2016-02-26

Identification and Characterization of MicroRNA Modulators in Caenorhabditis Elegans: A Dissertation

Zhiji Ren
University of Massachusetts Medical School

IDENTIFICATION AND CHARACTERIZATION OF MICRORNA MODULATORS IN *CAENORHABDITIS ELEGANS*

A Dissertation Presented

By

Zhiji Ren

Submitted to the Faculty of the
University of Massachusetts Graduate School of Biomedical Sciences, Worcester
in partial fulfillment of the requirements for the degree of

DOCTOR OF PHILOSOPHY

February 26, 2016

Interdisciplinary Graduate Program

IDENTIFICATION AND CHARACTERIZATION OF MICRORNA MODULATORS IN *CAENORHABDITIS ELEGANS*

A Dissertation Presented

By

Zhiji Ren

The signatures of the Dissertation Defense Committee signify completion and approval as to style and content of the Dissertation

Victor Ambros, Thesis Advisor

William Theurkauf, Member of Committee

Sean Ryder, Member of Committee

Amy Walker, Member of Committee

Dennis Kim, Member of Committee

The signature of the Chair of the Committee signifies that the written dissertation meets the requirements of the Dissertation Committee

Silvia Corvera, Chair of Committee

The signature of the Dean of the Graduate School of Biomedical Sciences signifies that the student has met all graduation requirements of the school.

Anthony Carruthers, Ph.D.,
Dean of the Graduate School of Biomedical Sciences

Interdisciplinary Graduate Program

February 26, 2016

DEDICATION

I would like to dedicate this thesis to my loving family, especially my mom. They have always put my education first. Without their support and encouragement, this work would not exist.

ACKNOWLEDGEMENTS

First and foremost, I want to thank my advisor, Victor Ambros, who not only enthusiastically encouraged me to pursue my scientific interest, but also generously provided me with the means to do so. Because of his guidance, I feel that I have grown tremendously as a scientist. For this and many other things, I am forever grateful.

Next, I thank Candy Lee and Darla Cavanaugh for their support and guidance both inside and outside of the lab. I would like to thank past and present members of the Ambros lab who have made our lab such an innovative and collaborative research environment. Particularly, I would like to express my gratitude to Isana Veksler-Lublinsky and Sungwook Choi for their collaboration on the Staufen project and LIN-28 project respectively. In addition, I want to thank Charles Nelson, Catherine Sterling, Samantha Burke, Katherine McJunkin, Isana Veksler-Lublinsky, Alejandro Vasquez Rifo and Sungwook Choi for their editing of chapters in this thesis. I also want to thank Omid Harandi, who taught me first things about *C. elegans* and generously offered me guidance during my graduate career.

Last, I would like to thank all my committee members throughout my graduate study. Silvia Corvera, Dennis Kim, Bill Theurkauf, Sean Ryder and Amy Walker have helped and supported me in developing my thesis. Craig Mello, Fen-Biao Gao, and Mark Alkema also served on my committees and offered me great advice.

ABSTRACT

MicroRNAs (miRNAs) are endogenous non-coding small RNAs that post-transcriptionally regulate gene expression primarily through binding to the 3' untranslated region (3'UTR) of target mRNAs, and are known to play important roles in various developmental and physiological processes. The work presented in this thesis was centered on understanding how *Caenorhabditis elegans* miRNAs are modulated by genetic, environmental, or physiological factors and how these small RNAs function to maintain the robustness of developmental processes under stressful conditions.

To identify modulators of the miRNA pathway, I developed sensitized genetic backgrounds that consist of a panel of miRNA gene mutants and miRNA biogenesis factor mutants with partially penetrant phenotypes. First, I found that upon infection of *Caenorhabditis elegans* with *Pseudomonas aeruginosa*, an opportunistic pathogen of diverse plants and animals, *let-7* family miRNAs are engaged in reciprocal regulatory interactions with the p38 MAPK innate immune pathway to maintain robust developmental timing despite the stress of pathogen infection. These *let-7* family miRNAs, along with other developmental timing regulators, are also integrated into innate immune regulatory networks to modulate immune responses. Next, I demonstrated that loss-of-function mutations of Staufen (*stau-1*), a double-stranded RNA-binding protein, increase miRNA activity for several miRNA families, and this negative modulation of Staufen on miRNA activity acts downstream of miRNA biogenesis, possibly by

competing with miRNAs for binding to target mRNA 3'UTRs.

In summary, these studies provide a better understanding on how miRNAs are modulated by various environmental and cellular components, and further support the role of the miRNA pathway in conferring robustness to developmental processes under these perturbations.

TABLE OF CONTENTS

LIST OF TABLES

LIST OF FIGURES

PREFACE

Chapter II was previously published as “Ren Z. and Ambros V. (2015). *Caenorhabditis elegans* microRNAs of the *let-7* family act in innate immune response circuits and confer robust developmental timing against pathogen stress. *Proc Natl Acad Sci U S A*: 2015 May 5; 112(18):E2366-75. doi: 10.1073/pnas.1422858112”. Permission is not required by Proceedings of the National Academy of Sciences of United States of America for inclusion in a dissertation.

The CRISPR/Cas9 experiments and the construction of plasmids for *lin-28* gene isoforms in Chapter III were carried out by Sungwook Choi.

Most of Chapter IV of this thesis was submitted to the journal of G3: Gene, Genome, Genetics on January 18, 2016 as “Ren Z, Veksler-Lublinsky, I, Morrissey D, Ambros V. Staufen negatively modulates microRNA activity in *Caenorhabditis elegans*”. This manuscript was accepted for publication on February 22, 2016. The CLIP experiment was not included in the manuscript. Permission is not required by Genetics Society of America for inclusion in a dissertation. The data analysis of the small RNA sequencing libraries was carried out by Isana Veksler-Lublinsky. David Morrissey provided the original idea of testing Staufen for its modulation of miRNA activity.

Victor Ambros aided in the experimental design and data interpretation of the results presented from Chapter II to Chapter V.

CHAPTER I: Introduction

Establishing and maintaining proper gene expression requires various regulatory mechanisms including post-transcriptional regulation by microRNAs (miRNAs). These small RNAs have been demonstrated to regulate a variety of biological processes (1, 2). Therefore, it is important to understand how miRNAs are modulated by various genetic, physiological and environmental perturbations. Here I describe the current knowledge of the regulation of the miRNA pathway, our approach to identify modulators of the miRNA pathway, and roles of miRNAs in maintaining biological robustness.

I.A. The microRNA pathway

1. Discovery.

In the last decades, our knowledge of the complexity of gene expression regulation in eukaryotes has been dramatically expanding. One of the most significant advances is the discovery of miRNAs. In 1993, the laboratories of Victor Ambros and Gary Ruvkun made the breakthrough finding that a regulator of developmental timing in *Caenorhabditis elegans* (*C. elegans*), *lin-4*, actually encodes a small noncoding RNA that post-transcriptionally regulates the expression of LIN-14 (3, 4). Seven years later, another developmental timing regulator *let-7* was found to generate a 21-nucleotide RNA that is well-conserved across animal phylogeny (5, 6). Since then, the field of miRNA biology has really

taken off, and miRNAs have been shown to play important roles in many developmental and physiological processes (1, 2).

2. Biogenesis.

MiRNAs are endogenous single-stranded non-coding small RNAs that post-transcriptionally regulate gene expression through translational inhibition and/or mRNA decay (7, 8). Although some miRNAs are located in the introns of protein-coding genes, they are usually present in the genome as independent genes and these miRNAs are transcribed into primary transcripts (pri-miRNAs) by RNA polymerase II in the nucleus (Figure 1.1). Pri-miRNAs fold into stem-loop structures and are processed into precursor miRNAs (pre-miRNAs) by the Microprocessor complex that consists of RNase III Drosha/DRSH-1 and its cofactor DGCR8/PASH-1. The interaction between DGCR8/PASH-1 and apical elements of the pri-miRNA's stem-loop structure ensures the precise cleavage of pri-miRNAs by Drosha/DRSH-1, which in turn generates pre-miRNAs with a two nucleotide overhang at the 3' end (9, 10). The hairpin-structured pre-miRNAs are exported into the cytoplasm by Ran-GTP and Exportin-5 (11, 12) and further processed by the RNase III Dicer/DCR-1 into RNA duplexes with two nucleotide overhangs at each 3' end (13, 14). One strand of the RNA duplex (guide strand) is the mature miRNA which is incorporated into the miRNA-specific Argonaute (AGO) protein (ALG-1 and ALG-2 in *C. elegans* (15)), whereas the other strand (passenger strand) is usually expelled and not functional (16).

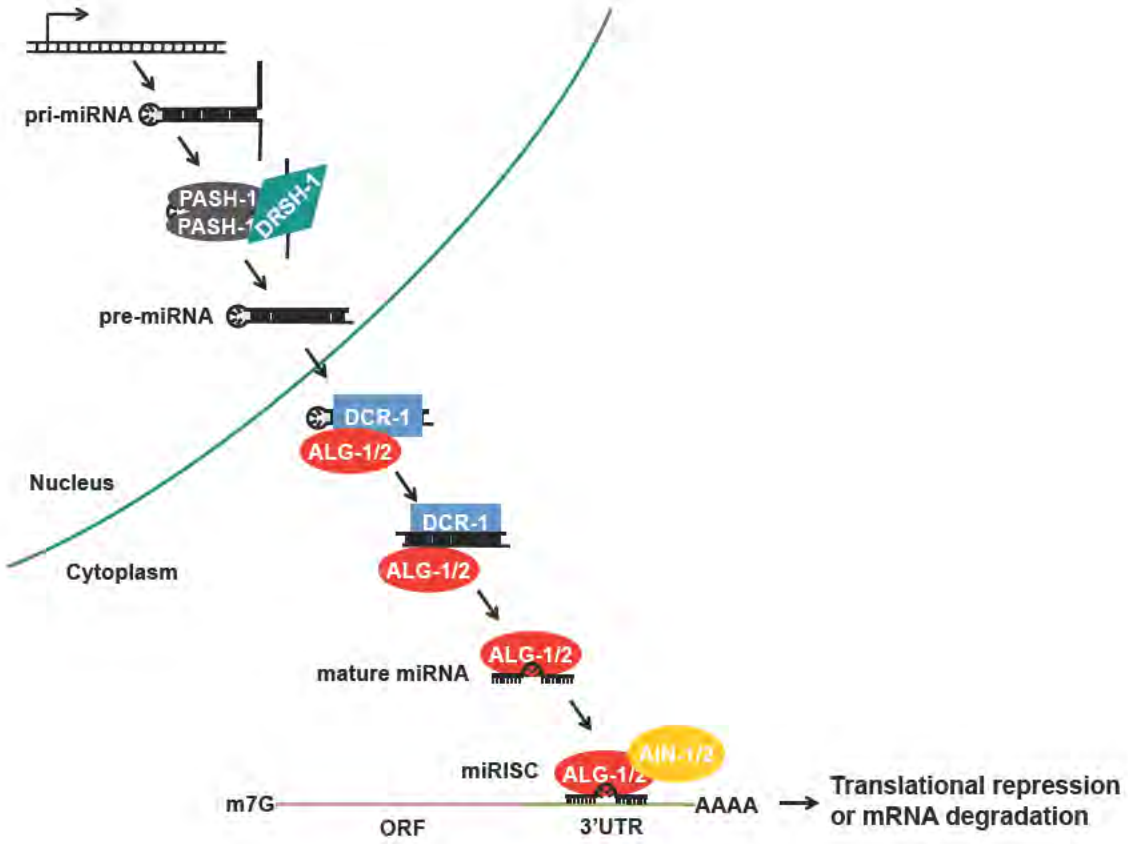

Figure 1.1 The *C. elegans* miRNA pathway.

3. Function.

MiRNAs exert their functions in translational inhibition and/or mRNA decay primarily through imperfect base-pairing to the 3' untranslated region (3'UTR) of their target mRNAs (17). The seed sequence (nucleotides 2-7) of a mature miRNA dictates the specificity of miRNA's recognition on target mRNAs. There is usually no mismatch between the seed sequence and the miRNA target site on the 3'UTR. Therefore, miRNAs with the same seed sequence are grouped into a family and predicted to potentially share the same set of target mRNAs (18). In addition to the seed sequence, the assembly of a ribonucleoprotein complex named miRNA-induced silencing complex (miRISC) on the 3'UTR of target mRNAs is also crucial for miRNAs to exhibit their regulation. Besides the AGO protein, another core component of miRISC is the AGO binding partner GW182 protein (AIN-1 and AIN-2 in *C. elegans* (19, 20)) (21, 22). GW182 proteins can serve as scaffolds for the binding of numerous silencing effectors on miRISC in order to carry out the miRNA-mediated gene silencing (23-29).

Because different miRNAs could potentially regulate the expression of different sets of genes with diverse functions, miRNAs have been shown to play important roles in numerous physiological and pathological processes, including development, differentiation, immune response, metabolism, neurodegeneration and cancer (3, 5, 30-34). Misregulation of miRNAs could lead to large-scale changes in gene expression, which in turn lead to disease conditions. For example, the upregulation of RAS and cell proliferation pathways caused by

reduced expression of *let-7* promotes the tumorigenesis of human lung cancer (35-38). Since miRNAs are such important regulators of many biological processes, it is not too surprising that the activity of miRNAs is subject to extremely sophisticated regulation.

4. The regulation of the microRNA pathway.

The activity of miRNAs can be regulated at several levels, including transcription, processing, target accessibility, miRISC activity and turnover.

The regulation of miRNA transcription is similar to the transcription regulation of protein coding genes. Complex control of miRNA transcription is usually observed, which consists of various types of autoregulatory feedback loops. One example is that transcription factor PITX3 and *mir-133b* form a negative feedback loop to control the differentiation of dopaminergic neuron. The transcription of *mir-133b* is activated by PITX3, which subsequently suppresses PITX3 expression (39).

The processing of miRNAs can be regulated through changes in the activity of miRNA biogenesis factors and through modifications on the miRNA sequence (40-46). The best-studied negative regulator of miRNA processing is an RNA-binding protein LIN-28, which specifically affects the processing of *let-7* family miRNAs on several different levels (47). First, LIN-28 can bind to the primary transcripts and precursors of the *let-7* family miRNAs, blocking Drosha and Dicer processing respectively (48, 49). Second, upon binding to the *pre-let-7*, LIN-28 also induces the 3’-terminal polyuridylation on *pre-let-7* by recruiting

TUT4 terminal poly(U) polymerase, which prevents Dicer processing and promotes the degradation of *pre-let-7* (50-54). The regulation between LIN-28 and *let-7* is highly conserved and plays an important role in the regulation of cell fate decisions including the developmental timing in *C. elegans*, the pluripotency of mammalian embryonic stem cells, and oncogenesis (47).

In order to carry out miRNA-mediated gene silencing, miRNAs need to physically bind to the target sites on the 3'UTR of target mRNAs, which can be subject to regulation by various 3'UTR binding proteins. Interestingly, 3'UTR binding proteins can have both positive and negative effects on the target accessibility of miRNAs. PUF proteins can act as positive regulators of miRNA activity through binding proximally to the miRNA target sites to increase miRNA target site accessibility (55, 56). By contrast, because the binding sites of the RNA-binding protein Dead end 1 (Dnd1) overlap with miRNA target sites, Dnd1 was found to impede the binding of miRNAs to their target 3'UTRs, thereby negatively regulating miRNA-mediated gene silencing (57). HuR proteins in some cases can function as positive regulators of miRNA activity in a similar manner as PUF proteins (58, 59), but in other cases, HuR proteins can negatively regulate miRNA activity by forming oligomers on the 3'UTR to block the miRNA target sites (60-62). Therefore, many 3'UTR binding proteins can affect the miRNA target accessibility, resulting in significant regulation on miRNA activity.

Another mode of regulation on miRNA activity is through affecting miRISC. Both core components of miRISC, AGO and GW182, can be regulated at the

level of expression and activity (63-65). However, other protein factors could also affect the activity of miRISC. For example, *C. elegans* TRIM-NHL protein NHL-2 was found to be associated with miRISC and promoted the potency of miRNA action without affecting miRNA biogenesis (66).

Regulators of the miRNA turnover process could affect the steady state level of miRNAs, which in turn regulates miRNA activity. So far, there is still a lack of comprehensive understanding on how mature miRNAs are degraded. However, certain exonucleases were found to carry out the turnover of mature miRNAs (67, 68). Additionally, several studies have shown that under certain conditions interaction with targets can contribute to the decay of a miRNA (69-71).

Although many regulators has been shown to dramatically affect the miRNA pathway, some factors such as NHL-2 only exhibit moderate effects on miRNA activity, and they are named miRNA modulators. A few studies so far have suggested that miRNA modulators could function to fine-tune the activity of miRNAs especially in response to developmental and physiological signals (66, 72). However, more studies on how the miRNA pathway is modulated by various genetic, physiological and environmental factors are needed to provide a better understanding of the biological significance of miRNA-mediated gene silencing.

I.B. Utilizing sensitized genetic backgrounds to identify microRNA modulators

1. The model organism: *C. elegans*.

To identify modulators of the miRNA pathway, we utilized the nematode *C. elegans* as our model organism. In the 1970s, *C. elegans* was first used by Sydney Brenner to study neuronal development (73), and it has since been proven to be a fantastic genetic model that has significantly propelled biomedical research in the last decades.

C. elegans is normally a self-fertilizing hermaphrodite organism that has a simple life cycle consisting of the embryonic stage, four larval stages (L1, L2, L3 and L4) and the adult stage (Figure 1.2). Upon fertilization, embryos go through proliferation and organogenesis to establish the main body plan. In the presence of food after hatching, larvae normally pass through four stages to reach adulthood with an increase in body size. At the end of each larval stage, worms enter a lethargic period called molt, during which a new, stage-specific cuticle is synthesized and the old one is shed. Under starvation, high temperature and crowding, L2 larvae can adopt an alternative developmental program and molt into an arrested stage named dauer. Dauer larvae can withstand the unfavorable conditions and survive for several months, and they will resume normal development when favorable conditions occur.

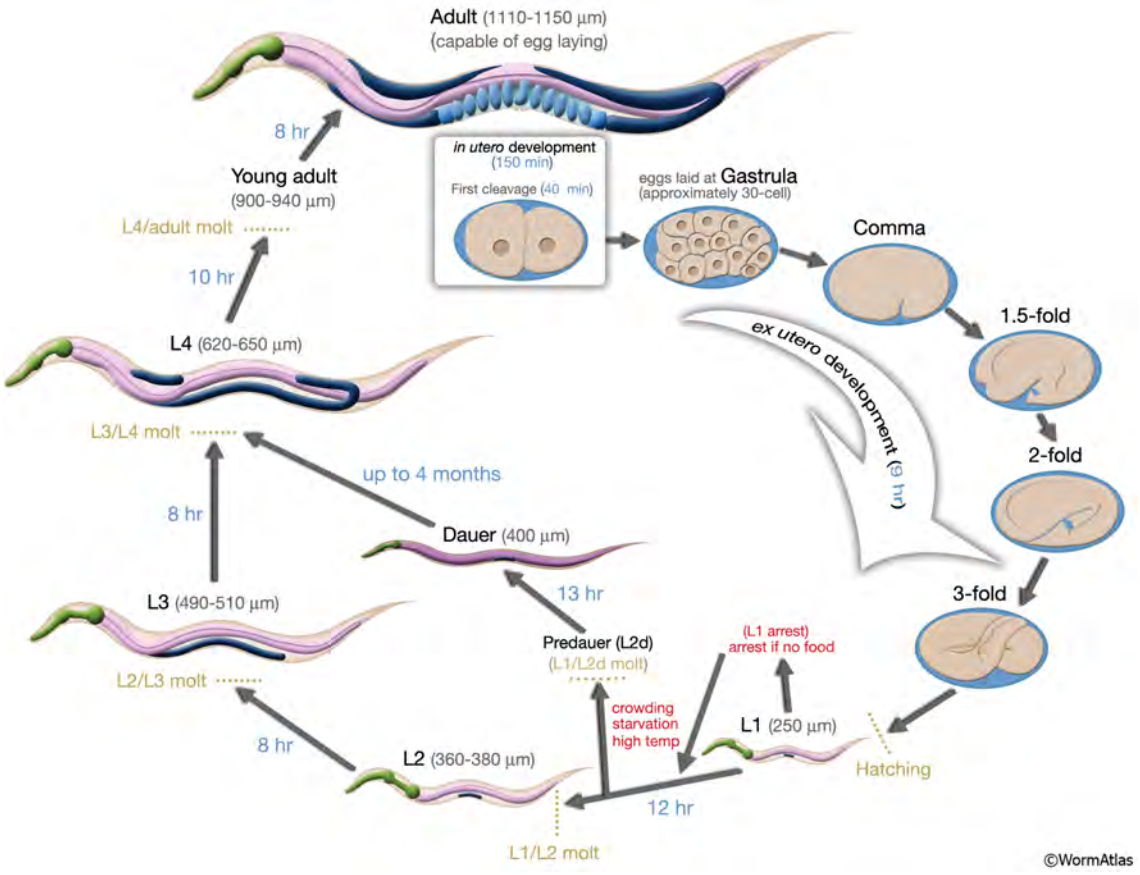

Figure 1.2 The life cycle of *C. elegans*. Image is from WormAtlas (http://wormatlas.org/index.html).

Extensive studies have been conducted in *C. elegans* to show that miRNAs are important in the regulation of several developmental processes (3, 5, 74-76), which provides me with a great system to study modulators of the miRNA pathway.

2. Sensitized genetic backgrounds.

Genetic loss-of-function mutants of miRNA modulators usually do not exhibit any miRNA related phenotype in an otherwise wild type genetic background. Therefore, to identify modulators of miRNA activity, we established a panel of worm strains containing mutations designed to produce sensitized genetic backgrounds with compromised activity of specific miRNA families or miRNA biogenesis factors (Figure 1.3). There are three categories of mutations in these sensitized genetic backgrounds: 1) null mutations of a subset of genes encoding a miRNA family; 2) hypomorphic (non-null partial loss-of-function) mutations of a particular miRNA; 3) hypomorphic mutations of a miRNA biogenesis factor or miRISC component. One essential feature of the sensitized genetic backgrounds is that these mutants all have partially penetrant phenotypes. This feature allows the identification of either positive or negative modulators of miRNA activity by testing for enhancement or suppression, respectively, of these sensitized phenotypes after knockdown of candidate gene activity or applying various stress conditions.

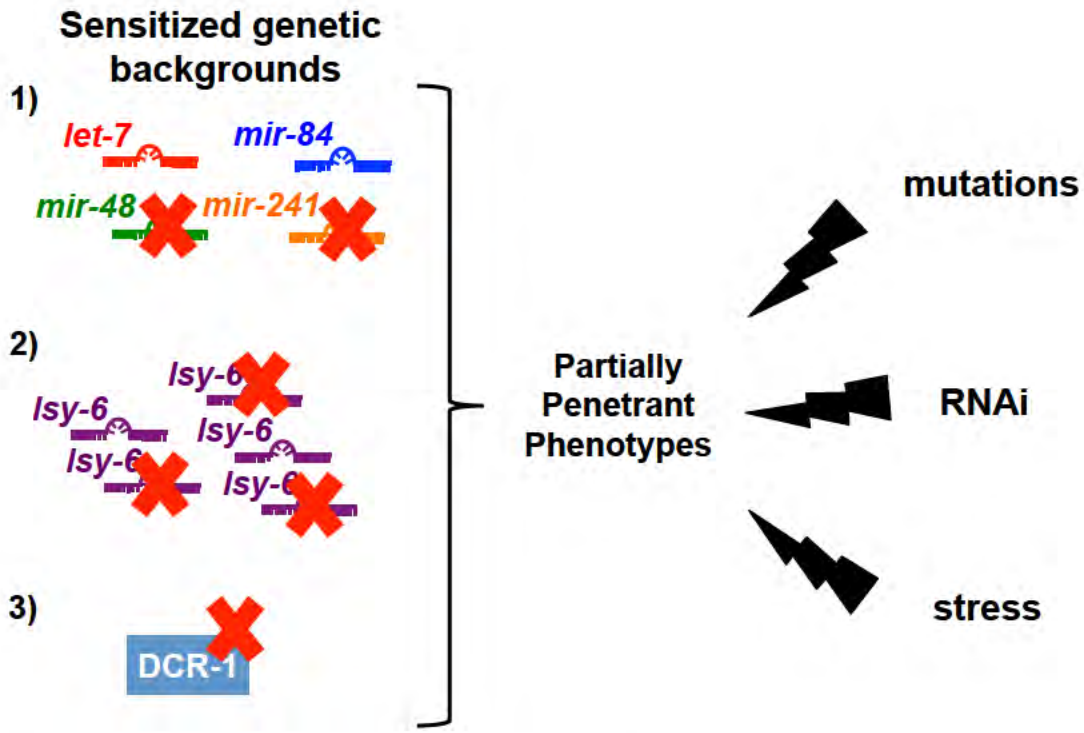

Figure 1.3 A diagram showing the approach of using sensitized genetic backgrounds to identify miRNA modulators.

3. The developmental timing pathway.

The first identified miRNAs, *lin-4* and *let-7*, are known to function in the heterochronic pathway to regulate the developmental timing of the hypodermal seam cell V lineage in *C. elegans* (3, 5, 77) (Figure 1.4). During larval development, wild type animals exhibit a distinct seam cell division pattern at each larval stage, and after the L4 molt, seam cells will differentiate and produce adult specific cuticle structure, called adult alae which are three longitudinally oriented ridges above the seam cells on the lateral sides of adult worms (Figure 1.4A and B). If a mutant animal reiterates an early larval stage seam cell division at later stage, it is named a retarded mutant. And a precocious mutant will skip a particular larval stage seam cell division causing the early occurrence of later stage divisions.

The expression of the *lin-4* miRNA starts in the mid-L1 stage to suppress the expression of two core heterochronic genes, *lin-14* and *lin-28* (4, 78) (Figure 1.4E and H). The transcription factor *lin-14* functions to promote the L1 stage seam cell division which is skipped in the *lin-14* loss-of-function mutant thereby resulting in a precocious phenotype (77, 79). In the absence of *lin-4*, *lin-14* expression level remains high, which results in the continuous reiteration of the L1 stage seam cell division (Figure 1.4A). When *lin-28* is disrupted, the L2 stage proliferative seam cell division is skipped and worms end up with a precocious heterochronic phenotype with decrease seam cell number and precocious adult

alae (Figure 1.4A). *lin-28* exhibits this function mainly through its regulation on *let-7* family miRNAs and *hbl-1*, a target of *let-7* family miRNAs (80).

So far, four of the *C. elegans let-7* family miRNAs, *let-7*, *mir-48*, *mir-84* and *mir-241*, are known to regulate developmental timing. Three of the *let-7* family miRNAs (*mir-48*, *mir-241* and *mir-84*) are expressed starting at the L2 stage and function redundantly to downregulate the expression of a transcription factor *hbl-1* (74) (Figure 1.4F and H). *hbl-1* is required to promote the L2 stage proliferative seam cell division that is reiterated when *mir-48*, *mir-241* and *mir-84* are all deleted. Therefore, all the seam cells in worms lacking *mir-48*, *mir-241* and *mir-84* continue to go through the proliferative division after the L2 stage, resulting in worms with an increased number of seam cells and no adult alae at the adult stage (Figure 1.4A). Since these three *let-7* family miRNAs function redundantly, in doubly-mutant worms missing only *mir-48* and *mir-241* not all the seam cells reiterates the L2 stage proliferative division, which leads to a partially penetrant phenotype with gaps in the adult alae and extra seam cells at the adult stage (Figure 1.4A, C-D). This partially penetrant phenotype of the *mir-48 mir-241* mutant can therefore be used to identify modulators of *let-7* family miRNA activity.

Finally, the larval-to-adult transition of seam cells is regulated by the upregulation of *let-7* miRNA from the L3 stage, which results in the repression of *lin-41* and *hbl-1* (81, 82) (Figure 1.4G and H). *lin-41* and *hbl-1* function to

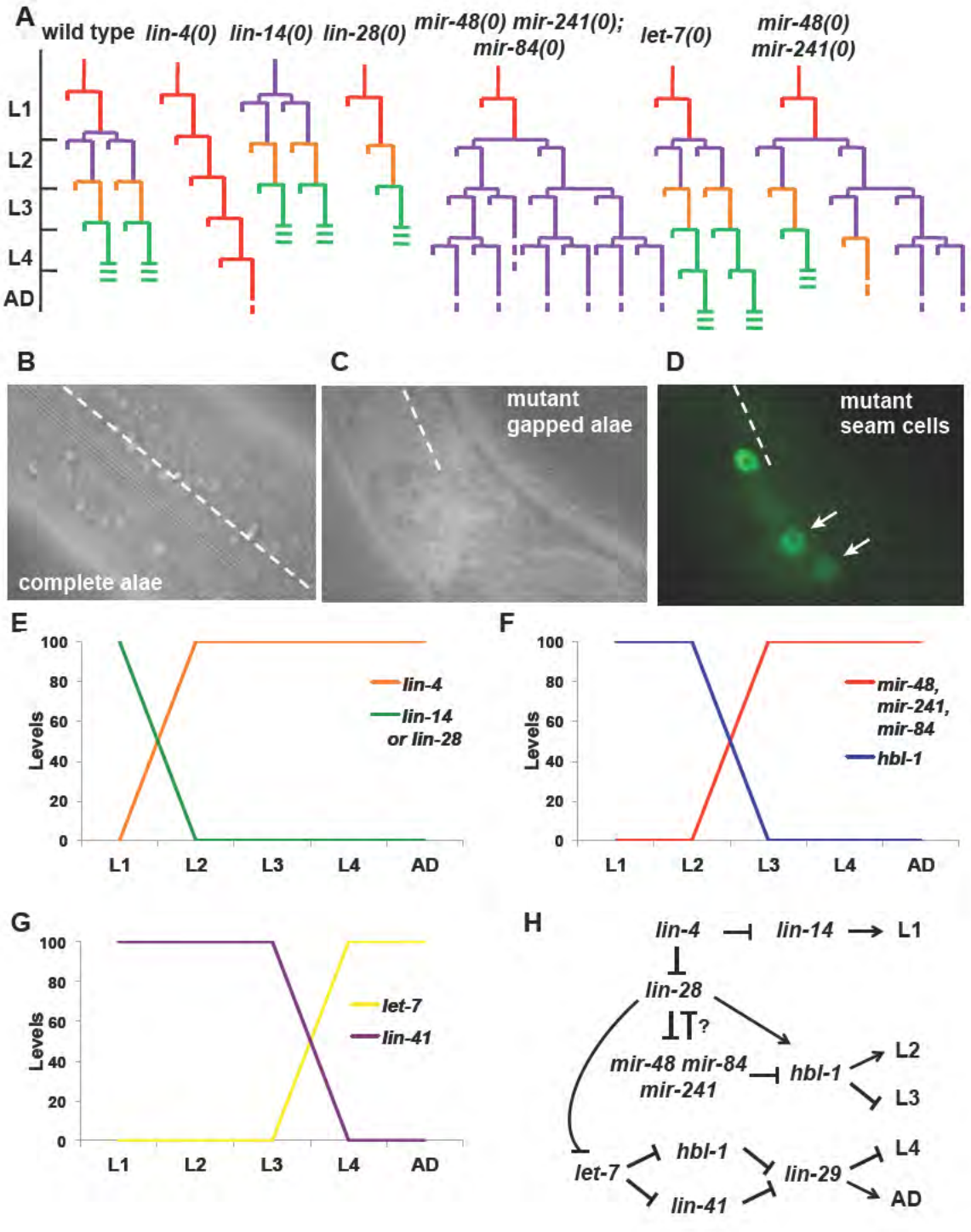
A
wild type
lin-4(0)
lin-14(0)
lin-28(0)
mir-48(0) mir-241(0); mir-84(0)
let-7(0)
mir-48(0) mir-241(0)
L1
L2
L3
L4
AD
B
complete alae
C
mutant gapped alae
D
mutant seam cells
E
Levels
lin-4
lin-14 or lin-28
F
mir-48, mir-241, mir-84
hbl-1
G
let-7
lin-41
H
lin-4
lin-14
lin-28
mir-48 mir-84 mir-241
hbl-1
let-7
lin-41
lin-29

Figure 1.4 The *C. elegans* developmental timing pathway. (A) A diagram of seam cell V lineage (V1-V4, V6) in wild type and various heterochronic gene mutants. The three horizontal lines indicate adult alae formation. (B) Image of complete adult alae in wild type animal. (C) Image of gapped adult alae in a *let-7* family miRNA mutant, and the seam cells of the same animal were shown in (D). These seam cells pointed by arrows are going through a proliferative division instead of differentiation at the L4 molt, and these cells fail to produce the adult alae, which leads to the gap in adult alae. Developmental expression patterns of (E) *lin-4*, *lin-14* and *lin-28*; (F) *mir-48*, *mir-241*, *mir-84* and *hbl-1*; (G) *let-7* and *lin-41*. (H) The genetic interactions within the developmental timing pathway.

regulate the expression of a zinc finger transcription factor LIN-29 that triggers the cellular events associated with seam cell terminal differentiation (83). Therefore, seam cells in the *let-7* null mutant fail to differentiate at the L4 molt, resulting in the absence of adult alae at the young adult stage and the recurrence of the L4 stage seam cell division after adulthood (Figure 1.4A).

Besides *lin-4* and *let-7* family miRNA, mutants of the miRNA biogenesis factor and miRISC components have been shown to exhibit developmental timing defects possibly due to the reduced activity of these miRNAs (15, 19, 20, 84).

4. Other microRNA regulated developmental processes in *C. elegans*.

Similar to the developmental timing regulation elicited by *lin-4* and *let-7* family miRNAs, certain other *C. elegans* miRNAs have been shown to play important roles in developmental processes. The mutants of these miRNAs can also be used as sensitized genetic backgrounds.

lsy-6 is a miRNA identified in a forward genetic screen for mutants in which the cell fate decision of a pair of morphologically bilaterally symmetric gustatory neurons is inappropriately executed (75) (Figure 1.5A). Specifically, the two of neurons are ASE left (ASEL) and ASE right (ASER) and they undergo a left/right asymmetric diversification in cell fate during embryonic development. *lsy-6* is expressed only in the ASEL neuron to suppress its target transcription factor *cog-1*, thereby promoting the expression of genes required for ASEL neuronal cell fate. Whereas in the ASER neuron, *lsy-6* expression is turned off,

and another set of genes are expressed to specify the cell fate of ASER. One of the genes downstream of *lsy-6* is *lim-6* that is present specifically in the ASEL neuron in wild type animals. In the null mutant of *lsy-6*, the ASEL neuron adopts the fate of ASER neuron, which results in the complete loss of *lim-6* expression in the ASEL neuron. There is an allele of *lsy-6* (*lsy-6(ot150)*) with weak penetrance due to the impaired *lsy-6* biogenesis, which makes it an ideal candidate of a sensitized genetic background to identify miRNA modulators.

Loss of all *mir-35* family miRNAs (*mir-35* through *mir-42*) results in an embryonic lethal phenotype in *C. elegans*, however, a partially penetrant temperature-sensitive embryonic or L1 larval lethal phenotype was observed in worms without *mir-35-41* (76) (Figure 1.5B). Therefore, *mir-35-41* loss-of-function mutant could be utilized as sensitized genetic background to identify modulators of miRNAs as well.

I.C. MicroRNAs function to confer biological robustness

Proper animal development requires the robust execution of cell fates under diverse genetic, physiological and environmental perturbations. Therefore, numerous mechanisms have evolved to confer the robustness of biological processes (85). Recent studies have shown that miRNAs participate in feedback and feedforward regulatory circuits (86-88), and in doing so, they maintain biological robustness under various stresses (89-92).

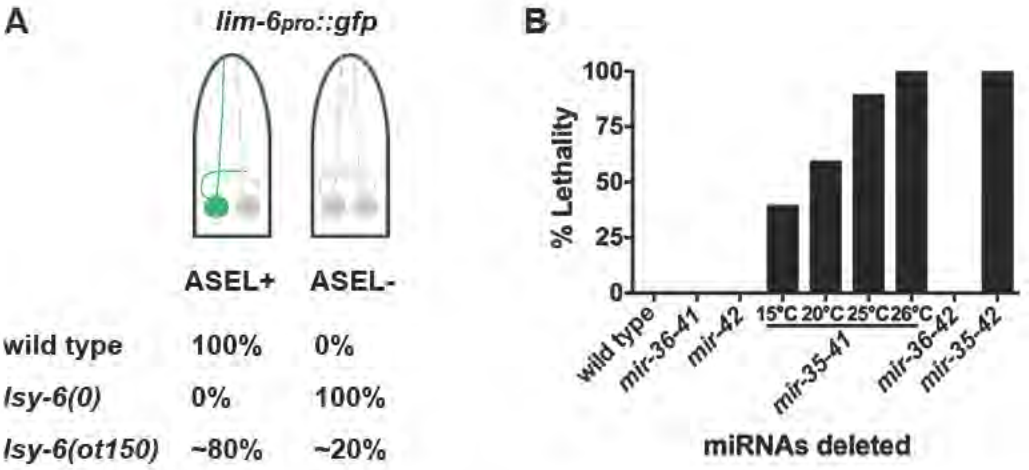

Figure 1.5 Phenotypes of other *C. elegans* miRNA mutants. (A) The ASE neuron specification phenotypes wild type, *lsy-6(0)* and *lsy-6(ot150)* animals. (B) The embryonic lethality phenotype of *mir-35* family miRNA mutants. This data image in (B) is from (76).

In some regulatory circuits, miRNAs could oppose the actions of an upstream regulator to create tightly controlled outcome. For example, work in *Drosophila melanogaster* has shown that *mir-7* acts in two feedforward loops to refine downstream gene expression, which in turn maintains the robustness of eye development against temperature fluctuation (93). Similar study in *C. elegans* demonstrated that *mir-34* and *mir-83* protect the robust migration of distal tip cells under temperature changes (94). Furthermore, *let-7* family miRNAs and the DAF-12 nuclear hormone receptor function in a feedback loop to ensure the robust seam cell fate under different environmental signals (72).

In contrast, miRNAs in other regulatory circuits can reinforce the regulation by an upstream factor to generate genetic switches. Upon the activation of an inflammatory signal, mammalian *let-7* family miRNAs are involved in a positive feedback loop with NF-κB, LIN-28, IL6 and Ras to promote an epigenetic switch from immortalized breast cells to stably transformed cancer cells (95). Moreover, the double negative feedback loops between *mir-223* and the transcription factor NFI-A control the retinoic acid-induced cell fate differentiation in granulocytes (96).

Additionally, several miRNA modulators have been shown to act through miRNAs to regulate biological robustness. As a positive modulator of the miRNA pathway, NHL-2 was proposed to modulate the efficacy of miRNAs in response to developmental and physiological signals thereby ensuring the robustness of miRNA regulated pathways (66). Another RNA-binding protein TDP-43 was

found to positively regulate the expression of *mir-9a* in *Drosophila*, which is important for the robust cell fate specification of sensory organ precursor cells when the environmental temperature changes (97).

Taken together, these studies demonstrate a critical role for miRNAs and miRNA modulators in maintaining robustness of biological processes under various conditions. Therefore, by identifying new modulators of miRNA pathway, we can achieve a better understanding of this important function of miRNAs.

The proceeding chapters will describe novel environmental and cellular modulators of the *C. elegans* miRNA pathway. First, reciprocal interactions between heterochronic genes and the p38 innate immune pathway help to ensure the robust developmental cell fate during infection. Second, the double-stranded RNA-binding protein Staufen can negatively modulate the efficacy of miRNAs in *C. elegans*, suggesting a role for Staufen in buffering miRNA-mediated gene silencing in developmental, physiological and environmental contexts. These findings underscore the importance of miRNA pathway in conferring robustness to developmental programs under stressful conditions.

CHAPTER II: *C. elegans let-7* family microRNAs act in innate immune response circuits and confer robust developmental timing against pathogen stress

II.A. Abstract

Animals maintain their developmental robustness against natural stresses through numerous regulatory mechanisms, including the post-transcriptional regulation of gene expression by miRNAs. *Caenorhabditis elegans let-7* family miRNAs (*let-7*, *mir-48*, *mir-241* and *mir-84*) function semi-redundantly to confer robust stage-specificity of cell fates in the hypodermal seam cell lineages. Here we show reciprocal regulatory interactions between *let-7* family miRNAs and the innate immune response pathway in *C. elegans*. Upon infection of *C. elegans* larvae with the opportunistic human pathogen *Pseudomonas aeruginosa* (*P. aeruginosa*), the developmental timing defects of certain *let-7* family miRNA mutants are enhanced. This enhancement is mediated by the p38 MAPK innate immune pathway acting in opposition to *let-7* family miRNA activity, possibly via the downstream transcription factor ATF-7. Furthermore, *let-7* family miRNAs appear to exert negative regulation on the worm's resistance to *P. aeruginosa* infection. Our results show that the inhibition of pathogen resistance by *let-7* involves downstream heterochronic genes and the p38 MAPK pathway. These findings suggest that *let-7* family miRNAs are integrated into innate immunity gene regulatory networks, such that this family of miRNAs modulates immune

responses while also ensuring robust timing of developmental events under pathogen stress.

II.B. Introduction

During development, animals routinely encounter environmental, physiological, and nutritional challenges that threaten to compromise the robust execution of developmental programs. Therefore, the genetic programming of development includes mechanisms to ensure that developmental events occur flawlessly despite stressful conditions (85, 91). Several studies indicate that miRNAs are utilized to maintain the robustness of biological processes under stress conditions (90, 93, 97-102). MiRNAs are endogenous non-coding small RNAs that post-transcriptionally regulate gene expression primarily through binding to the 3' untranslated region (3'UTR) of target mRNAs, which results in translation inhibition and/or mRNA degradation (103). MiRNAs with the same seed sequence (nucleotides 2-7 of the mature miRNA sequence), which are predicated to potentially share the same set of targets (18), are grouped into a family.

lin-4 and *let-7* family miRNAs are central to the regulation of pluripotency and differentiation in many animal systems, including mammals (3-5, 74, 104, 105). Four *C. elegans let-7* family miRNAs, *let-7, mir-48, mir-84* and *mir-241*, function in concert to repress key heterochronic gene targets, including *daf-12*, *lin-41,* and *hbl-1,* to stage-specifically regulate the timing of the hypodermal seam

cell divisions (74, 81, 82, 106, 107). In *C. elegans*, the temporal patterns of cell division and cell fate during larval development are exquisitely invariant, even though larvae develop as free-living inhabitants of a changing environment in soil and decaying plant materials.

In the wild, worms encounter a variety of bacteria species as food sources. Several of these species are proven to be pathogenic to *C. elegans* (108), thus representing environmental stressors. Interestingly, recent studies have shown that *let-7* family miRNAs seem to not only regulate developmental events, but also regulate the antibacterial and inflammatory response in several animal systems (95, 109-112) . At least two of the *C. elegans let-7* family miRNAs are shown to regulate worm's survival to *P. aeruginosa* infection (112). These previous findings suggest that *let-7* family miRNAs could possibly coordinate developmental timing and innate immune responses, so as to contribute to the robustness of development during pathogen infection.

Here we show that *let-7* family miRNAs are engaged in reciprocal interactions with innate immune pathways. Using genetically sensitized backgrounds, we find that the developmental timing phenotypes of *let-7* family miRNA mutants are modified by bacterial diet, particularly by growth on pathogenic *P. aeruginosa*. *let-7* family miRNA activity is negatively regulated on *P. aeruginosa* by the p38 MAPK pathway. Moreover, *let-7* family miRNAs exhibit negative regulation on pathogen resistance, possibly through several pathways, including the p38 MAPK signaling and also downstream heterochronic genes,

particularly the *let-7* family miRNA targets *lin-41* and *hbl-1*. Our findings suggest that genetic redundancy among *let-7* family miRNAs enables these miRNAs to robustly control the expression of developmental cell fates, while also modulating innate immune responses according to the pathogenicity of the worm's bacterial diet.

II.C. Materials and methods

Nematode and bacteria methods. *C. elegans* were cultured on nematode growth media (NGM) (73) and fed with *E. coli* HB101, unless otherwise noted. All the *C. elegans* strains used in this study are listed in Table 2.1. Synchronized populations of developmentally staged worms were obtained by standard methods (113). To test different bacterial foods for effects on heterochronic phenotypes, all the *E. coli* strains and *Comamonas sp.* were seeded onto NGM plates from saturated cultures. Procedures for culturing *P. aeruginosa* and *S. enterica* for feeding nematodes were carried out as described in (114).

Heterochronic phenotype analysis. Gravid adult animals raised at 20°C were placed on control or treatment plates at 20°C, and their progeny were scored at the young adult stage for adult lateral alae formation and seam cell number. Nomarski DIC microscopy and fluorescence microscopy with the *maIs105* [*col-19::gfp*] transgene to mark lateral hypodermal cell nuclei were used to score alae formation and seam cell number, respectively.

Table 2.1 *C elegans* strains used in Chapter II.

Name	Genotype
AU78	*agIs219* [*T24B8.5p::gfp::unc-54-3'UTR + ttx-3::gfp::unc-54-3'UTR*] III
CT11	*hbl-1(mg285)* X
KU25	*pmk-1(km25)* IV
KU4	*sek-1(km4)* X
MT7626	*let-7(n2853)* X
N2	wild type
VC1518	*atf-7(gk715)* III
VT1064	*mir-48(n4097) mals105* V*; mir-84(n4037)* X
VT1153	*mals137* [*Plet-7(2kb)::gfp + unc-119(+)*]
VT1159	*mals138* [*Pmir-84(2kb)::gfp + unc-119(+)*]
VT1259	*mals150* [*Pmir-48(1.5kb)::gfp + unc-119(+)*]
VT1296	*mir-48 mir-241(nDf51) mals105* V
VT1307	*mir-48(n4097) mals105* V
VT1313	*mir-84(n4037)* X*; mals105* V
VT1365	*let-7(mg279)* X*; mals105* V
VT1367	*mals105* [*col-19::gfp*] V (wild type[§])
VT1423	*mir-48 mir-241(nDf51) mals105* V*; mir-84(n4037)* X
VT1718	*mir-48(n4097)* V*; mir-84(n4037)* X
VT2692	*let-7(n2853)* X*; mals105* V
VT2731	*nsy-1(ky397)* II
VT2769	*nsy-1(ky397)* II*; mir-48 mir-241(nDf51) mals105 V*
VT2770	*sek-1(km4)* X*; mir-48 mir-241(nDf51) mals105* V
VT2771	*pmk-1(km25)* IV*; mir-48 mir-241(nDf51) mals105* V
VT2788	*let-7(n2853) mir-84(n4037)* X*; mals105* V
VT2816	*pmk-1(km25)* IV*; mals138*
VT2817	*let-7(mg279) mir-84(n4037)* X*; mals105* V
VT2855	*let-7(mg279)* X
VT2890	*tir-1(qd4)* III*; let-7(mg279)* X
VT2891	*nsy-1(ky397)* II*; let-7(mg279)* X
VT2892	*sek-1(km4) let-7(mg279)* X
VT2893	*pmk-1(km25)* IV*; let-7(mg279)* X
VT2909	*atf-7(gk715)* III*; mir-48 mir-241(nDf51) mals105* V
VT2923	*pmk-1(km25)* IV*; mals137*
VT2924	*pmk-1(km25)* IV*; mals150* V
VT2933	*lin-41(ma104)* I*; let-7(mg279)* X
VT2934	*hbl-1(mg285) let-7(mg279)* X
VT2936	*tir-1(tm3036)* III*; mir-48 mir-241(nDf51) mals105* V
VT2937	*tir-1(ok1052)* III*; mir-48 mir-241(nDf51) mals105* V
VT2955	*atf-7(qd22) agIs219* III*; mir-48 mir-241(nDf51) mals105* V
VT2956	*atf-7(qd22qd130) agIs219* III*; mir-48 mir-241(nDf51) mals105* V
VT3037	*mals380* [*let-7(+) + unc-119(+)*] II; *unc-119(ed3)* III
VT3047	*let-7(n2853)* X*; mals380* II
VT3049	*let-7(mg279)* X*; mals380* II
VT3051	*mir-48(n4097)* V*; mir-84(n4037)* X*; mals380* II
VT3053	*mir-48 mir-241(nDf51); mals380* II
VT3086	*mals380* II
VT432	*lin-41(ma104)* I
ZD101	*tir-1(qd4)* III

[§] This strain was used as wild type in all the heterochronic phenotype assays.

***P. aeruginosa* killing assays and lifespan assays.** *P. aeruginosa* PA14 and *E. coli* HB101 were cultured in Luria broth (LB), seeded onto slow-killing plates (114) containing 100μM 5-fluorodeoxyuridine (FUdR, Sigma) for *P. aeruginosa* killing assay and lifespan assay, respectively. The seeded plates were incubated at 37°C for 24 hours and then transferred to 25°C for 24 hours before use. Assays were conducted by transferring L4 stage animals raised on *E. coli* HB101 to *P. aeruginosa* killing assay plates and lifespan assay plates at 25°C. Animals that died prematurely due to developmental abnormalities (leading to bagging and bursting vulva), or that expired after crawling off the plate, were censored. Data were normalized by adjusting the numbers of live animals at each time point so as to derive a total population size of 100 for each technical replicate. Then, the normalized data for three technical replicates were averaged, and survival curves were compared using log-rank test and Fisher's exact test in OASIS (Online Application for Survival Analysis of Lifespan Assays) (115). All experiments were independently performed at least twice.

RNA extraction. Animals were collected and flash frozen in liquid nitrogen. Total RNA was extracted using Trizol reagent (Invitrogen).

Firefly microRNA assay. 2μg of total RNA was used for Firefly microRNA assay (http://www.fireflybio.com/). Standard protocol provided by the manufacture was followed. Guava easyCyte 8HT was used for analysis. Signals (arbitrary unit) were normalized to small nucleolar RNA U18 and then to the control group (HB101).

Confocal microscopy. Animals were mounted on glass slides with 2% agarose pads and anesthetized with 10mM levamisole. A Leica TCS SPE microsystem was used to acquire images. The mean intensities were calculated with Leica Application Suite Advanced Fluorescence software platform.

Transgenic constructs. pZR001 plasmid was made by cloning the 2459 bp of *let-7* genomic rescue region (5) into MosSCI destination vector pCFJ150. An integration *maIs380* at the Chromosome II *ttTi5605* site was obtained using MosSCI protocol (116).

Western blot analysis. For p38 western blots, synchronized L4 stage animals grown on *E. coli* HB101 at 20°C were transferred to *P. aeruginosa* slow-killing assay plates (114) at 25°C. At each indicated time point, animals were washed off plates with M9 buffer and flash frozen in liquid nitrogen. Lysates were prepared by resuspending samples in lysis buffer (50mM Tris-HCl pH7.4, 150mM NaCl, 2mM EDTA, 1% NP-40, 2mM DTT, PhosSTOP (Roche), Protease inhibitor (Roche)) and sonicated briefly with Branson SLPe sonicator. Lysates were centrifuged at 164,000rpm for 20 minutes at 4°C and the supernatants were collected. Protein concentration was measured by BioRad Protein Assay Dye Reagent Concentrate (Cat# 500-0006). 60µg of proteins were used for the immunoblot analysis. The activated p38 was recognized by anti-ACTIVE p38 pAb (Cell Signaling) at a 1:1000 dilution. The total PMK-1 polyclonal antibody was applied at 1:1000 dilution (a gift from Dr. Kunihiro Matsumoto), and anti-α-tubulin antibody (Sigma-Aldrich Cat# T6074) was used at 1:20000 dilution.

Electron microscopy. Wild type (N2) and *let-7(mg279)* animals were synchronized and grown on NGM plates seeded with *E. coli* HB101. L4 stage animals were transferred onto *P. aeruginosa* slow-killing plates and incubated at 25°C for 8, 24 and 48 hours. Worms were harvested and prepared for transmission EM as described (117).

RNAi knockdown. Gene knockdown by RNAi was carried out using bacterial feeding RNAi (118). RNAi clones were obtained from Ahringer RNAi feeding library (119). Gravid adult animals were placed on the RNAi plates and their progeny were scored for their heterochronic phenotypes.

Epifluorescence Microscopy. Animals carrying transgene *agIs219*[*T24B8.5p::gfp::unc-54-3'UTR*]) were used as an indication of the p38 MAPK pathway activity in the RNAi experiments for *vhp-1* (120). Images were acquired using Zeiss SteREO Discovery.V12 microscope with Zeiss AxioCam MRc camera and Zeiss ZEN 2012 (blue edition) software.

***P. aeruginosa* avoidance behavior assay:** L4 stage animals were put on *P. aeruginosa* slow-killing plates (114), and numbers of animals on and off the bacterial lawn were counted 2, 4, 6, 8, 12 and 24 hours later.

II. D. Results

1. Growth on *P. aeruginosa* aggravates the heterochronic phenotypes of *let-7* family miRNA mutants.

let-7 family miRNAs act semi-redundantly in controlling the developmental timing of certain stage-specific hypodermal seam cell fates in *C. elegans*. Loss of *let-7* family miRNAs results in reiterations of early larval seam cell division patterns at later stages, and many seam cells in these mutants also fail to properly differentiate adult specific cuticular structures (called adult alae) at the L4 molt (5, 74) (Figure 2.1A). These heterochronic *let-7* family miRNA mutant phenotypes are easily quantified by using microscopy to measure the number of seam cells and to score for the formation of adult alae in young adults. To investigate whether different bacterial food sources could impact the regulation of developmental timing by *let-7* family miRNAs, we employed a genetically sensitized *let-7* family miRNA mutant strain (*mir-48 mir-241(nDf51)*) that exhibits a partially penetrant heterochronic phenotype. Wild type animals have an average number of 16 seam cells and 100% of the animals have complete adult alae at the young adult stage, while *mir-48 mir-241(nDf51)* animals display an average of 18.5 seam cells and approximately 60% of the animals exhibit incomplete adult alae.

We scored seam cell numbers and adult alae formation for wild type and *mir-48 mir-241(nDf51)* animals after development on six different bacterial diets including three strains of *E. coli* that are typically used as laboratory food sources

(HB101, OP50, HT115), and three other bacterial species (*Comamonas sp.* DA1877, *P. aeruginosa* PA14, *Salmonella enterica* SL1344) that have been shown to significant effect the physiology of *C. elegans* (108, 121). As expected, wild type animals exhibited no evidence of developmental timing abnormalities regardless of the bacterial diet (Figure 2.1B, Table 2.2). However, *mir-48 mir-241(nDf51)* animals showed quantitatively different seam cell phenotype, dependent upon the bacterial food source (Figure 2.1B). Notably, when grown on *P. aeruginosa, mir-48 mir-241(nDf51)* animals exhibited an enhanced seam cell phenotype compared to growth on HB101 (Figure 2.1B). Consistent with this enhanced seam cell phenotype, *mir-48 mir-241(nDf51)* animals also exhibit enhanced adult alae phenotype on *P. aeruginosa* (Table 2.2). These results suggest that bacterial food source can modulate the activity of the heterochronic gene pathway. Since animals with all *let-7* family miRNAs intact showed no heterochronic phenotypes on any of the bacterial diets, these results indicate that *let-7* family miRNAs act redundantly to maintain the robustness of developmental timing under the influence of dietary stress.

The most dramatic effect of diet on the developmental timing phenotypes of *mir-48 mir-241(nDf51)* animals was from growth on the pathogenic bacterium *P. aeruginosa*. Therefore, we focused our further studies on the effects of *P. aeruginosa*. The heterochronic phenotype enhancement in *mir-48 mir-241(nDf51)* animals on *P. aeruginosa* suggests that the activity of the remaining

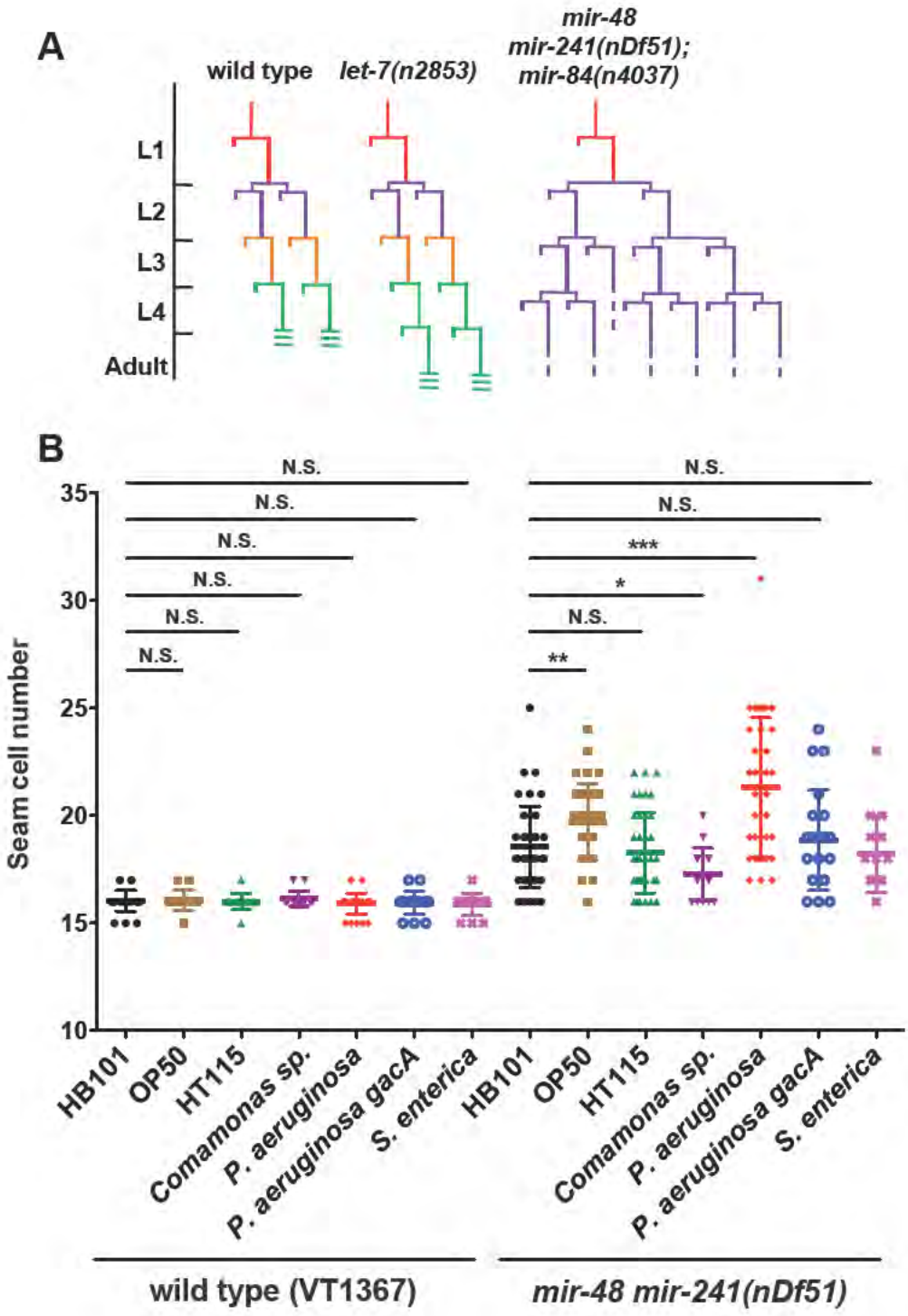
A
wild type
let-7(n2853)
mir-48
mir-241(nDf51);
mir-84(n4037)
L1
L2
L3
L4
Adult
B
Seam cell number
35
30
25
20
15
10
N.S.
N.S.
N.S.
N.S.
N.S.
N.S.
N.S.
N.S.
***
*
N.S.
**
HB101
OP50
HT115
Comamonas sp.
P. aeruginosa
P. aeruginosa gacA
S. enterica
wild type (VT1367)
mir-48 mir-241(nDf51)

Figure 2.1 Effects of bacterial food on the heterochronic phenotype of a *let-7* family partial loss-of-function mutant. (A) Diagrams of seam cell V lineage in wild type (N2), *let-7(n2853)* and *mir-48 mir-241(nDf51); mir-84(n4037)* animals. L1 to L4 are the four larval stages in *C. elegans* post-embryonic development. (B) Scatter plot of seam cell number for wild type (VT1367) and *mir-48 mir-241(nDf51)* animals raised on seven different bacteria, *E. coli* (HB101, OP50, HT115), *Comamonas sp*.(DA1877), *P. aeruginosa* (PA14), *P. aeruginosa* (PA14 *gacA*), *S. enterica* (SL1344). Wild type animals in this experiment are the strain of VT1367 that carries an integrated *col-19* (an adult specific collagen) transcriptional reporter (*maIs105*) to assist the quantification of seam cell numbers. *maIs105* is also present in the genetic background of all the other stains used in heterochronic phenotype analysis. *E. coli* HB101 was used as control. In this and all subsequent scatter plots, the line in the middle is the mean value; error bars represents standard deviations (SDs). * $p < 0.05$, ** $p < 0.01$, *** $p < 0.001$, N.S. not significant, two-tailed *t*-test. ($n \geq 15$).

Table 2.2. Adult alae phenotypes of wild type and *let-7* family miRNA mutants cultured on different bacterial food sources

		Percentage of Animals with Different Adult Alae Phenotypes				
Genotype	**Treatment**	**Complete**	**Gapped**	**No alae**	**(n)**	**Test[1]**
wild type (VT1367)	*E. coli* HB101 (control)	100	0	0	30	
	E. coli OP50	100	0	0	15	N.S.
	E. coli HT115	100	0	0	15	N.S.
	Comamonas sp. DA1877	100	0	0	15	N.S.
	P. aeruginosa PA14	100	0	0	30	N.S.
	P. aeruginosa PA14 *gacA*	100	0	0	15	N.S.
	S. enterica SL1344	100	0	0	15	N.S.
mir-48 mir-241(nDf51)	*E. coli* HB101	40	60	0	42	
	E. coli OP50	28	72	0	39	N.S.
	E. coli HT115	60	40	0	40	N.S.
	Comamonas sp. DA1877	40	60	0	15	N.S.
	P. aeruginosa PA14	8	92	0	37	***
	P. aeruginosa PA14 *gacA*	30	70	0	21	N.S.
	S. enterica SL1344	27	73	0	15	N.S.
mir-48(n4097); mir-84(n4037)	*E. coli* HB101	100	0	0	31	
	P. aeruginosa PA14	93	7	0	30	N.S.
let-7(n2853)	*E. coli* HB101	0	77	23	30	
	P. aeruginosa PA14	0	42	58	26	**

[1] The chi-square test was used for comparison between *E. coli* HB101 (control) and other bacterial treatment for the same genotype. N.S. not significant, ** $p < 0.01$, *** $p < 0.001$.

family members (chiefly *let-7* and *mir-84*) may be decreased upon exposure to *P. aeruginosa*. To examine whether this decrease of *let-7* family miRNA activity is restricted to certain members of the family, we tested a series of other *let-7* family miRNA mutants for their developmental timing phenotypes upon *P. aeruginosa* treatment. Two other *let-7* family miRNA mutants showed enhancement in their heterochronic phenotypes on *P. aeruginosa*. Specifically, *mir-48(n4097); mir-84(n4037)* animals showed an enhancement in seam cell phenotype (Figure 2.2), while *let-7(n2853)* animals exhibited an adult alae phenotype enhancement (Table 2.2). These results suggest the activity of *mir-241* and *mir-48* could also be decreased by *P. aeruginosa* treatment. In conclusion, the activities of all four *let-7* family miRNAs appear to be decreased upon growth on *P. aeruginosa*.

2. Modulation of *let-7* family miRNA activity by the p38 MAPK pathway in response to *P. aeruginosa* infection.

The observed effects of bacterial diet on the developmental timing phenotypes of *let-7* family miRNA mutants could be caused by various properties of the bacterial food, such as nutritional quality and pathogenic toxicity. This is of particular interest in the case of *P. aeruginosa*, which can support *C. elegans* larval development as a sole food source, yet is also a pathogen capable of infecting *C. elegans*. To determine if the pathogenicity of *P. aeruginosa* is required for the modulation of heterochronic phenotypes elicited in *let-7* family miRNA mutants, we cultured *mir-48 mir-241(nDf51)* larvae on the *gacA* mutant of

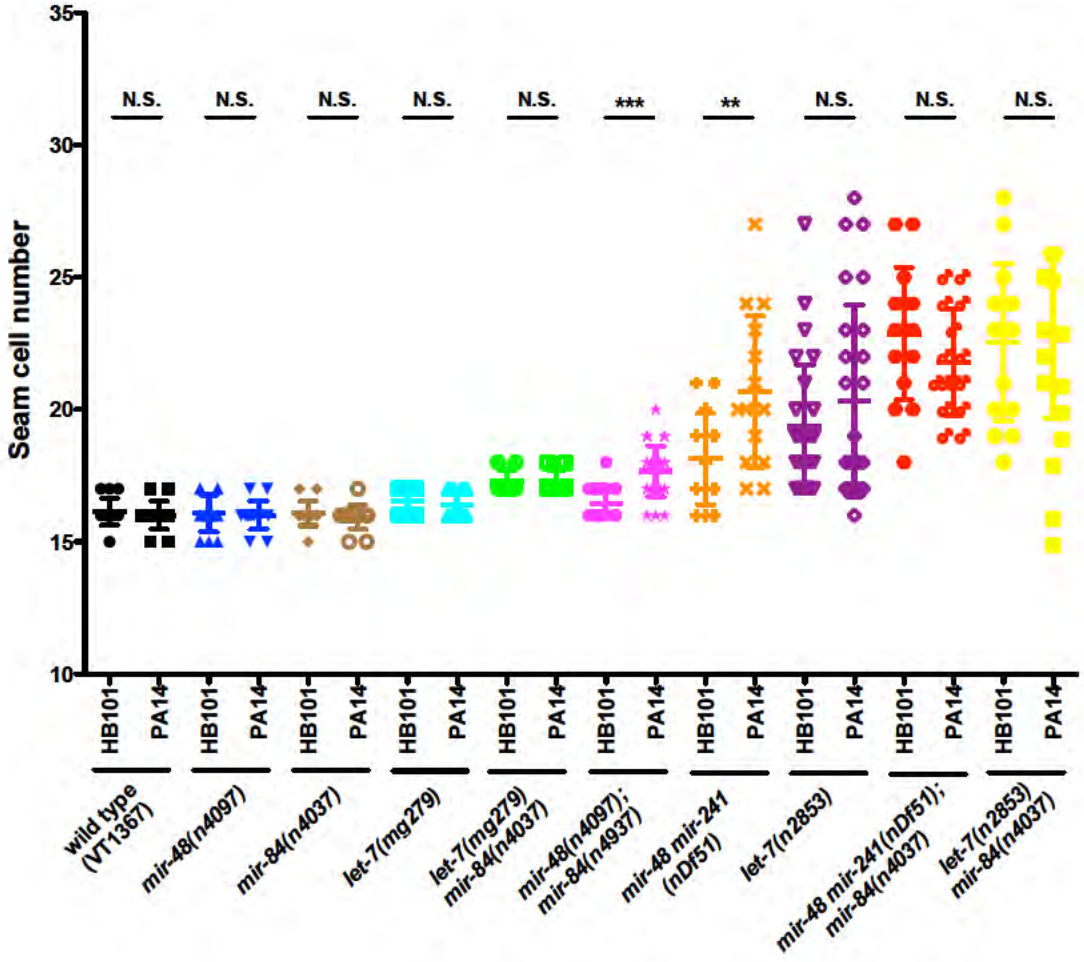

Figure 2.2. Effects of *P. aeruginosa* on seam cell phenotypes of *let-7* family miRNA mutants. Seam cell number of several *let-7* family miRNA mutants grown on *E. coli* HB101 and *P. aeruginosa* PA14. * $p < 0.05$, ** $p < 0.01$, *** $p < 0.001$, N.S. not significant, two-tailed *t*-test. $n \geq 15$.

P. aeruginosa PA14*. gacA* is an important regulator of the cell-density-dependent gene expression in *P. aeruginosa* and it is required for the production of exoenzymes and secondary metabolites (122). The pathogenicity of PA14 *gacA* strain is dramatically decreased compared to the wild type PA14 (123). We observed that the enhancement of *let-7* family miRNA mutant phenotypes was substantially reduced for larvae grown on PA14 *gacA*, compared to larvae grown on wild type PA14 (Figure 2.1B, Table 2.2). This suggests that the pathogenicity of *P. aeruginosa* is crucial for the modulation of *let-7* family miRNA activity.

Although *C. elegans* can develop throughout postembryonic development and into adult stage with *P. aeruginosa* as a sole food source, adults succumb to *P. aeruginosa* infection within a few days. A key pathway that enables larvae to survive on *P. aeruginosa* is the conserved p38 MAPK cascade (TIR-1-NSY-1-SEK-1-PMK-1) that initiates the innate immune response for antibacterial defenses (124, 125). We found that genetic removal of any p38 MAPK pathway component blocks the enhancement of the *let-7* family miRNA mutant phenotypes on *P. aeruginosa* (Figure 2.3A and C). We interpret this result to indicate that the p38 MAPK pathway activation in larvae grown on *P. aeruginosa* is required for the downregulation of *let-7* family miRNA activity. Furthermore, one of the major downstream transcription factors of the p38 MAPK pathway is ATF-7 (120). We therefore tested whether ATF-7 is involved in the modulation of *let-7* family miRNA mutant phenotypes. We observed that *mir-48 mir-241(nDf51)* animals homozygous for a null mutation of ATF-7 (*atf-7(qd22qd130)*) or for a

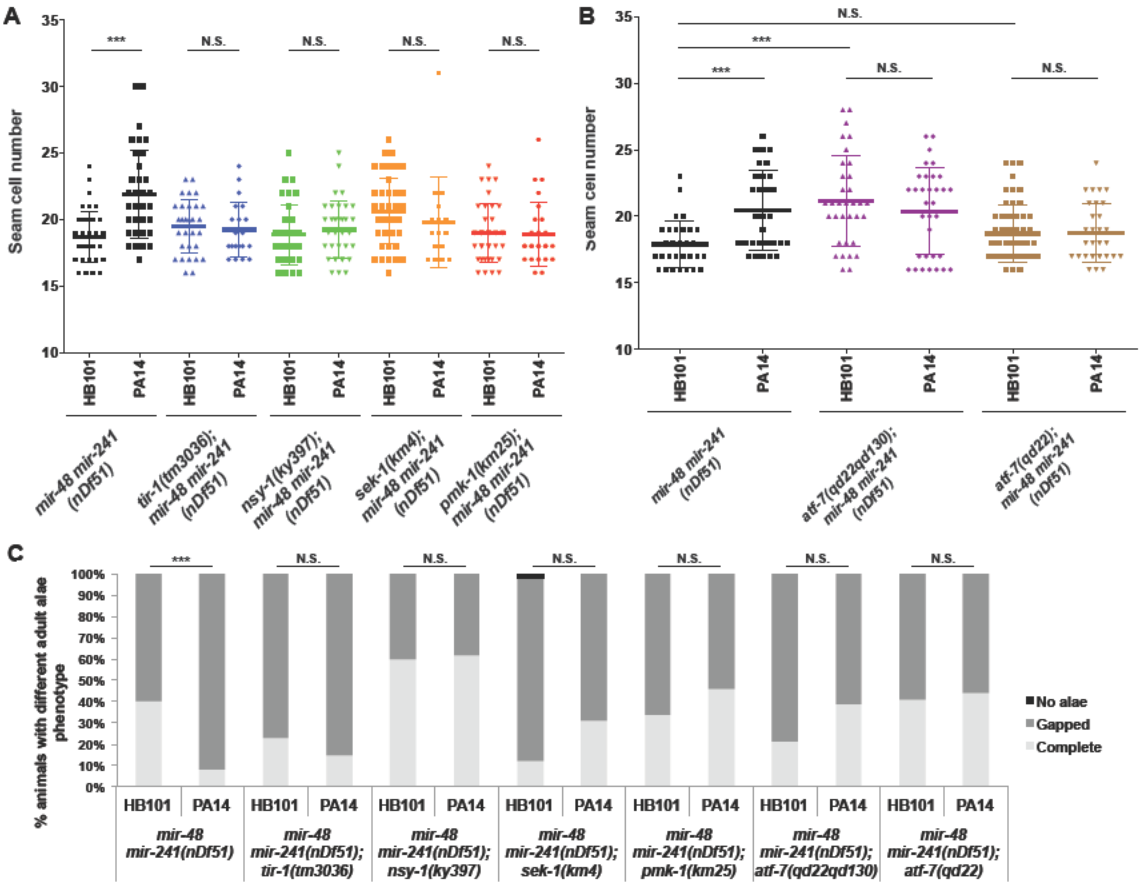

Figure 2.3 The p38 MAPK pathway and its downstream transcription factor *atf-7* are required for the suppression of *let-7* family miRNA activity on *P. aeruginosa*. (A) Deletion of any p38 MAPK pathway component blocks the enhancement of *mir-48 mir-241(nDf51)* animals' seam cell phenotype on *P. aeruginosa*. (B) Seam cell number of *atf-7(qd22qd130); mir-48 mir-241(nDf51)* and *atf-7(qd22); mir-48 mir-241(nDf51)* animals treated with either HB101 (control) or PA14. *qd22qd130* is a putative null allele of *atf-7*. *** $p < 0.001$, N.S. not significant, two-tailed *t*-test. ($n \geq 15$). (C) Adult alae phenotype for double mutants of *mir-48 mir-241(nDf51)* and p38 MAPK pathway components. *** $p < 0.001$, N.S. not significant, chi-square test. ($n > 15$).

phosphorylation-defective allele of ATF-7 (*atf-7(qd22)*) (120), did not exhibit enhanced heterochronic phenotypes on *P. aeruginosa* (Figure 2.3B and C). Interestingly, even for animals grown on *E coli*, loss of ATF-7 led to a significant enhancement of heterochronic phenotypes in *mir-48 mir-241(nDf51)* animals (Figure 2.3B). Therefore, ATF-7 seems to exhibit a positive regulation on *let-7* family miRNA activity when animals are on *E. coli*, and upon *P. aeruginosa* infection this regulation could be altered depending on the phosphorylation potential of ATF-7. Models for the effects of different *atf-7* alleles on *let-7* family miRNA activity are shown in Figure 2.4B-D.

3. Effects of *P. aeruginosa* infection and p38 signaling on *let-7* family miRNA gene expression

To investigate possible mechanisms for the apparent reduction of *let-7* family miRNA activity upon *P. aeruginosa* infection, we first measured the mature *let-7* family miRNA levels in animals exposed to *P. aeruginosa* throughout larval development to young adults. We observed an approximately two-fold decrease in *mir-241*, but no significant change in the levels of other *let-7* family miRNAs on *P. aeruginosa* (Figure 2.5). Because we did not observe any reduction of *mir-84* or *let-7* levels on *P. aeruginosa*, the enhanced heterochronic phenotypes of *mir-48 mir-241(nDf51)* animals cannot be simply accounted for by a reduction of *let-7* family miRNA levels in whole animals. It is possible that, upon *P. aeruginosa* infection, *let-7* family miRNAs are regulated through modulation of the potency of their action, without affecting their overall levels. However, because our miRNA

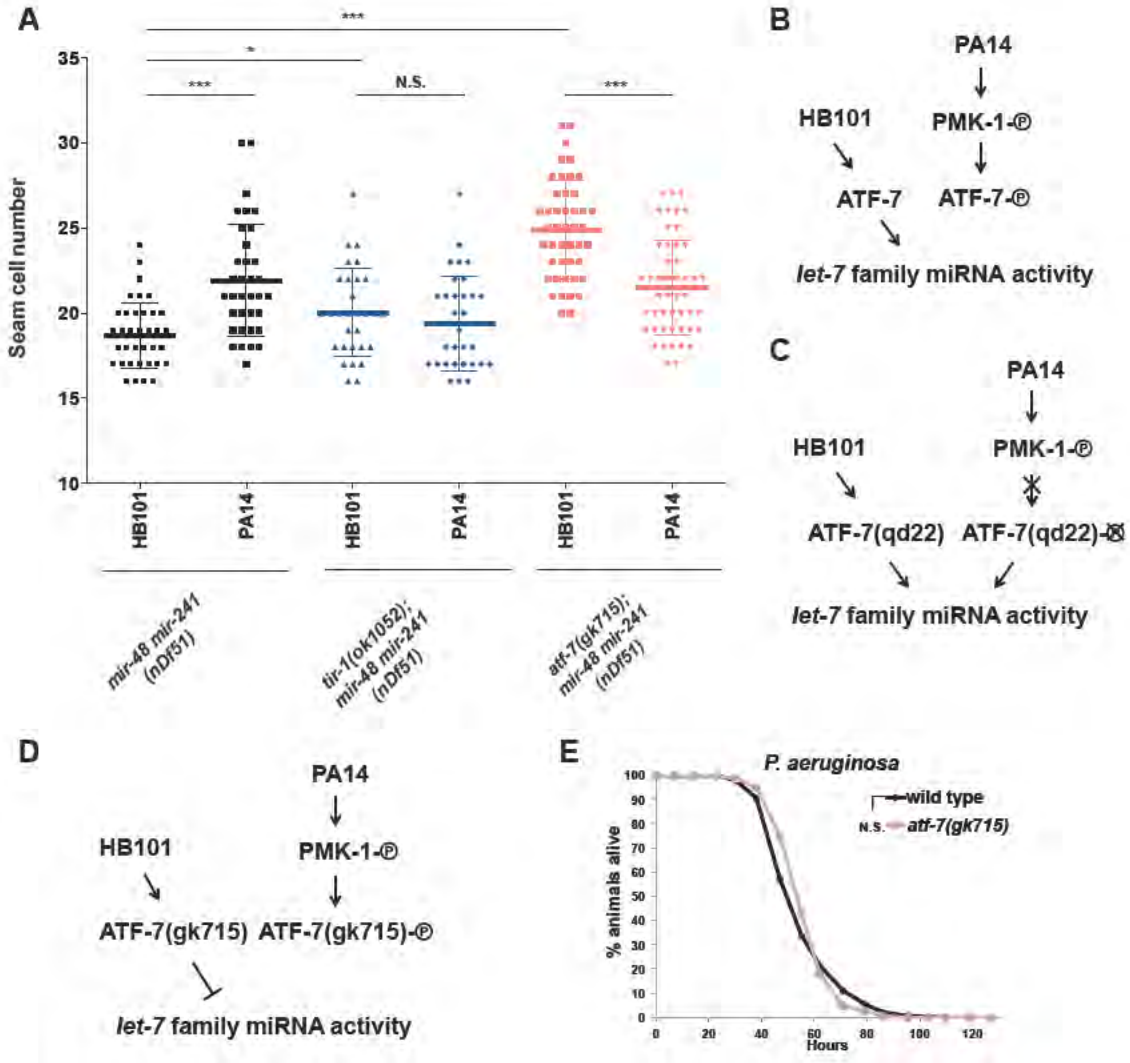
A
***
*
***
N.S.
***
Seam cell number
35
30
25
20
15
10
HB101
PA14
HB101
PA14
HB101
PA14
mir-48 mir-241 (nDf51)
tir-1(ok1052); mir-48 mir-241 (nDf51)
atf-7(gk715); mir-48 mir-241 (nDf51)
B
PA14
HB101
PMK-1-P
ATF-7
ATF-7-P
let-7 family miRNA activity
C
PA14
HB101
PMK-1-P
ATF-7(qd22)
ATF-7(qd22)-P
let-7 family miRNA activity
D
PA14
HB101
PMK-1-P
ATF-7(gk715)
ATF-7(gk715)-P
let-7 family miRNA activity
E
P. aeruginosa
wild type
N.S.
atf-7(gk715)
% animals alive
100
90
80
70
60
50
40
30
20
10
0
0
20
40
60
80
100
120
Hours

Figure 2.4. The effects of *atf-7* on *let-7* family miRNA activity. (A) Effects of *tir-1(ok1052)* and *atf-7(gk715)* alleles on the seam cell phenotype of *mir-48 mir-241(nDf51)* animals on *E. coli* HB101 and *P. aeruginosa* PA14. (B-D) Models for how different *atf-7* alleles affect *let-7* family miRNA activity. (B) On *E. coli* HB101, the unphosphorylated ATF-7 positively regulates *let-7* family miRNA activity. After being phosphorylated by PMK-1 upon *P. aeruginosa* PA14 infection, ATF-7 loses its positive regulation on *let-7* family miRNAs, which results in the heterochronic phenotype enhancement of *let-7* family miRNA mutants. (C) The regulation of ATF-7 on *let-7* family miRNAs depends on the phosphorylation potential of ATF-7. Therefore, the phosphorylation-inactive form of ATF-7 (*qd22* allele) does not affect *let-7* family mutant heterochronic phenotypes with or without *P. aeruginosa* infection. (D) ATF-7 (gk715) negatively regulates *let-7* family miRNA activity on HB101. Because *atf-7(gk715)* animals have no enhanced susceptibility to *P. aeruginosa* infection (E), the phosphorylation activity of ATF-7(gk715) is likely still intact. After infected with *P. aeruginosa*, ATF-7 is phosphorylated and this releases its negative regulation on *let-7* family miRNAs, therefore, the heterochronic phenotypes are suppressed compared to the ones from control HB101 group.

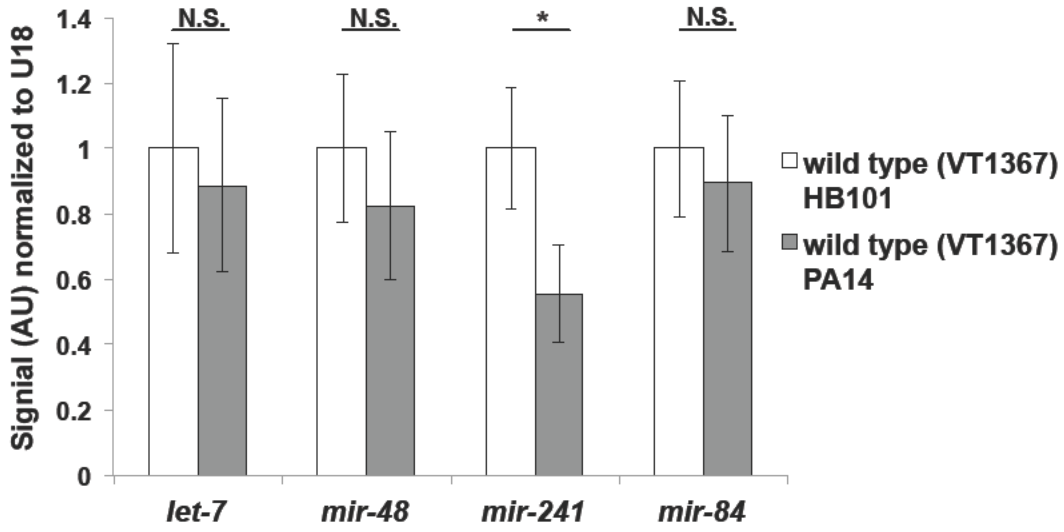

Figure 2.5 Mature *let-7* family miRNA levels upon *P. aeruginosa* infection. Total RNA from whole animals was used to perform Firefly microRNA assays. Animals (VT1367) were raised on either HB101 (control) or PA14 from synchronized L1 stage to young adult stage at 20°C. Error bars, SDs. * $p < 0.05$, N.S. not significant, two-tailed *t*-test. AU, arbitrary unit.

quantitation was performed on total RNA from whole worms, we would not necessarily detect tissue-specific changes in *let-7* family miRNA levels.

The results of our phenotypic analysis indicate that the activities and/or levels of *let-7* family miRNAs are modulated by the p38 MAPK pathway. Since the p38 MAPK pathway is known to ordinarily regulate gene expression transcriptionally, we examined whether p38 loss-of-function could affect the transcriptional activities of *let-7* family miRNA genes. For these studies, we employed transgenic worms carrying transcriptional reporters expressing GFP from *let-7* family miRNA gene promoters. We observed stage- and tissue-specific increases of GFP expression for *Pmir-48::GFP, Pmir-84::GFP*, and *Plet-7::GFP* in the *pmk-1* mutant compared to wild type animals (Figure 2.6). The developmental stages at which we detected differences in reporter activities between wild type and *pmk-1* mutant animals were L4 and young adult for *Pmir-48::GFP*; day-one adult for *Pmir-84::GFP*; L3, young adult and day-one adult for *Plet-7::GFP*. For *mir-48* and *mir-84*, the upregulation on these reporters by loss of *pmk-1* was observed in the hypodermis, suggesting a cell-autonomous effect of *pmk-1* signaling on *let-7* family miRNA transcription (Figure 2.6 A-B, D-E). Also, loss of *pmk-1* resulted in detectable *Pmir-84::GFP* expression in the hyp7 syncytium, compared to essentially undetected expression of *Pmir-84::GFP* in hyp7 for wild type animals. For the *let-7* transcriptional reporter, an increase of reporter activity in the absence of *pmk-1* was apparent in the intestine but not in the hypodermis (Figure 2.6C and F). These data suggest that the p38 MAPK

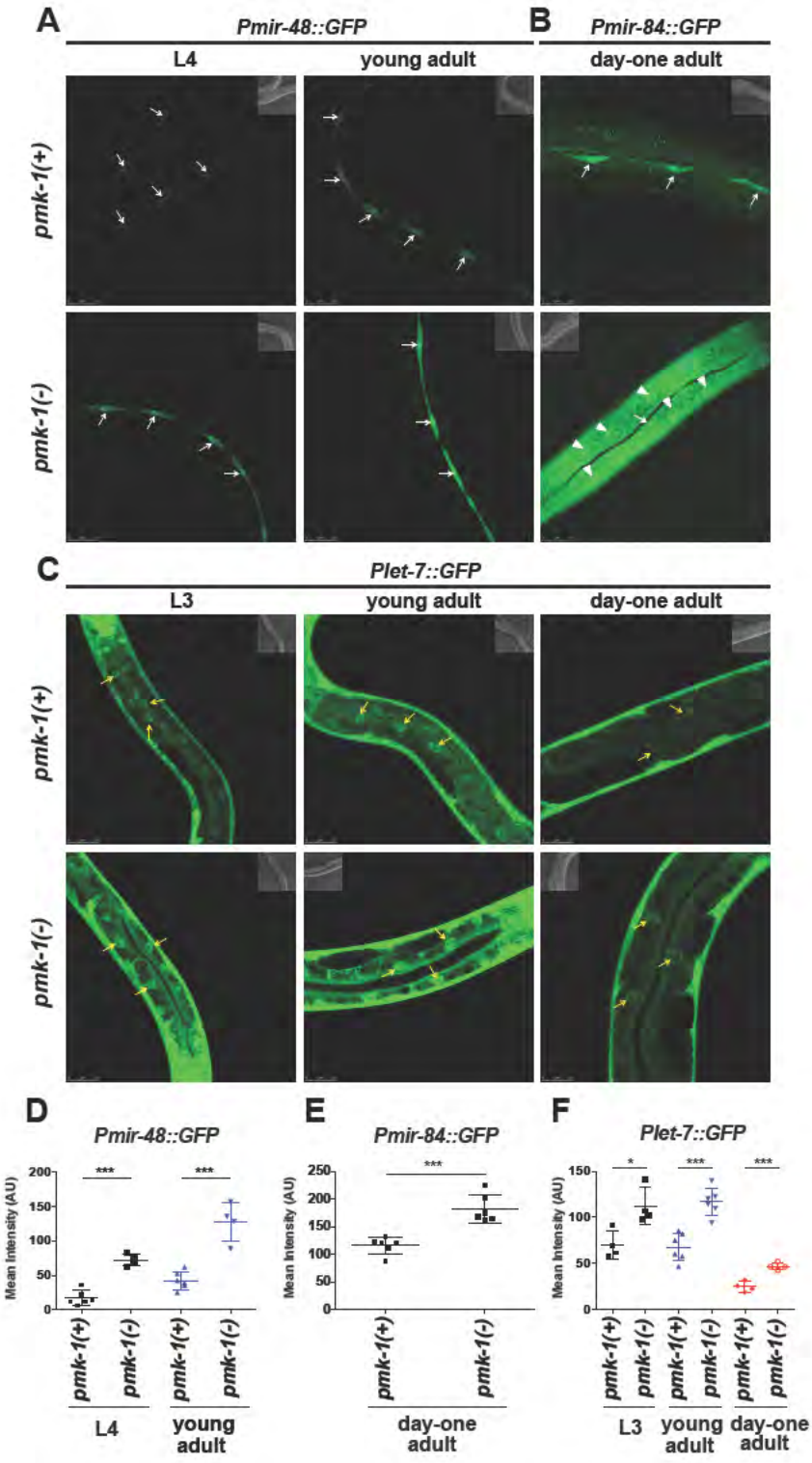
A
Pmir-48::GFP
L4
young adult
B
Pmir-84::GFP
day-one adult
pmk-1(+)
pmk-1(-)
C
Plet-7::GFP
L3
young adult
day-one adult
pmk-1(+)
pmk-1(-)
D
Pmir-48::GFP
Mean Intensity (AU)
***
***
pmk-1(+)
pmk-1(-)
pmk-1(+)
pmk-1(-)
L4
young adult
E
Pmir-84::GFP
Mean Intensity (AU)
***
pmk-1(+)
pmk-1(-)
day-one adult
F
Plet-7::GFP
Mean Intensity (AU)
*
***
***
pmk-1(+)
pmk-1(-)
pmk-1(+)
pmk-1(-)
pmk-1(+)
pmk-1(-)
L3
young adult
day-one adult

Figure 2.6 *pmk-1* regulates the transcriptional activity of *let-7* family miRNA genes*.* Confocal images showing that the transcriptional reporters of (A) *mir-48* (*maIs150*), (B) *mir-84* (*maIs138*) and (C) *let-7* (*maIs137*) in wild type (*pmk-1(+)*) and *pmk-1(km25)* (*pmk-1(-)*) animals. Animals were raised on *E. coli* HB101 at 20°C. Stages of the animals are as indicated. White arrows indicate seam cells; white arrowheads indicate hyp7 nuclei; yellow arrows point to representative intestine nuclei. (D), (E) and (F) The mean intensities of the intended tissues in (A-C). Error bars, SDs. * $p < 0.05$, *** $p < 0.001$, two-tailed *t*-test.

pathway negatively regulates the transcription of *let-7* family miRNAs and this regulation is tissue and stage specific.

4. *let-7* family miRNAs exhibit negative roles in resistance to *P. aeruginosa* infection.

Our results indicate that during larval development, worms actively downregulate their *let-7* family miRNA activity upon exposure to *P. aeruginosa*. Additionally, we found that *pmk-1* regulates the transcription of *let-7* in the intestine, a major tissue for pathogen resistance in *C. elegans* (126). Therefore, we hypothesized that this inhibition of *let-7* family miRNA activity may reflect a survival response to the presence of pathogen during larval development. Central to this hypothesis is the premise that *let-7* family miRNAs may negatively regulate pathogen resistance and hence the downregulation of their activity would promote survival. Accordingly, we examined the survival capacity of several *let-7* family miRNA mutants placed on *P. aeruginosa* beginning as L4 stage animals.

First, we measured the survival of animals homozygous for *let-7(mg279),* a weak loss-of-function allele (with very weak developmental timing phenotypes), and animals homozygous for *let-7(n2853)*, a stronger loss-of-function allele (with developmental timing phenotypes resembling the *let-7* null mutant) on *P. aeruginosa*. We observed that *let-7(mg279)* animals displayed a dramatic improvement in survival against *P. aeruginosa* infection compared to wild type (Figure 2.7A), whereas *let-7(n2853)* animals displayed the opposite, a decreased

survival on *P. aeruginosa* (Figure 2.7B). Interestingly, populations of double mutants *mir-48 mir-241(nDf51)* and *mir-48(n4097); mir-84(n4037)* animals exhibited bi-phasic survival curves (Figure 2.7A). Apparently, for each of these double mutants, a portion of the population dies faster than wild type while the remainder of the population survives longer than wild type on *P. aeruginosa*.

To confirm that the opposite pathogen survival phenotypes of distinct *let-7* mutants are attributable to the reduction of *let-7* gene activity, we tested the ability of a single-copy *let-7* transgene (*maIs380*), which fully rescues the developmental phenotypes of both *let-7* alleles (Figure 2.8A and B), to also rescue the characteristic survival phenotypes of *let-7(mg279)* and *let-7(n2853)* mutants. *maIs380* rescued the extended survival phenotype of *let-7(mg279)* animals (Figure 2.8C) and the shortened survival phenotype of *let-7(n2853)* animals on *P. aeruginosa* (Figure 2.8D). Interestingly, the *let-7* rescuing transgene also rescued the bi-phasic survival phenotype of *mir-48 mir-241(nDf51)* and *mir-48(n4097); mir-84(n4037)* animals (Figure 2.8E and F). These results support the conclusion that *let-7* family miRNAs function redundantly to regulate survival on *P. aeruginosa* and all the survival phenotypes of *let-7* family miRNA mutants on *P. aeruginosa* result from different degrees of *let-7* family miRNA loss-of-function.

To determine whether the complex survival phenotypes of *let-7* family miRNA mutants on *P. aeruginosa* could reflect underlying effects of *let-7* family miRNAs on overall fitness of the animals (regardless of diet), we examined the

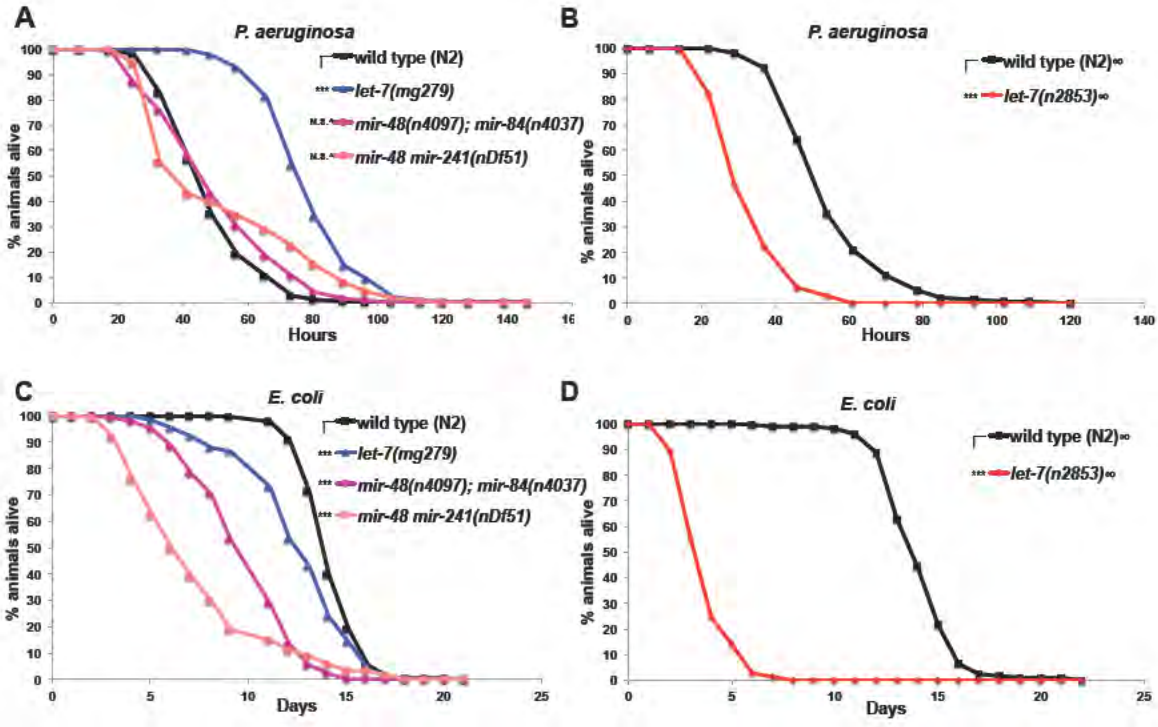
A
P. aeruginosa
wild type (N2)
*** let-7(mg279)
N.S. mir-48(n4097); mir-84(n4037)
N.S. mir-48 mir-241(nDf51)
% animals alive
Hours
B
P. aeruginosa
wild type (N2)∞
*** let-7(n2853)∞
% animals alive
Hours
C
E. coli
wild type (N2)
*** let-7(mg279)
*** mir-48(n4097); mir-84(n4037)
*** mir-48 mir-241(nDf51)
% animals alive
Days
D
E. coli
wild type (N2)∞
*** let-7(n2853)∞
% animals alive
Days

Figure 2.7 *let-7* family miRNAs regulate pathogen resistance against *P. aeruginosa* and lifespan on *E. coli.* (A) Survival of wild type (N2), *let-7(mg279)*, *mir-48(n4097); mir-48(n4037)* and *mir-48 mir-241(nDf51)* animals on *P. aeruginosa*. (B) Survival of wild type (N2) and *let-7(n2853)* animals on *P. aeruginosa*. (C) Lifespan of wild type (N2), *let-7(mg279)*, *mir-48(n4097); mir-48(n4037)* and *mir-48 mir-241(nDf51)* animals on *E. coli* HB101. (D) Lifespan of wild type (N2) and *let-7(n2853)* animals on *E. coli* HB101. Animals were usually raised at 20°C prior to being transferred to *P. aeruginosa* killing assay and lifespan assay at 25°C, except for experiments with *let-7(n2853)* (noted with ∞ next to the strain names) in which strains were raised at 15°C (to reduce the number of bursting adults) prior to being transferred to 25°C for the *P. aeruginosa* killing assay and lifespan assay. *** p< 0.001, N.S. not significant, log-rank test. For the *let-7* family miRNA mutants that exhibit different survival kinetics on *P. aeruginosa* compared to wild type, Fisher's exact tests were applied (data in Table 2.3). ^ indicates a statistically significant outcome in Fisher's exact test.

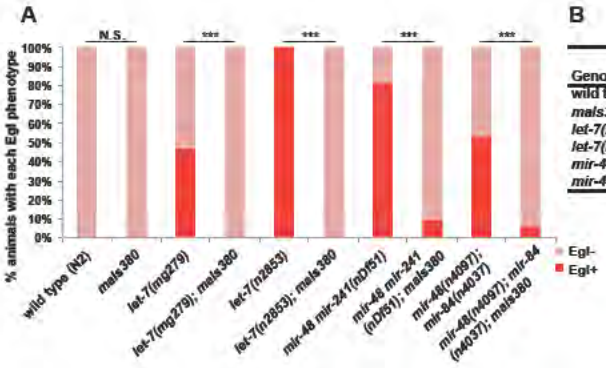

B

Genotype	Percentage of Animals with Different Adult Alae				
	Complete	Gapped	No alae	(n)	
wild type (N2)	100	0	0	15	
mals380	100	0	0	30	N.S.
let-7(n2853)	0	44	56	25	
let-7(n2853); mals380	100	0	0	30	***
mir-48 mir-241(nDf51)	33	67	0	30	
mir-48 mir-241(nDf51); mals380	27	73	0	30	N.S.

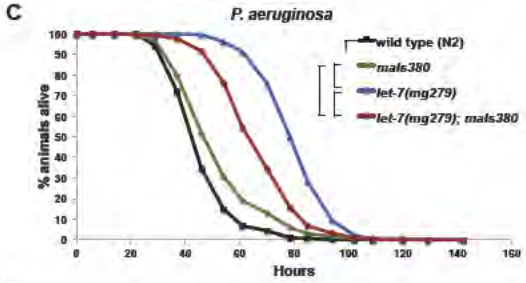

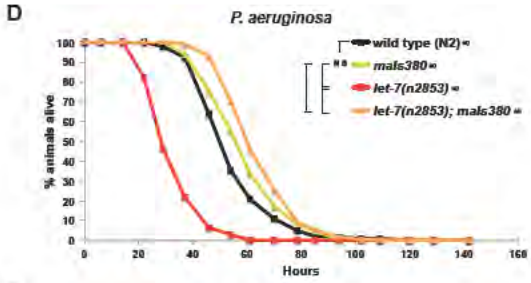

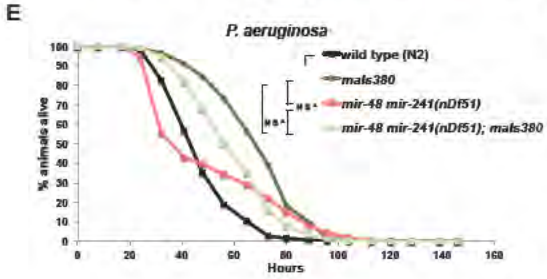

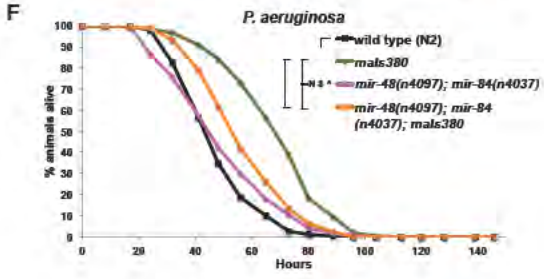

Figure 2.8 The effects of a *let-7*-rescuing transgene on the phenotypes of *let-7* family miRNA mutants. (A) Egg laying defective phenotype of *let-7* family miRNA mutants in combination with the *let-7* rescuing transgene, *maIs380*. Egl-, wild type for egg laying, Egl+, egg laying defective. *** p< 0.001, N.S. not significant, chi-square test, for comparison in the same genetic background with and without transgenes, n ≥ 100 (except *let-7(n2853)*, n = 36). Interestingly, the *let-7* transgene rescued the egg laying defective phenotype of *mir-48 mir-241(nDf51)* and *mir-48(n4097); mir-84(n4037)* animals, suggesting a redundancy within the family in the regulation of vulva development. (B) Adult alae phenotype of *let-7* family miRNA mutants with the transgene *maIs380*. Since 100% of *let-7(mg279)* and *mir-48(n4097); mir-84(n4037)* animals have complete adult alae, this phenotype was not used to confirm the transgene's rescue of these strains. *** p< 0.001, N.S. not significant, chi-square test, for comparison in the same genetic background with and without transgene. The *maIs380 let-7*-expressing transgene did not rescue the adult alae phenotype of *mir-48 mir-241(nDf51)* animals, indicating that although *let-7* seems to function together with the other *let-7* family miRNAs in several processes, the roles of *let-7* family miRNAs in regulating developmental timing are more distinct. Survival phenotypes of *let-7(mg279)* (C), *let-7(n2853)* (D), *mir-48 mir-241(nDf51)* (E) and *mir-48(n4097); mir-84(n4037)* (F) animals with *let-7* rescuing transgenes *maIs380* on *P. aeruginosa*. The *maIs380* strain used in (E and F) was not backcrossed. *unc-119(ed3)* mutation and/or other possible mutations were suspected to cause the further enhanced survival than the same transgene in (C and D). * p < 0.05, ** p < 0.01, *** p< 0.001, N.S. not significant, log-rank test. Fisher's exact test has also been performed for *mir-48 mir-241(nDf51)* and *mir-48(n4097); mir-84(n4037)* groups. ^ indicates a statistically significant outcome in Fisher's exact test (Table 2.3).

Table 2.3. Fisher's exact test results for comparing survival curves of various *C. elegans* strains on *P. aeruginosa*

Comparison	Fisher's Exact Test				Log-Rank Test
	P-value at 25%	P-value at 50%	P-value at 75%	P-value at 90%	P-value
wild type (N2) *vs. mals380*	9.10E-09	1.20E-12	1.20E-11	3.60E-05	< 1.0E-10
wild type (N2) *vs. mir-48 mir-241(nDf51)*	0.0001	0.0657	0.0011	0.0003	0.0509
wild type (N2) *vs. mir-48 mir-241(nDf51); mals380*	0.0001	2.60E-06	3.30E-05	0.0008	2.30E-08
mals380 vs. mir-48 mir-241(nDf51)	9.90E-13	0.0002	0.7037	1	0.0011
mals380 vs. mir-48 mir-241(nDf51); mals380	0.0013	0.0044	0.0568	0.1338	0.0004
mir-48 mir-241(nDf51) vs. mir-48 mir-241(nDf51); mals380	2.20E-11	0.0218	0.3676	0.2134	0.2488
wild type (N2) *vs. mir-48(n4097); mir-84(n4037)*	0.7753	0.1947	0.0486	0.0185	0.0752
wild type (N2) *vs. mir-48(n4097); mir-84(n4037); mals380*	5.00E-04	0.0001	0.0052	0.0055	7.50E-06
mals380 vs. mir-48(n4097); mir-84(n4037)	9.70E-08	4.80E-08	3.70E-06	0.0331	< 1.0E-10
mals380 vs. mir-48(n4097); mir-84(n4037); mals380	0.0007	2.60E-05	0.0153	0.0582	1.20E-06
mir-48(n4097); mir-84(n4037) vs. mir-48(n4097); mir-84(n4037); mals380	0.0022	0.1079	0.24	0.7674	0.0475

longevity of these mutants on *E. coli* HB101. All the *let-7* family miRNA mutants we tested displayed a degree of shortened lifespan compared to wild type animals (Figure 2.7C and D), which indicates that *let-7* family miRNAs function positively to regulate longevity in *C. elegans*. Therefore, the decreased survival phenotype of the stronger loss-of-function mutant *let-7(n2853)* animals on *P. aeruginosa* could be simply due to reduced longevity of these animals. However, importantly, the weak loss-of-function mutant *let-7(mg279)* animals exhibit an improved survival against *P. aeruginosa* infection despite the fact that these animals have a shortened lifespan. This suggests that *let-7* family miRNAs negatively modulate pathogen resistance, while also positively regulating longevity, such that a mild reduction in *let-7* family miRNA activity (by *let-7(mg279)*) promotes survival on *P. aeruginosa* because the longevity of these animals is not severely compromised. With regard to the bi-phasic survival phenotype of *mir-48 mir-241(nDf51)* and *mir-48(n4097); mir-84(n4037)* animals on *P. aeruginosa*, we propose that there are variations in the extent of reduced *let-7* family miRNA activity within the population in these mutants, such that animals with mildly reduced *let-7* family miRNA activity exhibit enhanced pathogen resistance while others with greater reduced *let-7* family miRNA activity show decreased survival on *P. aeruginosa* possibly due to a reduced longevity in general.

In summary, *let-7* family miRNAs exhibit negative regulation on animals' resistance to *P. aeruginosa* infection, as evidenced by the increased survival on

P. aeruginosa for *let-7(mg279)* animals. On the other hand, some *let-7* family miRNA mutants exhibited decreased survival on *P. aeruginosa*, which probably results from an epistatic function of *let-7* family miRNAs in promoting longevity.

5. Downstream heterochronic genes may mediate the enhanced survival of *let-7(mg279)* animals on *P. aeruginosa*.

To further investigate the mechanism by which *let-7* family miRNAs negatively regulate pathogen resistance, we focused on understanding the enhanced survival phenotype of *let-7(mg279)* animals. This emphasis was for several reasons. First, *let-7* family miRNAs contribute redundantly to survival on *P. aeruginosa*. Hence *let-7* can serve as a proxy for the other *let-7* family miRNA genes in our genetic analyses. Additionally, *let-7(mg279)* animals exhibit a striking survival phenotype on *P. aeruginosa* that we expected would be more tractable for genetic analysis than the complex survival phenotypes of the other *let-7* family miRNA mutants. Lastly, among the *let-7* family mutants tested here, *let-7(mg279)* animals exhibited the least reduced lifespan on *E. coli*. Therefore, employing *let-7(mg279)* animals to explore the mechanism of *let-7* family miRNAs in pathogen resistance could minimize potentially confounding effects of lifespan in our analysis.

let-7 family miRNAs regulate a set of specific target gene mRNAs during larval development to control developmental timing. For *let-7*, the most prominent targets are *lin-41* and *hbl-1* (81, 82, 107). To determine if *lin-41* and *hbl-1* are downstream of *let-7* in the regulation of pathogen resistance, we tested the

survival of *let-7(mg279)* animals on *P. aeruginosa* in the presence of *lin-41* or *hbl-1* loss-of-function mutations. Interestingly, animals with partial loss of function for *lin-41* exhibited a decreased survival upon *P. aeruginosa* infection, and *lin-41* also suppressed the enhanced survival phenotype of *let-7(mg279)* animals (Figure 2.9A). These findings suggest that aside from its developmental timing role downstream of *let-7*, *lin-41* is also possible to be one of the targets of *let-7* for the regulation of pathogen resistance.

hbl-1(mg285) also suppressed the enhanced survival phenotype of *let-7(mg279)* on *P. aeruginosa*, but unlike *lin-41(ma104)*, the *hbl-1(mg285)* mutation alone did not cause any obvious survival phenotype (Figure 2.9B). Because *hbl-1(mg285)* is only a partial loss-of-function mutation, epistasis cannot be interpreted unequivocally, but these results are consistent with both *hbl-1* and *lin-41* functioning downstream of *let-7* for pathogen sensitivity. We note that *hbl-1* has been shown to negatively regulate the transcription of *let-7* (127). Therefore, the suppression of *let-7(mg279)* enhanced survival phenotype by *hbl-1(mg285)* could reflect a derepression of *let-7* gene transcription.

In addition, we examined the longevity on *E. coli* HB101 of *lin-41(ma104)* and *hbl-1(mg285)* animals along with animals mutant for *lin-41(ma104)* or *hbl-1(mg285)* in combination with *let-7(mg279)* (Figure 2.9C and D). The results suggest that *lin-41* and *hbl-1* positively regulate lifespan on *E. coli*. However, since *hbl-1(mg285)* animals exhibit similar survival on *P. aeruginosa* compared to wild type animals (Figure 2.9B), the suppression of *hbl-1(mg285)* on

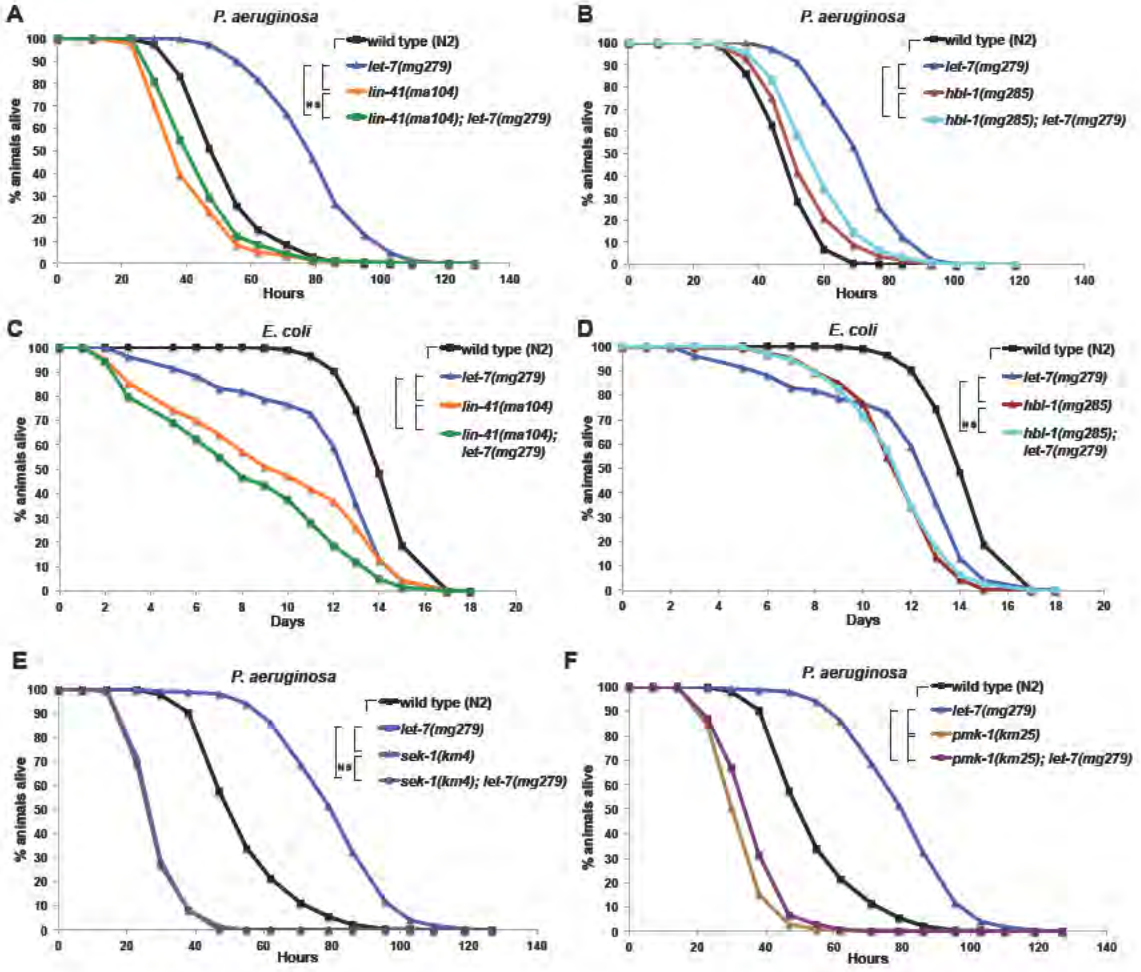

Figure 2.9 *lin-41*, *hbl-1* and p38 MAPK pathway modulate the enhanced pathogen resistance of *let-7(mg279)* animals. (A) *lin-41(ma104)* and (B) *hbl-1(mg285)* suppress the enhanced survival phenotype of *let-7(mg279)* animals on PA14. (C) Lifespan of strains used in (A) on *E. coli* HB101. (D) Lifespan of strains used in (B) on *E. coli* HB101. *sek-1* (E) and *pmk-1* (F) are also required for the enhanced survival phenotype of *let-7(mg279)* animals on PA14. * $p < 0.05$, ** $p < 0.01$, *** $p < 0.001$, N.S. not significant, log-rank test.

let-7(mg279) animals' enhanced survival phenotype on *P. aeruginosa* is likely caused by a role of *hbl-1* in pathogen resistance, rather than longevity. On the other hand, the suppression of *let-7(mg279)* animals' survival phenotype on *P. aeruginosa* by *lin-41* could be contributed in part by the role of *lin-41* in animal's longevity and in part by a role in pathogen resistance.

6. The p38 MAPK pathway is required for the prolonged survival phenotype of *let-7(mg279)* animals on *P. aeruginosa*.

In addition to targeting *lin-41* and *hbl-1*, *let-7* could also (directly or indirectly) regulate genes in the innate immune response pathways in order to negatively regulate pathogen resistance. Interestingly, in the p38 MAPK pathway, *tir-1*, *nsy-1* and *sek-1* are all predicted targets of *let-7* family miRNAs according to mirWIP (128). Therefore, we hypothesized that *let-7* could function upstream of the p38 MAPK pathway to regulate animal's survival on *P. aeruginosa*. Accordingly, we examined the survival of animals doubly mutant for *let-7(mg279)* and loss-of-function mutations in p38 MAPK pathway components. We observed that loss of any p38 MAPK pathway component could suppress the enhanced survival phenotype of *let-7(mg279)* animals (Figure 2.9E and F, Figure 2.10). Also, previous studies indicate that the p38 MAPK pathway does not affect animal's longevity (124, 129). Therefore, these results indicates that *let-7(mg279)* animals' enhanced pathogen resistance phenotype requires the p38 MAPK pathway.

To examine whether *let-7* may regulate factors upstream of p38 in the

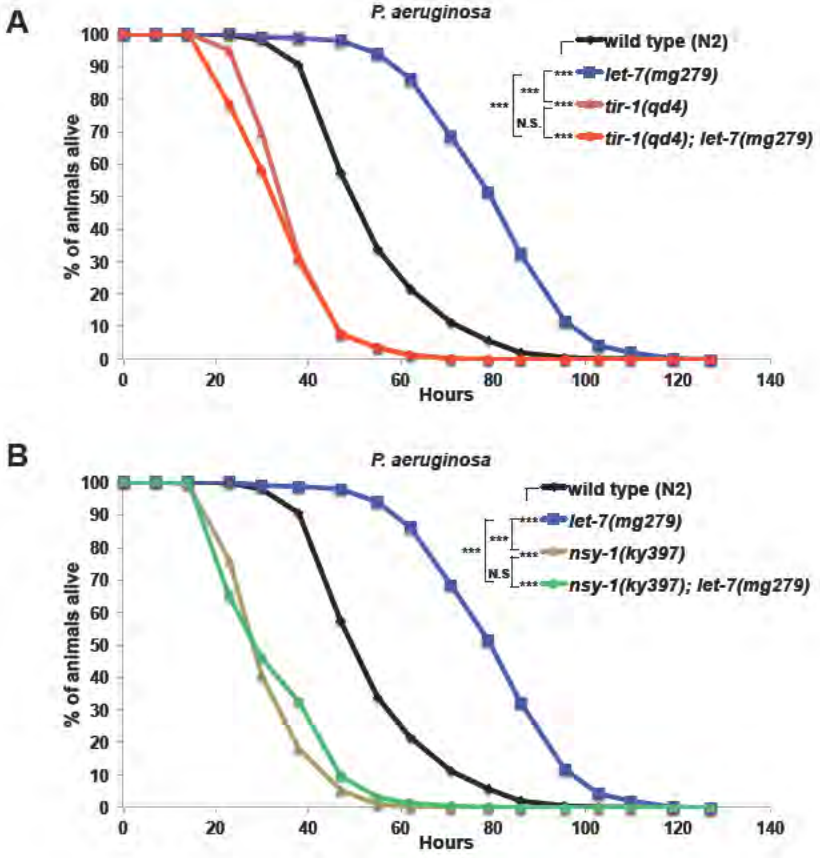

Figure 2.10 Survival on PA14 of adults doubly-mutant for *let-7(mg279)* and *tir-1(qd4)* (A) or *nsy-1(ky379)* (B). *** p< 0.001, N.S. not significant, log-rank test.

MAPK pathway, we tested for an elevated level of phosphorylated p38 in protein extracts of *let-7(mg279)* animals compared to that of wild type. These experiments did not conclusively reveal an impact of *let-7* on p38 phosphorylation (Figure 2.11). However, since these assays for phosphorylated p38 were performed on extracts of whole animals, it is possible that *let-7* may function upstream of the p38 MAPK pathway in a tissue specific manner. Although genetically the p38 MAPK pathway is downstream of *let-7* in regulating animal's survival on *P. aeruginosa*, we cannot rule out the possibility that it might function in parallel with *lin-41* and *hbl-1* for the prolonged survival of *let-7(mg279)* animals on *P. aeruginosa*.

7. *let-7(mg279)* animals exhibit reduced accumulation of outer membrane vesicles in the intestine during *P. aeruginosa* infection.

To further explore the basis for why *let-7(mg279)* animals survive better than wild type on *P. aeruginosa*, we examined the intestines of infected worms using transmission electron microscopy (TEM). At 8 or 24 hours after infection, we did not observe any difference in the intestinal cytopathology between wild type and *let-7(mg279)* animals (Figure 2.12). However, after 48 hours infection, we observed a significant reduction of outer membrane vesicles (OMV) in the intestinal lumen of *let-7(mg279)* animals compared to that of wild type (Figure 2.13). OMVs are secreted by *P. aeruginosa* and known to function as a virulence factor and toxin delivery platform (117). These results suggest that the prolonged

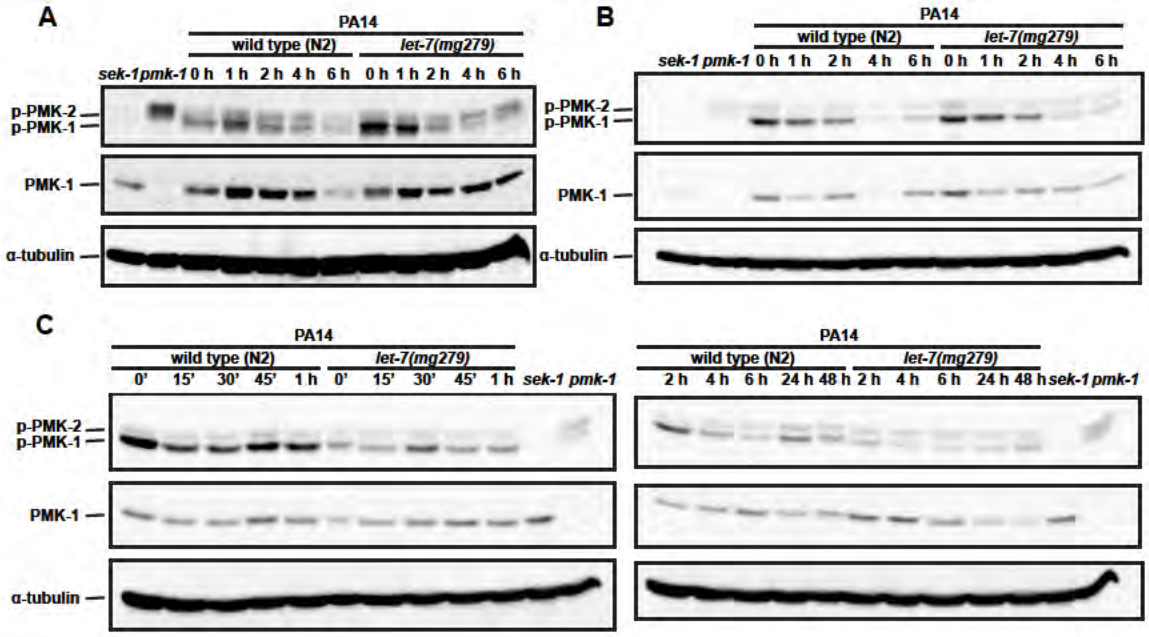

Figure 2.11. Western blots of whole animal lysates of wild type, *let-7(mg279)*, *sek-1(km4)* and *pmk-1(km25)* animals. All the animals were grown on HB101 before treated with PA14. *sek-1(km4)* and *pmk-1(km25)* animals were collected at the L4 stage. L4 stage (0 h) wild type and *let-7(mg279)* animals were treated with PA14 and collected at the time points accordingly. (A-C) three independent experiments.

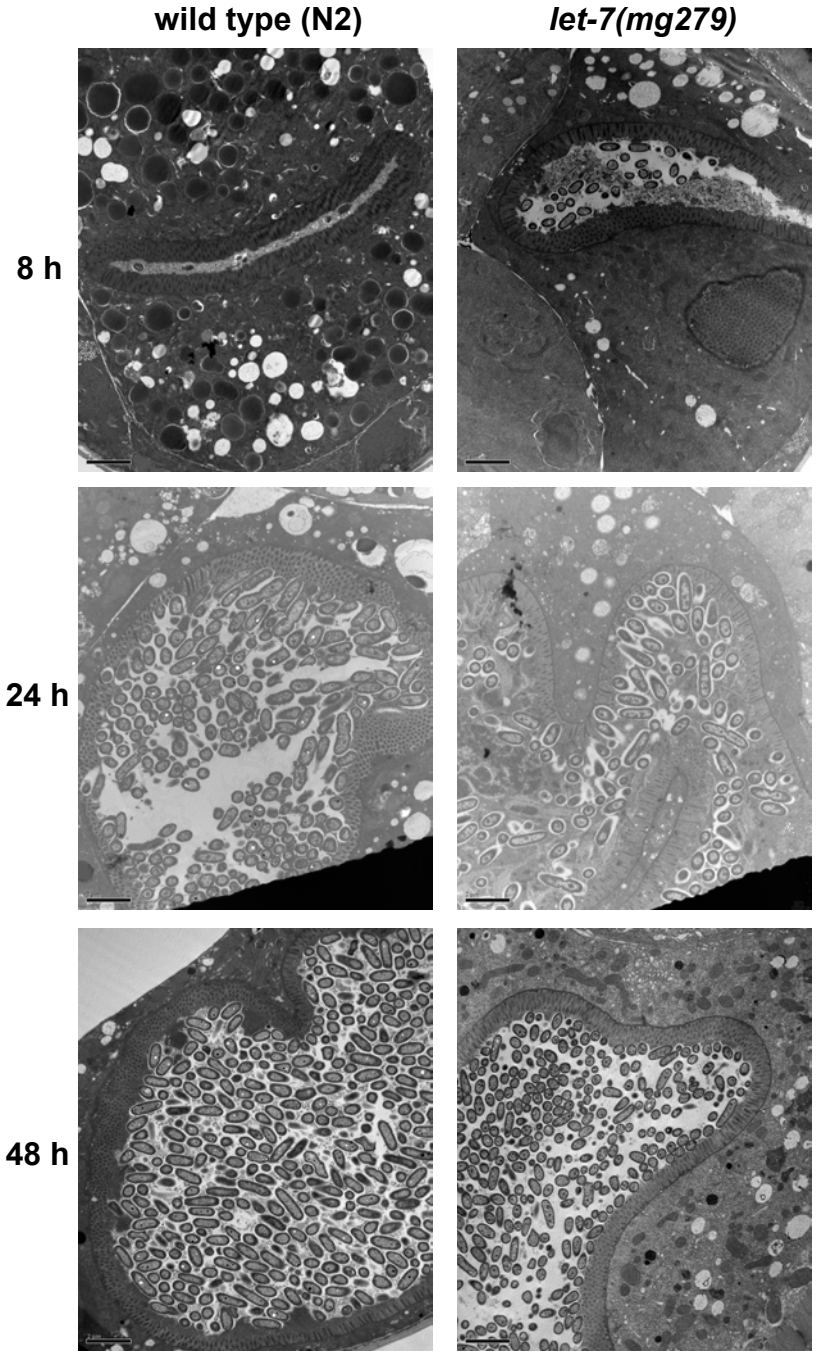

Figure 2.12 TEM images of wild type (N2) and *let-7(mg279)* animals upon *P. aeruginosa* infection for 8h, 24h and 48h. Scale bar, 2µm.

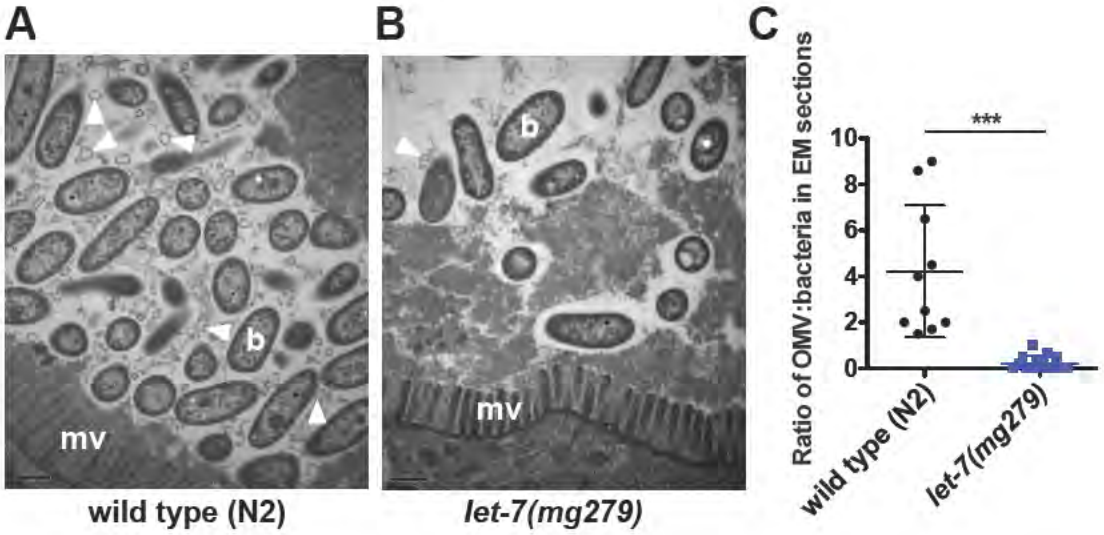

Figure 2.13 *let-7(mg279)* animals exhibit reduced abundance of bacterial outer membrane vesicles in their intestinal lumen during *P. aeruginosa* infection. Transmission electron micrographs of transversal midbody sections of (A) wild type (N2) animal and (B) *let-7(mg279)* animal infected with *P. aeruginosa* PA14 for 48 hours. b, bacterial cell; mv, microvilli; arrowheads point to representative outer membrane vesicles (OMVs); scale bar, 0.5μm (C) Ratio of OMVs to bacteria in electron micrographs. Randomly sample the electron micrographs with 1μm square five times and count the number of OMVs and bacteria within the square. Two animals for both wild type and *let-7(mg279)* groups. Error bars, SDs. *** $p < 0.001$, two-tailed *t*-test.

survival of *let-7(mg279)* animals on *P. aeruginosa* reflects an enhanced counter-virulence activity compared to that in wild type animals.

II. E. Discussion

Animals are challenged by diverse physiological and environmental stresses during development, but nevertheless execute temporal and spatial patterns of developmental events with remarkable robustness. *let-7* family miRNAs function in the heterochronic gene pathway to regulate the specification and execution of stage-specific cell fates during *C. elegans* larval development (5, 74). Here we report evidence that the activity of *let-7* family miRNAs is regulated by the p38 innate immune response pathway during growth on the bacterial pathogen *P. aeruginosa* (Figure 2.14A). Furthermore, we show that *let-7* family miRNAs and several other heterochronic genes also function in the modulation of animal's resistance against *P. aeruginosa* infection (Figure 2.14B). Our findings uncover fundamental connections between the heterochronic gene pathway and innate immune response pathway, and suggest that these connections could serve to optimize the coordination of temporal cell fate specification and antibacterial responses in the developing larvae.

An important implication of our findings is that the collective function of *let-7* family miRNAs provides robustness to the specification of temporal fates in wild type *C. elegans* larvae, especially when they are challenged by pathogenic bacteria. This conclusion is based on a few interesting findings in our study. First,

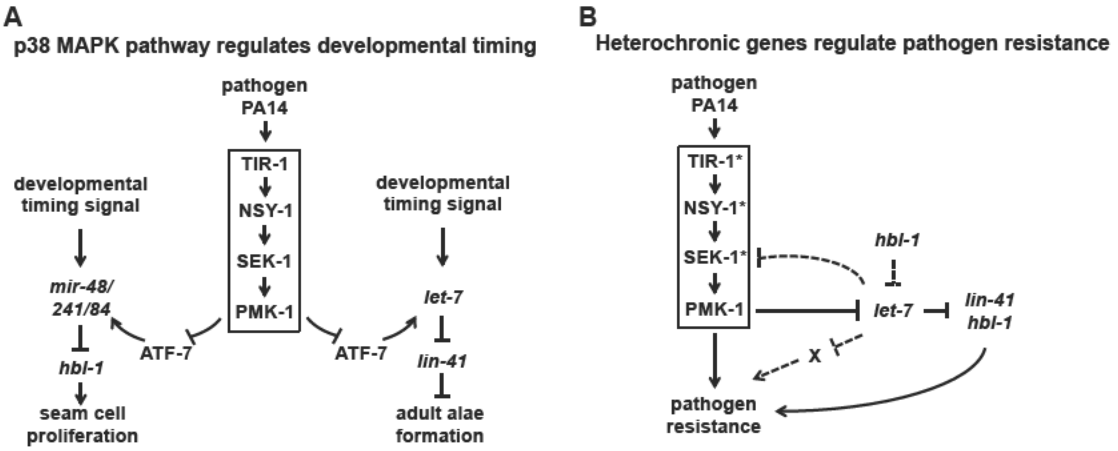

Figure 2.14 Model. (A) A model for the regulation of developmental timing by *P. aeruginosa* and the p38 MAPK pathway in *C. elegans*. (B) A model for the roles of heterochronic genes in pathogen resistance on *P. aeruginosa*. * indicates the predicated targets of *let-7* family miRNAs in the p38 MAPK pathway. X represents other possible pathways that are regulated by *let-7* to promote pathogen resistance on *P. aeruginosa*. The dotted line indicates proposed regulatory interactions not yet tested experimentally.

growth on pathogen affects temporal seam cell fate phenotypes only in sensitized genetic backgrounds where the full complement of *let-7* family miRNAs is compromised by mutation. For wild type, and for most of the single mutants and for *let-7(mg279) mir-84(n4037)* animals, developmental timing phenotypes were not affected by *P. aeruginosa* infection (Figure 2.2), which indicates that the downregulation of *let-7* family miRNA activity caused by *P. aeruginosa* is tolerated in these animals (without compromising temporal cell fate specification) due to the genetic redundancy of *let-7* family miRNAs. Moreover, we also observed an increase in the variation of seam cell number in *let-7* family miRNA mutants as the activity of this miRNA family declines, and the variation in seam cell number is enhanced by *P. aeruginosa* infection in those same *let-7* family miRNA mutants where we observed *P. aeruginosa* induced heterochronic phenotype enhancement (Figure 2.15). This variation of seam cell number could reflect noisy target gene expression caused by reduction of *let-7* family miRNA activity and could also represent a breakdown in the robustness of seam cell fate determination. This further supports the idea that *let-7* family miRNAs function to protect the robustness in the temporal patterns of seam cell program, especially in face of *P. aeruginosa* infection.

We observed that certain other bacterial food sources, besides *P. aeruginosa*, can also modulate the seam cell phenotype in the *let-7* family miRNA sensitized genetic background, albeit with less potency than *P. aeruginosa* (Figure 2.1B). One surprising result is that *E. coli* OP50, a routine

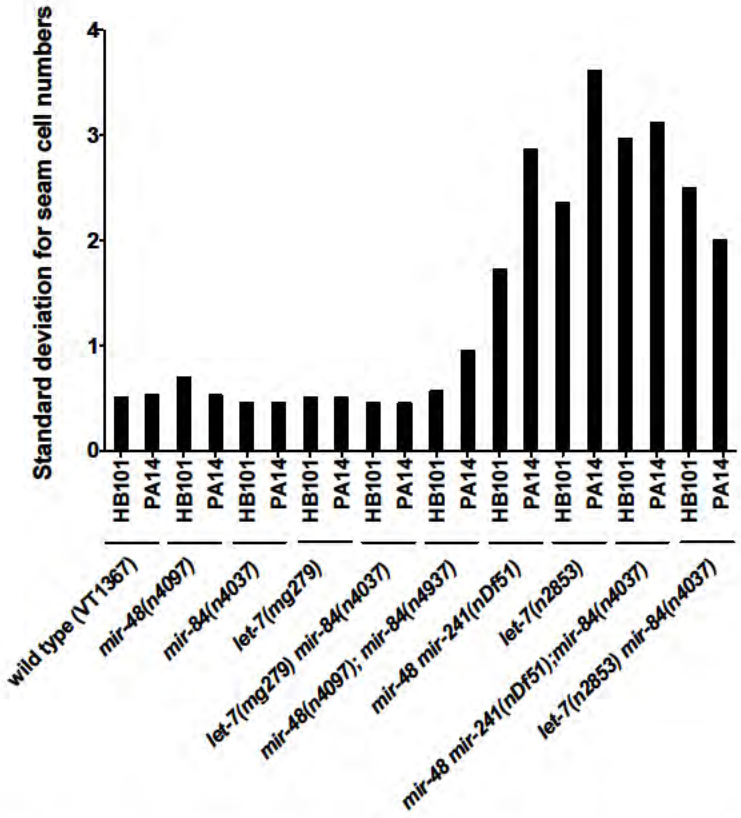

Figure 2.15 The variation in seam cell number of *let-7* family miRNA mutants is enhanced by *P. aeruginosa* infection. Standard deviation for Seam cell number of several *let-7* family miRNA mutants grown on *E. coli* HB101 and *P. aeruginosa* PA14.

food source for most laboratories, also enhances the seam cell numbers of *mir-48 mir-241(nDf51)* animals (although this enhancement is very mild compared to the effects of *P. aeruginosa*, and there is no change in adult alae phenotype). Interestingly, *pmk-1(km25)* partially suppresses the enhanced heterochronic phenotypes of *mir-48 mir-241(nDf51)* animals on OP50 (Figure 2.16), consistent with previous findings which suggested that OP50 could be slightly pathogenic to worms (130). Therefore, the enhanced seam cell phenotype of the *let-7* family miRNA mutant on OP50 could be partially due to the slight pathogenicity of the bacteria. However, other properties of OP50 could contribute to the phenotype as well because *pmk-1(km25)* did not fully suppress all the enhanced heterochronic phenotype of *mir-48 mir-241(nDf51)* animals on OP50 (Figure 2.16C). Nevertheless, it is noteworthy that wild type larvae exhibit robustly normal developmental timing regardless of the bacterial diets tested here, supporting our conclusion that the full *let-7* family miRNA genotype underlies the robustness of developmental timing to dietary and/or pathogenic stress.

Our findings that *P. aeruginosa* elicits phenotypic modulation of *let-7* family miRNA mutants reveals a regulatory circuit connecting the p38 MAPK innate immunity pathway and the heterochronic gene developmental timing pathway via *let-7* family miRNAs. The role of p38 pathway in this process is supported by our observation that loss-of-function mutations that disable the p38 MAPK pathway block the phenotypic enhancement of *let-7* family miRNA mutants on *P. aeruginosa*. Also in support of this conclusion is our result that

A

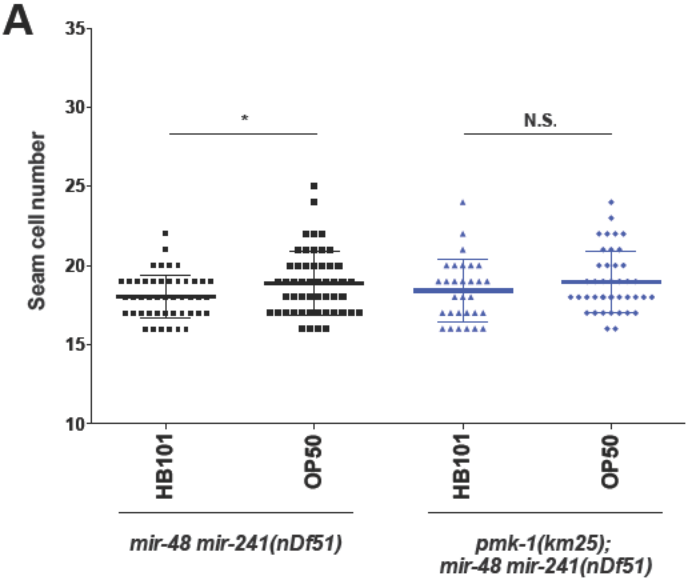

B

		Percentage of Animals with Different Adult Alae Phenotypes				
Genotype	Treatment	Complete	Gapped	No alae	(n)	
mir-48 mir-241(nDf51)	HB101	37	63	0	35	
	OP50	37	63	0	35	N.S.
mir-48 mir-241(nDf51); pmk-1(km25)	HB101	27	73	0	15	
	OP50	20	80	0	25	N.S.

N.S. not significant. χ2 test, for comparison between *E. coli* HB101 (control) and *E. coli* OP50

C

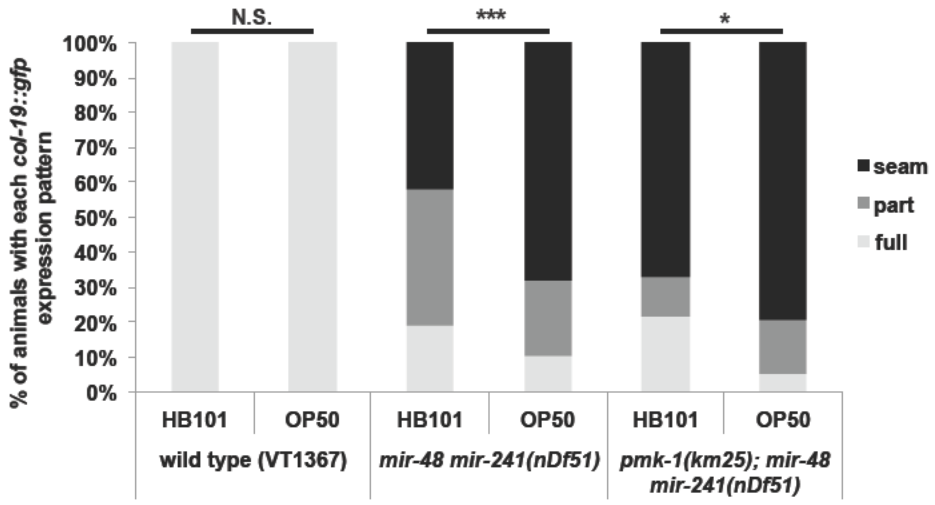

χ2 test, for comparison between *E. coli* HB101 (control) and *E. coli* OP50

Figure 2.16 Effects of *E. coli* OP50 on heterochronic phenotypes of *let-7* family miRNA mutants. Seam cell phenotype (A), adult alae phenotype (B) and *col-19::gfp* expression pattern phenotype (C) of *mir-48 mir-241(nDf51)* and *pmk-1(km25); mir-48 mir-241(nDf51)* animals on *E. coli* HB101 and *E. coli* OP50. *col-19* is an adult specific collagen whose expression pattern is regulated by *let-7* family miRNAs (81, 83, 131). seam, *col-19::gfp* is only expressed in the seam cells; part, *col-19::gfp* is expressed in the seam cells and part of the hyp7 nuclei; full, *col-19::gfp* is expressed in all the seam cells and hyp7 nuclei. All the wild type animals have full *col-19::gfp* expression pattern, and *let-7* family miRNA mutants loss a degree of *col-19::gfp* expression in hyp7 nuclei depending on the level of *let-7* family miRNA activity in the mutants. Hence, *col-19::gfp* expression pattern can be used as an indication of *let-7* family miRNA activity: the less *let-7* family miRNA activity there is, the less *col-19::gfp* expression there is in the hyp7 nuclei. The *col-19::gfp* expression pattern phenotype was scored using Zeiss SteREO Discovery.V12 microscope.

constitutive activation of p38 by knocking down of a negative regulator of p38 signaling, *vhp-1* (the p38 phosphatase (132, 133)), phenocopied the *P. aeruginosa* induced heterochronic phenotype enhancement in *let-7* family miRNA mutants (Figure 2.17).

Although our findings show that the p38 MAPK pathway is involved in regulation of *let-7* family miRNA activity, certain aspects of this regulatory circuit differ in interesting ways from canonical p38 innate immune signaling. First, the *tir-1(ok1052)* allele that lacks the N-terminal Heat/Armadillo motif of the protein blocks the enhancement of *let-7* family miRNA mutant phenotypes as well (Figure 2.4A), even though this motif has been shown to be dispensable for pathogen resistance (134, 135). This result suggests that activation of the p38 MAPK pathway is necessary for the regulation of *let-7* family miRNA activity upon *P. aeruginosa* infection, but p38 signaling alone without the activity of the Heat/Armadillo motif of TIR-1 is not sufficient. Moreover, we observed that ATF-7 exerts complex and allele-specific modes of regulation on *let-7* family miRNA activity with and without *P. aeruginosa* infection, presumably depending on its phosphorylation potential (Figure 2.4B-E). This is consistent with previously published observations that upon phosphorylation by PMK-1 in face of *P. aeruginosa* infection, ATF-7 switches its regulation on the *pmk-1*/p38-mediated gene expression (120). More intriguingly, the *atf-7(gk715)* allele enhances the phenotypes of the *let-7* family miRNA mutant even more than the *atf-7* null allele does, and the phenotype is suppressed when animals were exposed to *P.*

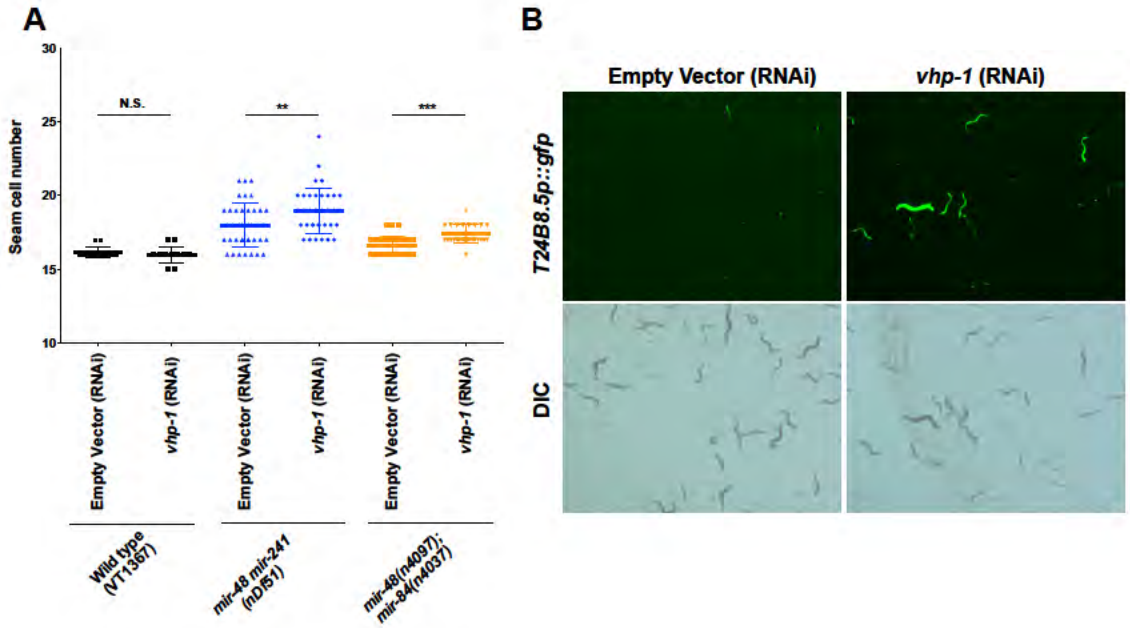

Figure 2.17 The effects of *vhp-1* on *let-7* family miRNA activity. (A) *vhp-1* positively regulates *let-7* family miRNA activity. (B) p38 MAP Kinase is activated by *vhp-1* RNAi as indicated by transgene reporter *agIs219*[*T24B8.5p::gfp::unc-54-3'UTR*]). * $p < 0.05$, ** $p < 0.01$, *** $p < 0.001$, N.S. not significant, two-tailed *t*-test. $n \geq 15$.

aeruginosa (Figure 2.4A). This *atf-7(gk715)* allele removes the first exon from two *atf-7* gene isoforms, leaving the remaining isoforms unaffected. This suggests that there is an activation domain in the N-terminal region of ATF-7 protein. Removal of this region in the *gk715* allele results in a reversal of function for the protein. Previous findings suggested that the N-terminal region of mammalian ATF-7 homologs is essential for transcriptional activity (136, 137), a situation which, according to our results, appears to be evolutionally conserved in *C. elegans*. Even though there are still caveats in the interpretations of these non-canonical functions of TIR-1 and ATF-7 on *let-7* family miRNA activity that might benefit from further confirmation, our results provide a beginning in the understanding of mechanisms involved for p38 MAPK pathway's regulation on *let-7* family miRNAs.

Our experiments using *let-7* family miRNA gene transcriptional reporters in wild type and *pmk-1* mutant growing on *E coli* suggest that p38 signaling could inhibit *let-7* family miRNA activity at least in part at the transcriptional level. Thus, upon *P. aeruginosa* infection, activated p38 could further reduce *let-7* family miRNA gene expression relative to growth on *E. coli*, which correlates with the enhanced heterochronic phenotype of *let-7* family miRNA mutants on *P. aeruginosa*. However, we were not able to directly explore the GFP reporter activity of *let-7* family miRNA genes upon *P. aeruginosa* infection, due to an apparent nonspecific degradation of GFP (possibly caused by cellular autophagy and/or necrosis) when animals were treated with *P. aeruginosa*. Additionally, it

should be noted that the transcriptional regulation of p38 on *let-7* family miRNAs could be more complex than observed here, because the reporter transgenes used in our study may not have necessarily contained all relevant regulatory elements (138).

The negative regulation of *let-7* family miRNAs upon *P. aeruginosa* infection is presumably beneficial to worms and can enhance their response to pathogen. This conclusion is supported by our observation that *let-7(mg279)* animals with mildly reduced activity of *let-7* exhibit an enhanced survival in the face of *P. aeruginosa* infection. Even though we have shown that the p38 MAPK pathway and the *let-7* targets *lin-41* and *hbl-1* are required for this phenotype, it is also possible that additional downstream stress response effectors, such as *skn-1* (112), could also mediate the regulation for pathogen resistance by *let-7* family miRNAs. Predicted targets of *let-7* family miRNAs include components of several pathways involved in pathogen resistance including the p38 MAPK pathway, the unfolded protein response pathway, the oxidative stress response pathway, and the autophagy pathway (112, 124, 139, 140). We propose that *let-7* family miRNAs could function during normal, unstressed development to dampen several stress response pathways, and that under stress conditions such as *P. aeruginosa* infection, the downregulation of *let-7* family miRNA activity reported here would broadly augment animal's stress response.

Intestine, hypodermis and neurons have been shown previously to be involved in host response to pathogen infection in *C. elegans* (126, 134).

Although tissue specific rescue and knock out experiments will be required to determine the anatomical site(s) of action, and to test for cell autonomy of *let-7* family miRNAs for their regulation of pathogen resistance, our findings suggest that *let-7* family miRNAs may impact pathogen resistance by acting in intestine and possibly hypodermis. We did not observe any noticeable difference in the pathogen avoidance behavior between *let-7(mg279)* animals and wild type (Figure 2.18), arguing against an exclusively neuronal effect. However, our electron microscopy results indicate that *let-7(mg279)* animals actively fight off *P. aeruginosa* infection in the intestine. Lastly, based on the transcriptional reporter results, *let-7* family miRNAs are specifically regulated in the intestine and the hypodermis.

Implications of our findings include intriguing possibilities for evolutionarily conserved roles of *let-7* family miRNAs in cell fate and innate immune gene regulatory networks. In mammalian cells, *let-7* family miRNA levels have been shown to be reduced in response to infection by the bacterium *Salmonella* (109, 114), or the parasitic protozoan *Cryptosporidium parvum* (110, 111), or an inflammatory response of Src activation (95). In the latter context, *let-7* family miRNA levels were regulated by *lin-28* (95), which also functions in the heterochronic pathway with *let-7* family miRNAs in *C. elegans* (74, 141). In the context of *Salmonella* infection, Toll-like receptor (TLR4) and NFκB pathway and possibly other innate immune signals appear to mediate the downregulation of *let-7* family miRNAs (142). This is analogous to the p38 MAPK pathway's

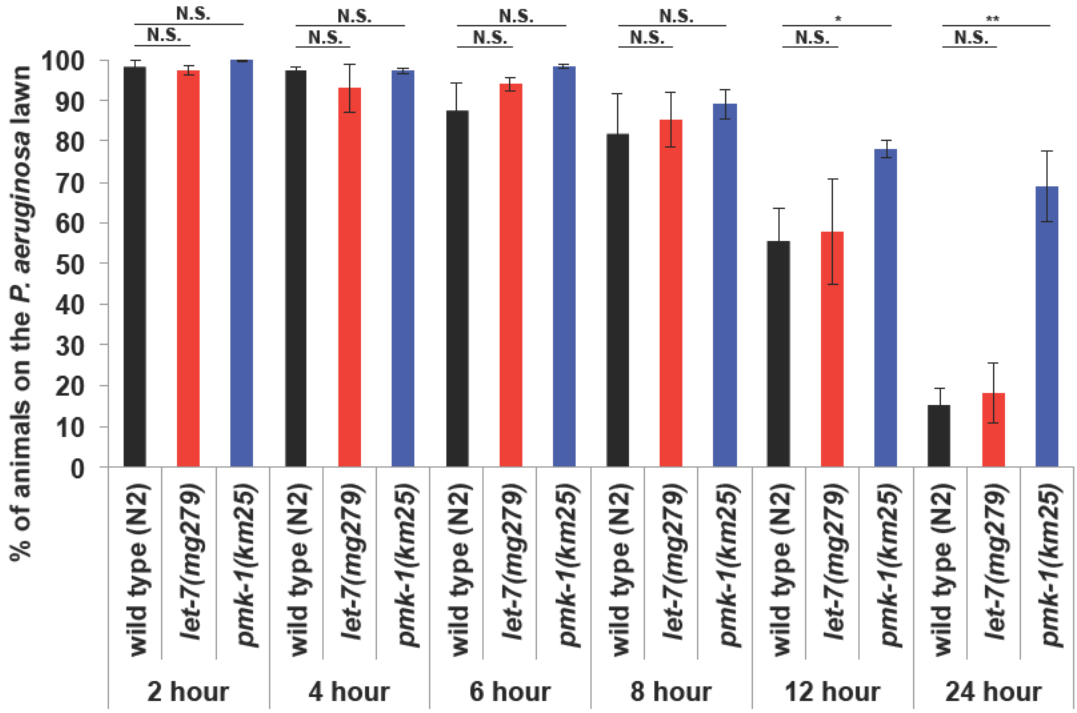

Figure 2.18 *P. aeruginosa* avoidance behavior for wild type (N2), *let-7(mg279)* and *pmk-1(km25)* animals at different time points. * $p < 0.05$, ** $p < 0.01$, N.S. not significant, two-tailed *t*-test. Error bars, SD. ($n \geq 30$).

regulation of *let-7* family miRNAs in the context of *P. aeruginosa* infection of *C. elegans*, whose genome does not contain an NFκB homolog (143, 144). It is not currently clear whether p38 could contribute to the regulation of *let-7* family miRNAs in mammalian cells upon innate immune activation.

In conclusion, our study demonstrates that *let-7* family miRNAs function in a feed-forward loop with the p38 MAPK pathway to promote pathogen resistance upon infection, and that the evolutionary advantage of genetic redundancy in *let-7* family miRNAs assists animals in maintaining their robust developmental programs under various stress conditions.

CHAPTER III: Investigating the interplay between heterochronic genes and pathogen resistance pathways

III.A. Abstract

In Chapter II, I have shown that the reciprocal interactions between *let-7* family miRNAs and the p38 MAPK innate immune pathway function to coordinate developmental timing with pathogen defense. In this chapter, we further investigated the interactions between the developmental timing pathway and pathogen resistance pathways in the context of *P. aeruginosa* infection. I found that the developmental timing regulator *lin-28* functions upstream of *let-7* family miRNAs in a manner that is independent of its regulation on developmental timing to promote pathogen resistance against *P. aeruginosa* infection. Interestingly, we observed that only one of the two major gene isoforms of *lin-28* is upregulated upon *P. aeruginosa* infection and this isoform is also phosphorylated regardless of the developmental stage and diet. Moreover, results in the rest of this chapter further validate that *let-7* family miRNAs and the p38 MAPK pathway contribute to the interactions between the developmental timing pathway and the innate immune pathway upon *P. aeruginosa* infection. The findings in this chapter may provide information about the functional divergence of the developmental and non-developmental roles of the heterochronic genes.

III.B. Introduction

I previously found that the activity of *let-7* family miRNAs is downregulated upon *P. aeruginosa* infection possibly through transcriptional regulation by the p38 MAPK pathway. However, whether *lin-28*, another known regulator of *let-7* family miRNAs, could be involved in the downregulation of *let-7* family miRNAs in response to *P. aeruginosa* infection remains to be investigated.

lin-28 encodes a well-conserved RNA-binding protein with a cold shock domain and two retroviral-type (CCHC) zinc finger motifs (78). *lin-28* was discovered in *C. elegans* as a developmental timing regulator, and the loss-of-function mutants of *lin-28* skip the L2 stage seam cell division resulting in precocious heterochronic phenotypes (77, 78). The protein expression of LIN-28 in *C. elegans* starts in the embryos and it is dramatically downregulated by *lin-4* and *let-7* family miRNAs after the L2 stage (78). *lin-28* has also been shown to regulate the biogenesis of *let-7* family miRNAs during development and disease processes in various organisms (47, 141). Mammalian LIN28 has also been shown to be induced by inflammation to promote cell transformation through *let-7* family miRNAs (95). This study echoes our findings of the reciprocal interactions between the p38 MAPK innate immune pathway and *let-7* family miRNAs in seam cell fate and pathogen resistance regulation. Therefore, I hypothesized that *lin-28* could function with *let-7* family miRNAs to regulate pathogen resistance against *P. aeruginosa* infection.

Additionally, I sought to determine the heterochronic phenotype enhancement of *let-7* family miRNA mutants on *P. aeruginosa* is solely caused by the p38 MAPK pathway. Besides the p38 MAPK pathway, multiple innate immune pathways are activated upon *P. aeruginosa* infection. First, a previous study has shown that the protein kinase D DFK-2 functions upstream of p38 to promote innate immune response upon *P. aeruginosa* infection (145). Second, the G-protein coupled receptor FSHR-1 is known to regulate innate immune response genes that partially overlap with the downstream targets of the p38 MAPK pathway (146). Another innate immune pathway against *P. aeruginosa* infection is controlled by the transcription factor ZIP-2 in a p38 independent manner (147). Additionally, the FOXO transcription factor DAF-16 has been demonstrated to act downstream of the insulin receptor DAF-2 to regulate innate immunity and stress response in dependent from the p38 MAPK pathway as well (129). The β-catenin/BAR-1 and the HOX transcription factor/EGL-5 were identified to be required for survival against *Staphylococcus aureus* infection, but they also play a role in pathogen resistance against *P. aeruginosa* (148). Last, although the only Toll-like receptor homolog in *C. elegans* TOL-1 is not required for survival on *P. aeruginosa*, it is important for the pathogen resistance against *Salmonella enterica* and the avoidance behavior in response to pathogenic *Serratia marcescens* (144, 149). Therefore, I tested if these innate immune response pathways are required for the heterochronic phenotype enhancement of the *let-7* family miRNA mutant on *P. aeruginosa*.

Building upon the results in Chapter II, I found that *lin-28* functions upstream of *let-7* family miRNAs in adults to regulate pathogen resistance against *P. aeruginosa* infection. Additionally, the reciprocal regulation between developmental timing and pathogen resistance observed in Chapter II seems to be specifically elicited by the p38 MAPK pathway and *let-7* family miRNAs.

III.C. Materials and methods

The following are methods not previously described in Chapter II.

Western blot analysis of LIN-28 and CIP reaction. For LIN-28 western blots, animals were washed off plates with M9 buffer and flash frozen in liquid nitrogen. Lysates were prepared by resuspending samples in lysis buffer (50mM Tris-HCl pH7.4, 150mM NaCl, 2mM EDTA, 1% NP-40, 2mM DTT, PhosSTOP (Roche), Protease inhibitor (Roche)) and were then homogenized with Branson SLPe sonicator. Lysates were centrifuged at 164,000rpm for 20 minutes at 4°C and the supernatants were collected. BioRad Protein Assay Dye Reagent Concentrate (Cat# 500-0006) was used to measure the protein concentration. LIN-28 was recognized by an anti-serum (150) at 1:1000 dilution, and anti-α-tubulin antibody (Sigma-Aldrich Cat# T6074) was used at 1:20000 dilution.

For the CIP treatment, 50 units of Calf Intestinal Alkaline Phosphatase (CIP, NEB Cat# M0290) were used for each sample and the reaction was carried out at 37°C for 30 minutes. Also, in order to get better separation between the doublet bands, samples were run slowly on a 12% SDS-PAGE gel at 80V.

Generation of transgenic animals and CRISPR/Cas9 experiments. To generate transgenic animals carrying extrachromosomal arrays, a mixture containing 50ng/µl pBlueScript, 50ng/µl pCFJ150, 15ng/µl *sur-5::gfp* and 10ng/µl of either *lin-28a* (pSW30) or *lin-28b* (pSW22) was injected into post-dauer *lin-28(n719)* animals. F1 and F2 generation was screen for *sur-5::gfp* expression and transmission of the extrachromosomal arrays respectively. Two independent lines were established for both *lin-28a* and *lin-28b*.

For the CRISPR/Cas9 experiment, wild type (N2) animals were injected with a mixture containing 50ng/µl *eft-3::cas9* vector, 50ng/µl *lin-28a* sgRNA-1 vector (pSW12), 50ng/µl *lin-28a* sgRNA-2 vector (pSW15), 20ng/µl *dpy-10* sgRNA vector and 15ng/µl *sur-5::gfp* vector for *lin-28a*, or 50ng/µl *eft-3::cas9* vector, 50ng/µl *lin-28b* sgRNA-1 vector (pSW48), 50ng/µl *unc-22* sgRNA vector and 50ng/µl *myo-2::mcherry* vector for *lin-28b*. F1 animals with dumpy phenotype were sequenced for mutations in the *lin-28* gene.

Immunoprecipitation and silver staining. For LIN-28 IP, lysates were prepared by resuspending samples in the IP lysis buffer (60mM HEPES pH 7.4, 100mM KCl, 0.2% TritonX-100, 4mM $MgCl_2$, 20% glycerol, 2mM DTT, Protease inhibitor (Roche), Phosphatase inhibitor cocktail 2 and 3(Sigma)) and then samples were lysed in a medal dounce homogenizer. Lysates were centrifuged at 164,000rpm for 20 minutes at 4°C and the supernatants were collected.

3.17mg and 0.33mg of protein lysate inputs were used for wild type and *lin-28(n719)* samples, respectively. 150µl of 50% suspension of Dynabeads

Protein A (Thermo) and 50µl of the LIN-28 antiserum was used for each sample. Beads were first washed 3 times with IP lysis buffer, and then LIN-28 antiserum was added to the beads solution. 0.8ml volume was made up for each sample by compensating with IP lysis buffer. Beads and LIN-28 antiserum were incubated at 4°C with gentle rotating for 3 hours. Meanwhile, protein lysates were pre-cleared by adding 40µl of 50% suspension of Dynabeads Protein A and incubating at 4°C with gentle rotating for 1 hour. The beads/antibody suspension was added to each pre-cleared protein lysate and incubated at 4°C with gentle rotating for 3 hours. Afterwards, supernatants were saved for further analysis. Beads were washed 3 times with wash buffer (30mM HEPES pH 7.4, 100mM KCl, 0.1% TritonX-100, 2mM $MgCl_2$, 10% glycerol, 1mM DTT, Protease inhibitor (Roche)) and then boiled in 50µl of 2xSDS/BME sample buffer at 95°C for 15 minutes.

For silver staining, SilverQuest staining kit (Invitrogen Cat# LC6070) was used following the manufacturer's protocol.

ASE neuron phenotypic analysis. The ASE neuron phenotype was scored by the expression of *otIs114* [*lim-6::gfp*] (ASEL marker) in the larvae of each genotype under Zeiss SteREO Discovery.V12 microscope (66).

Quantitative RT-PCR (qRT-PCR). Total RNA was digested with DNase I (NEB) to eliminate genomic DNA contamination. QuantiFast SYBR Green RT-PCR kit (Qiagen) was used for *lin-28* qRT-PCR analysis, while SensiMix SYBR One Step kit (BIOLINE) was used for qRT-PCR analysis of pathogen response

genes. 1ng/µl RNA was used for each reaction. Primer sequences are listed in Table 3.1.

Exotoxin A, tunicamycin and *S. aureus* treatment. For exotoxin A treatment, previously published protocol (151) was used with our modification. Gravid adults (P0) were put on each treatment plates to produce progeny (F1 generation), and the F1 adults were transferred to fresh plates seeded with the same bacteria to produce F2 generation. The heterochronic phenotypes of F2 young adults were scored.

For tunicamycin treatment, 1µg/ml tunicamycin was added to NGM plates and seeded with *E. coli* HB101. Synchronized L1 stage animals were put on the control or treatment plates and their heterochronic phenotypes were scored at young adult stage.

For *S. aureus* treatment, plates were made following the procedure described in (114). L2 stage animals were put on the treatment plates and their heterochronic phenotypes were scored at young adult stage. The control group is NGM plates seeded with *E. coli* HB101 because we suspect that *E. coli* might behave quite differently on the *S. aureus* plates, which could cause changes in the heterochronic phenotypes of *let-7* family miRNA mutants and would not be a good control.

Table 3.1. Primer sequences for qRT-PCR

Gene	Forward Primer	Reverse Primer
lin-28a	AGAGGCTCCCGTCACCAACA	CTTCACCGGTGATGTCATCGATCAC
lin-28b	CGGTGCCCATCAAATCTCAATTGTC	CTTCACCGGTGATGTCATCGATCAC
tir-1	AGAACGACACCGACCACCAAAG	GATGGCCCAGTACGGCTTACT
gst-4	GTGACGCTGATCATATTAACAAAGTACGTT	CCTGATTTACTCTTGGCCAGGAAC
tsp-1	TTCGTGTTTGGCTCATCGTTGTATTC	CGTTTTGGCCAAACACTTGAAATCATTC
ilys-5	CTCCTTTCTGTCGCTATTGCGTAC	CCAACGTCCATGTGGCAACC
lys-3	CTATCTGGATTCAAGTAACTTCTCCAACAA	CAAGCCCAGATTCTTCGCACTTCTA
C17H12.8	CGTTCAGAAGACCAACGAACCAAAT	TCTCGGATAATCATATACAGCTGTGAAGT
F55G11.4	GATCCGTGTATTTGGCTGGAATCG	CATATGTGCTCCCGCGTTCAC
tba-1	TGACAAGGCTTACCATGAGGCTCTC	ATCGCACTTCACCATTTGGTTGGCT

III.D. Results

1. *lin-28* functions upstream of *let-7* family miRNAs in the regulation of pathogen resistance.

Since *let-7* family miRNAs are involved in pathogen resistance against *P. aeruginosa*, we investigated if *lin-28*, the well-studied post-transcriptional regulator of *let-7* family miRNAs could play a role in pathogen resistance as well. The loss-of-function mutant *lin-28(n719)* dies faster on *P. aeruginosa* compared to wild type animals, and this phenotype is suppressed by *let-7* family miRNAs (Figure 3.1). This suggests that *lin-28* is genetically upstream of *let-7* family miRNAs in the regulation of survival on *P. aeruginosa*.

In addition, we failed to observe any significant reduction in either *mir-48* or *mir-241* levels of the L4 stage *lin-28(n719)* animals compared to wild type animals after 24 hour *P. aeruginosa* treatment (Figure 3.2), which is consistent with the *P. aeruginosa* survival results showing that *lin-28* acts upstream of *let-7* family miRNAs. These results here indicate that *lin-28* is probably required for the downregulation of mature *let-7* family miRNA levels upon *P. aeruginosa* infection after the L4 stage.

2. *lin-28* is not required for the heterochronic phenotype enhancement of *let-7* family miRNA mutants on *P. aeruginosa*.

Since *lin-28* affects developmental timing of *C. elegans* through its negative regulation on *let-7* family miRNAs, I investigated into whether *lin-28* is required for the heterochronic phenotype enhancement of the *let-7* family miRNA

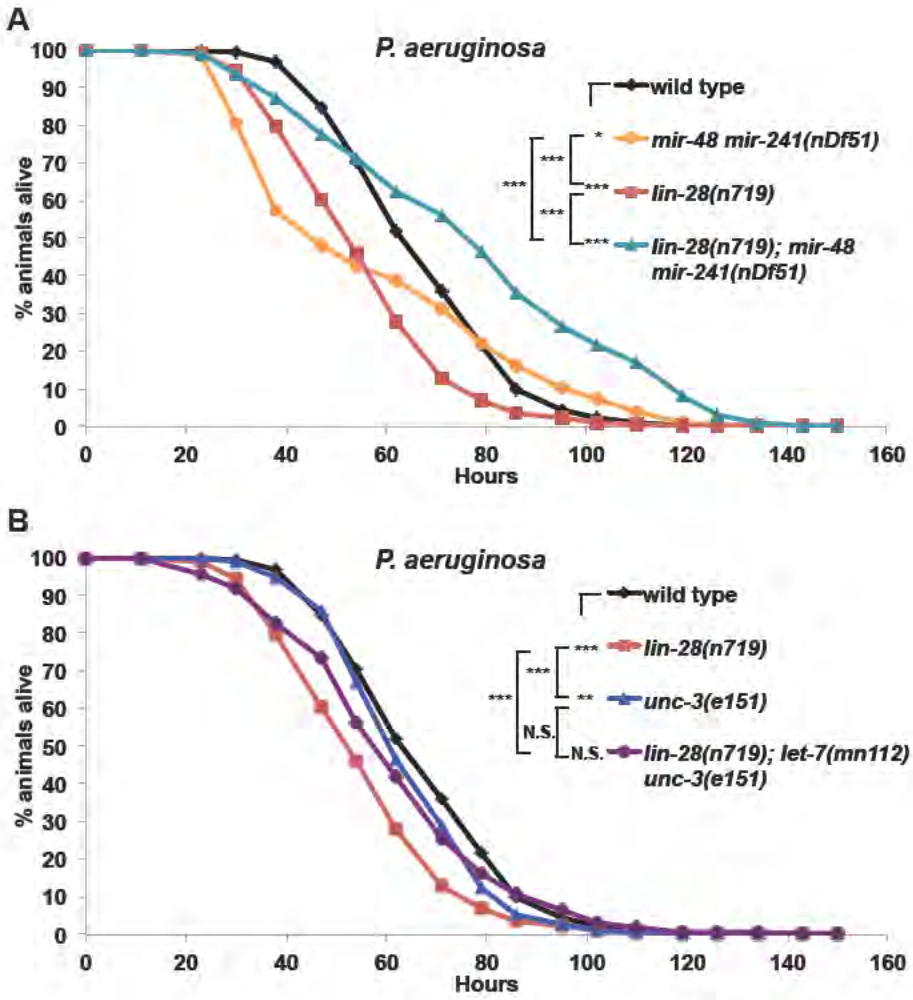

Figure 3.1 *lin-28* acts upstream of *let-7* family miRNAs in worm's survival on *P. aeruginosa*. (A) Survival of wild type (N2), *mir-48 mir-241(nDf51)*, *lin-28(n719)* and *mir-48 mir-241(nDf51); lin-28(n719)* animals on *P. aeruginosa*. (B) Survival of wild type (N2), *unc-3(e151)*, *lin-28(n719)* and *let-7(mn112) unc-3(e151); lin-28(n719)* animals on *P. aeruginosa*. * $p < 0.05$, ** $p < 0.01$, *** $p < 0.001$, N.S. not significant, log-rank test.

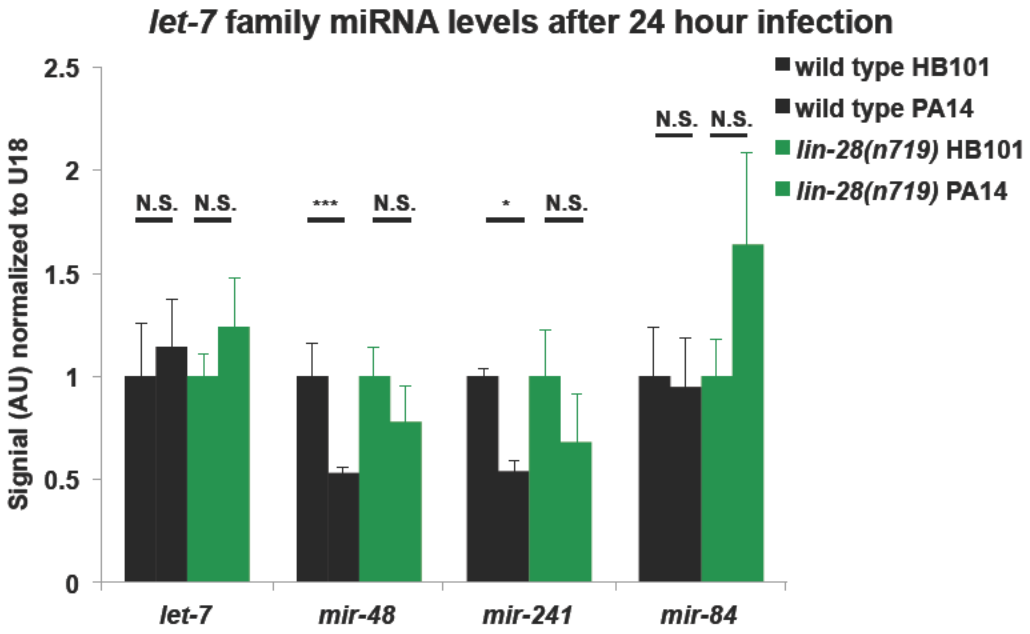

Figure 3.2 The downregulation of two *let-7* family miRNAs on *P. aeruginosa* is impaired in *lin-28(n719)* animals. Mature *let-7* family miRNA levels of wild type (N2) and *lin-28(n719)* animals after 24 hours of *P. aeruginosa* infection compared to control (HB101) at 25°C. Error bars, SDs. * $p < 0.05$, ** $p < 0.01$, *** $p < 0.001$, N.S. not significant, two-tailed *t*-test.

mutants on *P. aeruginosa*. To do that, I tested if *P. aeruginosa* infection could still elicit the heterochronic phenotype enhancement in *let-7* family miRNA mutants in the absence of LIN-28. Loss of function for *lin-28* results in a precocious heterochronic phenotype where seam cells skip the L2 stage symmetric division, resulting in less seam cells and formation of adult alae at the L3 molt. I believe that this precocious heterochronic phenotype of *lin-28(n719)* might be too dominant to be modulated by *P. aeruginosa* even if *lin-28* is not required for the regulation. Therefore, I used a strain that contains a suppressor mutation of *lin-28(n719)*, *lin-46(ma164)*, but the double mutant *lin-28(n719); lin-46(ma164)* exhibits almost completely normal heterochronic phenotypes that do not fall into the sensitized genetic background range. Finally, I built a strain that deletes one of the *let-7* family miRNAs (*mir-48*) in the *lin-28(n719); lin-46(ma164)* background. This strain (*lin-28(n719); lin-46(ma164) mir-48(n4097)*) has a partially penetrant retarded heterochronic phenotype that allows the detection of any heterochronic phenotype enhancement elicited by *P. aeruginosa* infection. Indeed, the heterochronic phenotype of this mutant is enhanced on *P. aeruginosa* (Figure 3.3). This suggests that *lin-28* could not be solely required for the heterochronic phenotype enhancement of *let-7* family miRNA mutants on *P. aeruginosa*, which is consistent with our previous finding that p38 MAPK pathway is required for phenotypic enhancement of *let-7* family miRNA mutants on *P. aeruginosa* (152).

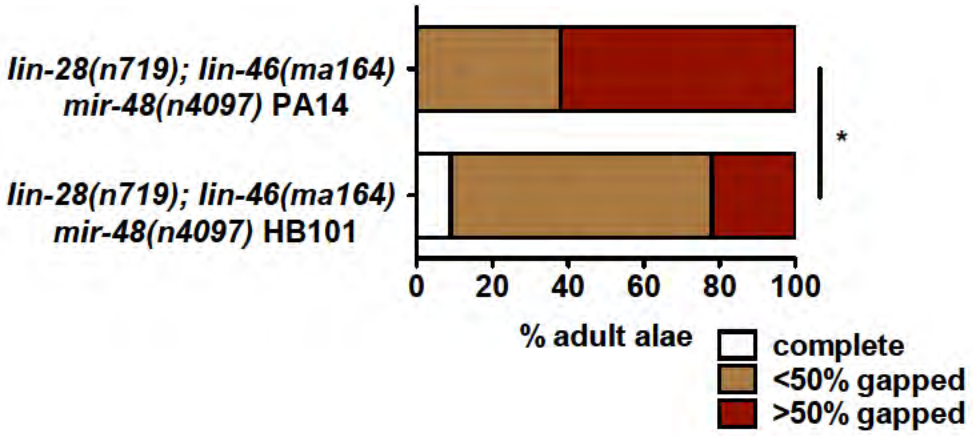

Figure 3.3 *lin-28* is not required for the heterochronic phenotype enhancement on *P. aeruginosa*. Adult alae phenotype of *lin-28(n719); lin-46(ma164) mir-48(n4097)* animals developed on *E. coli* control (HB101) and *P. aeruginosa* (PA14). * $p < 0.05$, ** $p < 0.01$, *** $p < 0.001$, N.S. not significant, chi-square test for adult alae phenotype and two-tailed *t*-test for seam cell phenotype.

3. *lin-28*'s role in pathogen resistance might be separate from its role in larval development.

Since *lin-28* is not required for the regulation of developmental timing phenotypes of *let-7* family miRNA mutants on *P. aeruginosa*, I wondered if the roles of *lin-28* in development and pathogen resistance could be separated. Because the developmental phenotypes of *lin-28(n719)* animals are dramatically suppressed by going through the dauer stage (153), I tested the survival of post-dauer animals of wild type and *lin-28(n719)* animals on *P. aeruginosa*. Interestingly, these post-dauer *lin-28(n719)* animals still die faster than wild type even though the general fitness of these animals is not significantly compromised (Figure 3.4). This suggests that the pathogen resistance phenotype of *lin-28(n719)* animals is probably independent from their developmental timing phenotype.

To summarize all the results above, upon *P. aeruginosa* infection, *lin-28* seems to positively regulate pathogen resistance upstream of *let-7* family miRNAs in adults. Also, *lin-28* is not required for the heterochronic phenotype enhancement of *let-7* family miRNA mutants on *P. aeruginosa*. Therefore, the pathogen resistance role of *lin-28* might be distinct from its function in developmental timing.

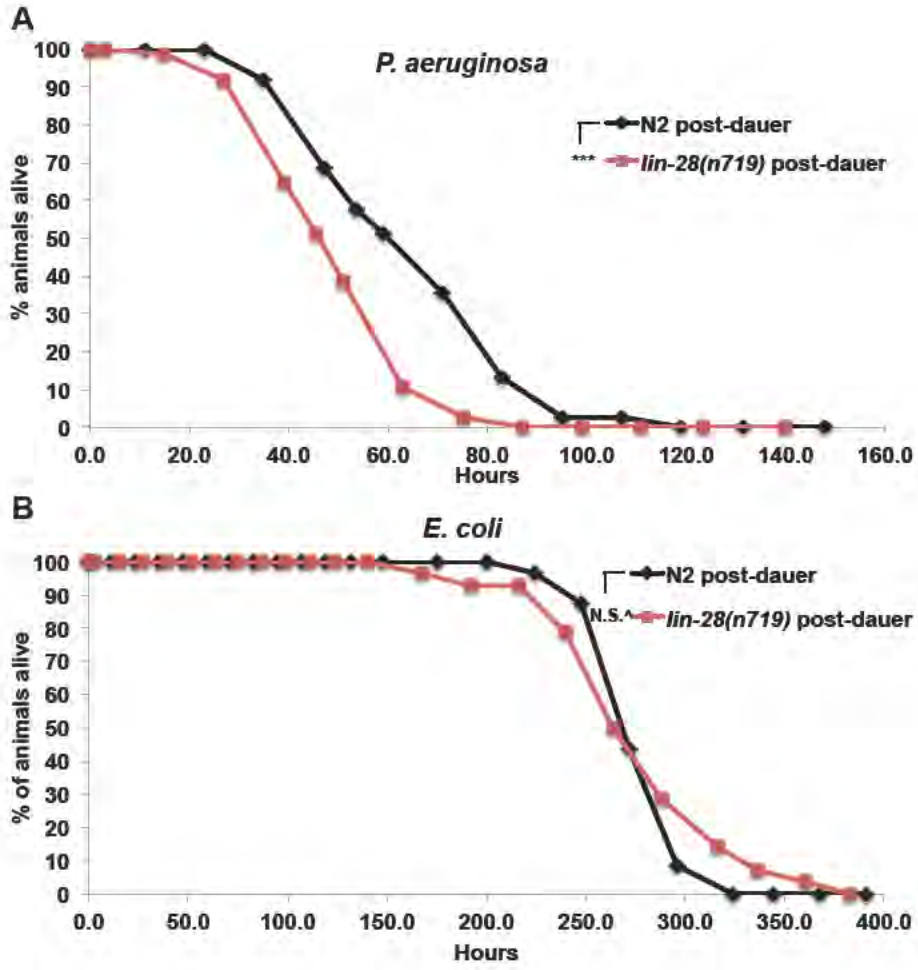

Figure 3.4 The effects of post-dauer on *lin-28(n719)* animals lifespan and survival on *P. aeruginosa*. (A) Survival of post-dauer wild type (N2) and *lin-28(n719)* animals on *P. aeruginosa*. (B) Lifespan of post-dauer wild type (N2) and *lin-28(n719)* animals on *E. coli* HB101. *** p< 0.001, N.S. not significant, log-rank test. ^ indicates a statistically significant outcome in Fisher's exact test (p=3.8e-06 at 25% and p=0.0065 at 75%).

4. One of two major gene isoforms of *lin-28* is upregulated upon *P. aeruginosa* infection.

Since *lin-28* is involved in pathogen resistance, I examined the protein levels of LIN-28 in response to *P. aeruginosa* infection. Because previously LIN-28 protein expression was not observed after the L3 stage (150), I looked into the LIN-28 protein levels of wild type animals on *E. coli* or *P. aeruginosa* at different larval stages. First, our results are consistent with previous studies showing that there are two protein bands for LIN-28, and that the expression of LIN-28 proteins starts from embryo stage and dramatically downregulated after the L2 stage on *E. coli* (Figure 3.5A) (150). *P. aeruginosa* appears to delay the downregulation of LIN-28 proteins (Figure 3.5A), which could be caused by the downregulation of *let-7* family miRNAs upon *P. aeruginosa* treatment since *let-7* family miRNAs can suppress LIN-28 expression as well.

Because *lin-28* probably exhibits its role in pathogen resistance from the L4 stage, I investigated into the LIN-28 protein levels of L4 animals upon *P. aeruginosa* infection. Interestingly, I observed that only one of the LIN-28 protein isoforms is present at the L4 stage and there is an increase of this LIN-28 protein isoform in both wild type and *let-7(mg279)* animals upon *P. aeruginosa* infection (Figure 3.5B). The upregulation of the LIN-28 protein isoform in wild type compared to *let-7(mg279)* animals were similar, which indicates that *let-7* might not be required for this upregulation of LIN-28 protein level on *P. aeruginosa*.

Furthermore, I looked into whether this upregulation of LIN-28 protein isoform is specific to *P. aeruginosa* infection and if the p38 MAPK pathway is required for this upregulation. Unfortunately, the results were not very conclusive because the increase of LIN-28 protein levels in this experiment was very mild (less than two-fold change)(Figure 3.5C and D), and further experiments are needed to address these questions. Nonetheless, from Figure 3.5C, I found that the LIN-28 protein isoform present in the L4 stage is the one with higher molecular weight.

To my knowledge, the results here are the first indication that LIN-28 proteins are still present after the L3 stage even though in very low abundance. Because only one of LIN-28 protein isoform appears to be regulated upon *P. aeruginosa* infection, it is very important to characterize the identity of these two LIN-28 protein isoforms. *C. elegans lin-28* is present only at one genomic locus, but there are two gene isoforms (*lin-28a* and *lin-28b*) with different first exons (Figure 3.6A). We took two complementary approaches to determine if the two LIN-28 protein isoforms correspond to the two gene isoforms: 1) generate specific knockout mutations of *lin-28a* and *lin-28b* by CRISPR/Cas9 technology; 2) rescue *lin-28(n719)* animals with extrachromosomal arrays expressing each gene isoform specifically (Figure 3.6B). Both *lin-28a* and *lin-28b* extrachromosomal arrays rescued the vulva developmental phenotype of *lin-28(n719)* animals (data not shown), which suggests that both *lin-28a* and *lin-28b*

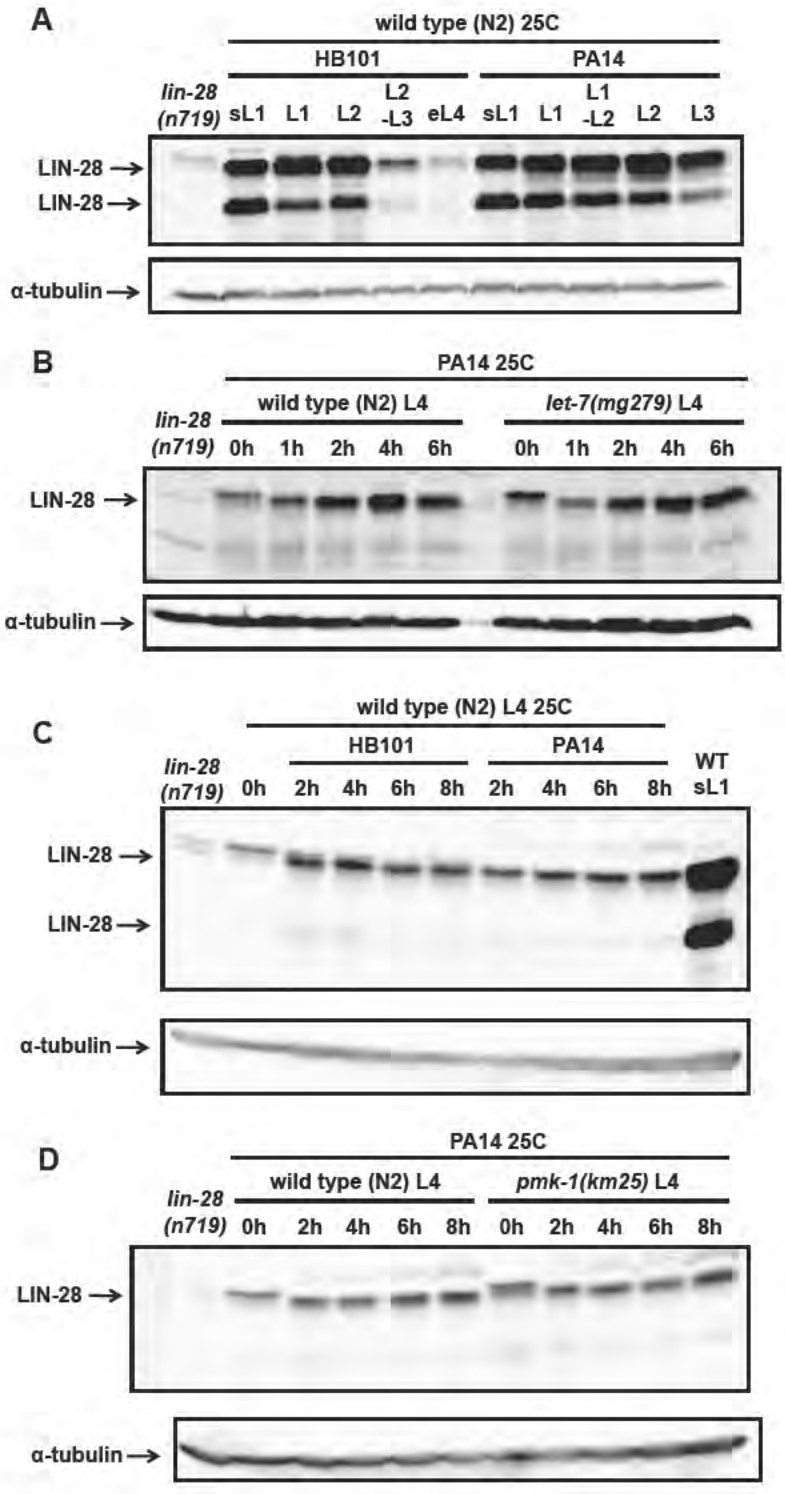
A
wild type (N2) 25C
HB101
PA14
lin-28 (n719)
sL1
L1
L2
L2 -L3
eL4
sL1
L1
L1 -L2
L2
L3
LIN-28
LIN-28
α-tubulin
B
PA14 25C
wild type (N2) L4
let-7(mg279) L4
lin-28 (n719)
0h
1h
2h
4h
6h
0h
1h
2h
4h
6h
LIN-28
α-tubulin
C
wild type (N2) L4 25C
HB101
PA14
lin-28 (n719)
0h
2h
4h
6h
8h
2h
4h
6h
8h
WT sL1
LIN-28
LIN-28
α-tubulin
D
PA14 25C
wild type (N2) L4
pmk-1(km25) L4
lin-28 (n719)
0h
2h
4h
6h
8h
0h
2h
4h
6h
8h
LIN-28
α-tubulin

Figure 3.5 Changes in LIN-28 protein levels upon *P. aeruginosa* infection. (A) Western blots of LIN-28 in wild type (N2) animals at different larval stages on HB101 and PA14. (B) Western blots of LIN-28 protein levels in L4 stage wild type (N2) and *let-7(mg279)* animals upon infection with PA14. (C) Western blots of LIN-28 in L4 stage wild type (N2) animals on HB101 and PA14. (D) Western blots of LIN-28 in L4 stage wild type (N2) and *pmk-1(km25)* animals on PA14. sL1, starved L1 animals (obtained by incubating embryos in M9 for 24 hours).

transgenes are functional. Moreover, as it is shown in Figure 3.6C, *lin-28a* and *lin-28b* transgenes specifically generate the bigger and smaller protein isoform respectively, and the *lin-28a* deletion animals only produce the smaller protein band. These results indicate that the bigger and smaller protein bands of LIN-28 correspond to LIN-28A and LIN-28B respectively. The reason we observe less LIN-28A and LIN-28B in the extrachromosomal array strains is that only a small percentage of animals actually carry the transgenes. And the lower level of LIN-28B in *lin-28a* deletion mutant (Figure 3.6C) is likely because the sample consists of a mix stage population with majority of the animals at the L4 and young adult stage. At the embryonic stage, there might be even a slight upregulation of LIN-28B level in the *lin-28a* knockout strain (Figure 3.6D), which suggests that there might be compensatory regulation between the two *lin-28* isoforms.

From these results, it seems like the LIN-28 gene isoform that is upregulated on *P. aeruginosa* is LIN-28A. Consistently, I also observed that only *lin-28a* is upregulated at the mRNA level upon *P. aeruginosa* infection (Figure 3.6E). This indicates that the upregulation of LIN-28 by *P. aeruginosa* could be either through transcriptional activation or inhibition of mRNA decay.

5. LIN-28A is phosphorylated.

From the experiment in Figure 5C, we noticed that LIN-28A protein exhibits a doublet band pattern. Additionally, the size of LIN-28A in western blot analysis (~30kD) is different from the predicated sizes of LIN-28A (25.4kD).

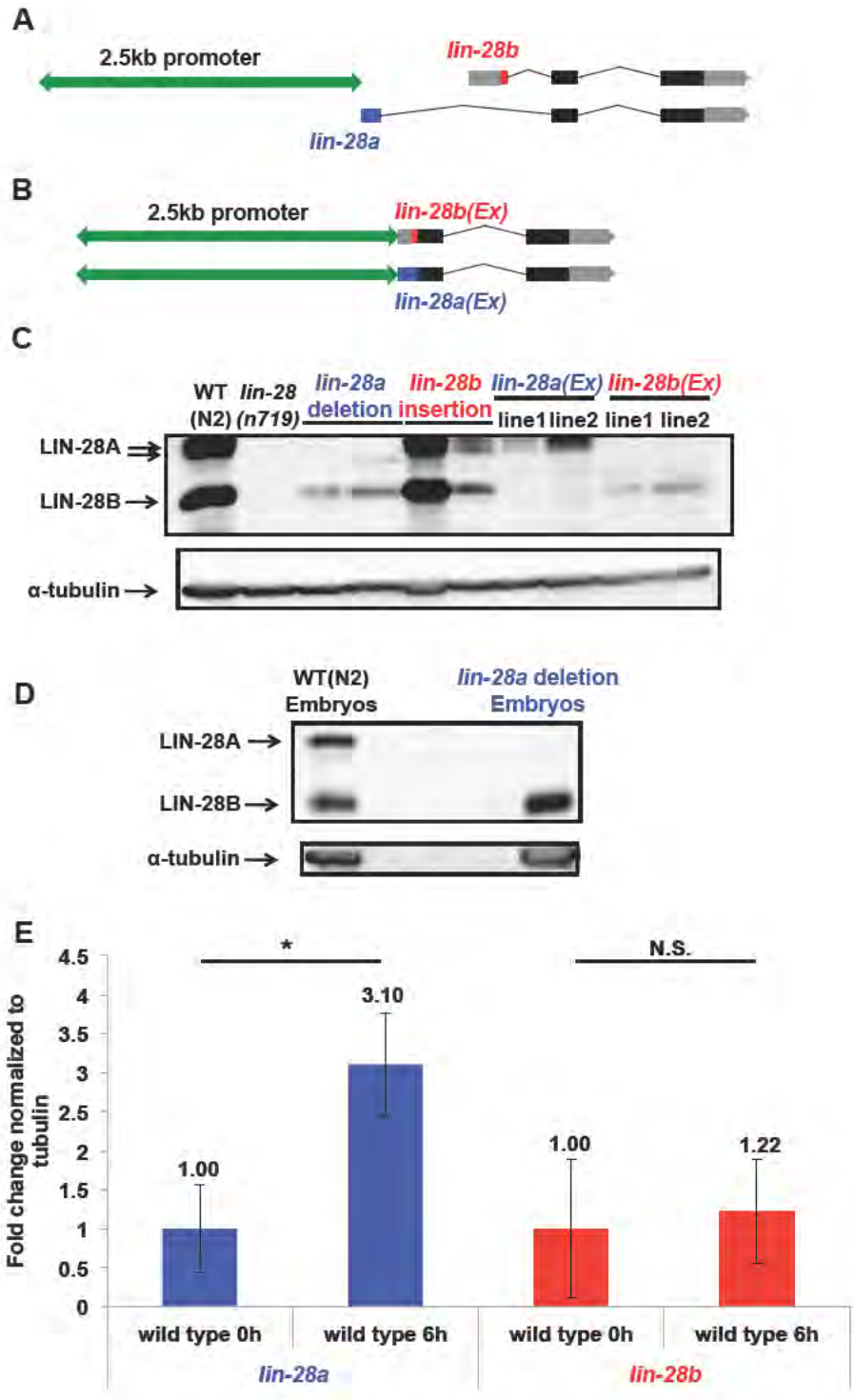
A
2.5kb promoter
lin-28b
lin-28a
B
2.5kb promoter
lin-28b(Ex)
lin-28a(Ex)
C
WT (N2)
lin-28 (n719)
lin-28a deletion
lin-28b insertion
lin-28a(Ex) line1
lin-28a(Ex) line2
lin-28b(Ex) line1
lin-28b(Ex) line2
LIN-28A
LIN-28B
α-tubulin
D
WT(N2) Embryos
lin-28a deletion Embryos
LIN-28A
LIN-28B
α-tubulin
E
*
N.S.
Fold change normalized to tubulin
4.5
4
3.5
3
2.5
2
1.5
1
0.5
0
1.00
3.10
1.00
1.22
wild type 0h
wild type 6h
wild type 0h
wild type 6h
lin-28a
lin-28b

Figure 3.6 *lin-28* gene isoforms respond differently upon *P. aeruginosa* infection. (A) A diagram of the *lin-28* gene locus. There are two gene isoforms, *lin-28a* (in blue) and *lin-28b* (in red), sharing the same second and third exons. (B) A diagram of the design of extrachromosomal arrays specifically expressing either *lin-28a* (*lin-28a(Ex)*) or *lin-28b* (*lin-28b(Ex)*). 2.5kb of upstream promoter region was used for both *lin-28* isoforms and *lin-28b(Ex)* also contains 82nt of upstream sequence (grey) from the first exon of *lin-28b*. (C) Western blots of LIN-28 in wild type (N2), several *lin-28* mutants and transgenic animals carrying the extrachromosomal arrays. The *lin-28a* deletion is the *lin-28(ma289)* strain which has a frame-shift (4bp) deletion in the *lin-28a* exon 1 resulting in a pre-mature stop codon. The *lin-28b* insertion strain is *lin-28(ma288)* which has in-frame nucleotide changes resulting in an insertion of one amino acid, which is not expected to change the LIN-28B expression. (D) Western blots of LIN-28 in wild type (N2) and *lin-28a* deletion embryos. (E) *lin-28a* and *lin-28b* mRNA levels in wild type (N2) animals upon *P. aeruginosa* infection for 6 hours. Error bars, SDs. * $p < 0.05$, N.S. not significant, two-tailed *t*-test.

These results suggest that there might be post-translational modifications for LIN-28A. Although the doublet band pattern does not reflect well on the scanned images, it is present at all different larval stages on *E. coli* and *P. aeruginosa* for wild type animals (Figure 3.7A) and in *pmk-1(km25)* animals on *P. aeruginosa* (Figure 3.7B), which suggests that p38 is not required for this potential post-translational modification. Based on the size difference of the doublet bands, I hypothesized that LIN-28A might be phosphorylated. Accordingly, I performed CIP experiments on protein lysates of wild type and *lin-28(n719)* embryos. As expected, there is phosphorylation on LIN-28A isoform specifically (Figure 3.7C). A previous study has shown that LIN28A in mammals is phosphorylated suggesting an evolutionary conserved role of LIN28 phosphorylation (154). From the protein sequences, there are five potential phosphorylation sites specifically on LIN-28A (Figure 3.7D), but it is also possible that serine, threonine and tyrosine residues shared by LIN-28A and LIN-28B are phosphorylated only on LIN-28A.

Mass spectrometry analysis could help identify which amino acids of LIN-28A are phosphorylated. First step of mass spectrometry is to purify the protein of interest. I attempted to pull down LIN-28 with an anti-serum (Figure 3.7E and F). Even though the IP seems to be successful, I could not identify the LIN-28 protein bands on the silver staining gel due to the enormous amount of IgG eluted from the beads. So, future experiments should be performed by crosslinking antibody to the beads to eliminate the IgG contamination.

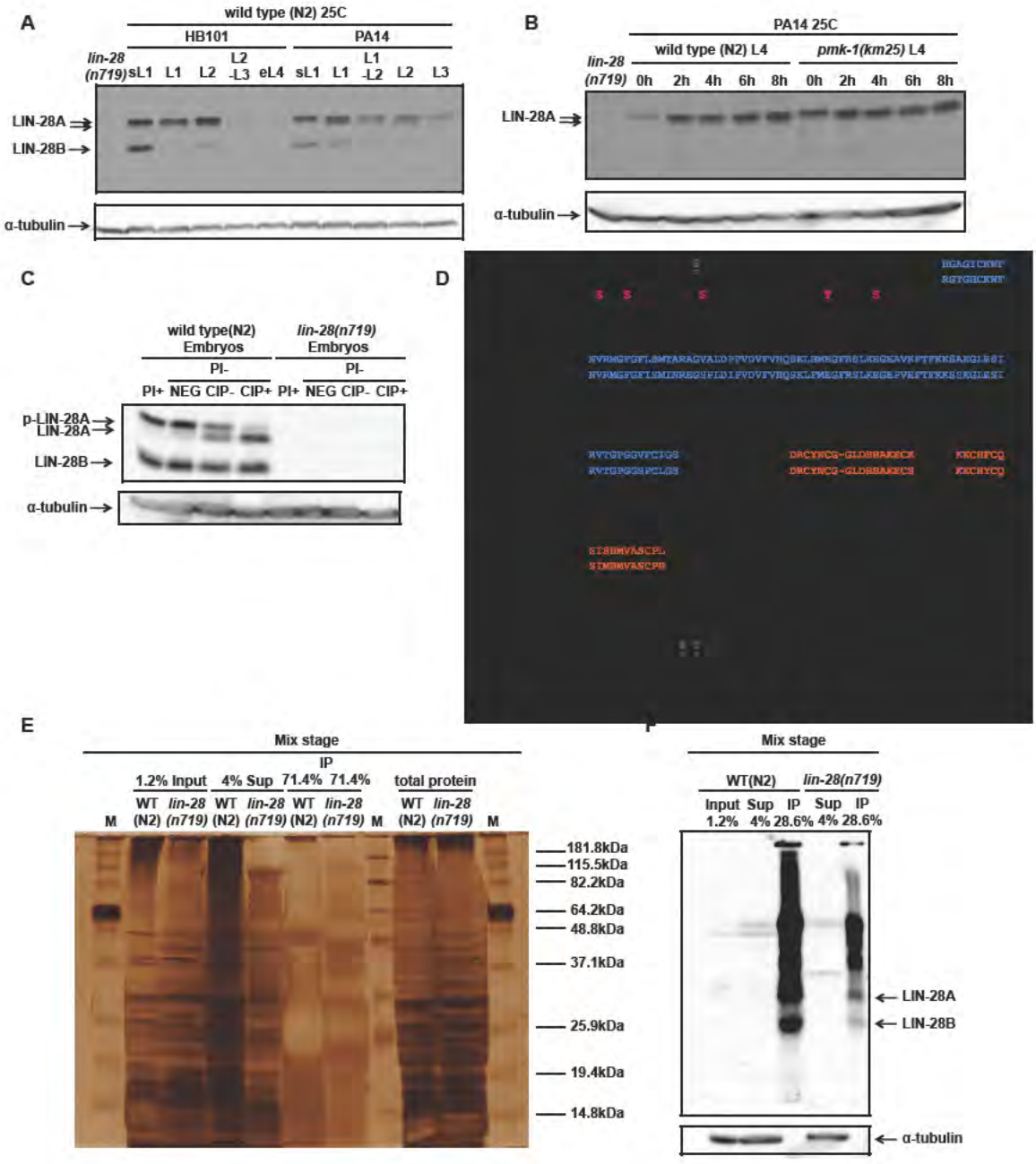
A
wild type (N2) 25C
HB101
PA14
lin-28 (n719)
sL1 L1 L2 L2 -L3 eL4 sL1 L1 L1 -L2 L2 L3
LIN-28A
LIN-28B
α-tubulin
B
PA14 25C
wild type (N2) L4
pmk-1(km25) L4
lin-28 (n719)
0h 2h 4h 6h 8h 0h 2h 4h 6h 8h
LIN-28A
α-tubulin
C
wild type(N2) Embryos
lin-28(n719) Embryos
PI-
PI+ NEG CIP- CIP+ PI+ NEG CIP- CIP+
p-LIN-28A
LIN-28A
LIN-28B
α-tubulin
D
E
Mix stage
IP
1.2% Input 4% Sup 71.4% 71.4% total protein
WT (N2) lin-28 (n719) WT (N2) lin-28 (n719) WT (N2) lin-28 (n719) M WT (N2) lin-28 (n719) M
M
181.8kDa
115.5kDa
82.2kDa
64.2kDa
48.8kDa
37.1kDa
25.9kDa
19.4kDa
14.8kDa
F
Mix stage
WT(N2) lin-28(n719)
Input 1.2% Sup 4% IP 28.6% Sup 4% IP 28.6%
LIN-28A
LIN-28B
α-tubulin

Figure 3.7 Phosphorylation of LIN-28A. (A) Western blots of LIN-28 in wild type (N2) animals at different larval stages on HB101 and PA14. (B) Western blots of LIN-28 in L4 stage wild type (N2) and *pmk-1(km25)* animals on PA14. (C) Western blots of LIN-28 in wild type (N2) and *lin-28(n719)* embryos with CIP treatment. PI (phosphatase inhibitor); NEG (no phosphatase inhibitor, no CIP and did not go through the CIP reaction); CIP- (no phosphatase inhibitor, no CIP but went through the CIP reaction); CIP+ (no phosphatase inhibitor, with CIP and went through the CIP reaction). (D) Sequence alignment of *lin-28* genes in *C. elegans* (Celin-28a and Celin-28b) and human (hLin28a and hLin28b). Cold shock domain and zinc-finger domains are highlighted in blue and orange respectively. The known phosphorylation sites in human LIN-28A are shown in purple, and the potential phosphorylation sites in *C. elegans* LIN-28A are shown in red. (E) Silver stain and (F) western blots of LIN-28 for the LIN-28 IP experiment. M, marker. Sup, supernatant. Percentage of sample run on the gel is as indicated.

Interestingly, I observed protein bands similar to the size of LIN-28 in the IP sample of *lin-28(n719)* lysates (Figure 3.7F), which suggests that there might be very small amount of read through protein products produced from this nonsense mutation. Other *lin-28* mutants should be used as negative control for the future mass spectrometry experiment.

6. Loss of *lin-28a* does not affect worm's survival against *P. aeruginosa* infection.

Since *lin-28a* is the predominant isoform expressed at the L4 stage, and is upregulated isoform upon *P. aeruginosa* infection, it is reasonable to propose that *lin-28a* could be solely responsible for the pathogen resistance phenotype observed in *lin-28(n719)* animals on *P. aeruginosa*. However, I observed no difference in survival on *P. aeruginosa* for *lin-28(ma289)* (*lin-28a* deletion) animals compared to wild type (Figure 3.8A). Interestingly, *lin-28(ma289)* animals might have an extended lifespan (Figure 3.8B) which requires further experimental confirmation. So, it seems that the pathogen resistance phenotype of *lin-28(n719)* is not solely from the *lin-28a* isoform, but it is also possible that LIN-28B might be upregulated in *lin-28(ma289)* animals to compensate the loss of LIN-28A for the pathogen resistance phenotype. Western blot analysis of LIN-28 protein levels in L4 stage wild type and *lin-28(ma289)* animals is needed to test this hypothesis.

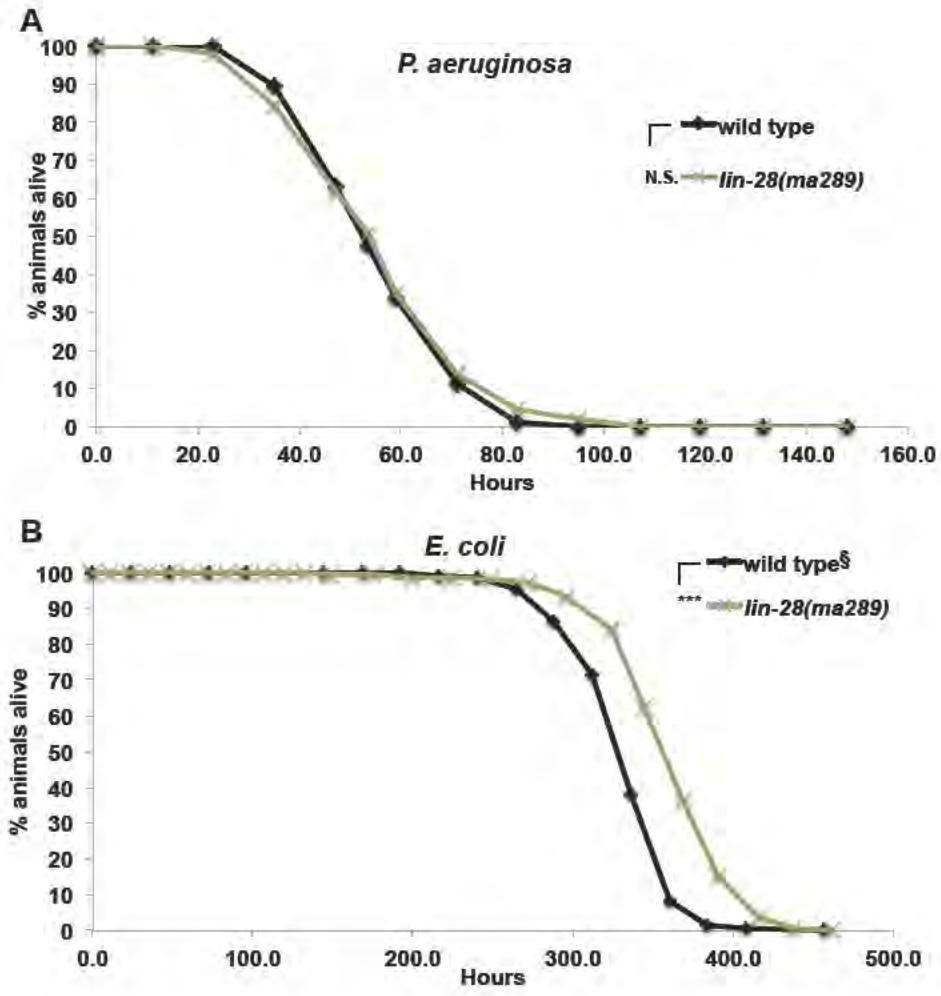

Figure 3.8 *lin-28a* is not required for survival on *P. aeruginosa*. (A) Survival of wild type (N2) and *lin-28(ma289)* animals on *P. aeruginosa*. (B) Lifespan of wild type (N2) and *lin-28(ma289)* animals on *E. coli* HB101. *** $p < 0.001$, N.S. not significant, log-rank test. § indicates that the wild type data here were not obtained in parallel since the plate were contaminated for the wild type samples in same experiment with *lin-28(ma289)*.

7. The enhancement of *let*-7 family miRNA mutant's heterochronic phenotypes on *P. aeruginosa* occurs during larval development.

The heterochronic phenotype enhancement of *let-7* family miRNA mutants on *P. aeruginosa* was observed at young adult stage. In order to confirm that this phenotype is due to enhancement of heterochronic defects during larval development instead of only at the L4 to adult transition, I examined the seam cell phenotype of early L4 stage wild type and *mir-48 mir-241(nDf51)* animals on *P. aeruginosa*. As expected, I still observed the enhancement of seam cell defects for the L4 stage *mir-48 mir-241(nDf51)* animals on *P. aeruginosa* (Figure 3.9). Therefore, the heterochronic phenotype enhancement of *let-7* family miRNA mutant on *P. aeruginosa* could not be simply caused by an over-proliferation of seam cells at the L4 molt.

8. *P. aeruginosa* infection does not seem to cause a general impairment of the miRNA pathway.

Thus far, I observed that *let-7* family miRNA activity is suppressed upon *P. aeruginosa* infection. I wondered if this effect of *P. aeruginosa* on *let-7* family miRNA activity might reflect a general inhibition of the miRNA pathway that could also affect other miRNAs. Therefore, I tested mutants of miRNA pathway components in *C. elegans* (*alg-1*, *alg-2*, *nhl-2*) (15) for the heterochronic phenotypes on *P. aeruginosa*, and I observed enhanced heterochronic phenotypes for *alg-1(gk214)* and *nhl-2(ok818); mir-48(n4097)* animals (Figure 3.10A and B). I think the reason why there is no phenotypic enhancement for

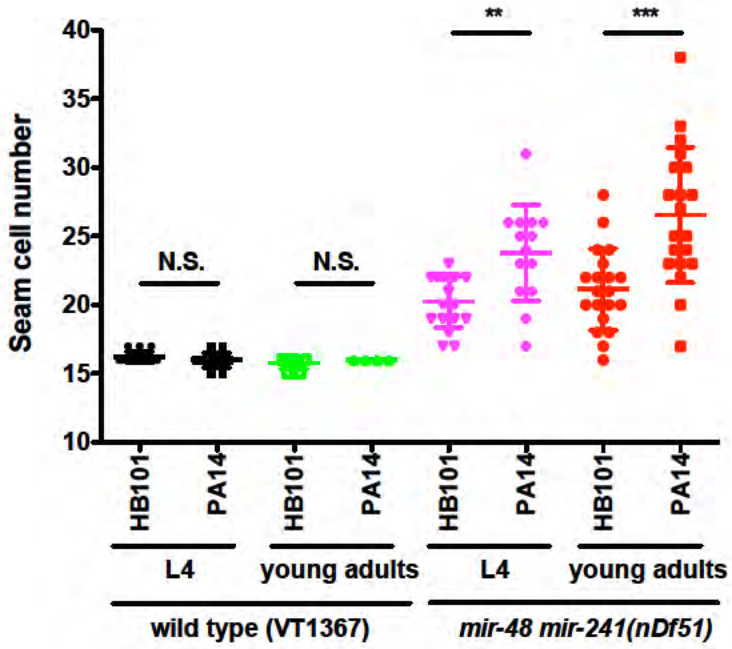

Figure 3.9 Seam cell phenotype of L4 and young adult stage wild type and *mir-48 mir-241(nDf51)* animals on HB101 and PA14. Error bars, SDs. * $p < 0.05$, ** $p < 0.01$, *** $p < 0.001$, N.S. not significant, two-tailed *t*-test.

alg-2(ok304) animals on *P. aeruginosa* could be because the phenotype of this mutant was not sufficiently sensitized genetically. These results suggest that *P. aeruginosa* could not solely act on either *alg-1* or *nhl-2* to regulate *let-7* family miRNA activity, which is consistent with our previous results that p38 regulates the transcription of *let-7* family miRNAs directly.

Next, if *P. aeruginosa* infection leads to a compromised miRNA pathway in general, I would expect that the phenotype of other miRNA mutants, besides *let-7* family, could be enhanced on *P. aeruginosa*. So, I tested if the ASE neuron phenotypes of *lsy-6(ot150)* animals could be affected by *P. aeruginosa*. As it is shown in Figure 3.10C, there is no effect of *P. aeruginosa* on the ASE neuron phenotypes of *lsy-6(ot150)* animals. This suggests that the downregulation of *let-7* family miRNA activity upon *P. aeruginosa* infection is probably specific to *let-7* family miRNAs and may not reflect a generally compromised miRNA pathway.

9. The expression changes of several pathogen response genes in wild type and *let-7(mg279)* animals upon *P. aeruginosa* infection.

In Chapter II, we observed that upon *P. aeruginosa* infection *let-7(mg279)* accumulates much less bacterial outer membrane vesicles compared to wild type animals, and I suspect that this could be caused by a hyper-activation of the innate immune pathway in *let-7(mg279)* animals. Therefore, I performed qRT-PCR of wild type and *let-7(mg279)* animals for several genes that are known to be regulated by *P. aeruginosa* infection (120, 129). The genes exhibited statistically significant changes are shown in Figure 3.11. Even though upon *P.*

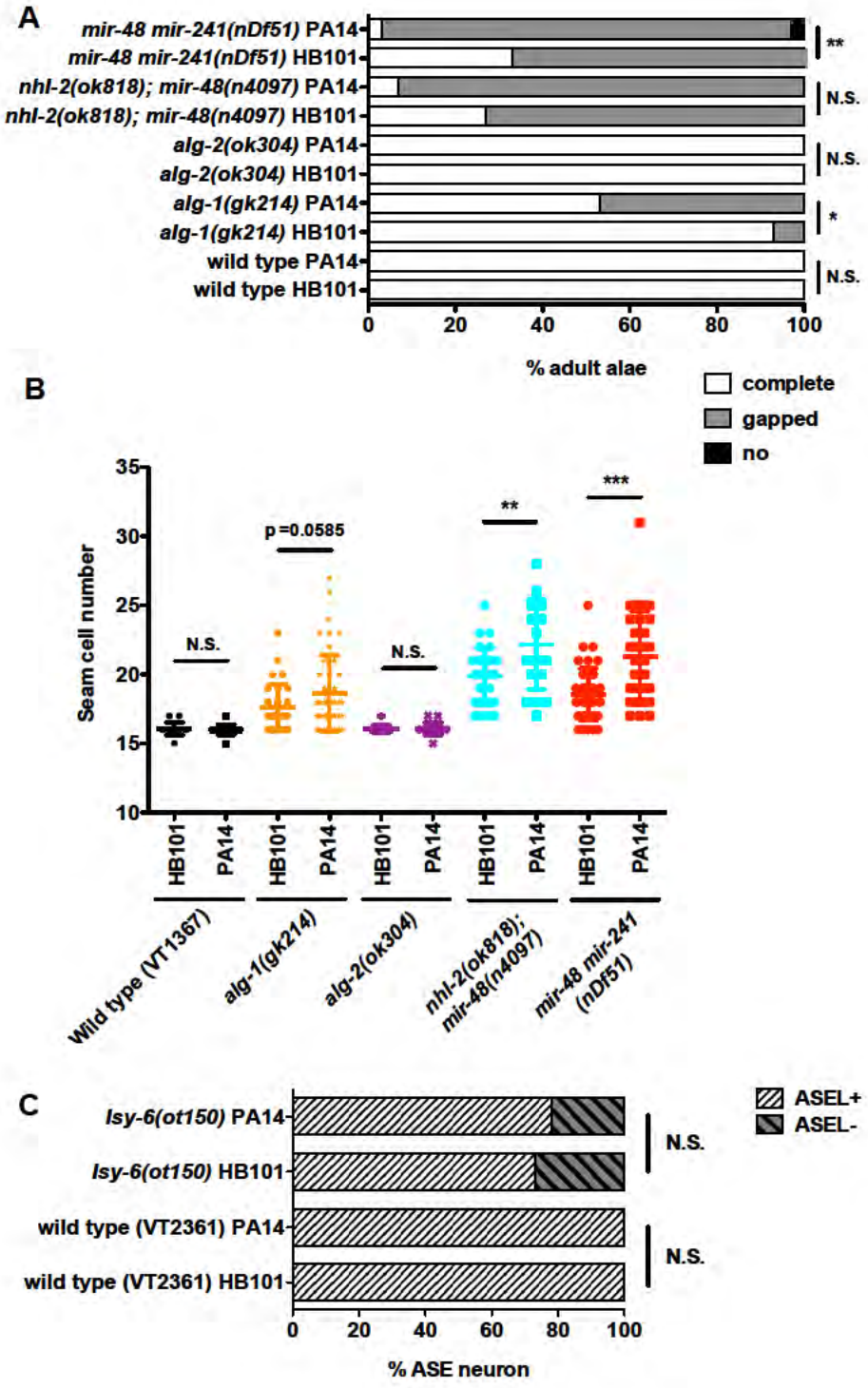
A
mir-48 mir-241(nDf51) PA14
mir-48 mir-241(nDf51) HB101
nhl-2(ok818); mir-48(n4097) PA14
nhl-2(ok818); mir-48(n4097) HB101
alg-2(ok304) PA14
alg-2(ok304) HB101
alg-1(gk214) PA14
alg-1(gk214) HB101
wild type PA14
wild type HB101
**
N.S.
N.S.
*
N.S.
0 20 40 60 80 100
% adult alae
complete
gapped
no
B
Seam cell number
35 30 25 20 15 10
N.S.
p =0.0585
N.S.
**
***
HB101 PA14 HB101 PA14 HB101 PA14 HB101 PA14 HB101 PA14
Wild type (VT1367)
alg-1(gk214)
alg-2(ok304)
nhl-2(ok818); mir-48(n4097)
mir-48 mir-241 (nDf51)
C
lsy-6(ot150) PA14
lsy-6(ot150) HB101
wild type (VT2361) PA14
wild type (VT2361) HB101
N.S.
N.S.
0 20 40 60 80 100
% ASE neuron
ASEL+
ASEL-

Figure 3.10 *P. aeruginosa* does not seem to affect the miRNA pathway in general. (A) Adult alae and (B) seam cell phenotypes of wild type (VT1367), *alg-1(gk214)*, *alg-2(ok304)*, *nhl-2(ok818); mir-48(n4097)* and *mir-48 mir-241(nDf51)* animals on HB101 and PA14. (C) ASE neuron phenotype of wild type (VT2361) and *lsy-6(ot150)* animals on HB101 and PA14. ASEL+ means ASEL neuron has *lim-6::gfp* expression and ASEL- indicates that there is no *lim-6::gfp* expression in the ASEL neuron. Error bars, SDs. * $p < 0.05$, ** $p < 0.01$, *** $p < 0.001$, N.S. not significant, chi-square test for adult alae phenotype and ASE neuron phenotype, two-tailed *t*-test for seam cell phenotype.

A

Genes	Proteins	Change on PA14	PMK-1 dependent	SKN-1 target
tir-1	TIR domain adaptor protein	up		
gst-4	Glutathione S-Transferase	down		YES
tsp-1	trans membrane protein	up	NO	
ilys-5	lysozyme	down		
lys-3	lysozyme	up		
C17H12.8	CUB like domain	up	YES	
F55G11.4	CUB like domain	up		

B

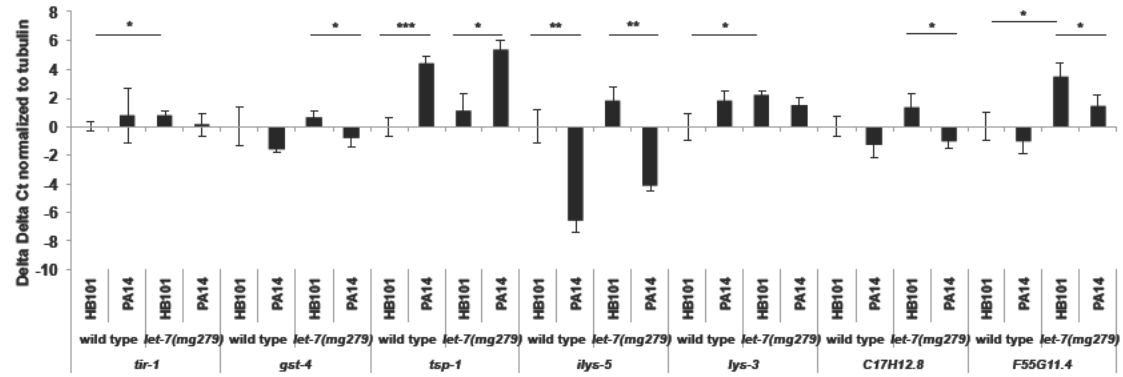

Figure 3.11 Expression levels of *P. aeruginosa*-response genes in wild type and *let-7(mg279)* animals. (A) A list of genes whose expression level changes on PA14. (B) Delta Delta Ct of *P. aeruginosa*-response genes after 24 hour treatment on HB101 or PA14. Data were normalized to tubulin and then to the wild type HB101 group. Error bars, SDs. * $p < 0.05$, ** $p < 0.01$, *** $p < 0.001$, two-tailed *t*-test. Only the statistically significant results were shown on the graph.

aeruginosa infection we did not observe any hyper-activation of these genes in *let-7(mg279)* animals compared to wild type, I did notice that several genes were already upregulated in *let-7(mg279)* animals on *E. coli*, especially *tir-1* (the upstream adaptor for the p38 MAPK pathway). This indicates that *let-7(mg279)* animals may have an elevated basal level of innate immune response, which could contribute to the enhanced survival of these animals on *P. aeruginosa* However, whole-genome studies are needed to prove this hypothesis.

10. The effects of other stresses, pathogen and innate immune pathways on the developmental timing phenotypes of *mir-48 mir-241(nDf51)* animals.

We found that the pathogenicity of *P. aeruginosa* is required for the downregulation of *let-7* family miRNA activity, thus, I wonder if one of the known pathogenicity factors of *P. aeruginosa* (exotoxin A (ToxA) (151)) could induce this downregulation. ToxA is an AB toxin that catalyzes ADP ribosylation of elongation factor 2, which blocks protein synthesis, and E575 of ToxA is required for the ribosylation reaction (155, 156). In order to test if ToxA is responsible for the downregulation of *let-7* family miRNAs, I utilized *E. coli* HT115 strains that express ToxA, mutant form of ToxA (ToxA E575Δ) and vector control. Interestingly, ToxA has no effect on the heterochronic phenotypes of *mir-48 mir-241(nDf51)* animals (Figure 3.12A and B), which suggests that ToxA might not be the *P. aeruginosa* pathogenicity factor required for the regulation of *let-7* family miRNAs.

Next, since the ER stress pathway is activated when worms are infected with *P. aeruginosa* (125), I wanted to test if ER stress could induce the downregulation of *let-7* family miRNA activity. So, I examined if the ER stress inducer, tunicamycin, could affect the heterochronic phenotypes of *mir-48 mir-241(nDf51)* animals. As it is shown in Figure 3.12C and D, I did not observe any enhancement of the heterochronic phenotypes of *mir-48 mir-241(nDf51)* animals on tunicamycin, which suggests that simply inducing ER stress could not suppress *let-7* family miRNA activity.

Besides the bacteria diets shown in Chapter II, I also tested if another bacterial pathogen *Staphylococcus aureus* (*S. aureus*) could affect the developmental timing phenotype of the *let-7* family miRNA mutant. Since worms could not develop from L1 to adults on *S. aureus*, I performed this experiment starting with the L2 stage animals. With this caveat, there is no change in the heterochronic phenotypes of wild type or *mir-48 mir-241(nDf51)* animals on *S. aureus* (Figure 3.12E and F).

Although our results indicate that ToxA, tunicamycin or *S. aureus* could not affect the activity of *let-7* family miRNAs, there is still a caveat that the efficacy of these stressors might not be strong enough due to the experimental feasibility. Alternatively, I can test if any of the known innate immune pathways activated by these stresses could affect the *let-7* family miRNA activity. Therefore, I knocked down each gene that is important for other innate immune response pathways in the parental generation and scored the heterochronic

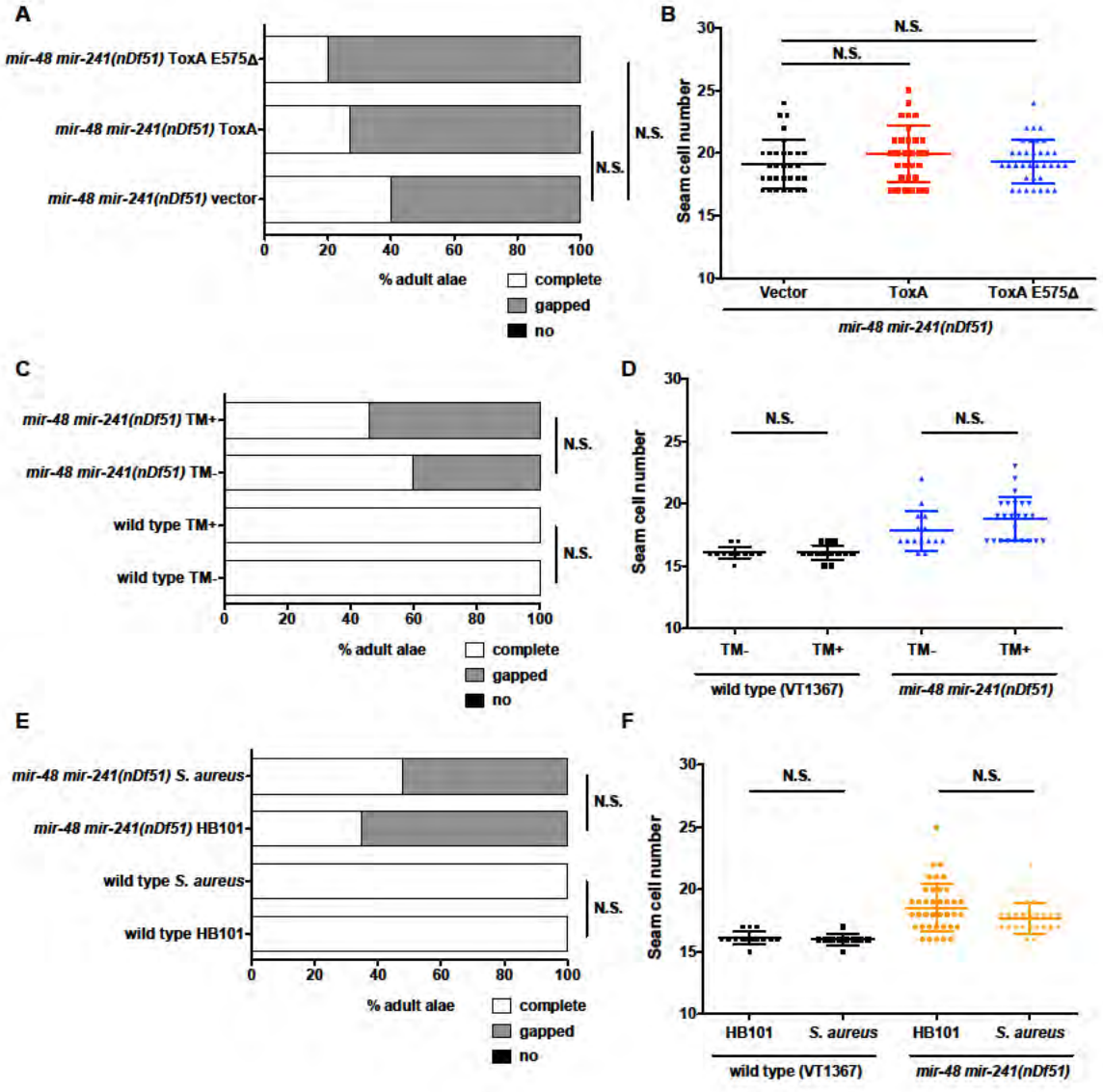
A
mir-48 mir-241(nDf51) ToxA E575Δ
mir-48 mir-241(nDf51) ToxA
mir-48 mir-241(nDf51) vector
N.S.
N.S.
0
20
40
60
80
100
% adult alae
complete
gapped
no
B
N.S.
N.S.
Seam cell number
30
25
20
15
10
Vector
ToxA
ToxA E575Δ
mir-48 mir-241(nDf51)
C
mir-48 mir-241(nDf51) TM+
mir-48 mir-241(nDf51) TM-
wild type TM+
wild type TM-
N.S.
N.S.
% adult alae
complete
gapped
no
D
N.S.
N.S.
Seam cell number
TM-
TM+
TM-
TM+
wild type (VT1367)
mir-48 mir-241(nDf51)
E
mir-48 mir-241(nDf51) S. aureus
mir-48 mir-241(nDf51) HB101
wild type S. aureus
wild type HB101
N.S.
N.S.
% adult alae
complete
gapped
no
F
N.S.
N.S.
Seam cell number
HB101
S. aureus
HB101
S. aureus
wild type (VT1367)
mir-48 mir-241(nDf51)

Figure 3.12 Heterochronic phenotypes of *mir-48 mir-241(nDf51)* animals upon different stresses. (A) Adult alae and (B) seam cell phenotypes of *mir-48 mir-241(nDf51)* animals on Vector, ToxA and ToxA E575Δ. (C) Adult alae and (D) seam cell phenotypes of wild type and *mir-48 mir-241(nDf51)* animals on ER stress inducer tunicamycin (TM). (E) Adult alae and (F) seam cell phenotypes of wild type and *mir-48 mir-241(nDf51)* animals on *S. aureus*. Error bars, SDs. * $p < 0.05$, ** $p < 0.01$, *** $p < 0.001$, N.S. not significant, chi-square test for adult alae phenotype and two-tailed *t*-test for seam cell phenotype.

phenotypes of the progeny after development on *E. coli* or *P. aeruginosa*. Because the effect of RNAi in *C. elegans* is transferable through generations (157), I expect that the progeny should have lower levels of the gene knocked down in their parental generation. I found that knocking down several innate immune pathways (*daf-16*, *zip-2*, *egl-5*, *bar-1* and *tol-1*) (129, 144, 147, 148) that function in parallel to the p38 MAPK pathway did not affect the enhancement of heterochronic phenotypes of *mir-48 mir-241(nDf51)* animals on *P. aeruginosa* (Figure 3.13). *zip-2* is an important downstream regulator for ToxA's effect on *C. elegans* (151), and beta-catenin (*bar-1*) and HOX transcription factor (*egl-5*) are the major innate immune response pathway against *S. aureus* infection (148). Therefore, our results here provide additional support that the downregulation of *let-7* family miRNA activity on *P. aeruginosa* is specifically elicited by the p38 MAPK pathway. However, given the nature of RNAi, it is likely that there is still residual expression of the knocked down genes, which could lead to false negative results. Experiments with genetic knockouts of other innate immune response pathway genes are required to confirm our results from the RNAi experiment.

Interestingly, *dkf-2* encodes a protein kinase D upstream of the p38 MAPK pathway (145) and the G-protein coupled receptor FSHR-1 are required for the regulation of *let-7* family miRNA activity on *P. aeruginosa* (Figure 3.13). It has been previously shown that even though *fshr-1* and the p38 MAPK pathway mostly function in parallel in response to *P. aeruginosa* infection, they share

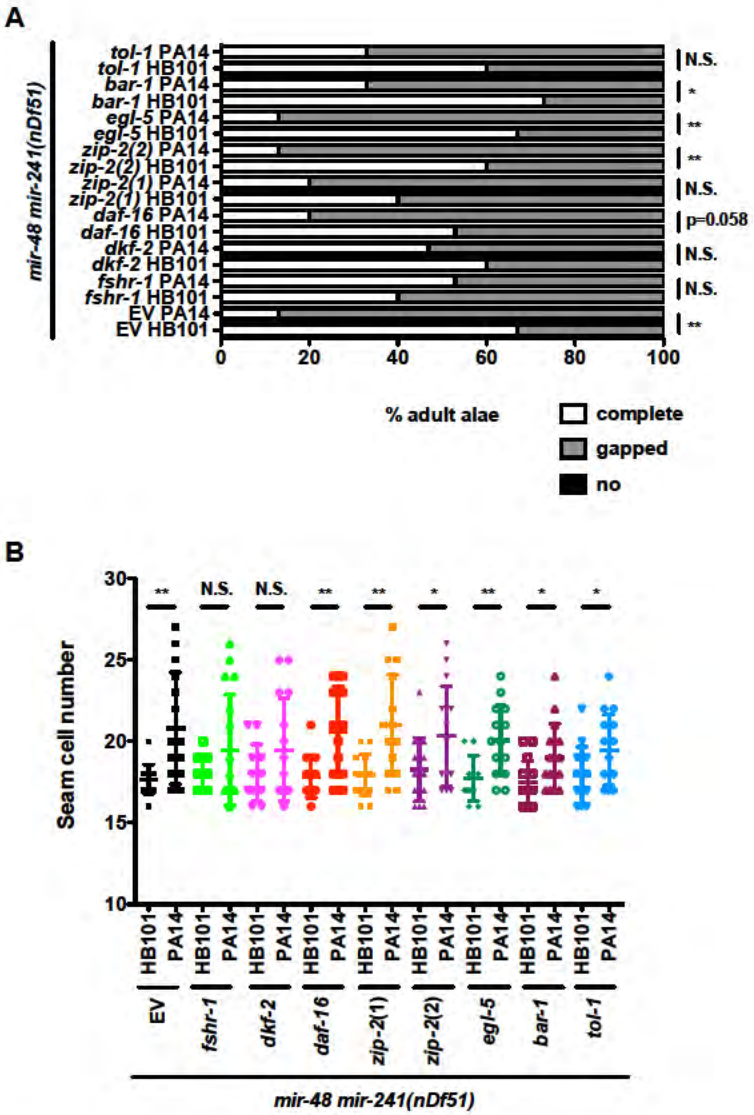

Figure 3.13 The effects of several pathogen response pathways on the heterochronic phenotypes of *mir-48 mir-241(nDf51)* animals upon *P. aeruginosa* infection. (A) Adult alae and (B) seam cell phenotypes of *mir-48 mir-241(nDf51)* animals on HB101 and PA14 after knocking down the genes indicated. There are two *zip-2* RNAi clones (*zip-2*(1) is from the ORF library and *zip-2*(2) is from the Ahringer library). Error bars, SDs. * $p < 0.05$, ** $p < 0.01$, *** $p < 0.001$, N.S. not significant, chi-square test for adult alae phenotype and two-tailed *t*-test for seam cell phenotype.

some downstream factors. Our results suggest that the shared downstream factors between *fshr-1* and the p38 MAPK pathway might be important for the regulation of *let-7* family miRNAs on *P. aeruginosa*.

III.E. Discussion

In *C. elegans*, many developmental regulators could have alternative functions in other tissues and/or at different stages. For example, the p38 MAPK pathway was first shown to regulate the asymmetric cell fate decisions in the olfactory AWC neurons in the embryos (158-160), and it was later on shown to control the innate immune response at larval and adult stages (124). Similarly, I found here that the developmental timing regulator *lin-28* is also involved in the regulation of pathogen resistance against *P. aeruginosa* infection through the *let-7* family miRNAs. This regulation between *lin-28* and *let-7* family miRNAs in pathogen resistance seems to be distinct from their roles in developmental timing.

Interestingly, I observed that *mir-48 mir-241(nDf51)* suppressed the pathogen resistance phenotype of *lin-28(n719)* animals on *P. aeruginosa*. However, the phase in which *mir-48 mir-241(nDf51)* animals die faster than wild type seems to be suppressed by *lin-28(n719)* as well (Figure 3.1A). Our previous study indicates that this phase in which *mir-48 mir-241(nDf51)* animals initially die faster than wild type is probably due to the reduced fitness of *mir-48 mir-241(nDf51)* animals (152). Therefore, I propose that besides being upstream of

let-7 family miRNAs in pathogen resistance, *lin-28* is also possibly downstream of *mir-48* and *mir-241* in the regulation of worm's general fitness, however, longevity assays for these mutants are needed to test this hypothesis.

The downregulation of LIN-28 protein during larval development seems to be dramatically delayed when worms were treated with *P. aeruginosa* (Figure 3.5A). I proposed that this delay could be due to the suppression of *let-7* family miRNA activity on *P. aeruginosa*. However, there could be another possible explanation for this result. When cultured on *P. aeruginosa* , worms tend to go through larval development slower than when cultured on *E. coli*. This developmental delay affects individual worms to a different degree, which results in asynchronous population of worms on *P. aeruginosa*. Therefore, the stages labeled on Figure 3.5A in *P. aeruginosa* treatment represent the majority of the population while some earlier stage animals were actually present in the sample as well, which could lead to this higher LIN-28 protein levels on *P. aeruginosa* since LIN-28 is very abundant in the early larval stages. However, this caveat does not affect our experiments regarding LIN-28 protein levels of the L4 stage animals because they were treated with *P. aeruginosa* for a maximum of 8 hours and no significant developmental delay was observed for that short period of time.

Because I did not observe a significant increase of LIN-28 protein levels on *P. aeruginosa* in Figure 3.5C and D, it still remains unknown whether the upregulation of LIN-28 is specifically caused by *P. aeruginosa* and the p38 MAPK

pathway. The *P. aeruginosa* treatment was carried out at 25°C on adults that had developed at 20°C. Therefore, it is possible that the temperature shift could elicit the upregulation of LIN-28, which should be tested in future studies. Additionally, *lin-28* mRNA and protein levels in wild type and *pmk-1(km25)* animals upon *P. aeruginosa* infection should be examined to determine if the p38 MAPK pathway is required for the upregulation of LIN-28 on *P. aeruginosa*.

Interestingly, only one of the two gene isoforms of *lin-28*, *lin-28a*, seems to be present and upregulated at the L4 stage upon *P. aeruginosa* infection. However, deleting *lin-28a* does not have any effect on worm's survival against *P. aeruginosa* infection. It is possible that there might be compensation in LIN-28B protein expression when *lin-28a* is removed. Alternatively, *lin-28a* and *lin-28b* could function redundantly for pathogen resistance against *P. aeruginosa* infection in early developmental stages (Embryonic stage to L3 stage). Interestingly, the *lin-28a* mutant might have an increased lifespan in our lifespan assay that was performed at 25°C with SK plates containing FUDR (Figure 3.8B). The reason for this lifespan assay condition is to control for the *P. aeruginosa* killing assay, but this condition could also be considered stressful for *C. elegans*. Therefore, the prolonged life span observed for *lin-28a* mutant could be due to *lin-28a*'s role in regulating stress response.

Another interesting finding from this study is that LIN-28A protein is phosphorylated, and the amount of mobility shift due to phosphorylation suggests that more than one phosphate group is on LIN-28A (Figure 3.7C). Mass

spectrometry experiment is needed to identify the phosphorylation sites and creating mutations in the phosphorylation sites by CRISPR/Cas9 technology will allow us to study the functions of the phosphorylation. Furthermore, it seems that LIN-28A is the only phosphorylated LIN-28 protein isoform in *C. elegans*, which echoes a study showing that there is phosphorylation on human LIN28A. In that study, one of the phosphorylation sites of human LIN28A was regulated during the early differentiation of embryonic stem cells (154). Although I observed the doublet band pattern in all larval developmental stages, there could still be specific *C. elegans* LIN-28A phosphorylation sites being regulated during development. Protein phosphorylation is known to play important roles in regulating signal transduction, protein localization, and protein stability (161). Mammalian LIN28A and LIN28B have been shown to exhibit different modes of regulation on *let-7* and different sub-cellular localizations (162). Whether *C. elegans* LIN-28A and LIN-28B also have distinct regulatory mechanisms and whether the phosphorylation of LIN-28A is important for the potential distinction remain to be investigated. Additionally, in order to identify specific functions for these two *lin-28* isoforms, a two-color splicing reporter system (163) will be used to identify differences in temporal and spatial expression patterns between *lin-28a* and *lin-28b*, which could indicates potentially diverse functions for these two gene isoforms.

A previous study showed that there might be a broad role for miRNAs in suppressing basal activity of *C. elegans* pathogen response in the intestine

(164), consistent with our finding that *let-7(mg279)* animals shown elevated basal levels of pathogen response gene expression. However, the mechanisms of how elevated level of basal pathogen resistance could affect survival on *P. aeruginosa* remains to be investigated. The same previous study also showed that the inactivation of miRNA-induced silencing complex by loss of *ain-1* (*C. elegans* GW182 protein) enhanced the worm's survival on *P. aeruginosa* (164). Therefore, I examined if *P. aeruginosa* treatment could affect miRNA pathway in general to exhibit the enhancement of heterochronic phenotypes in *let-7* family miRNA mutants. However, I found that neither *alg-1* nor *nhl-2* is solely required for the downregulation of *let-7* family miRNA activity on *P. aeruginosa*, and the activity of *lsy-6* was not affected upon *P. aeruginosa* infection. Even though whole-genome studies are needed, I think our results to date along with other studies (112, 165) suggest that the effect of *P. aeruginosa* on miRNA pathway might be specific to certain miRNA families, and the enhanced survival phenotype of *ain-1* mutants could be due to the reduce activity of *let-7* family miRNAs.

In conclusion, we provided more information in this chapter on the roles of another developmental timing regulator (*lin-28*) in pathogen resistance against *P. aeruginosa* infection. This finding along with our previous data on *let-7* family miRNAs suggest that the developmental timing pathway and the innate immune pathway in *C. elegans* are highly integrated perhaps to maintain the robust developmental processes in face of a pathogen infection.

CHAPTER IV: Staufen negatively modulates microRNA activity in *Caenorhabditis elegans*

IV.A. Abstract

The double-stranded RNA-binding protein Staufen has been implicated in various post-transcriptional gene regulatory processes. Here we demonstrate that the *Caenorhabditis elegans* homolog of Staufen, STAU-1, functionally interacts with microRNAs. Loss-of-function mutations of *stau-1* significantly suppress phenotypes of *let-7* family microRNA mutants, a hypomorphic allele of *dicer* and a *lsy-6* microRNA partial loss-of-function mutant. Furthermore, STAU-1 modulates the activity of *lin-14*, a target of *lin-4* and *let-7* family microRNAs, and this modulation is abolished when the 3' untranslated region of *lin-14* is removed. Deep sequencing of small RNA cDNA libraries reveals no dramatic change in the levels of microRNAs, or other small RNA populations between wild type and *stau-1* mutant, with the exception of certain endogenous siRNAs in the WAGO pathway. The modulation of microRNA activity by STAU-1 does not seem to be associated with the previously reported enhanced exogenous RNAi (Eri) phenotype of *stau-1* mutants since *eri-1* exhibits the opposite effect on microRNA activity. Altogether, our results suggest that STAU-1 negatively modulates microRNA activity downstream of biogenesis, possibly by competing with microRNAs for binding on the 3' untranslated region of target mRNAs.

IV.B. Introduction

MicroRNAs (miRNAs) are a class of endogenous non-coding small RNAs that post-transcriptionally regulate gene expression primarily through binding to the 3’ untranslated region (3’UTR) of target mRNAs, and inhibiting translation and/or mRNA stability (8). MiRNAs are usually transcribed into primary transcripts (pri-miRNAs) by RNA polymerase II. Pri-miRNAs are processed into hairpin structured precursor miRNAs (pre-miRNAs) by Drosha-DGCR8 complex in the nucleus, and then pre-miRNAs are exported into cytoplasm and further processed by Dicer to generate the ~21 nucleotide-long mature miRNAs (166). The seed sequence (nucleotides 2-7) of a mature miRNA dictates the specificity of miRNA’s recognition on target mRNAs, therefore, miRNAs with the same seed sequence are grouped into a family and predicated to potentially share the same set of target mRNAs (18).

MiRNAs exert their repression on mRNAs through the assembly of miRNA-induced silencing complex (miRISC) on the 3’UTR of target mRNAs. MiRISC is a ribonucleoprotein complex with a miRNA-specific Argonaute (AGO) protein loaded with a mature miRNA and a AGO binding partner GW182 protein (167). Besides AGO and GW182, other RNA-binding proteins have been shown to affect miRNA activity through biogenesis, such as the case of LIN-28 (47), miRISC activity, as for NHL-2 (66) and target site accessibility, as shown for Pumilio, HuR and Dnd1 (55-57, 60-62, 168).

Staufen is a conserved double-stranded RNA-binding protein that contains five double-stranded RNA-binding domains, and that was first identified in *Drosophila* to regulate mRNA localization and translation (*oskar* in oocytes, *bicoid* in embryos and *prospero* in neuroblasts) (169-171). For example, Staufen binding to the 3'UTR of *bicoid* and *prospero* mRNAs is required for their localization (172-174). In mammalian neurons, Staufen homologs (Staufen1 and Staufen2) are also known to regulate mRNA transport and the activation of localized mRNA translation (175, 176). Two groups have shown that Staufen1 can bind to long-range RNA duplexes in the 3'UTR of mRNAs (177, 178). Besides regulating mRNA localization and translation, mammalian Staufen can also mediate mRNA decay through interaction with the nonsense medicated decay regulator Upf1 (179). In *Caenorhabditis elegans* (*C. elegans*), there is only one Staufen homolog, *stau-1*, and it has been shown to have high binding affinity for double-stranded RNA *in vitro*. STAU-1 is expressed at all developmental stages in *C. elegans* and partial loss-of-function mutants (*stau-1(tm2266)* and *stau-1(q798)*) exhibit phenotypes that include enhanced transgene silencing, enhanced exogenous RNAi and mild germline defects (180).

Previous studies demonstrate that miRISC components and miRNAs are present in Staufen-containing RNA granules (181, 182), which indicates that Staufen might affect the miRNA pathway, perhaps by influencing miRNA biogenesis and/or function. Here we report genetic evidence that *C. elegans* STAU-1 exerts activity in opposition to certain miRNAs; we show that loss of

function for *stau-1* genetically suppresses the phenotypes of mutants in several distinct miRNA genes and a miRNA biogenesis factor. Further, our small RNA sequencing data show that STAU-1 does not have any significant effect on the levels of mature miRNAs, indicating that Staufen can inhibit the activity of miRNAs downstream of miRNA biogenesis. Finally, we report data suggesting that Staufen-mediated opposition of miRNA activity acts via the 3'UTR of miRNA target mRNAs.

IV.C. Materials and methods

The following are methods not previously described in Chapter II and III.

Targeted genome editing by CRISPR/Cas9. In order to generate *stau-1* null mutants, we adapted previously described co-CRISPR strategies (183, 184) with our modifications. Wild type animals (N2) were injected with a mixture containing 40ng/µl *eft-3::cas9* vector, 35ng/µl *unc-22* sgRNA vector, 35ng/µl *dpy-10* sgRNA vector, 35ng/µl *stau-1* sgRNA-1 vector, 35ng/µl *stau-1* sgRNA-2 vector and 15ng/µl *sur-5::gfp* vector. The sequences for *stau-1* sgRNAs are: GGATGGAGTGATGATAGTAC (sgRNA-1) and TACGGATCTGGCAGATACTT (sgRNA-2). F1 worms exhibiting any of the dumpy and/or twitching phenotypes, and/or *sur-5::gfp* expression were picked individually to plates and allowed to produce F2 progeny. These F1 animals were lysed in 10µl single-worm lysis buffer (50mM KCl, 10mM Tris-HCl pH 8.2, 2.5mM $MgCl_2$, 0.45% NP-40, 0.45% Tween-20, 0.01% Gelatin, 60 ng/µl proteinase K) at 60°C for 1 hour, and PCR

reactions were performed with primers (TCCTTCAATCGATGTGGCCAA and TGGCTCACATTTTGTTAAACGACA) and the sequence of PCR products was determined using Sanger sequencing. Both of the two mutations recovered were from CRISPR/Cas9 editing events by sgRNA-1.

To create endogenously tagged STAU-1, I performed CRISPR/Cas9 experiment with homology-directed recombination. Wild type animals (N2) were injected with a mixture containing 40ng/µl *eft-3::cas9* vector, 40ng/µl *unc-22* sgRNA vector, 40ng/µl *rol-6* vector, 40ng/µl *stau-1* sgRNA-3 vector, 40ng/µl *3xflag::stau-1* donor repair vector, 40ng/µl *pie-1* sgRNA vector and 40ng/µl *pie-1::gfp* donor repair vector. The sequence for *stau-1* sgRNA-3 is TACCTCCTCTGTCCCAATGC. The *3xflag::stau-1* donor repair vector was made with 800bp of homology flanking region at each side and PAM sequence was mutated from “NGG” to “NAG”. F1 worms exhibiting twitching, rolling, rolling and twitching phenotypes were picked individually to plates and allowed to produce F2 progeny. These F1 animals were genotyped with primers (TTGTCTGAAGCACGTCGCAG and GCCGCAGCTTGTTGAATCG) and PCR products were digested with BspHI to test for *3xflag* insertion. PCR products were also sent to Sanger sequencing to confirm the *3xflag* insertion. The two independent alleles generated were named *ma329* and *ma330*.

Western blot analysis. For STAU-1 western blots, samples were prepared from populations of mixed stage embryos and synchronized L4 stage larvae grown on *E. coli* HB101 at 20°C. Animals were washed off plates with M9

buffer and flash frozen in liquid nitrogen. Lysates were prepared by resuspending samples in lysis buffer (25mM HEPES pH7.5, 100mM NaCl, 0.25mM EDTA, 0.1% NP-40, 2mM DTT, PhosSTOP (Roche), Protease inhibitor (Roche)) and homogenized with a Branson SLPe sonicator. Lysates were centrifuged at 164,000rpm for 15 minutes at 4°C and the supernatants were collected. BioRad Protein Assay Dye Reagent Concentrate (Cat# 500-0006) was used to measure the protein concentration. 80µg of protein were used for the immunoblot analysis. STAU-1 was recognized by an anti-serum generated in Dr. Marvin Wickens laboratory (180) at 1:1000 dilution, gel loading was calibrated by re-probing blots with anti-α-tubulin antibody (Sigma-Aldrich Cat# T6074) at 1:20000 dilution. ALG-1 protein was recognized by a purified polyclonal antibody (185) at a 1:1000 dilution. The DCR-1 polyclonal antibody was applied at 1:1000 dilution (186), and anti-α-tubulin antibody (Sigma-Aldrich Cat# T6074) was used at 1:20000 dilution.

RNA extraction and small RNA cDNA cloning. Wild type (N2) and *stau-1(tm2266)* young adults were collected and flash frozen in liquid nitrogen. Three biological replicates were analyzed for each strain. Total RNA was extracted using Trizol reagent (Invitrogen). 20µg of total RNA for each sample was used to isolation small RNA populations. RNA samples were run on 15% PAGE/urea gel and small RNA populations were isolated from the gel with the size range from 18 nucleotide (nt) to 26 nt. A previously published small RNA cloning protocol (187) was used to generate cDNA libraries with the following modifications: 1) 3’ ligation reactions were performed at 4°C overnight; 2) 100 units of Superscript III

Reverse Transcriptase were used for first-strand cDNA synthesis for each sample and the Reverse Transcriptase reaction was performed at 42°C for 90 minutes. The Sterling CH *et al*. (2015) protocol involves only one RNA ligation to the 3’ end of the RNA, and hence recovers RNA species regardless of 5’ end structure.

Computational analysis of small RNA libraries. cDNA libraries were sequenced on the Ion Torrent (Proton) instrument according to manufacturer's protocols. Sequencing files in FastQ formats were processed using the Cutadapt method (version 1.2.1) (188) to remove the adapter sequences with the following options -e 0.25 -g ATTGATGGTGCCTACAG -a GATCGTTCGGACTGTAGATC.

Sequence files were split into libraries according to barcode sequences, and reads shorter than 16 nt were removed. For each library, reads with identical sequences were combined and the combined count was saved in Fasta files. Reads were then aligned to the *C. elegans* genome (WormBase release WS215) using bowtie (189) with arguments, -v 3 -f -B 1 -a–best –strata. Alignments were then filtered based on the length of the reads and the number of mismatches as follows: for sequence lengths 16-17, 18-19, 20-24, or >24: zero, one, two, or three mismatches were allowed, respectively.

Annotations of coding genes, transposons, tRNAs, rRNAs, piRNAs, and miRNAs were obtained from WormBase (release WS215) and miRBase (190) (Release 20). An in-house developed code was used to analyze the mapping results. To assign read counts to the miRNA sequences, we considered all reads

that mapped to the miRNA genomic loci starting within -5 to +5 nucleotides of the annotated 5’ end of mature miRNAs. For all the other small RNA species and genomic features (e.g. coding genes and transposons), we counted all reads that mapped within the annotated region in sense and anti-sense orientations separately.

For endo-siRNA analysis, we considered all reads that mapped anti-sense to the 5'UTR, coding exons and 3'UTR regions of each annotated gene. Annotations of target genes in the CSR-1, WAGO, ALG-3/4, and ERGO-1 pathways were downloaded from (191).

Differential expression analysis was performed using edgeR package in R (192).

Crosslinking immunoprecipitation (CLIP) Mix stage animals were raised on 24 of 6cm NGM plates for each of both tagged strains and wild type (N2). Right after animals consumed all the bacteria on the plates, UV crosslink in Stratalinker was done at energy setting 3000 (3kJ/m^2). Non-crosslinked samples from the tagged strains were also collected at the same time. Worm pellets were washed with M9 for 3 times and flash frozen in liquid nitrogen and then stored at -80°C. The CLIP experiment was adapted from previously published protocol (193).

Before each experiment, worm pellets (~1ml) were thawed on ice and 1ml of cold homogenization buffer (100mM NaCl, 25mM HEPES pH 7.5, 250uM EDTA, 0.10% NP-40, 2mM DTT, Complete mini protease inhibitor (Roche)) were

added to each sample. For the homogenization buffer, 25U/ml RNAse inhibitor and PhosSTOP (Roche) were also added to the buffer for CLIP and IP respectively. Samples were homogenized in Branson SLPe sonicator with the pulse of 20 seconds on, 60 seconds off at 20% power (30W). Lysates were centrifuged at 164,000rpm for 15 minutes at 4°C and the supernatants were collected. BioRad Protein Assay Dye Reagent Concentrate (Cat# 500-0006) was used to measure the protein concentration.

3mg and 6mg of lysates were used for IP and CLIP experiments respectively. Sigma anti-FLAG beads were used to capture the FLAG tagged proteins. 50µl of bead slurry was used for each sample and the bead slurry was washed with 500µl cold homogenization buffer for 3 times before adding to the samples. Lysates with washed beads were incubated at 4°C overnight with rotating. After incubation, beads were magnetized and supernatant were collected for western blot analysis. Beads were then washed 2 times with 500µl ice-cold wash buffer (20mM Tris-HCl pH 7.4, 137mM NaCl, 0.10% SDS, 0.50% sodium deoxycholate, 0.50% NP-40), 2 times with 500µl ice-cold high-salt wash buffer (100mM Tris-HCl pH 7.4, 685mM NaCl, 0.10% SDS, 0.50% sodium deoxycholate, 0.50% NP-40), and 2 times with 500µl ice-cold PNK buffer (50mM Tris-HCl pH 7.4, 10mM $MgCl_2$, 0.50% NP-40).

For IP experiments, SDS sample buffer was added to the beads and boiled at 95°C for 15 minutes, and then samples were run on SDS-PAGE run

and FLAG was recognized by anti-FLAG antibody (Thermo Pierce, Catalog#: PA1-984B) at 1:1000 dilution.

For CLIP experiments, after washing the beads, DNase digestion was carried out with Turbo DNase at 37°C for 15 minutes with intermittent shaking (1200rpm for 1min, then 1200rpm for 15 seconds every 3 minutes) and 1µl Ribolock/RNAse inhibitor were added in each sample before the incubation. After DNase reaction, beads were washed 1 time with ice-cold PNK-EDTA buffer (50mM Tris-HCl pH 7.4, 20mM EDTA, 0.50% NP-40) and 2 times with ice-cold PNK buffer.

Next, RNA trimming was performed with Micrococcal Nuclease at 1:100 dilution in MNase buffer (50mM Tris-HCl pH 7.9, 5mM $CaCl_2$). Reactions were carried out at 4°C for 10 minutes with rotating. Beads were washed afterwards 2 times with ice-cold PNK-EGTA buffer (50mM Tris-HCl pH 7.4, 20mM EGTA, 0.50% NP-40), 2 times with ice-cold wash buffer, and 2 times with ice-cold PNK buffer.

CIP reactions were used next to perform 3’ end de-phosphorylation. 3µl of CIP was used in 80µl reaction and samples were incubated at 37°C for 10 minutes with intermittent shaking (1200rpm for 15 seconds every 3 minute). Beads were then washed 2 times with PNK+EGTA buffer and 2 times with PNK buffer.

5’ end labeling was preformed with T4 PNK and P^{32}-gamma-ATP. 80µl reaction was used for each sample and incubated at 37°C for 10 minutes with

intermittent shaking at 1000rpm. Then, 10µl of 1mM nonradioactive ATP were added and incubated for 5 minutes at 37°C. Afterwards, beads were washed 3 times with PNK+EGTA buffer and resuspended in 30ul of PNK+EGTA buffer and 10ul of 4x NuPAGE LDS sample buffer. Samples were then incubated at 70°C for 10 minutes with optional shaking at 1000rpm.

Samples were run on a 10% Bis-Tris gel at 180V and gel was then transferred to a nitrocellulose membrane in the cold room at 40V for 4 hours. Membrane was rinsed with 1x PBS and wrapped in saran warp. Membrane was exposed to films (two sheets) and phosphor screen overnight. Films were developed in the dark room and phosphor imager was used to capture the image.

IV.D. Results

1. STAU-1 functionally modulates the activity of several miRNAs.

In order to identify if STAU-1 could modulate miRNA activity, I utilized sensitized genetic backgrounds described in Chapter I.

The first sensitized genetic backgrounds we investigated were the *let-7* family miRNA mutants. *C. elegans let-7* family miRNAs (including *let-7*, *mir-48*, *mir-84* and *mir-241*) function semi-redundantly in controlling the developmental timing of certain stage-specific hypodermal seam cell fates. Loss of *let-7* family miRNAs results in reiterations of early larval seam cell division patterns at later stages, and seam cells in these mutants also fail to properly differentiate adult

specific cuticular structures (called adult alae) at the young adult stage (Figure 4.1A). Three of the *let-7* family miRNAs (*mir-48*, *mir-84* and *mir-241*) are expressed starting at the L2 stage and function to regulate the L2 stage proliferative seam cell division, while the *let-7* miRNA is strongly upregulated from the L3 stage to control the larval-to-adult transition of seam cells (5, 74). These heterochronic *let-7* family miRNA mutant phenotypes are easily quantified by using microscopy to measure the formation of adult alae and to score the number of seam cells in young adults.

To test if STAU-1 modulates *let-7* family miRNA activity, we used two mutant strains (*mir-48 mir-241(nDf51)* and *let-7(n2853)*) that both have partially penetrant heterochronic phenotypes with gaps in adult alae and increased number of seam cells at the young adult stage. *mir-48 mir-241(nDf51)* mutant has two *let-7* family miRNAs removed while *let-7(n2853)* is a strong loss-of-function mutation at the seed region of *let-7* mature miRNA (5). Although the *stau-1* loss-of-function mutant does not exhibit any developmental timing defects in an otherwise wild type genetic background, we observed that both *stau-1(tm2266)* and *stau-1(q978)* significantly suppresses the heterochronic phenotypes of the *mir-48 mir-241(nDf51)* mutant (Figure 4.1B and C). Since *stau-1(tm2266)* and *stau-1(q978)* have similar effect on the phenotypes of *mir-48 mir-241(nDf51)* animals, we focused only on *stau-1(tm2266)* for further analysis. Besides suppressing the heterochronic phenotypes of *mir-48 mir-241(nDf51)* animals, *stau-1(tm2266)* also exerts significant suppression on the heterochronic

adult alae phenotype of *let-7(n2853)* animals (Figure 4.1B). We interpret this suppression of heterochronic phenotypes of *let-7* family miRNA mutants by *stau-1* loss of function to suggest that loss of *stau-1* function causes an increase in the activity of the remaining *let-7* family miRNAs. These results indicate that STAU-1 acts as a negative modulator of *let-7* family miRNA biogenesis or activity.

The second sensitized genetic background we tested is a *dicer* (*dcr-1*) hypomorphic allele, *bp132*. This mutation causes a single amino acid change in the RNase III domain of DCR-1 and has been previously shown to have developmental timing defects as indicated by increased number of seam cells and failure to form complete adult alae at the young adult stage (Figure 4.1A). The phenotypes of this partial loss-of-function mutant *dcr-1(bp132)* are stronger at 15°C and can be suppressed by a point mutation that alters the sequence of the *lin-4* miRNA precursor (3, 4, 84), indicating that the *dcr-1(bp132)* phenotypes reflect partially compromised *lin-4* biogenesis. We found that *stau-1(tm2266)* suppresses both adult alae and seam cell phenotypes of this *dcr-1(bp132)* mutant at 15°C (Figure 4.1D and E), suggesting that STAU-1 exerts a negative modulation of *lin-4* biogenesis or activity.

The third sensitized genetic background that we employed is a *lsy-6* miRNA hypomorphic mutant. *lsy-6* is known to regulate the asymmetric cell fate decision in the ASE neurons (75). The null allele of *lsy-6* causes a highly penetrant cell fate transformation phenotype where the ASEL neuron adopts the cell fate of the ASER neuron, which is detected by loss of expression of the

ASEL marker *lim-6*. The *lsy-6(ot150)* allele is a non-null (hypomorphic) point mutation 111 nt upstream of the *lsy-6* hairpin, which disrupts a *cis*-regulatory element required for *lsy-6* expression. The *lsy-6(ot150)* animals exhibit a weak phenotype with ~20% penetrance (194) (Figure 4.1F). *stau-1(tm2266)* animals do not exhibit any ASE neuron cell fate defects since all the animals have *lim-6* expression only in the ASEL neurons, yet the phenotype of *lsy-6(ot150)* animals is significantly suppressed by *stau-1(tm2266)* (Figure 4.1G). These results that loss-of-function of *stau-1* can potentiate the activity of *lsy-6* suggest that the role of STAU-1 as a negative modulator of miRNA activity is not restricted to miRNAs of the heterochronic pathway.

2. *stau-1* null mutants have the similar effect on miRNA activity as the partial loss-of-function mutants.

The *stau-1* mutants available so far are partial loss-of-function mutants that remove either the second (*tm2266*) or the fourth (*q798*) double-stranded RNA-binding domain (Figure 4.2A). Therefore, to test the effect of *stau-1* null mutants on miRNA activity and to determine if *stau-1* may have additional functions, we carried out CRISPR/Cas9 experiments to generate null mutants of *stau-1*. The guide RNA was designed to target the first exon of *stau-1* and we screened for frame-shift mutations that lead to premature stop codons. Two independent mutations were isolated: *ma327*, an 11 base-pair insertion, and *ma346*, a 5 base-pair deletion, both of which generate early premature stop codons (Figure 4.2A and B).

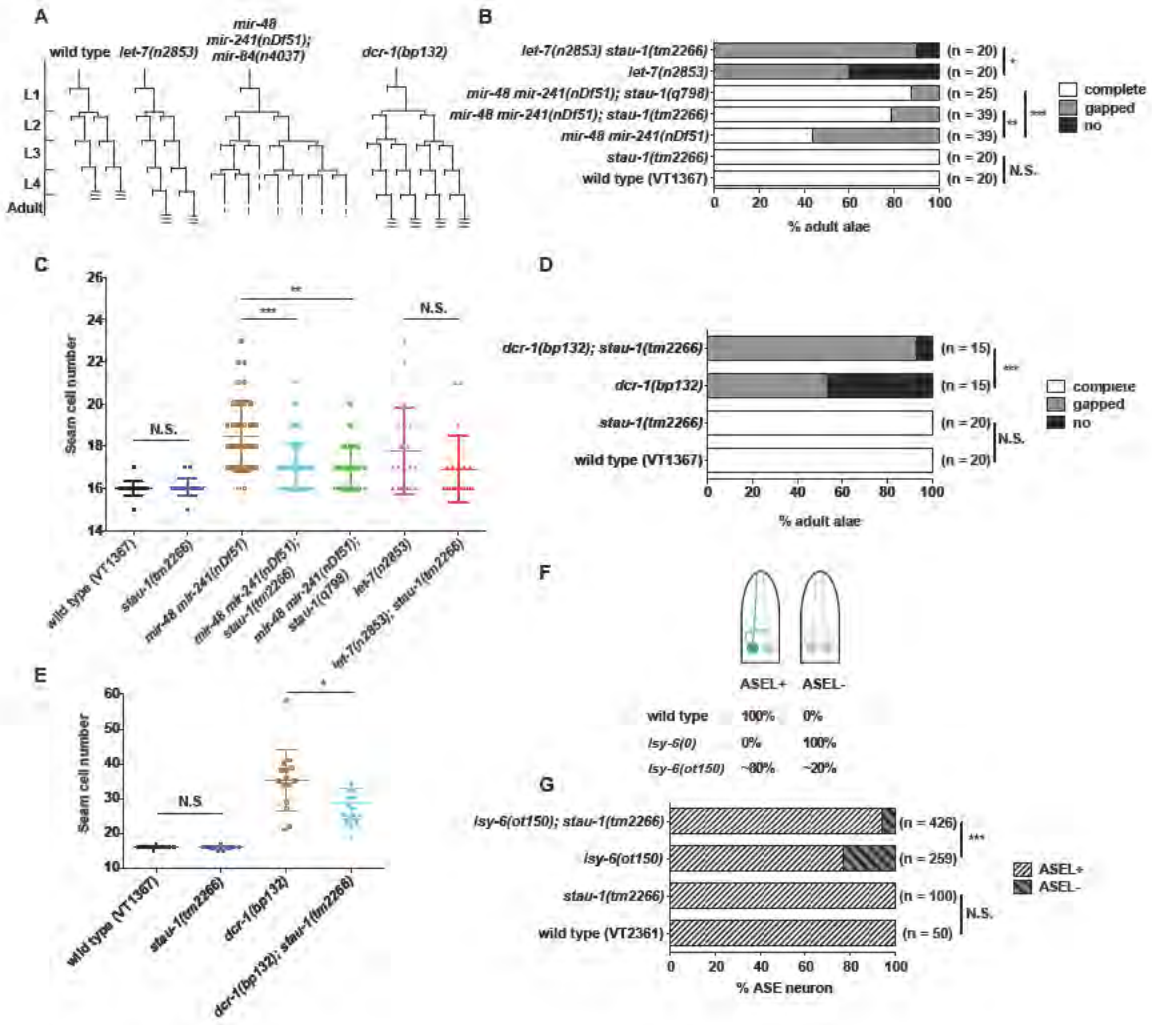
A
wild type
let-7(n2853)
mir-48 mir-241(nDf51); mir-84(n4037)
dcr-1(bp132)
L1
L2
L3
L4
Adult
B
let-7(n2853) stau-1(tm2266)
let-7(n2853)
mir-48 mir-241(nDf51); stau-1(q798)
mir-48 mir-241(nDf51); stau-1(tm2266)
mir-48 mir-241(nDf51)
stau-1(tm2266)
wild type (VT1367)
(n = 20)
(n = 20)
(n = 25)
(n = 39)
(n = 39)
(n = 20)
(n = 20)
*
**
***
N.S.
complete
gapped
no
0
20
40
60
80
100
% adult alae
C
Seam cell number
N.S.
***
**
N.S.
wild type (VT1367)
stau-1(tm2266)
mir-48 mir-241(nDf51)
mir-48 mir-241(nDf51); stau-1(tm2266)
mir-48 mir-241(nDf51); stau-1(q798)
let-7(n2853)
let-7(n2853); stau-1(tm2266)
D
dcr-1(bp132); stau-1(tm2266)
dcr-1(bp132)
stau-1(tm2266)
wild type (VT1367)
(n = 15)
(n = 15)
(n = 20)
(n = 20)
***
N.S.
complete
gapped
no
% adult alae
E
Seam cell number
N.S.
*
wild type (VT1367)
stau-1(tm2266)
dcr-1(bp132)
dcr-1(bp132); stau-1(tm2266)
F
ASEL+
ASEL-
wild type 100% 0%
lsy-6(0) 0% 100%
lsy-6(ot150) ~80% ~20%
G
lsy-6(ot150); stau-1(tm2266)
lsy-6(ot150)
stau-1(tm2266)
wild type (VT2361)
(n = 426)
(n = 259)
(n = 100)
(n = 50)
***
N.S.
ASEL+
ASEL-
% ASE neuron

Figure 4.1 Loss of function for *stau-1* suppresses the phenotypes associated with mutations of genes encoding miRNAs, or DCR-1, a miRNA biogenesis factor. (A) Diagrams of seam cell V lineage in wild type (N2), *let-7(n2853)*, *mir-48 mir-241(nDf51)*; *mir-84(n4037)* and *dcr-1(bp132)* animals. L1 to L4 are the four larval stages in *C. elegans* post-embryonic development. The three horizontal lines indicate adult alae formation. (B) Adult alae and (C) seam cell phenotypes of *stau-1* mutants in wild type and *let-7* family miRNA mutants' background. (D) Adult alae and (E) seam cell phenotypes of *stau-1(tm2266)* in combination with *dcr-1(bp132)*. The experiment with *dcr-1(bp132)* was carried out at 15°C. (F) A diagram of *C. elegans* larvae illustrating the ASE neuron phenotype of miRNA *lsy-6* mutants. The GFP expression in ASEL neuron is driven by *lim-6* promoter. *lsy-6(0)* indicates the null allele of *lsy-6*; *lsy-6(ot150)* is a partial loss-of-function mutation. (G) ASE neuron phenotype of *stau-1(tm2266)* and double mutant of *stau-1(tm2266)*; *lsy-6(ot150)*. * $p < 0.05$, ** $p < 0.01$, *** $p < 0.001$, N.S. not significant, chi-square test for adult alae phenotype and ASE neuron phenotype, two-tailed *t*-test for seam cell phenotype.

To confirm that *ma327* and *ma346* mutations are null alleles, we tested for expression of STAU-1 protein in these mutant animals. We performed western blot analysis of wild type and *stau-1* mutant embryos and L4 stage larvae using an anti-serum generated against the fourth double-stranded RNA-binding domain of STAU-1 (180) (Figure 4.2C). *stau-1(q798)* animals lacking the fourth double-stranded RNA-binding domain was used as negative control, and *stau-1(tm2266)* mutation results in a truncated STAU-1 protein recognizable by the anti-serum. In the embryos, we only observed full-length and truncated STAU-1 in wild type animals and *stau-1(tm2266)* mutant respectively, whereas neither *stau-1(ma327)* nor *stau-1(ma346)* embryos contained any detectable STAU-1 protein. In the L4 stage samples, there are non-specific bands close to the size of the truncated STAU-1 in the western blot, but the *stau-1(ma327)* and *stau-1(ma346)* mutants have the same band pattern as the negative control. Therefore, the *stau-1* alleles *ma327* and *ma346* generated in this study appear to be null alleles.

Next, we sought to characterize the phenotypes of these *stau-1* null alleles. Homozygous mutants of either *ma327* or *ma346* are viable, however, similar to *tm2266* and *q798*, these animals exhibit a 4 hour delay in larval development at 20°C and they are smaller in size compared to wild type animals at the young adult stage (Figure 4.3). Furthermore, to test if the *stau-1* null mutants also suppress phenotypes of miRNA mutants, we crossed the null alleles into the *let-7* family mutant *mir-48 mir-241(nDf51)*. As expected, both of these null alleles significantly suppress the adult alae and seam cell phenotypes

Figure 2

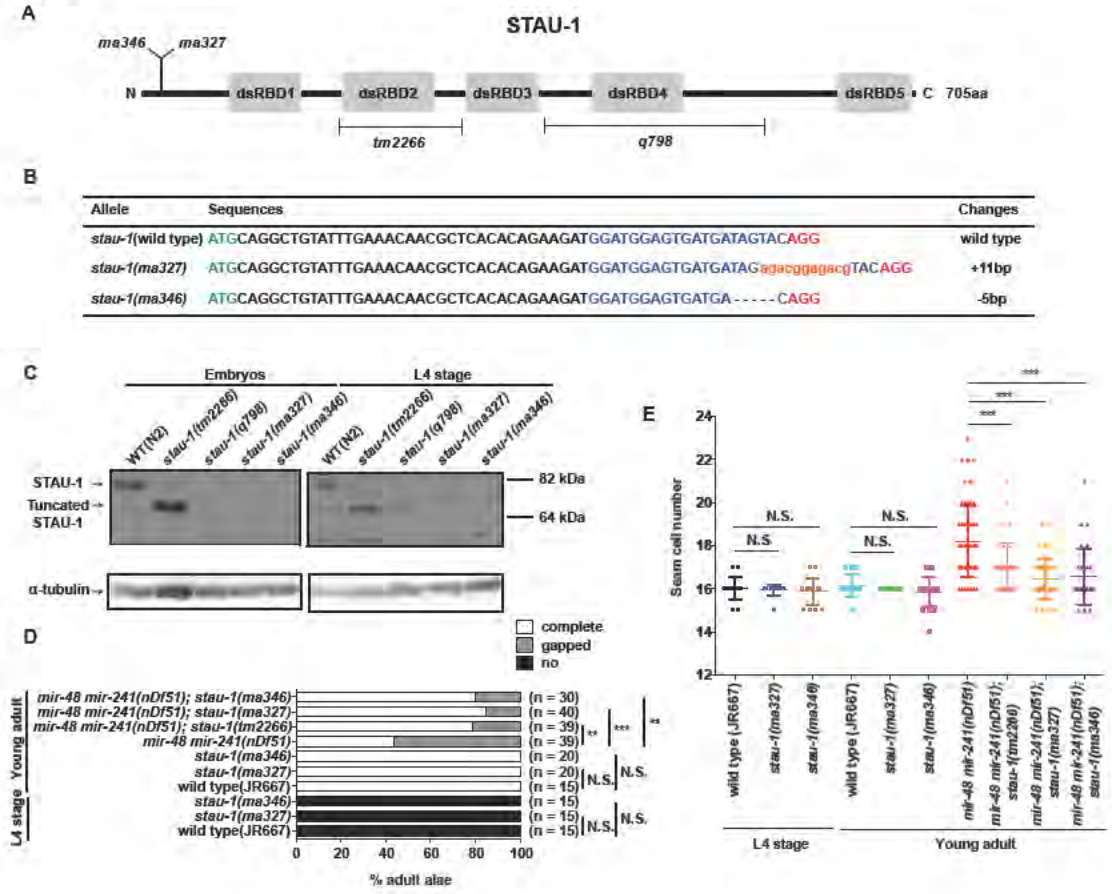
A
STAU-1
ma346
ma327
N
dsRBD1
dsRBD2
dsRBD3
dsRBD4
dsRBD5
C
705aa
tm2266
q798
B
Allele
Sequences
Changes
stau-1(wild type) ATGCAGGCTGTATTTGAAACAACGCTCACACAGAAGATGGATGGAGTGATGATAGTACAGG wild type
stau-1(ma327) ATGCAGGCTGTATTTGAAACAACGCTCACACAGAAGATGGATGGAGTGATGATAGagacggagacgTACAGG +11bp
stau-1(ma346) ATGCAGGCTGTATTTGAAACAACGCTCACACAGAAGATGGATGGAGTGATGA-----CAGG -5bp
C
Embryos
L4 stage
WT(N2)
stau-1(tm2266)
stau-1(q798)
stau-1(ma327)
stau-1(ma346)
STAU-1
Truncated STAU-1
α-tubulin
82 kDa
64 kDa
D
complete
gapped
no
Young adult
L4 stage
mir-48 mir-241(nDf51); stau-1(ma346)
mir-48 mir-241(nDf51); stau-1(ma327)
mir-48 mir-241(nDf51); stau-1(tm2266)
mir-48 mir-241(nDf51)
stau-1(ma346)
stau-1(ma327)
wild type(JR667)
(n = 30)
(n = 40)
(n = 39)
(n = 39)
(n = 20)
(n = 20)
(n = 15)
(n = 15)
(n = 15)
(n = 15)
**
***
**
N.S.
N.S.
N.S.
N.S.
0
20
40
60
80
100
% adult alae
E
Seam cell number
24
22
20
18
16
14
12
N.S.
N.S.
N.S.
N.S.
***
***
***
wild type (JR667)
stau-1(ma327)
stau-1(ma346)
wild type (JR667)
stau-1(ma327)
stau-1(ma346)
mir-48 mir-241(nDf51)
mir-48 mir-241(nDf51); stau-1(tm2266)
mir-48 mir-241(nDf51); stau-1(ma327)
mir-48 mir-241(nDf51); stau-1(ma346)
L4 stage
Young adult

Figure 4.2 Characterization of *stau-1* null alleles. (A) Nucleotide changes of *stau-1(ma327)* and *stau-1(ma346)* mutants. All the sequences shown here are in the beginning of *stau-1*'s first exon. The ATG start codon is in green. The sgRNA sequence is highlighted in blue and the PAM sequence is in red. The inserted sequence in *ma327* is in orange and lower case. The premature termination codons in *ma327* and *ma346* are 267nt and 195nt downstream of the start codon (not shown). (B) Western blots of STAU-1 and α-tubulin in wild type and *stau-1* mutants. Both mix stage embryos and L4 stage animals were used for this experiment. There are non-specific bands in the L4 stage blot. (C) Adult alae and (D) seam cell phenotypes of the *stau-1* null mutants at the L4 and the young adult stage in wild type and *mir-48 mir-241(nDf51)* background. * $p < 0.05$, ** $p < 0.01$, *** $p < 0.001$, N.S. not significant, chi-square test for adult alae phenotype and two-tailed *t*-test for seam cell phenotype.

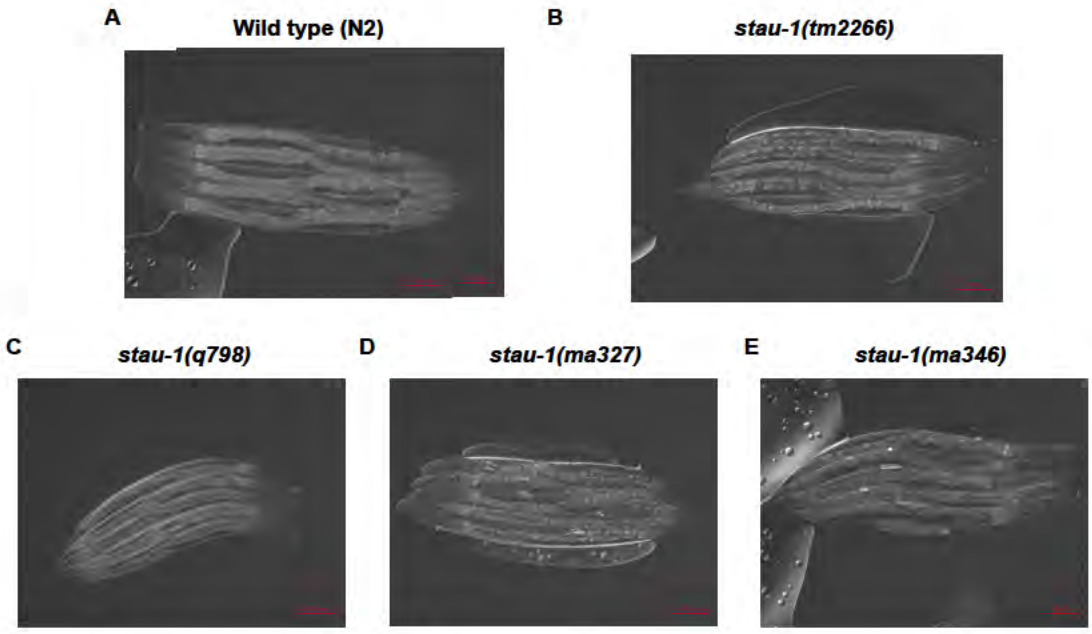

Figure 4.3 Body morphology phenotype of *stau-1* mutants. DIC images of young adult stage hermaphrodites: (A) wild type (N2), (B) *stau-1*(*tm2266*), (C) *stau-1*(*q798*), (D) *stau-1*(*ma327*), (E) *stau-1*(*ma346*). Scale bars are 100μm.

of *mir-48 mir-241(nDf51)* animals (Figure 4.2D and E). Interestingly, neither *stau-1(ma327)* nor *stau-1(ma346)* animals exhibit any heterochronic defects in an otherwise wild type genetic background (Figure 4.2D and E), indicating that the *let-7* family hyperactivity that would be resulted from the loss of STAU-1 appears to be below threshold to elicit a precocious developmental timing phenotype.

Since the effects of these *stau-1* null alleles on *let-7* family miRNA activity is similar to the effect of *stau-1(tm2266)*, subsequent studies were conducted using *stau-1(tm2266)*.

3. STAU-1 does not dramatically affect mature miRNA levels.

To investigate the mechanism on how *stau-1* modulates miRNA activity, we first performed small RNA high-throughput sequencing analysis of wild type and *stau-1(tm2266)* animals at the young adult stage. Three replicate samples were sequenced for each genotype and all the replicates yielded more than 5,000,000 reads, with ~80% of the reads mapping to *C. elegans* genome. Since the small RNA cloning technique we used is not dependent on the structure of the 5' nucleotide of the RNA (187), we were able to examine STAU-1's effect on diverse small RNA populations, including miRNAs, piRNAs and endogenous siRNAs. Based on the reads distribution data of small RNA populations, we did not observe any dramatic difference between wild type and *stau-1(tm2266)* animals (Figure 4.4A).

Furthermore, we focused our analysis on the levels of mature miRNAs. In our sequencing data, we identified a total of 239 miRNAs, however, only 12

miRNAs were significantly changed in *stau-1(tm2266)* compared to wild type animals (5 upregulated and 7 downregulated) (Figure 4.4B and C). None of the miRNAs that are differentially expressed in *stau-1(tm2266)* animals is known to be able to contribute to the phenotypes we observed earlier. Additionally, since the precocious expression of *let-7* at the L2 stage, rather than the overexpression at the young adult stage, could affect the developmental timing phenotypes (141), we therefore looked into the mature miRNA levels at the L2 stage. Similarly, no significant change in mature miRNA levels was detected in either *stau-1(tm2266)* or *stau-1(q798)* animals compared to wild type animals (Figure 4.5). Consistent with these results, we did not observe any significant change in the protein levels of two miRNA biogenesis factors (DCR-1 and ALG-1 (a *C. elegans* AGO)) in several *stau-1* mutants (Figure 4.6). Therefore, we conclude that the modulation of STAU-1 on miRNA activity is downstream of miRNA biogenesis.

4. STAU-1 does not dramatically affect other small RNA populations.

Since *stau-1* mutants exhibit enhanced RNAi and transgene silencing phenotypes (180), we examined if there is any change in other small RNA populations between wild type and *stau-1(tm2266)* animals. Besides miRNAs, *C. elegans* also possesses several classes of endogenous siRNAs (endo-siRNAs) and piRNAs. Since different functional classes of endo-siRNAs are loaded into distinct Argonaute proteins and endo-siRNAs in Argonaute CSR-1, WAGO, ALG-3/4 and ERGO-1 were previously identified (191), we mapped our sequencing

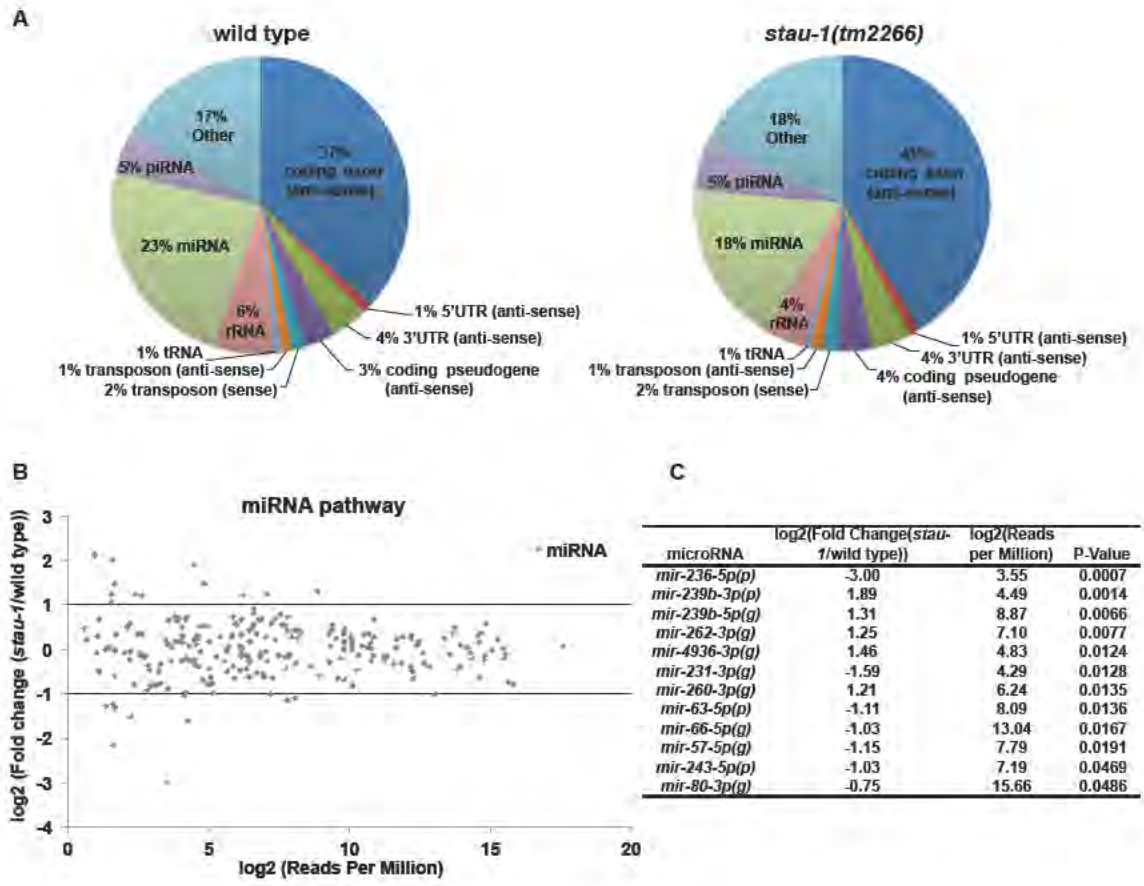

microRNA	log2(Fold Change(*stau-1*/wild type))	log2(Reads per Million)	P-Value
mir-236-5p(p)	-3.00	3.55	0.0007
mir-239b-3p(p)	1.89	4.49	0.0014
mir-239b-5p(g)	1.31	8.87	0.0066
mir-262-3p(g)	1.25	7.10	0.0077
mir-4936-3p(g)	1.46	4.83	0.0124
mir-231-3p(g)	-1.59	4.29	0.0128
mir-260-3p(g)	1.21	6.24	0.0135
mir-63-5p(p)	-1.11	8.09	0.0136
mir-66-5p(g)	-1.03	13.04	0.0167
mir-57-5p(g)	-1.15	7.79	0.0191
mir-243-5p(p)	-1.03	7.19	0.0469
mir-80-3p(g)	-0.75	15.66	0.0486

Figure 4.4 STAU-1 does not significantly affect mature miRNA levels. (A) Read distribution of small RNAs mapped to *C. elegans* genome in wild type and *stau-1(tm2266)* animals. All the anti-sense reads are endo-siRNA reads since *C. elegans* endo-siRNAs are mapped anti-sense to various regions of different gene transcripts (195). Most of reads in "other" were mapped to the sense strand of protein coding genes. (B) Differential gene expression analysis of miRNAs between wild type and *stau-1(tm2266)* animals. (C) List of miRNAs whose levels are significantly affected in *stau-1(tm2266)* animals. (g), miRNA guide strand. (p), miRNA passenger strand.

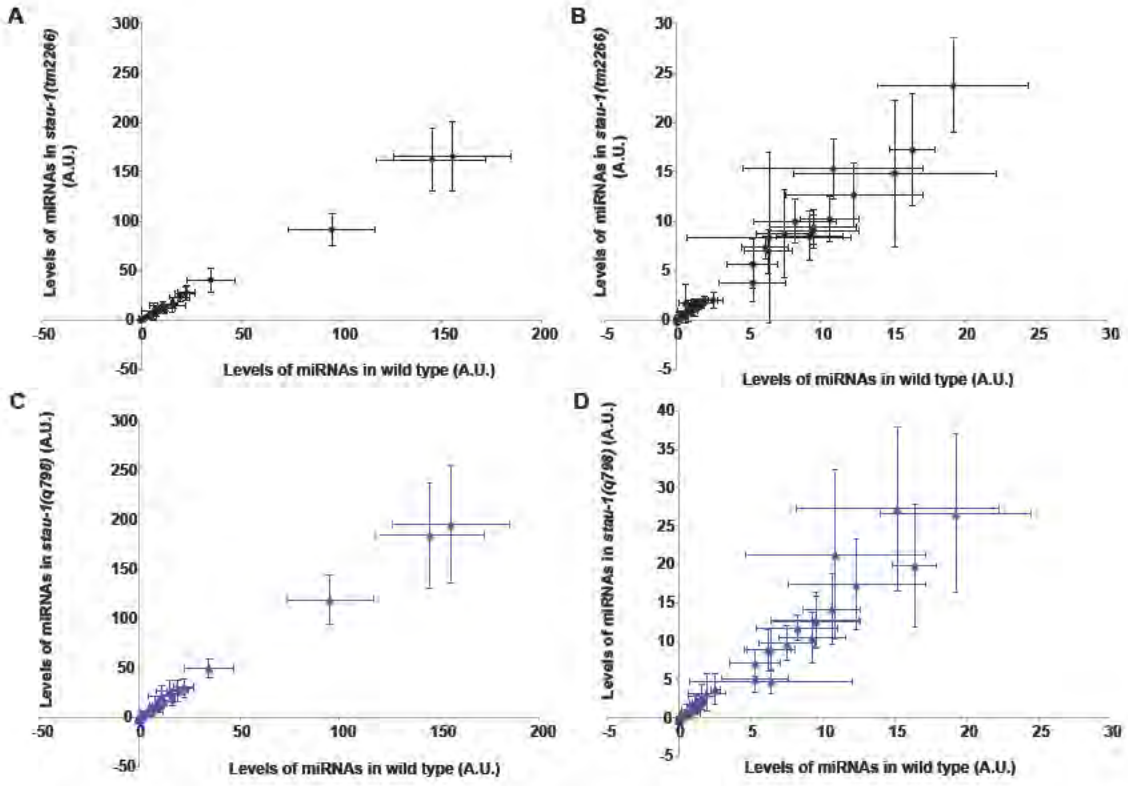

Figure 4.5 Mature miRNA levels in wild type and *stau-1* mutants at the L2 stage. (A-B) Levels of mature miRNAs in wild type (N2) and *stau-1*(*tm2266*) animals. (C-D) Levels of mature miRNAs in wild type (N2) and *stau-1*(*q798*) animals. Total RNA was used for a multiplex Firefly miRNA Quantification panel of 66 miRNAs. 54 miRNAs exhibited above background signals in at least one sample and were shown in (A) and (C). (B) and (D) show the miRNAs with lower expression levels in (A) and (C), respectively. All miRNA levels were normalized to U6 level in the same assay. There are three replicates for each sample. Two-tailed *t*-tests were performed, and no miRNA was statistically significantly changed by more than two-fold in either *stau-1* mutant compared to wild type animals.

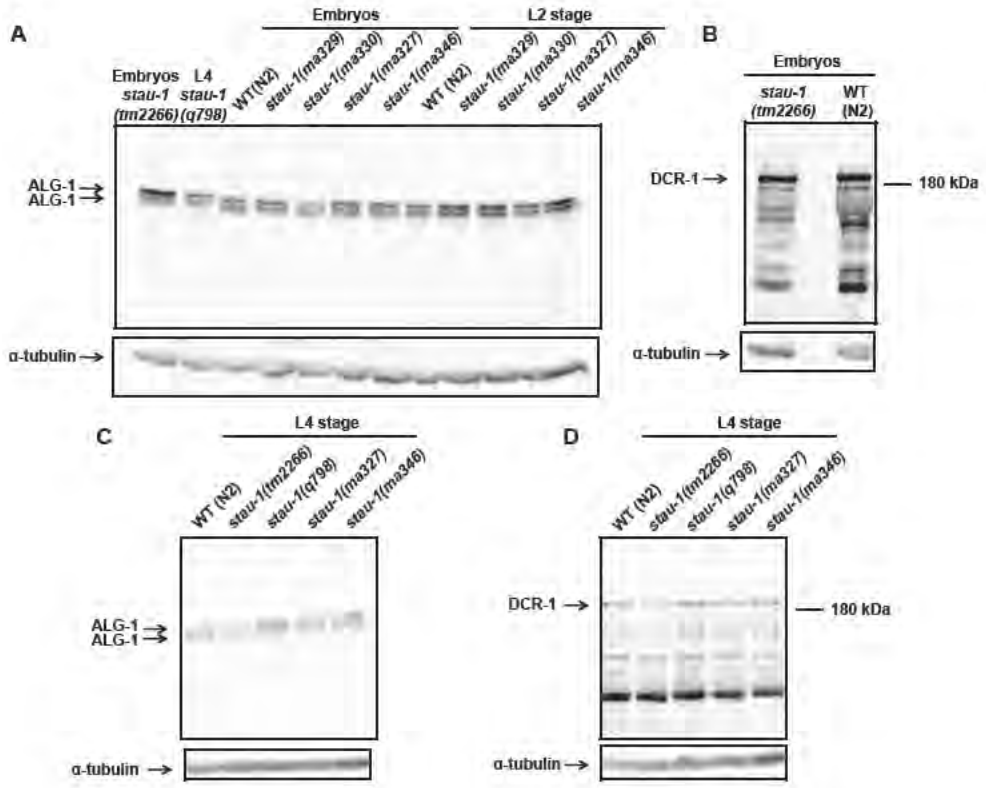

Figure 4.6 ALG-1 and DCR-1 protein levels in *stau-1* mutants. (A) Western blots showing ALG-1 protein levels in *stau-1* mutants at the embryo and the L2 stage. *stau-1*(*ma329*) and *stau-1*(*ma330*) are alleles which have N-terminal 3xFLAG tag at *stau-1*'s endogenous locus created by CRISPR/Cas9 with homologous recombination, however, they are not relevant in this study. (B) Western blots showing DCR-1 protein level in wild type (N2) and *stau-1*(*tm2266*) embryos. The L4 stage animals' ALG-1 and DCR-1 levels are shown in (C) and (D) respectively for wild type (N2) and *stau-1* mutants.

reads to these annotations and carried out differential gene expression analysis (Figure 4.7A-D). Of all these endo-siRNA categories, the most changes we observed were several WAGO endo-siRNAs that may function to maintain the silencing of “non-self” transcripts in *C. elegans* germline (196). STAU-1 does not seem to simply promote biogenesis of endo-siRNAs in the WAGO pathway since cases of upregulation and downregulation of endo-siRNAs were evident in *stau-1(tm2266)* animals (Figure 4.7B). The final class of small RNAs we analyzed was piRNAs, and there is no dramatic change in the piRNA levels between wild type and *stau-1(tm2266)* animals as well (Figure 4.7E).

5. The modulation of miRNA activity by *stau-1* mutations is likely independent of their enhanced RNAi phenotype.

C. elegans stau-1 mutants have been shown to exhibit an enhanced RNAi (Eri) phenotype, indicating that STAU-1 negatively modulates one or more RNAi pathways. This suggests the possibility that STAU-1’s negative modulation of miRNA activity we have shown here could reflect a common underlying effect of STAU-1 on small RNA silencing more broadly. In that case, one might expect other Eri mutants might also exhibit enhanced miRNA activity. Because *stau-1* mutants had been shown to interact genetically with *eri-1* (180), we tested if *eri-1* loss-of-function could affect the heterochronic phenotypes of *mir-48 mir-241(nDf51)* animals. Interestingly, loss-of-function of *eri-1* enhanced the adult alae and seam cell defects of *mir-48 mir-241(nDf51)* animals (Figure 4.8), which is opposite to the suppression caused by *stau-1* mutation. Therefore, the

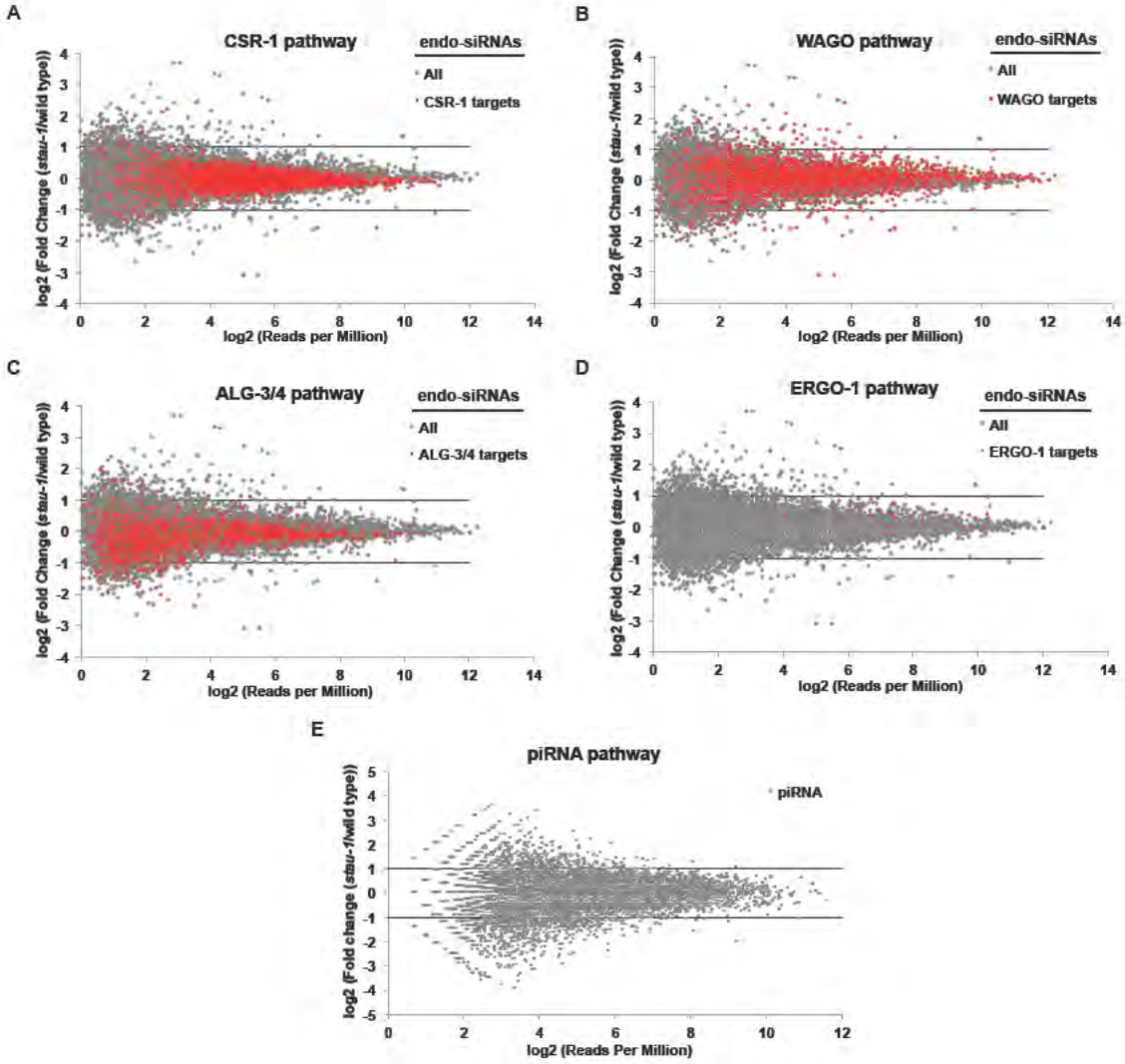

Figure 4.7 The effects of STAU-1 on small RNA pathways other than miRNAs. Comparisons between wild type and *stau-1(tm2266)* animals of expression of endo-siRNAs (A-D) associated with the CSR-1 (A), WAGO (B), ALG-3/4 (C), and ERGO-1 pathways (D), and piRNAs (E).

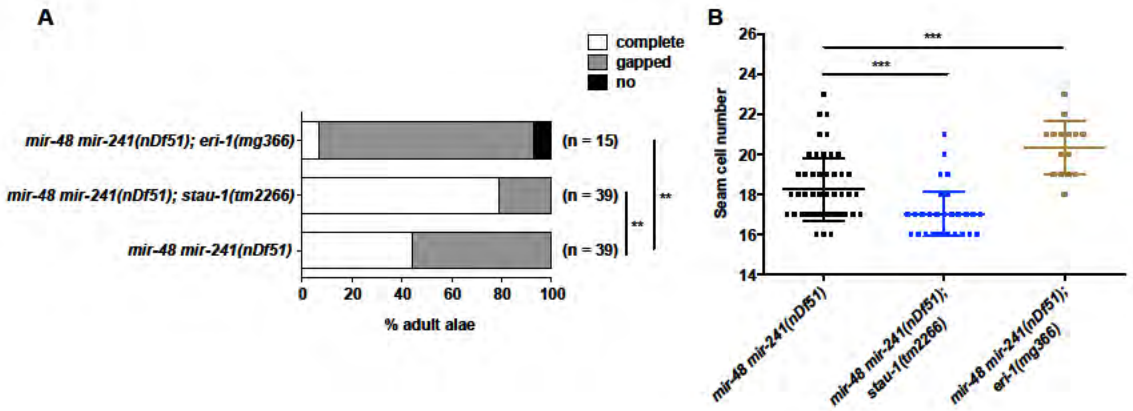

Figure 4.8 ERI-1 positively modulates *let-7* family miRNA activity. (A) Adult alae and (B) seam cell phenotype of *eri-1(mg366)* in combination with *mir-48 mir-241(nDf51)*. * $p < 0.05$, ** $p < 0.01$, *** $p < 0.001$, N.S. not significant, chi-square test for adult alae phenotype and two-tailed *t*-test for seam cell phenotype.

modulation of miRNA activity by STAU-1 is unlikely to be simply the result of a general enhancement of RNA interference.

6. STAU-1 may act through the 3'UTR of miRNA targets to modulate miRNA activity.

Staufen has been shown to promote the translation of its target mRNAs (177, 197, 198), suggesting that the negative effect of STAU-1 on miRNA activity shown here could reflect its role in promoting the translation of miRNA target mRNAs, either by binding to 3'UTR sequences (perhaps at or near miRNA binding sites), or conversely, to other regions of the mRNAs (such as 5'UTR and/or coding sequences). To investigate whether STAU-1 could oppose miRNA activity relatively directly, via the 3'UTR sequences of the target mRNAs, we utilized mutants of the heterochronic miRNA, *lin-4*, and its primary target, *lin-14* (3, 4).

The 3'UTR of *lin-14* possesses several *lin-4* and *let-7* family miRNA target sites (Figure 4.9A). The first strain we tested was *lin-4(e912); lin-14(n179)* which has a null mutation of *lin-4* and a point mutation in *lin-14*, and this double mutant exhibits a temperature sensitive heterochronic phenotype. At permissive temperature (15°C), *lin-4(e912); lin-14(n179)* animals exhibit a partially penetrant phenotype (~30% animals have gaps in the adult alae) and can be considered a sensitized genetic background, and *stau-1(tm2266)* significantly suppresses the adult alae phenotype of *lin-4(e912); lin-14(n179)* animals (Figure 4.9B). This indicates that STAU-1 could modulate the activity of *lin-14* possibly through *let-7*

family miRNAs or *mir-237* (the other member of *lin-4* family miRNAs in *C. elegans*).

Next, we used another *lin-14* mutant strain *lin-14(n355n679)*. *n355* is a breakpoint mutation in the 3'UTR of *lin-14*, which results in the removal of most *lin-14* 3'UTR including all the *lin-4* and *let-7* family miRNA binding sites (199). In combination with another point mutation (*n679*) that partially compromises LIN-14 function, the phenotype of *lin-14(n355n679)* is similar to *lin-4(e912); lin-14(n179)* animals. However, we failed to observe any suppression by *stau-1(tm2266)* on the adult alae phenotype on *lin-14(n355n679)* animals (Figure 4.9C). These data suggest that STAU-1 may modulate miRNA activity through the 3'UTR of miRNA targets.

7. An attempt to identify STAU-1 binding sites in *C. elegans*.

To further study the mechanism on how STAU-1 modulates miRNA activity, I attempted to perform high-throughput sequencing of RNA isolated by crosslinking immunoprecipitation (HITS-CLIP) experiment to identify STAU-1 binding sites in *C. elegans*. First, I utilized CRISPR/Cas9 technology to generate two independent alleles (*ma329* and *ma330*) of N-terminal 3xFLAG tagged STAU-1 at its endogenous locus. To test whether these allele affect the activity of STAU-1, I crossed them into *mir-48 mir-241(nDf51)* animals. If the 3xFLAG tag results in loss of function for STAU-1, I would expect that these alleles will suppress the heterochronic phenotypes of *mir-48 mir-241(nDf51)* animals similar to *stau-1(tm2266)* and the null alleles. However, instead of suppression, I

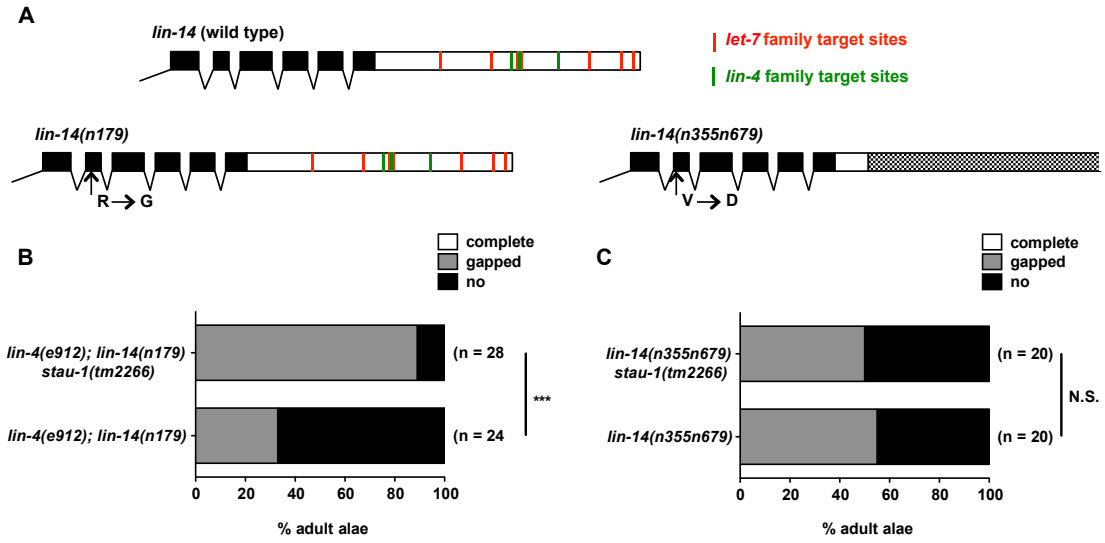

Figure 4.9 The 3'UTR of *lin-14* is required for modulation of *lin-14* gain-of-function phenotypes by *stau-1* mutation. (A) Diagrams of C-terminal end of *lin-14* gene in wild type, *lin-14(n719)* and *lin-14(n355n679)*. The black boxes represent exons and the white boxes represent 3'UTRs. The dotted box indicates the region of 3'UTR deleted in *lin-14(n355n679)*. The predicated *lin-4* family (green lines) and *let-7* family (red lines) target sites are indicated and the target site predication was obtained from TargetScan (200, 201). (B) Adult alae phenotype of *lin-4(e912)*; *lin-14(n179)* and *lin-4(e912)*; *lin-14(n179) stau-1(tm2266)* animals. (C) Adult alae phenotype of *lin-14(n355n679)* and *lin-14(n355n679) stau-1(tm2266)* animals. * $p < 0.05$, ** $p < 0.01$, *** $p < 0.001$, N.S. not significant, chi-square test for adult alae phenotype and two-tailed *t*-test for seam cell phenotype.

observed a mild enhancement of these alleles on the heterochronic phenotypes of *mir-48 mir-241(nDf51)* animals (Figure 4.10). This suggests that these two *3xflag* tagged *stau-1* alleles are not loss-of-function alleles and they might cause a slight overexpression of STAU-1, which may result in the mild phenotypic enhancement on the *let-7* family miRNA mutant.

Next, since the 3xFLAG does not significantly compromise the activity of STAU-1, I continued with the HITS-CLIP experiment. In parallel with STAU-1, I also used a positive control that is another RNA-binding protein SUP-26. 3xFLAG::STAU-1 and SUP-26::3xFLAG were both efficiently pulled down from the input and I observed that SUP-26 is much more abundant than STAU-1 (Figure 4.11A-C). Therefore, we doubled amount of input for STAU-1 CLIP compared to SUP-26. Although the positive control suggests that CLIP procedure was successful, I failed to obtain any STAU-1 ribonucleoprotein (RNP) complex in our experiment as indicated by the same signal pattern as the wild type (no tag) crosslinking sample (Figure 4.11D).

Because the double-stranded RNA-binding domain STAU-1 has does not interact with RNA bases (202) and the UV crosslinking requires the base interaction (203), therefore, the crosslinking reaction for STAU-1 might not be successful in our experiment. I proposed to perform formaldehyde crosslinking for STAU-1 instead of UV crosslinking in the future.

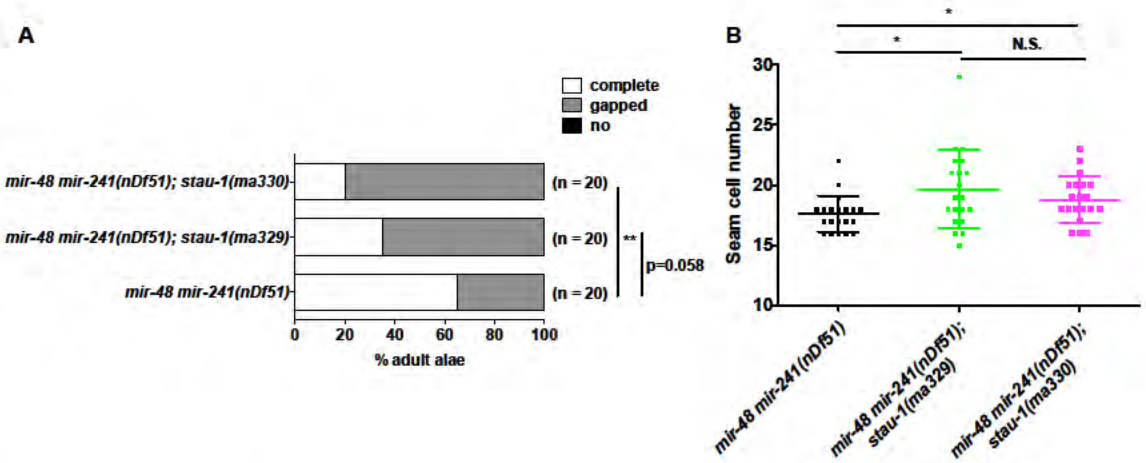

Figure 4.10 The effects of *3xflag::stau-1* on *let-7* family miRNA activity. (A) Adult alae and (B) seam cell phenotypes of *stau-1(ma329)* and *stau-1(ma330)* in *mir-48 mir-241(nDf51)* background. * $p < 0.05$, ** $p < 0.01$, *** $p < 0.001$, N.S. not significant, chi-square test for adult alae phenotype and two-tailed *t*-test for seam cell phenotype.

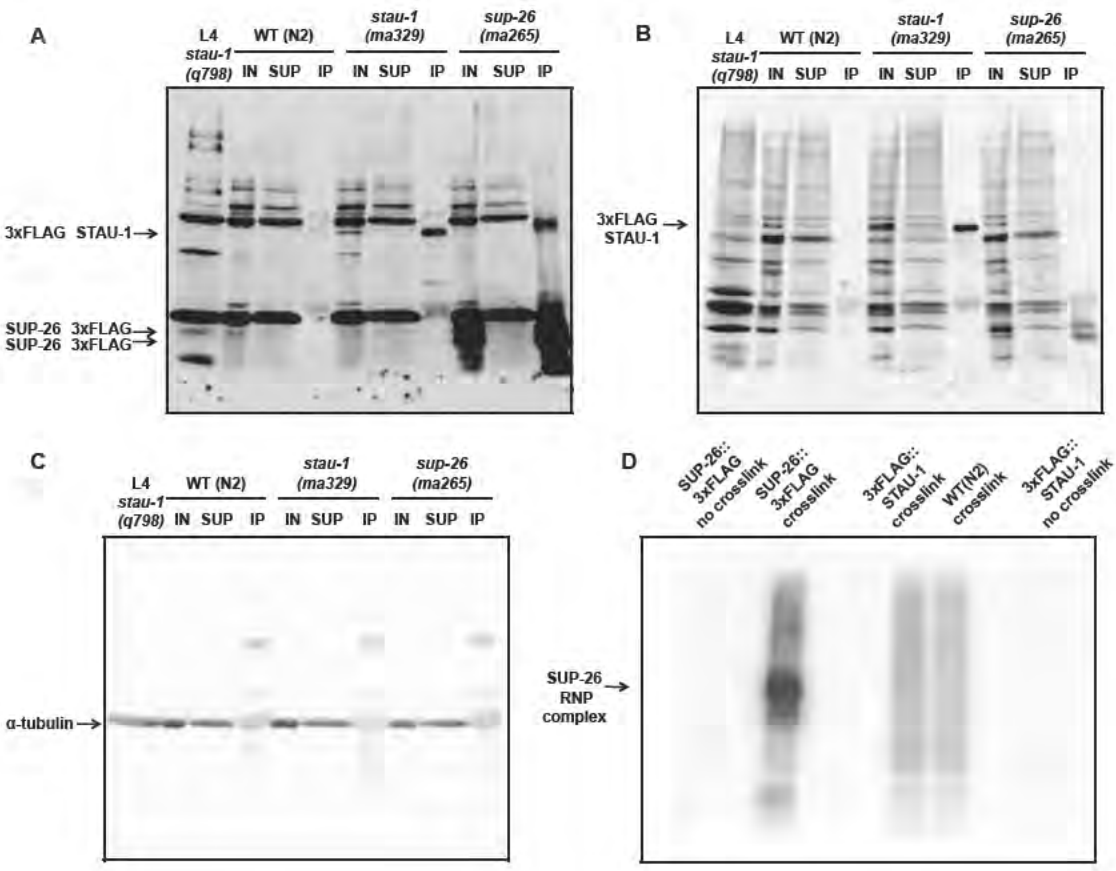

Figure 4.11 STAU-1 CLIP experiment. Western blots with (A) anti-FLAG, (B) anti-STAU and (C) anti-tubulin for testing the IP efficiency of 3xFLAG::STAU-1 protein. (D) Image captured by phosphor imager for STAU-1 CLIP experiment. IN, input; SUP, supernatant. A lot of non-specific bands for anti-FLAG and anti-STAU, but proteins of interest were pointed by arrows.

IV.E. Discussion

The double-stranded RNA-binding protein Staufen has been characterized as a master regulator of mRNA localization and translation in many metazoan species (204). Staufen is known to positively regulate translation upon localization through interactions with structured regions of mRNAs (3'UTR, coding sequences and 5'UTR) and various partner proteins and/or ribosomes (172, 177, 197, 198). Besides such positive roles in gene expression, Staufen can also negatively regulate gene expression by recruiting the nonsense-mediated decay factor Upf1 to the 3'UTR of mRNAs to trigger mRNA degradation (179). Because of these alternative positive or negative roles in post-transcriptional regulation of mRNA activity, we predicted that Staufen could be expected to potentially interact functionally with miRNA-mediated repression of mRNA targets, and could exert either promotion or inhibition of miRNA activity.

In this study, we found that loss of function Staufen (*stau-1*) mutations in *C. elegans* can suppress the phenotypes of miRNA partial loss of function, indicating that STAU-1 inhibits miRNA activity. This suggests that, at least with respect to the miRNAs whose functions we examined here, STAU-1 engages its translational enhancer function, rather than its mRNA decay activity. We show that *stau-1* loss of function mutation does not appreciably affect the levels of mature miRNAs; in particular, there was no detectable change, in *stau-1* mutants, of the levels of the *lin-4*, *let-7*, and *lsy-6* miRNAs whose function we monitored phenotypically in our genetic interaction experiments. This strongly

suggests that STAU-1 likely opposes the activity of these miRNAs independently of their biogenesis or turnover, and perhaps may act by binding to their target mRNAs. Consistent with a model where STAU-1 can modulate miRNA activity by binding to the 3'UTR of miRNA targets, our data show that the 3'UTR of a miRNA target, *lin-14*, is required for STAU-1-mediated modulation of *lin-14* heterochronic phenotypes.

Various possible molecular mechanisms could be the basis for an opposition of miRNA repression by STAU-1. STAU-1 bound to target mRNA could oppose miRNA activity by exerting an independent translational activation (Figure 4.12A), or perhaps also by directly inhibiting the binding (Figure 4.12B) or efficacy (Figure 4.12C) of miRISC. It should be noted that a target site occlusion model for STAU-1 (Figure 4.12B) would be similar to the action attributed to other 3'UTR binding proteins (Pumilio, HuR and Dnd1) that can apparently affect miRNA target accessibility by binding at or near miRNA sites (167).

All the models proposed here (Figure 4.12) involve a hypothetical physical interaction of STAU-1 with miRNA targets. Accordingly, one would predict that the miRNA target mRNAs that likely contribute to the phenotypes we observed here (*lin-14*, *hbl-1, lin-41* and *cog-1*) should be recoverable associated with STAU-1 immunoprecipitated from worms of the appropriate developmental stage (embryo for *cog-1*; L1 for *lin-14*, L2 for *hbl-1,* and L4/adult for *lin-41*). Our CLIP experiment so far did not work, but a previous study (180) did recover the *let-7* target *lin-41* as enriched in a STAU-1 RNA Immunoprecipitation (RIP) experiment

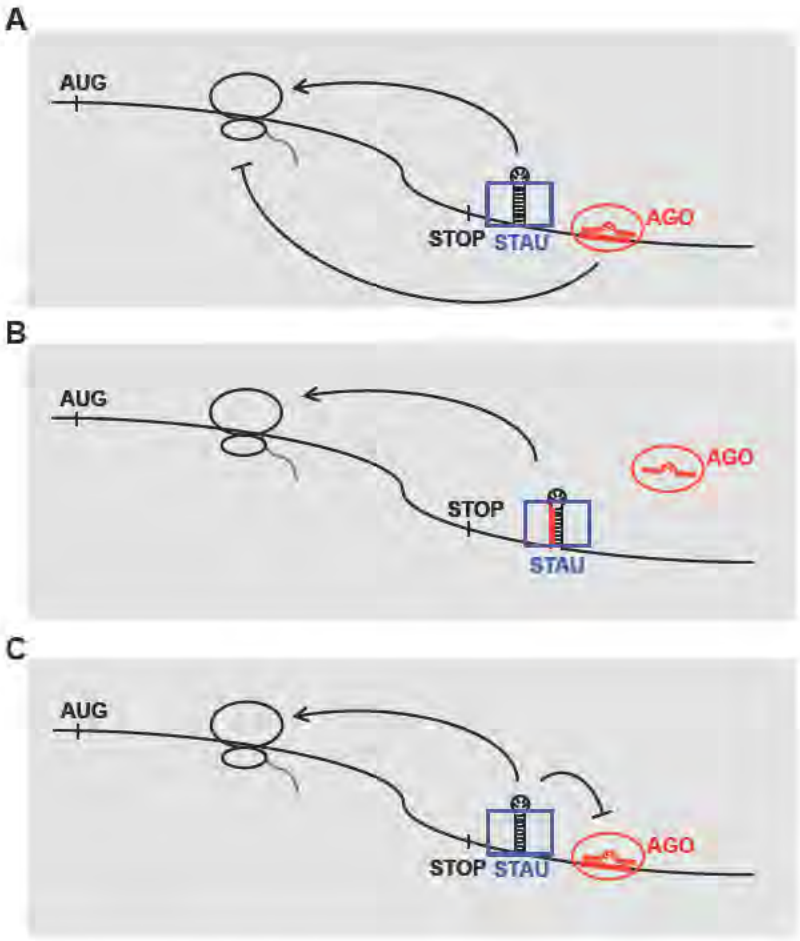

Figure 4.12 Alternative models for STAU-1-mediated modulation of miRNA activity wherein STAU-1 is proposed to bind to miRNA targets, for example via 3' UTR double-stranded RNA secondary structure. The previously-described translational activation function of Staufen could oppose, and hence inhibit the net potency of, miRNA-based translational repression (A); STAU-1 could also affect miRNA activity by binding at (or close to) the miRNA binding site and hence inhibiting miRISC binding (B) or activity (C). Blue rectangles are STAU-1 proteins and red ovals are AGO proteins. The red single stranded nucleic acids in AGO proteins represent miRNAs and red lines on mRNAs are miRNA binding sites. Brown curves are newly synthesized protein peptides from the mRNAs.

using extracts of *C. elegans* adults, supporting the model that STAU-1 could interact with miRNA targets. LeGendre JB *et al* (2013) did not recover *cog-1*, *lin-14*, or *hbl-1* in their RIP experiments, but this is perhaps not unexpected since larval stage extracts were not tested.

Our small RNA sequencing data indicate that *stau-1* loss of function mutation does not affect miRNA biogenesis in general, despite having clear effects on the developmental phenotypes of certain miRNA mutants. Importantly, the levels of the particular miRNAs responsible for those phenotypes were unchanged in *stau-1* mutants. However, we did not examine levels of these miRNAs in specific cell types, therefore, it is possible that STAU-1 could modulate miRNA biogenesis or stability cell type-specifically, and we might not have detected cell type-specific changes of those miRNAs in our RNA samples extracted from whole animals. Indeed, our sequencing data contain a hint that the abundance of some miRNAs could be affected by STAU-1; 11 miRNAs exhibited at least 2-fold change in levels in the *stau-1* mutant compared to wild type animals (Figure 4.4C). In such cases, perhaps STAU-1, through its double-stranded RNA-binding activity, can associate with secondary structure elements in miRNA primary transcripts and/or precursors and modulate their processing into mature miRNAs.

Prompted by the finding from a previous study that *C. elegans stau-1* mutants exhibit an enhanced RNAi (Eri) phenotype, and interact genetically with *eri-1* mutation (180), we tested whether an *eri-1* mutation, similarly to *stau-1,*

could suppress *let-7* family miRNA mutant's heterochronic phenotypes. Surprisingly, *eri-1(mg366); mir-48 mir-241(nDf51)* mutant exhibited enhanced heterochronic phenotypes, which is the opposite from the effect of *stau-1*. First of all, this finding indicates that the modulation of miRNA activity by STAU-1 is unlikely to stem simply from an enhanced exogenous RNAi pathway, otherwise, we would have expected that *eri-1(mg366)*, like *stau-1(loss-of-function)*, should suppress *mir-48 mir-241(nDf51)* mutant phenotypes. Rather, these findings, particularly the opposite effects of different Eri loci on *let-7* family miRNA phenotypes, suggest important, but as yet uncharacterized, interactions among RNAi and miRNA pathways in *C. elegans*. ERI-1 is known to be an exonuclease and important for the production of siRNAs in *C. elegans* (205), and a few studies have examined miRNA levels in *eri-1* loss of function context with mixed results, perhaps reflecting differences amongst experimental systems, and/or the particular miRNAs assayed (186, 206-208). It is clear that further studies are needed to characterize the mechanisms by which ERI-1 affects miRNA activity.

Interestingly, we did not observe any overt miRNA gain-of-function phenotypes for *stau-1* mutations in an otherwise wild type genetic background, as might be expected for loss of a potent miRNA inhibitor. Rather, the *stau-1* mutants' miRNA phenotypes were only detected in sensitized genetic backgrounds with compromised miRNA activity. These findings suggest a modulatory effect of STAU-1 on miRNA activity and underscore the importance of miRNA pathways in conferring robustness to biological systems. The

modulatory role of STAU-1 on miRNA activity could perhaps be important in refining the post-transcriptional regulation of important miRNA targets and to modulate the efficacy of miRNAs in response to physiological and environmental signals.

In conclusion, our study demonstrates that the RNA-binding protein STAU-1 negatively modulates miRNA activity downstream of miRNA biogenesis, possibly by interacting with the 3'UTR of miRNA targets. These findings reveal an expanded suite of RNA regulatory roles for STAU-1; besides regulating mRNA localization, translation and decay, Staufen also can exert post-transcriptional gene regulation through its engagement with miRNA targets. It should be noted that our results to date indicate that STAU-1 can inhibit the activity of *let-7* family, *lsy-6*, and perhaps *lin-4* miRNAs, but further studies are required to test for similar roles of STAU-1 in opposing the activity of other miRNAs; moreover, we should not rule out the possibility that STAU-1 could promote the activity of certain other miRNAs, for example through its known role in mediating mRNA decay (179).

CHAPTER V: Candidate-based RNAi screens to identify modulators of miRNA pathway

V.A. Abstract

In order to identify previously unknown cellular components that impact miRNA mediated gene silencing, I utilized the sensitized genetic backgrounds we have developed in Chapter I to perform candidate-base RNAi screens for the identification of positive and negative modulators of the miRNA pathway. The cellular pathways screened so far include endosomal trafficking, EGF signaling, Wnt ligands/retromer and RNA helicases. I found that the phenotypes of miRNA mutants could be modulated by various cellular components, but the modulation might not be directly through affecting the activity of miRNAs.

V.B. Introduction

Since the miRNA pathway is involved in the regulation of many fundamental processes, it is important to understand how different cellular pathways could affect miRNA activity. To build upon the findings in Chapter IV, I carried out several RNAi screens to test the effects of various cellular components on the activity of miRNAs.

Recent studies in *Drosophila* and mammalian cells have suggested that endosomal trafficking is linked to miRNA activity (209, 210). In these studies, it was observed that several important factors for miRNA's function (AGO, GW182,

Me31b) are coupled to late endosomes (also known as multivesicular bodies, or MVBs), and the level of the co-localization between these components varies from 60% to 93% depending on the cell type and organism. Additionally, blocking MVB formation by depleting ESCRT (endosomal sorting complexes required for transport) genes (*hrs*, *vps25*, *alix*) inhibits miRNA activity and results in loss of GW bodies, whereas blocking MVB turnover by knocking out genes controlling late endosome to lysosome transition (*dHPS4*, *dHPS1*) enhances miRNA activity and increases the number of GW bodies. These modifications in endosomal trafficking do not seem to affect the levels of mature miRNAs or several miRISC components.

Although these previous studies have provided insightful understandings of the connections between endosomal trafficking and miRNAs, yet they were limited based on lack of endogenous and quantifiable miRNA phenotypes. Therefore, I investigated whether important regulators of endosomal trafficking pathway (ESCRT genes and RAB genes) could modulate *C. elegans* miRNA activity. ESCRT genes form four major protein complexes (ESCRT-0, I, II, III, IV) to control the formation of MVBs and the sorting of cargo into these MVBs (211). RAB genes are small GTPases that regulate membrane identity and vesicle trafficking through the recruitment of effector proteins (212). Therefore, knocking down these two groups of genes by RNAi could significantly affect the endosomal trafficking pathway, which allows me to test the effect of endosomal trafficking pathway on miRNA activity.

In opposition to the previous results that depleting ESCRT genes inhibits miRNA activity (209, 210), I observed that knocking down several genes in the ESCRT complexes may not affect miRNA activity, and their effects on a GFP reporter phenotype of a miRNA mutant could be through the hyper-activation of autophagy activity caused by the depletion of ESCRT genes. Also, I observed that the master regulator of early to late endosome transition, RAB-7, seems to significantly modulate the phenotypes of several miRNA mutants. However, RAB-7 might act through EGFR/PI3K pathway to exhibit its modulation on miRNA mutant phenotypes instead of directly affecting miRNA activity. Additionally, I summarized data on several other genes that might affect miRNA activity. Last, I need to mention that a few of the results in this chapter are quite preliminary and experimental repeats and functional studies are required to confirm these findings.

V.C. Materials and methods

The following are methods not previously described in Chapter II, III and IV.

RNAi screens. All the candidate-based RNAi screens were performed using bacterial feeding RNAi (118). RNAi clones were obtained from Ahringer RNAi feeding library (119). RNAi feeding plates were made according to standard protocol (119). Gravid adult animals were placed on the RNAi plates and their progeny (F1) were transferred to a new RNAi plate seeded with the

same RNAi clone, and F2 animals were scored for various phenotypes and gene expression levels, except for the embryonic lethality phenotype of *mir-35* family mutant.

Embryonic lethality analysis of *mir-35* family mutant. The embryonic lethality phenotype of wild type and *mir-35-41(lf)* animals was assayed based on previously published studies (76, 102). Gravid adult animals were put on RNAi plates and the embryonic lethality phenotype of their progeny was examined at both 20°C and 25°C.

Taqman assay for miRNAs and *rab-7*. Young adult stage F2 animals on control and *rab-7* RNAi were collected for miRNA Taqman assay. Mix stage F2 animals on control and *rab-7* RNAi were collected for *rab-7* Taqman qRT-PCR. Two microliters of 12 ng/μl total RNA were used for multiplex miRNA Taqman reactions, and 1μg of total RNA was used for Taqman Gene Expression Assays for *rab-7*. All experiments were performed according to the manufacturer's protocol with an ABI 7900HT Fast-Real Time PCR System (Applied Biosystems).

V.D. Results

1. A summary of all candidate-based RNAi screens for the identification of miRNA pathway modulators.

In Chapter I, I described that sensitized genetic backgrounds could be utilized to identify modulators of miRNA pathways. Sensitized genetic backgrounds consist a panel of miRNA mutants with partially penetrant

phenotypes. By testing for enhancement or suppression of the partially penetrant phenotypes after knockdown of candidate gene activity, I can identify positive or negative modulators of miRNA pathway, respectively.

The establishment of these sensitized genetic backgrounds in combination of the ease of feeding RNAi in *C. elegans* provides us with great tools to study how miRNA pathway is affected by different cellular components. In this study, I employed candidate-based RNAi screens to examine the effects of several cellular pathways on miRNA activity. Three sensitized genetic backgrounds mainly utilized here are: 1) *mir-48 mir-241(nDf51)*; 2) *lsy-6(ot150)*; 3) *mir-35-41(lf)*.

The phenotypic readouts for the RNAi screens are *col-19::gfp* expression phenotype for *mir-48 mir-241(nDf51)*, the ASE neuron phenotype for *lsy-6(ot150)* and the embryonic lethality phenotype for *mir-35-41(lf)*. For the *let-7* family miRNA mutant, *col-19::gfp* expression phenotype was used instead of seam cell or adult alae phenotype as an indication of *let-7* family miRNA activity because *col-19::gfp* expression phenotype is experimentally feasible for large-scale screens. *col-19* encodes an adult specific collagen that is regulated by *let-7* family miRNAs through LIN-41 and LIN-29 (81, 83, 131). Wild type animals exhibit *col-19::gfp* expression in both seam cells and the hypodermis main body syncytium hyp7 at the young adult stage, and complete loss-of-function mutants of *let-7* family miRNAs fail to express *col-19::gfp* in hyp7 (74, 131). *mir-48 mir-241(nDf51)* animals exhibit a partially penetrant *col-19::gfp* expression phenotype

with a percentage of animals loss *col-19::gfp* expression in hyp7, which can be used as a reflection of *let-7* family miRNA activity. The ASE neuron phenotype of *lsy-6(ot150)* animals was described in Chapter IV and *lim-6::gfp* expression was used as the phenotypic readout. Last, *mir-35* family miRNAs were previously shown to regulate embryonic viability, and *mir-35-41(lf)* mutants have a temperature-sensitive embryonic lethal phenotype with mild embryonic lethality at 20°C and almost complete lethal at 25°C (76). I used both temperatures to test phenotypic enhancement or suppression of *mir-35-41(lf)* animals after knocking down candidate genes.

The cellular pathways I have screened are ESCRT complex, RAB genes, regulators of RAB activity, Wnt ligands/retromer, EGF signaling pathways, Notch pathway and RNA helicases. The genes that do not have any RNAi clones available in the Ahringer library were not screened. Therefore, the RNAi screens here were not exhausted. The result summary is shown in Table 5.1. The detailed studies on several candidate genes are shown in the rest of this chapter.

2. Endosomal trafficking regulator RAB-7 could modulate the phenotypes of several miRNA family mutants.

Several previous studies have shown that endosomal trafficking is linked to miRNA activity in *Drosophila* and mammalian cells (209, 210), therefore, I tested whether *C. elegans* miRNA pathway can also be modulated by endosomal trafficking. In order to do that, I performed RNAi screens to identify the effect of

Table 5.1 Result summary of all candidate-based RNAi screens														
			col-19 phenotype		ASE neuron phenotype		Embryonic lethality		Adult alaephenotype		Seam cell phenotype			
	Gene	Function	wild type	*mir-48 mir-241(nDf51)*	wild type	*lsy-6(ot150)*	wild type	*mir-35-41(lf)*	wild type	*mir-48 mir-241(nDf51)*	wild type	*mir-48 mir-241(nDf51)*		
ESCRT complex	*tsg-101*	ESCRT-I												Enhancement
	vps-37	ESCRT-I					20°C	20°C						No interaction
	vps-22	ESCRT-II												Suppression
	vps-25	ESCRT-II												Unable to test due to lethality
	vps-36	ESCRT-II												Not tested
	T27F7.1	ESCRT-III												
	vps-32.2	ESCRT-III						25°C					ER	endoplasmic reticulum
	vps-32.1	ESCRT-III											ee	early endosome
	hgrs-1	ESCRT-0					20°C	20°C					le	late endosome
	stam-1	ESCRT-0											re	recycling endosome
	alx-1	ESCRT-I												
	F23C8.6	ESCRT-III												
	T23G11.7	ESCRT-III												
RAB family	*rab-1*	ER to Golgi												
	rab-2	Golgi to ER												
	rab-5	ee												
	rab-6.1	Golgi												
	rab-6.2	Golgi												
	rab-7	le					20°C	20°C						
	rab-8	cilium												
	rab-10	re					20°C	20°C						
	rab-11.1	re												
	rab-11.2	re												
	rab-14	phagosome												
	rab-21	autophagy						25°C						
	rab-28	not known												
	rab-37	secretory												
	F11A5.3	lipid storage												
RAB regulators	*rme-6*	RAB-5 GEF												
	vps-34	kinase, PI(3)P												
	ccz-1	phagosome												
	vps-11	HOPS					20°C	20°C						
	vps-18	HOPS												
	vps-33.1	HOPS												
	vps-33.2	HOPS												
	vps-39	HOPS												
	vps-16	HOPS, AP-3												
	vps-41	HOPS, AP-3												
	tbc-2	RAB-5 GAP												
	glo-3	gut granule												
	glo-4	GEF												
	glo-5	AP-3												
	apb-3	AP-3												
	apm-3	AP-3												
	T27F6.6	not known												
	rabx-5	RAB-5 GEF												

Continued. Table 5.1 Result summary of all candidate-based RNAi screens

			col-19 phenotype		ASE neuron phenotype		Embryonic lethality		Adult alaephenotype		Seam cell phenotype			
	Gene	Function	wild type	*mir-48 mir-241(nDf51)*	wild type	*lsy-6(ot150)*	wild type	*mir-35-41(lf)*	wild type	*mir-48 mir-241(nDf51)*	wild type	*mir-48 mir-241(nDf51)*		
Wnt pathway and retromer	*dpy-23*	AP-2												Enhancement
	arl-1	trafficking												No interaction
	arf-1.2	trafficking												Suppression
	arf-3	trafficking												Unable to test due to lethality
	arf-6	trafficking												Not tested
	vps-34	PI3K												
	cogc-2	trafficking												
	sft-4	trafficking												
	F22G12.5	trafficking												
	ZK1098.5	trafficking												
	vps-26	retromer												
	vps-29	retromer												
	vps-35	retromer												
	snx-1	retromer												
	egl-20	Wnt ligand												
	cwn-1	Wnt ligand												
	cwn-2	Wnt ligand												
	lin-44	Wnt ligand												
	mom-2	Wnt ligand												
EGF and Notch pathway	*let-23*	EGFR												
	lin-2	EGFR localization												
	lin-7	EGFR localization												
	lin-10	EGFR localization												
	let-60	Ras												
	lin-3	EGF signaling												
	plc-3	PLCγ												
	itr-1	IP3 receptor												
	lfe-2	IP3K												
	hmr-1	EGF like												
	Y69H2.11	DLK2												
	glp-1	Notch												
	lin-12	Notch												
	age-1	PI3K												
	akt-1	Kinase												
	daf-18	PTEN												
	W03C9.5	autophagy												

Continued. Table 5.1 Result summary of all candidate-based RNAi screens

			col-19 phenotype		ASE neuron phenotype		Embryonic lethality		Adult alaephenotype		Seam cell phenotype			
	Gene	Function	wild type	*mir-48 mir-241(nDf51)*	wild type	*lsy-6(ot150)*	wild type	*mir-35-41(lf)*	wild type	*mir-48 mir-241(nDf51)*	wild type	*mir-48 mir-241(nDf51)*		
RNA helicase	*eri-7*	SF1- Upf1-like												Enhancement
	dna-2	SF1- Upf1-like												No interaction
	inf-1	Eukaryotic DEAD-box												Suppression
	F33D11.10	Eukaryotic DEAD-box												Unable to test due to lethality
	cgh-1	Eukaryotic DEAD-box												Not tested
	ddx-19	Eukaryotic DEAD-box												
	hel-1	Eukaryotic DEAD-box												
	B0511.6	Eukaryotic DEAD-box												
	T26G10.1	Eukaryotic DEAD-box												
	C46F11.4	Eukaryotic DEAD-box												
	ddx-23	Eukaryotic DEAD-box												
	F53H1.1	Eukaryotic DEAD-box												
	ZK686.2	Eukaryotic DEAD-box												
	F55F8.2	Eukaryotic DEAD-box												
	R05D11.4	Eukaryotic DEAD-box												
	mog-4	Eukaryotic DEAH / RHA												
	mog-5	Eukaryotic DEAH / RHA												
	F56D2.6	Eukaryotic DEAH / RHA												
	rha-2	Eukaryotic DEAH / RHA												
	drh-1	RIG-I-like DExH												
	dcr-1	RIG-I-like DExH												
	F01G4.3	Ski2-like DExH												
	Y54E2A.6	Ski2-like DExH												
	Y54E2A.4	Ski2-like DExH												
	C08F8.2	Ski2-like DExH												
Other	*pqn-29*	Prion-like												
	pqn-67	Prion-like												
	M88.5	FMRP												
	Y03D3A.4	homolog of Vpg												
	sid-1	RNAi spreading												
	sid-5	RNAi spreading												
	stau-1	dsRNA-binding protein												

important regulators of endosomal trafficking (ESCRT complex, RAB genes and RAB regulators) on miRNA activity.

From these screens, I identified that the RAB GTPase RAB-7 positively modulate the phenotypes of all the tested miRNA mutants. Specifically, knocking down *rab-7* enhances the *col-19::gfp* expression phenotype and the adult alae defects of *mir-48 mir-241(nDf51)* animals (Figure 5.1A-D), the embryonic lethality phenotype of *mir-35-41(lf)* animals (Figure 5.1E) and ASE neuron phenotype of *lsy-6(ot150)* animals (Figure 5.1F). This suggests that RAB-7 could function to positively modulate the activity of several miRNA families.

Since *rab-7* RNAi enhances the developmental timing phenotypes of a *let-7* family miRNA mutant, I would expect that knocking down *rab-7* should inhibit the repression of *let-7* family miRNA targets in the developmental timing pathway. As expected, I observed a signification delay in the downregulation of two *let-7* family miRNA targets (HBL-1(82, 107) and LIN-28 (20)) upon knocking down *rab-7* (Figure 5.2). This suggests that the effect of *rab-7* RNAi on the developmental timing phenotypes of *mir-48 mir-241(nDf51)* animals is likely due to a direct regulation of RAB-7 on the *let-7* family miRNA targets.

3. Knocking down *rab-7* does not affect mature miRNA levels.

Next, I wonder if the modulation of RAB-7 on miRNA activity could be through affecting miRNA biogenesis. So, I performed Taqman qRT-PCR for 103 *C. elegans* mature miRNAs in wild type and *mir-48 mir-241(nDf51)* animals upon knocking down *rab-7*. As it is shown in Figure 5.3, there is no significant change

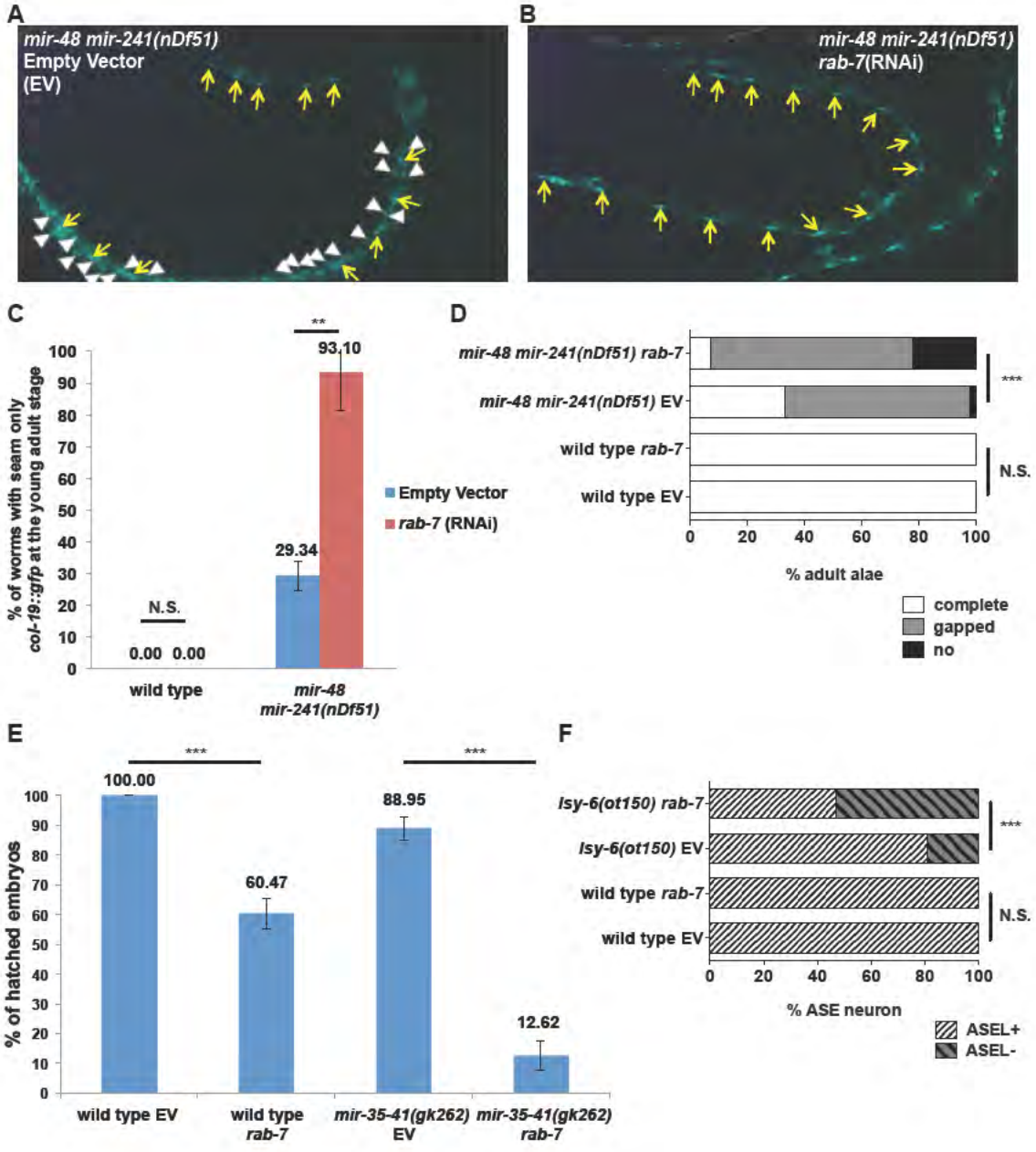
A
mir-48 mir-241(nDf51)
Empty Vector
(EV)
B
mir-48 mir-241(nDf51)
rab-7(RNAi)
C
% of worms with seam only
col-19::gfp at the young adult stage
**
93.10
29.34
N.S.
0.00 0.00
Empty Vector
rab-7 (RNAi)
wild type
mir-48
mir-241(nDf51)
D
mir-48 mir-241(nDf51) rab-7
mir-48 mir-241(nDf51) EV
wild type rab-7
wild type EV
***
N.S.
% adult alae
complete
gapped
no
E
% of hatched embryos
***
***
100.00
60.47
88.95
12.62
wild type EV
wild type
rab-7
mir-35-41(gk262)
EV
mir-35-41(gk262)
rab-7
F
lsy-6(ot150) rab-7
lsy-6(ot150) EV
wild type rab-7
wild type EV
***
N.S.
% ASE neuron
ASEL+
ASEL-

Figure 5.1 Knock down of *rab-7* enhances the phenotypes associated with several miRNA mutants. Images showing the *col-19::gfp* expression phenotype of *mir-48 mir-241(nDf51)* animals with control RNAi (Empty Vector (EV)) (A) and *rab-7* RNAi (B). Yellow arrows point to representative seam cells and white arrowheads point to representative hyp7 nuclei. (C) The *col-19::gfp* expression phenotype and (D) adult alae phenotype of wild type (VT1367) animals and *mir-48 mir-241(nDf51)* animals with EV and *rab-7* RNAi at the young adult stage. (E) Embryonic lethality phenotype of wild type (N2) and *mir-35-41(gk262)* animals with EV and *rab-7* RNAi. (F) ASE neuron phenotype of wild type (VT2361) and *lsy-6(ot150)* animals with EV and *rab-7* RNAi. * $p < 0.05$, ** $p < 0.01$, *** $p < 0.001$, N.S. not significant, chi-square test for adult alae phenotype and ASE neuron phenotype, two-tailed *t*-test for the *col-19::gfp* expression phenotype and embryonic lethality phenotype.

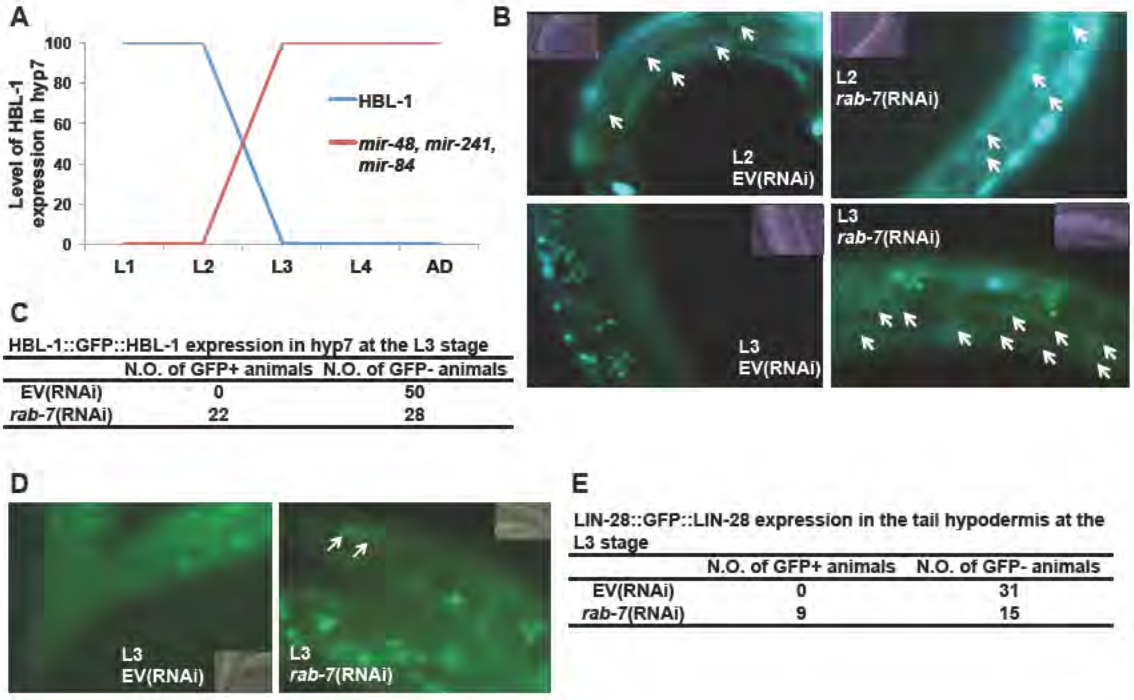

Figure 5.2 Knocking down *rab-7* delays the downregulation of two miRNA targets in the heterochronic pathway. (A) A diagram showing the regulation of HBL-1 by *let-7* family miRNAs (*mir-48*, *mir-241* and *mir-84*) during larval development in the hyp7. (B) Images and (C) quantification of HBL-1::GFP::HBL-1 expression in wild type animals with EV and *rab-7* RNAi. Arrows point to the hyp7 nuclei. (D) Images and (E) quantification of LIN-28::GFP::LIN-28 expression in wild type animals with EV and *rab-7* RNAi. Arrows point to the GFP+ hypodermal cells.

in the mature miRNA levels upon knocking down *rab-7* in either strain. This indicates that the modulation of RAB-7 on miRNA activity probably downstream of miRNA biogenesis.

4. VPS-11 exhibits similar effects as RAB-7 on the phenotypes of miRNA mutants.

Besides RAB-7, I proposed that regulators of RAB-7 in the endosomal trafficking pathway could also exhibit modulation on the phenotypes of miRNA mutants. Therefore, I performed another RNAi screen of genes encoding HOPS and AP-3 complexes on their effects on miRNA activity. HOPS complex is known to interact with RAB-7 in tethering late endosomal/lysosomal membrane fusion (213) and AP-3 complex is important in regulating cargo transport between various cellular organelles (214). From this screen, I identified that knocking down a HOPS gene *vps-11* exhibits similar effect on the phenotypes of both *mir-48 mir-241(nDf51)* animals and *lsy-6(ot150)* animals as *rab-7* RNAi, and *vps-11* is the only gene that have consistent effect on both strains (Figure 5.4A). Additionally, knocking down *vps-11* delays the downregulation of HBL-1 and enhances the embryonic lethality phenotype of *mir-35-41(lf)* animals (Figure 5.4B and C). Therefore, it seems that *vps-11* may function together with *rab-7* to elicit the positive modulation on the phenotypes of miRNA mutants.

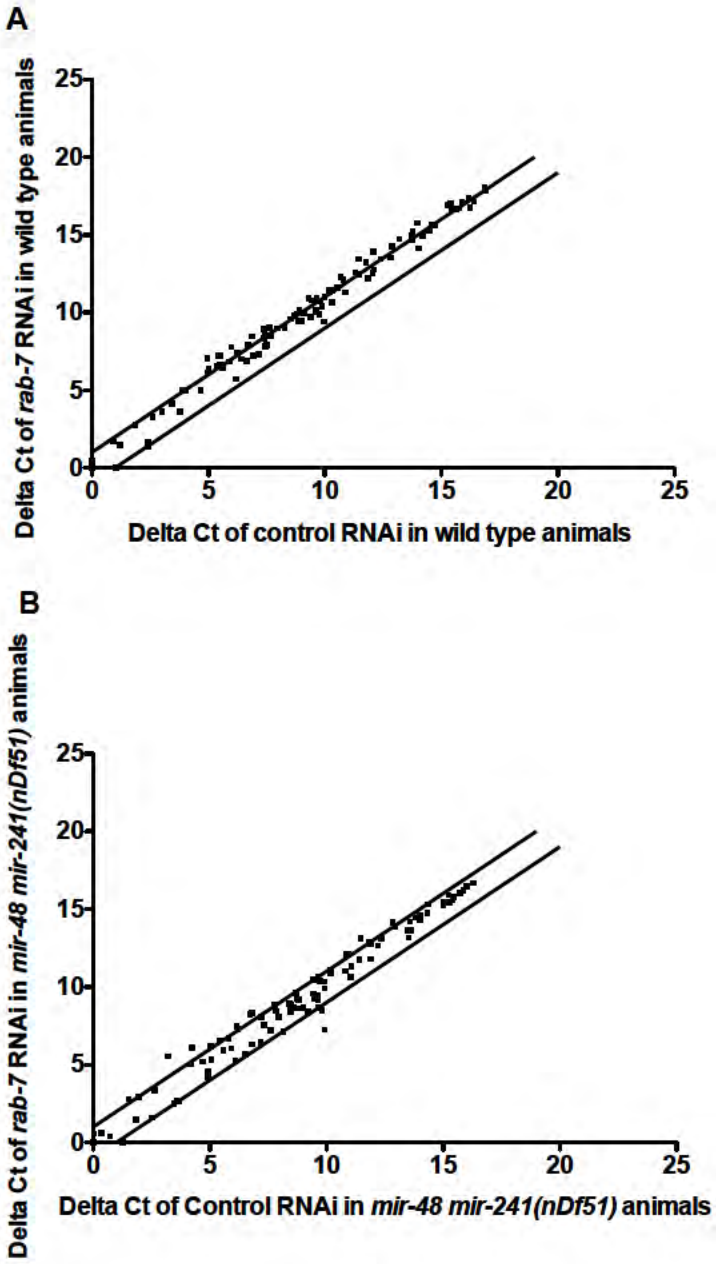

Figure 5.3 Knock down of *rab-7* does not affect mature miRNA levels. 103 mature miRNA levels wild type (VT1367) (A) and *mir-48 mir-241(nDf51)* (B) animals with EV and *rab-7* RNAi. Two-tailed *t*-tests were performed and not a single miRNA exhibit statistically significant two-fold change.

A

Gene	Function	Endosome association	Effect on *col-19::gfp* phenotype of *mir-48 mir-241(nDf51)*	Effect on ASE neuron phenotype of *lsy-6(ot150)*
rme-6	RAB-5 GEF	before early endosome		
vps-34	kinase, PI(3)P	before early endosome		
ccz-1		early endosome, RAB-5+	Suppression	
vps-11	HOPS	early endosome	Enhancement	Enhancement
vps-18	HOPS	early endosome	Suppression	
vps-33.1	HOPS	early endosome		Suppression
vps-33.2	HOPS	early endosome		Suppression
vps-39	HOPS	early endosome		
vps-16	HOPS, AP-3	late endosome		
vps-41	HOPS, AP-3	late endosome	Suppression	
tbc-2	RAB-5 GAP	late endosome, RAB-7+		
glo-3		late endosome		
glo-4	GEF	late endosome		Suppression
glo-5		late endosome		
apb-3	AP-3	late endosome		
apm-3	AP-3	late endosome		Suppression
T27F6.6		block exosome		

Enhancement

Suppression

B

HBL-1::GFP::HBL-1 expression in hyp7 at the L3 stage

	N.O. of GFP+ animals	N.O. of GFP- animals
EV(RNAi)	2	48
rab-7(RNAi)	32	52
vps-11(RNAi)	20	65

C

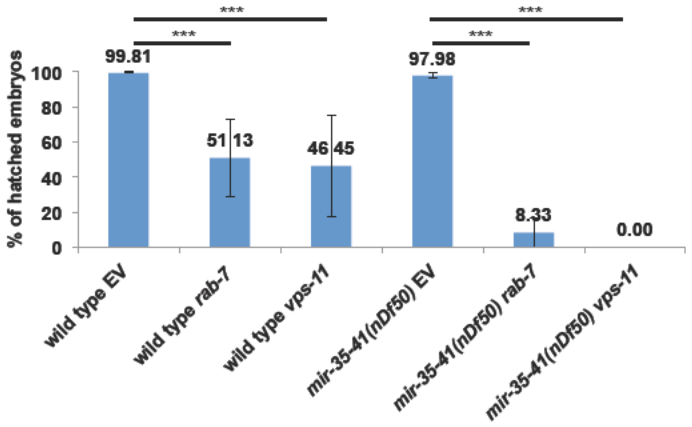

Figure 5.4 The effects of regulators of RAB GTPases on the miRNA mutants' phenotypes. (A) Result summary of the RNAi screen for the effects of RAB GTPase regulators on the phenotypes of *mir-48 mir-241(nDf51)* and *lsy-6(ot150)* animals. Blank boxes indicate no genetic interaction. (B) Quantification of HBL-1::GFP::HBL-1 expression in wild type animals with EV, *rab-7* and *vps-11* RNAi. (C) Embryonic lethality phenotype of wild type (N2) and *mir-35-41(nDf50)* animals with EV, *rab-7* and *vps-11* RNAi. *** $p < 0.001$, two-tailed *t*-test.

5. The genetic null mutant of *rab-7* does not exhibit the same effects on the miRNA mutant phenotypes as *rab-7* RNAi.

Furthermore, I examined if the genetic null mutant of *rab-7* (*rab-7(ok511)*) could have the same effect on miRNA mutant phenotypes as *rab-7* RNAi. The possible maternal contribution of RAB-7 protein allows *rab-7(ok511)* homozygote animals develop to adults even though they will lay dead embryos, which still allows us to test the effect of *rab-7(ok511)* on heterochronic phenotypes and the ASE neuron phenotype of miRNA mutants.

I expect that the *rab-7(ok511)* animals will exhibit similar effect on the phenotypes of miRNA mutants as *rab-7* RNAi. Although *rab-7(ok511)* enhances the adult alae phenotype of *mir-48 mir-241(nDf51)* animals, it suppresses the *col-19::gfp* expression phenotype (Figure 5.5 A and B). And *rab-7(ok511)* has no effect on the ASE neuron phenotype of *lsy-6(ot150)* animals (Figure 5.5C). Also, *rab-7(ok511)/mIn1* heterozygotes exhibit an enhancement of *col-19::gfp* expression of *mir-48 mir-241(nDf51)* animals, but it suppresses the adult alae phenotype. Next, based on our qRT-PCR and western blot analysis, I confirmed that the *rab-7* mRNA and protein levels were indeed decreased upon knocking down *rab-7* (Figure 5.6). This suggests that the *rab-7* RNAi I utilized before does reflect a loss-of-function for RAB-7.

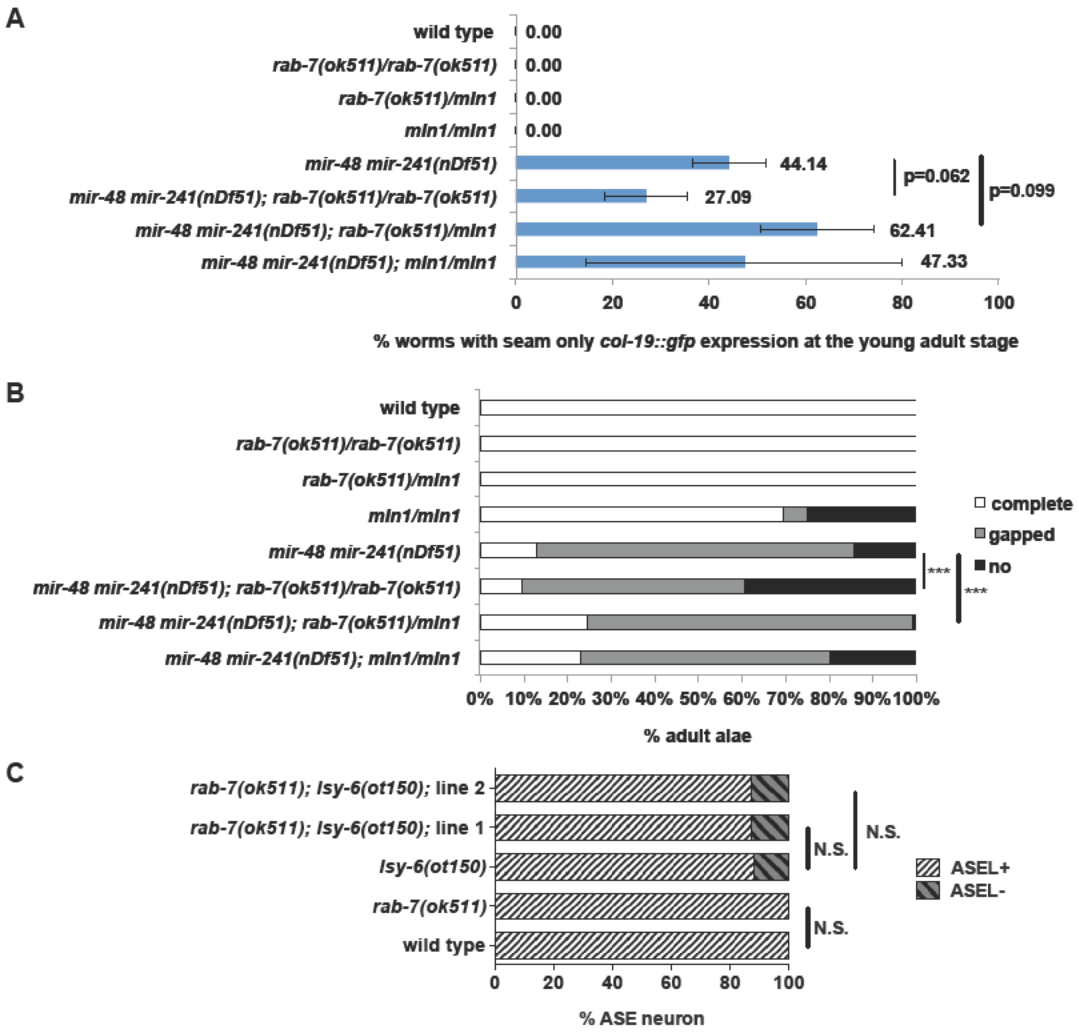

Figure 5.5 The effects of *rab-7(ok511)* on the phenotypes of miRNA mutants. (A) The *col-19::gfp* expression phenotype and (B) adult alae phenotype of *rab-7(ok511)* in wild type (VT1367) and *mir-48 mir-241(nDf51)* backgrounds at the young adult stage. *** $p < 0.001$, two-tailed *t*-test for the *col-19::gfp* expression phenotype and chi-square test for adult alae phenotype. (C) ASE neuron phenotype of *rab-7(ok511)* in wild type (VT2361) and *lsy-6(ot150)* backgrounds. N.S. not significant, chi-square test for ASE neuron phenotype.

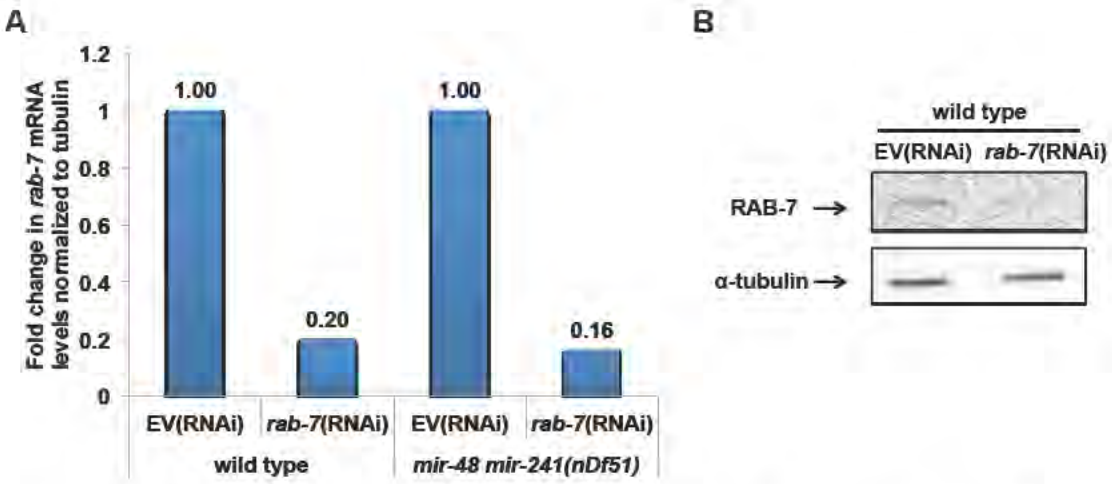

Figure 5.6 Validation of *rab-7* RNAi. (A) mRNA levels of *rab-7* in wild type (VT1367) and *mir-48 mir-241(nDf51)* animals upon EV and *rab-7* RNAi. (B) Western blots of RAB-7 and α-tubulin in wild type (VT1367) animals with EV and *rab-7* RNAi. RAB-7 is recognized with an antibody developed in Dr. Anne Spang's laboratory (215).

These results in the effects of *rab-7(ok511)* and *rab-7* RNAi on the phenotypes of miRNA mutants suggest that RAB-7's modulation on miRNA mutant phenotypes might be through different mechanisms and in a dosage-dependent manner.

6. The modulation of *rab-7* RNAi on miRNA mutant phenotypes might not be directly through miRNAs, but through EGFR/PI3K signaling pathway.

Since RAB-7 is an important regulator of endosomal trafficking and knocking down *rab-7* could have significant effects on various cellular pathways including protein degradation, endocytosis/exocytosis and signaling pathways, I sought to examine if the effect of *rab-7* RNAi on the phenotypes of miRNA mutants could be contributed by an indirect effect of RAB-7 on miRNA phenotypes.

First, since I observed adult alae and *col-19::gfp* expression phenotype enhancement of *mir-48 mir-241(nDf51)* animals when knocking down *rab-7*, I tested if the seam cell phenotype of *mir-48 mir-241(nDf51)* animals is enhanced as well. However, I failed to observe any change in the seam cell number of wild type or *mir-48 mir-241(nDf51)* animals upon knocking down *rab-7* (Figure 5.7). This suggests that the effect of *rab-7* RNAi on the adult alae and *col-19::gfp* expression phenotype might not be through directly affecting *let-7* family miRNA activity.

Next, previous studies have shown that *rab-7* can regulate EGF signaling pathway during *C. elegans* vulva development (216). Therefore, I wondered if the

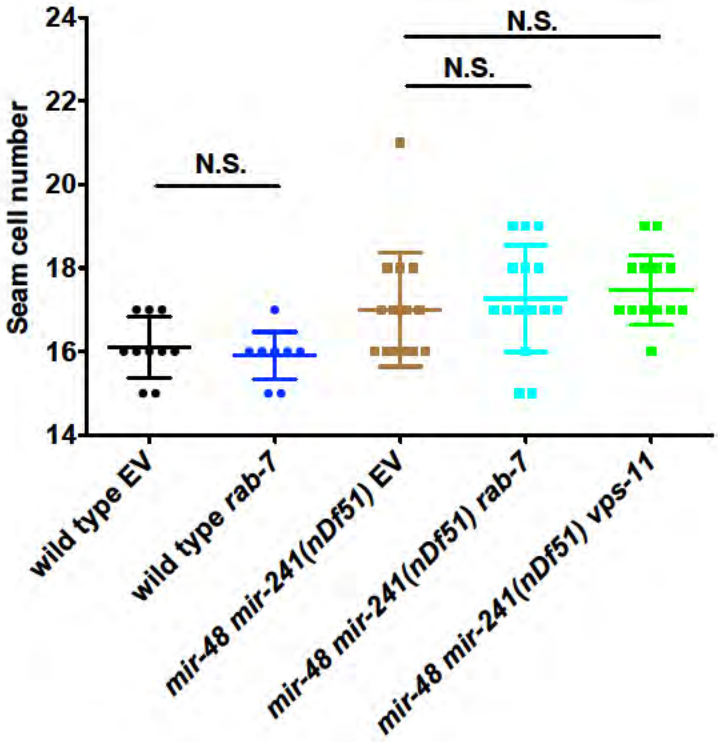

Figure 5.7 Knocking down *rab-7* and *vps-11* does not affect the seam cell phenotype of wild type and the *let-7* family mutant. Seam cell number of young adult stage wild type (VT1367) and *mir-48 mir-241(nDf51)* animals upon EV, *rab-7* and *vps-11* RNAi. N.S. not significant, two-tailed *t*-test.

phenotypic enhancement of *rab-7* RNAi on miRNA mutants could be due to the EGF signaling pathway. The gene that encodes *C. elegans* EGFR is *let-23*, and there are three possible signaling pathways downstream of LET-23: 1) Ras pathway; 2) PI3K/FOXO pathway; 3) PLCγ pathway (Figure 5.8) (217). Also, LIN-2 (membrane associated guanylate kinase (MAGUK) family) is known to be required for the correct localization of LET-23 in the basolateral membrane of the vulva precursor cells (218). Interestingly, loss-of-function mutant of *let-23* or *lin-2* blocks the enhancement of *col-19::gfp* expression phenotype of *mir-48 mir-241(nDf51)* animals upon knocking down *rab-7* or *vps-11* (Figure 5.9A). This suggests that the modulation of *rab-7* RNAi on *col-19::gfp* expression phenotype of the *let-7* family miRNA mutant is possibly through the EGF signaling pathway.

Interestingly, knocking down *let-23* or *lin-2* suppresses *col-19::gfp* expression phenotype of *mir-48 mir-241(nDf51)* animals and this suppression is diminished in the *rab-7(ok511)* animals (Figure 5.9B). This suggests that *rab-7* is also required for the modulation of *col-19::gfp* expression phenotype in *mir-48 mir-241(nDf51)* animals by the EGF signaling pathway. Additionally, *let-23* or *lin-2* RNAi mildly enhanced the ASE neuron phenotype of the *lsy-6(ot150)* animals, and the enhancement by *lin-2* RNAi is diminished in *rab-7(ok511)* animals (Figure 5.9C). Although further studies are needed to explain the opposite effects of EGF signaling pathway on the *col-19::gfp* expression phenotype and the ASE neuron phenotype, yet these results suggest that RAB-7 and EGF signaling

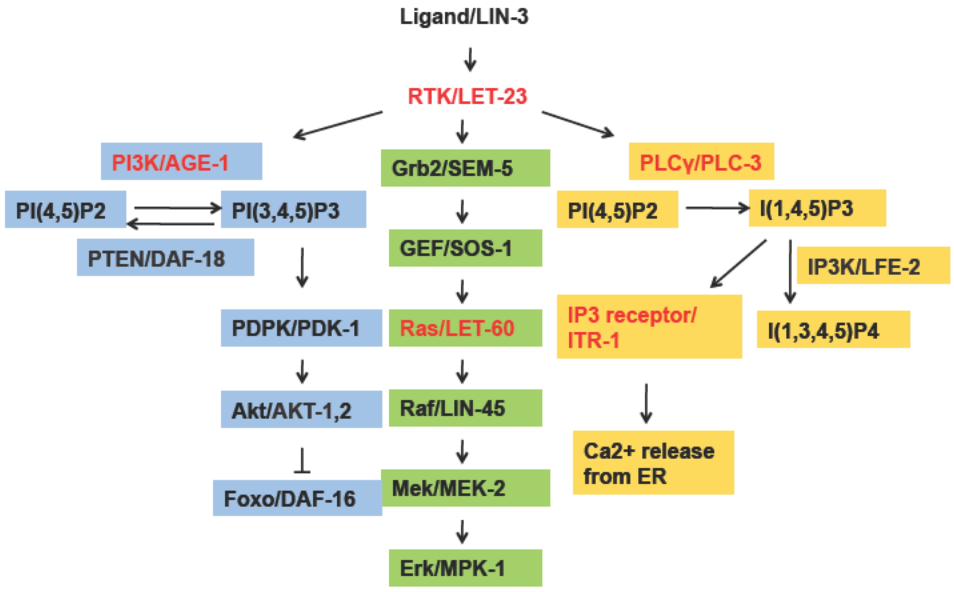

Figure 5.8 EGF signaling pathway in *C. elegans*. Blue boxes are PI3K pathway, green boxes are Ras pathway and yellow boxes are PLC pathway. Genes in red were used in later analysis.

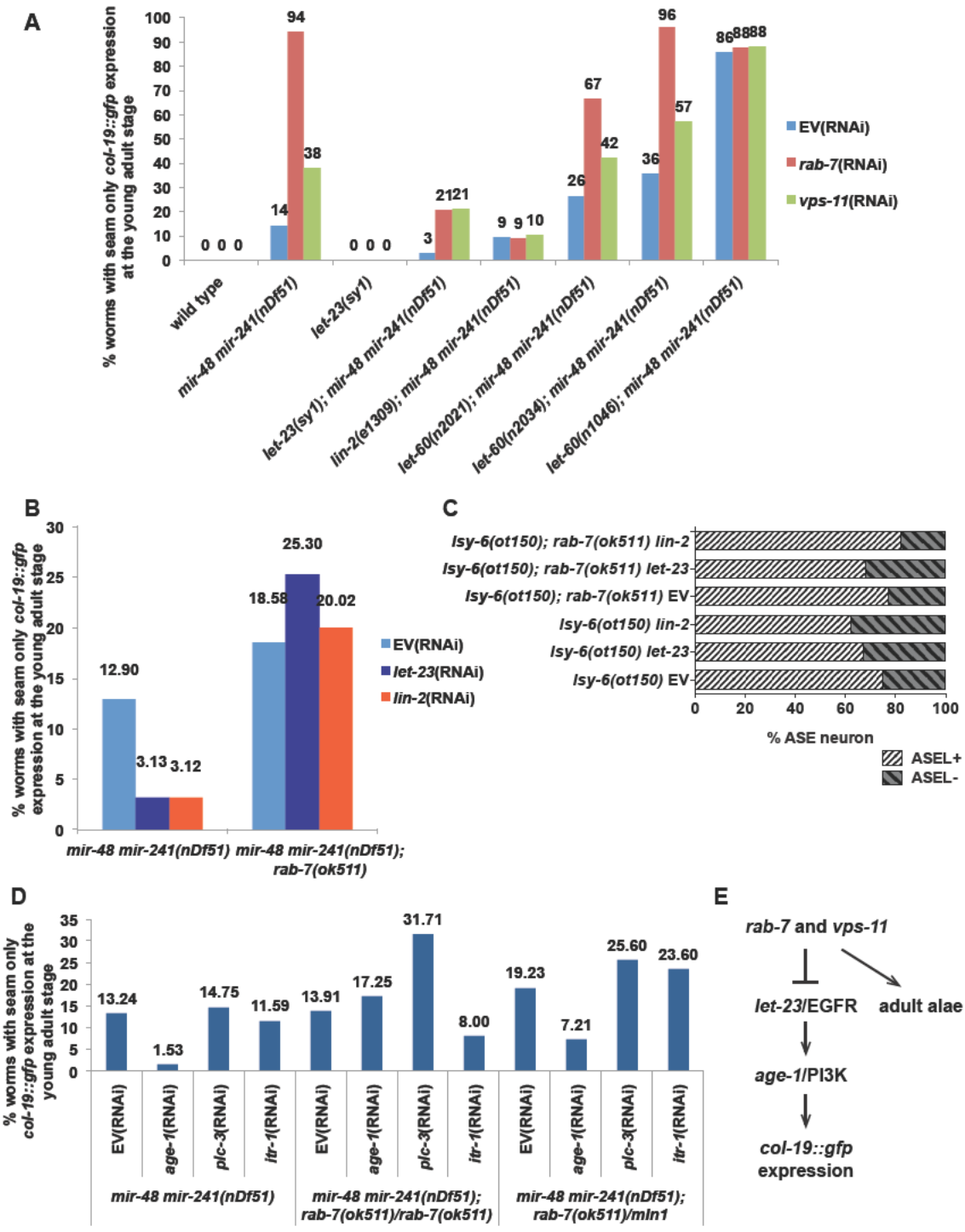
A
% worms with seam only col-19::gfp expression at the young adult stage
EV(RNAi)
rab-7(RNAi)
vps-11(RNAi)
wild type
mir-48 mir-241(nDf51)
let-23(sy1)
let-23(sy1); mir-48 mir-241(nDf51)
lin-2(e1309); mir-48 mir-241(nDf51)
let-60(n2021); mir-48 mir-241(nDf51)
let-60(n2034); mir-48 mir-241(nDf51)
let-60(n1046); mir-48 mir-241(nDf51)
B
% worms with seam only col-19::gfp expression at the young adult stage
EV(RNAi)
let-23(RNAi)
lin-2(RNAi)
mir-48 mir-241(nDf51)
mir-48 mir-241(nDf51); rab-7(ok511)
C
lsy-6(ot150); rab-7(ok511) lin-2
lsy-6(ot150); rab-7(ok511) let-23
lsy-6(ot150); rab-7(ok511) EV
lsy-6(ot150) lin-2
lsy-6(ot150) let-23
lsy-6(ot150) EV
% ASE neuron
ASEL+
ASEL-
D
% worms with seam only col-19::gfp expression at the young adult stage
EV(RNAi)
age-1(RNAi)
plc-3(RNAi)
itr-1(RNAi)
mir-48 mir-241(nDf51)
mir-48 mir-241(nDf51); rab-7(ok511)/rab-7(ok511)
mir-48 mir-241(nDf51); rab-7(ok511)/mln1
E
rab-7 and vps-11
let-23/EGFR
adult alae
age-1/PI3K
col-19::gfp expression

Figure 5.9 The EGFR/PI3K pathway seems to contribute to the effect of *rab-7* RNAi on the *col-19::gfp* expression phenotype of *mir-48 mir-241(nDf51)* animals. (A) The *col-19::gfp* expression phenotype of EGF pathway mutants in *mir-48 mir-241(nDf51)* background upon EV, *rab-7* and *vps-11* RNAi. (B) The *col-19::gfp* expression phenotype of *mir-48 mir-241(nDf51)* and *mir-48 mir-241(nDf51); rab-7(ok511)* animals upon knocking down *let-23* and *lin-2*. (C) ASE neuron phenotype of *lsy-6(ot150)* and *lsy-6(ot150)*; *rab-7(ok511)* animals upon knocking down *let-23* and *lin-2.* (D) The *col-19::gfp* expression phenotype of *mir-48 mir-241(nDf51)*, *mir-48 mir-241(nDf51); rab-7(ok511)* and *mir-48 mir-241(nDf51); rab-7(ok511)/mIn1* animals upon knocking down *age-1, plc-3* and *itr-1.* (E) Diagram on how *rab-7* and *vps-11* affect the *col-19::gfp* expression and adult alae phenotype.

pathway may function together to exhibit modulation on the miRNA mutant phenotypes.

Last, I wondered which downstream signaling pathway is required for the modulation of EGFR and RAB-7 on the *col-19::gfp* expression phenotype. First, loss-of-function mutants of *let-60*/Ras (*n2021* and *n2034*) do not suppress the *col-19::gfp* expression phenotype of *mir-48 mir-241(nDf51)* animals and *rab-7* and *vps-11* RNAi can still enhance the *col-19::gfp* expression phenotype of *mir-48 mir-241(nDf51)* animals in the *let-60(lf)* background (Figure 5.9A). This suggests that Ras pathway is probably not required for the modulation of the *col-19::gfp* expression phenotype by EGFR. Next, knocking down two major components of the PLCγ pathway (*plc-3*/PLCγ and *itr-1*/IP3 receptor) do not suppress the *col-19::gfp* expression phenotype of *mir-48 mir-241(nDf51)* animals (Figure 5.9D), which indicates that the PLCγ pathway is not required for this phenotype either. However, knocking down the PI3K (*age-1*) significantly suppresses the *col-19::gfp* expression phenotype of *mir-48 mir-241(nDf51)* animals and this suppression is diminished in *rab-7(ok511)* background (Figure 5.9D), similar to the effects of *let-23* and *lin-2* RNAi. These results indicate that the modulation of EGF signaling and RAB-7 on the *col-19::gfp* expression phenotype of *mir-48 mir-241(nDf51)* animals might act through PI3K pathway (Figure 5.9E).

In summary, the modulation of miRNA mutant phenotypes by RAB-7 might not be directly through affecting miRNAs, and certain phenotypic modulation of

rab-7 RNAi on miRNA mutants might be through RAB-7's effect on EGFR/PI3K pathway.

7. EGFR, Ras and PI3K pathways affect the developmental timing phenotypes of a *let-7* family miRNA mutant.

In addition to *col-19::gfp* expression phenotype, I also examined the adult alae and seam cell phenotypes of EGFR/Ras signaling pathway mutants in wild type and *mir-48 mir-241(nDf51)* background. Interestingly, as oppose to the suppression in *col-19::gfp* expression phenotype, *let-23(sy1)* and *lin-2(e1309)* significantly enhanced both adult alae and seam cell phenotypes of *mir-48 mir-241(nDf51)* animals (Figure 5.10). This suggests that the *col-19::gfp* expression phenotype and the adult alae/seam cell phenotype are not always consistent with each other and the effects of EGF signaling pathway on the *col-19::gfp* expression phenotype and the adult alae/seam cell phenotype of *mir-48 mir-241(nDf51)* animals might be due to different mechanisms. Indeed, I observed that both loss-of-function and gain-of-function mutants of *let-60* enhances the adult alae and seam cell phenotype of *mir-48 mir-241(nDf51)* animals (Figure 5.10). Therefore, it is possible that EGFR acts through Ras signaling pathway to positively modulate the adult alae and seam cell phenotypes of the *let-7* family miRNA mutant.

Since EGF signaling pathway's modulation on the *col-19::gfp* expression phenotype might be through PI3K/*age-1*, I tested the effects of *age-1* on the adult alae and seam cell phenotypes of *mir-48 mir-241(nDf51)* animals. Interestingly,

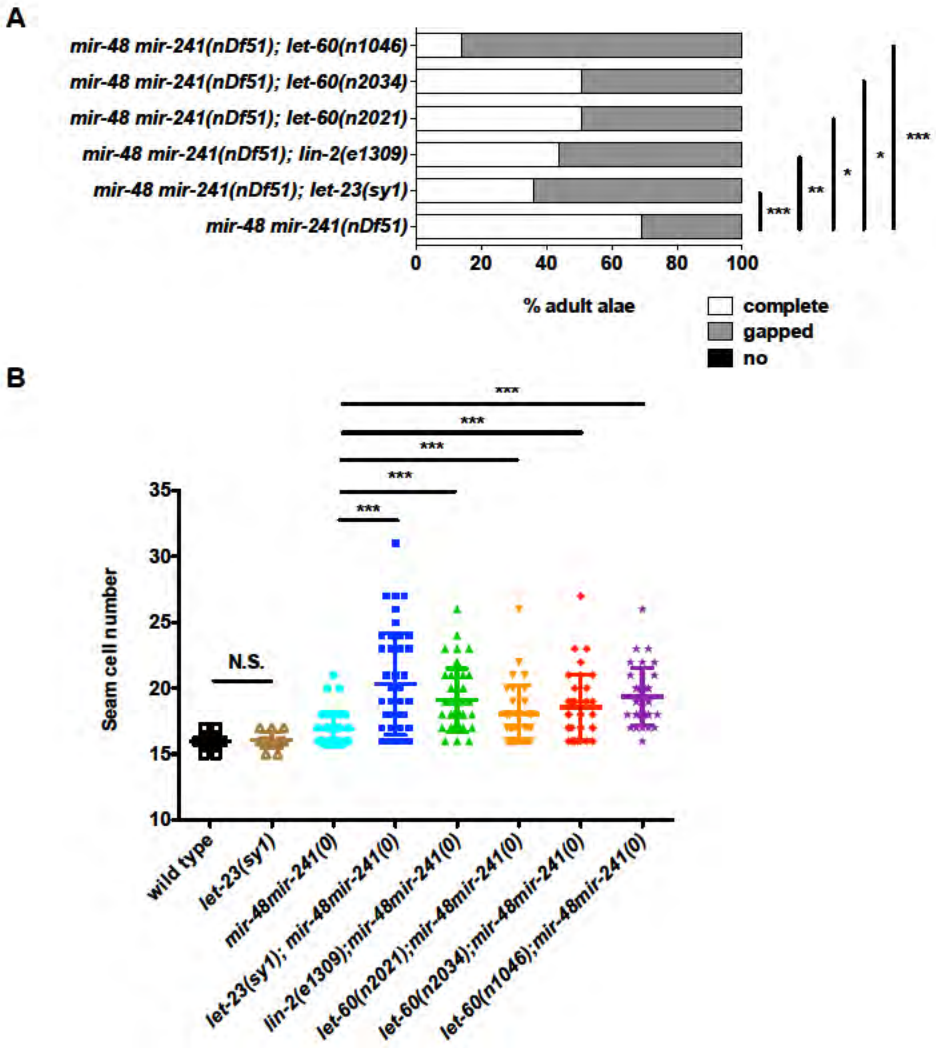

Figure 5.10 EGF signaling pathway can affect the developmental timing phenotype of *mir-48 mir-241(nDf51)* animals. (A) Adult alae and (B) seam cell phenotype of EGF signaling pathway mutants in wild type (VT1367) and *mir-48 mir-241(nDf51)* backgrounds at the young adult stage. * $p < 0.05$, ** $p < 0.01$, *** $p < 0.001$, N.S. not significant, chi-square test for adult alae phenotype, two-tailed *t*-test for seam cell phenotype.

consistent with the suppression in *col-19::gfp* expression phenotype, *age-1* RNAi mildly suppresses the seam cell phenotype of *mir-48 mir-241(nDf51)* animals as well (Figure 5.11). This indicates that the PI3K pathway might function to negatively modulate the heterochronic phenotypes of the *let-7* family miRNA mutant.

These results suggest that EGF signaling pathway could modulate the developmental timing phenotypes of the *let-7* family miRNA mutant, and the signaling pathways downstream of EGFR might have opposite effects on the phenotypes of *mir-48 mir-241(nDf51)* animals.

8. Knock down of ESCRT genes does not affect miRNA pathway, but leads to a general reduction of GFP reporter levels caused by an elevated autophagy activity.

In addition to *rab-7*, I also identified several genes in the ESCRT complex (*hgrs-1/hrs*, *vps-37* and *T27F7.1/vps-24*) that are able to modulate the phenotypes of miRNA mutants in the screen. Knocking down *hgrs-1*, *vps-37* or *T27F7.1* significantly enhanced the *col-19::gfp* expression phenotype of *mir-48 mir-241(nDf51)* animals (Figure 5.12A). However, the ASE neuron phenotype of *lsy-6(ot150)* animals was not affected by knocking down either *hgrs-1*, *vps-37* or *T27F7.1* (Figure 5.12B). Additionally, we examined the effect of *hgrs-1*, *vps-37* and *T27F7.1* RNAi on the levels of HBL-1 in several genetic backgrounds. Since *hgrs-1*, *vps-37* and *T27F7.1* RNAi enhances the *col-19::gfp* expression phenotype of *mir-48 mir-241(nDf51)* animals, I expect that there would be an

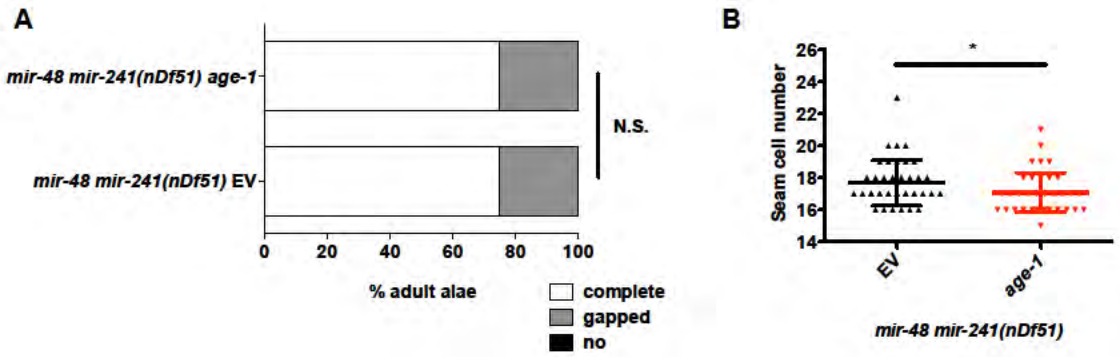

Figure 5.11 *age-1*/PI3K RNAi suppresses the seam cell phenotype of the *let-7* family miRNA mutant. (A) Adult alae and (B) seam cell phenotype of *mir-48 mir-241(nDf51)* animals upon knocking down *age-1* at the young adult stage. * $p < 0.05$, ** $p < 0.01$, *** $p < 0.001$, N.S. not significant, chi-square test for adult alae phenotype, two-tailed *t*-test for seam cell phenotype.

upregulation of HBL-1 upon depleting *hgrs-1*, *vps-37* and *T27F7.1*. However, I observed the opposite effect that is the levels of HBL-1 were downregulated when knocking down *hgrs-1*, *vps-37* and *T27F7.1* (Figure 5.12C). I also noticed that upon knocking down *hgrs-1*, *vps-37* and *T27F7.1*, worms became quite sick. Therefore, I wonder if the enhancement in the *col-19::gfp* expression phenotype upon *hgrs-1*, *vps-37* and *T27F7.1* RNAi could be due to a general reduction in the GFP levels. Indeed, I observed that *hgrs-1*, *vps-37* and *T27F7.1* RNAi lead to a reduction in the GFP levels for two other GFP reporters (*scm::gfp* and *sur-5::gfp*) whose levels are not known to be affected by the developmental timing pathway (Figure 5.12D and E). Therefore, it seems that the effects of *hgrs-1*, *vps-37* and *T27F7.1* RNAi on *col-19::gfp* expression phenotype of *mir-48 mir-241(nDf51)* animals might be through a general reduction of the GFP levels.

Next, we examined the possible mechanism in which knocking down the ESCRT complex *hgrs-1*, *vps-37* and *T27F7.1* could cause a reduction in the GFP expression. Loss-of-function mutants of ESCRT complex were previously shown to exhibit an elevated level of autophagy (219). Consistent with that, I observed a dramatic upregulation of the autophagy marker (LGG-1/Atg8) when knocking down *hgrs-1*, *vps-37* and *T27F7.1* (Figure 5.13A). Also, *lgg-1* RNAi suppresses the downregulation of *col-19::gfp* and *hbl-1::gfp::hbl-1* expression upon knocking down *hgrs-1*, *vps-37* and *T27F7.1* (Figure 5.13B and C). This indicates that the enhancement of *hgrs-1*, *vps-37* and *T27F7.1* RNAi on *col-19::gfp* expression phenotype of *mir-48 mir-241(nDf51)* animals is possible because of a general

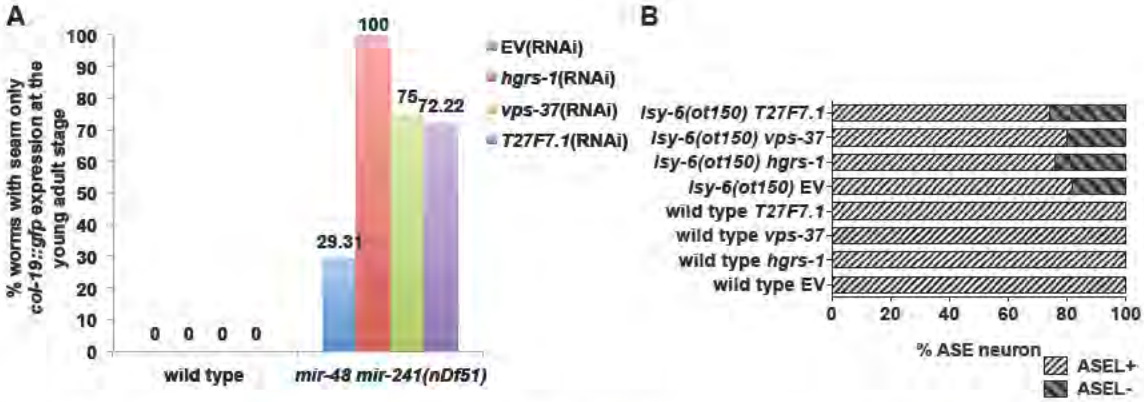

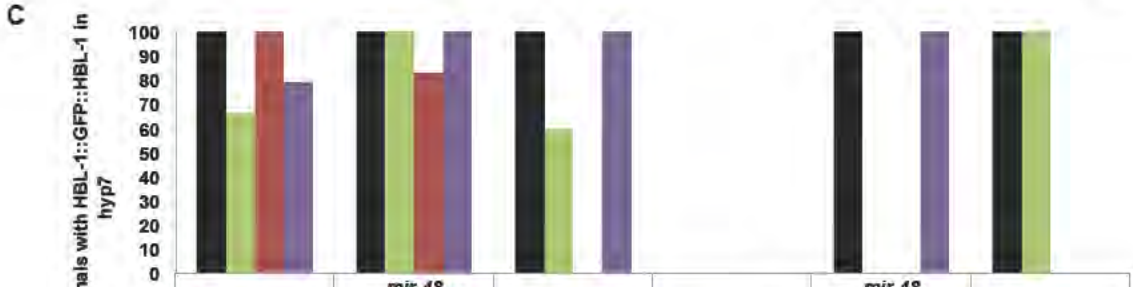

	wild type	mir-48 mir-241(nDf51); mir-84(n4037)	alg-1(tm492)	wild type	mir-48 mir-241(nDf51); mir-84(n4037)	alg-1(tm492)
	L2			L3		
EV(RNAi)	100	100	100	0	100	100
hgrs-1(RNAi)	66.66666667	100	60	0		100
vps-37(RNAi)	100	83.33333333		0	0	
T27F7.1(RNAi)	78.94736842	100	100	0	100	

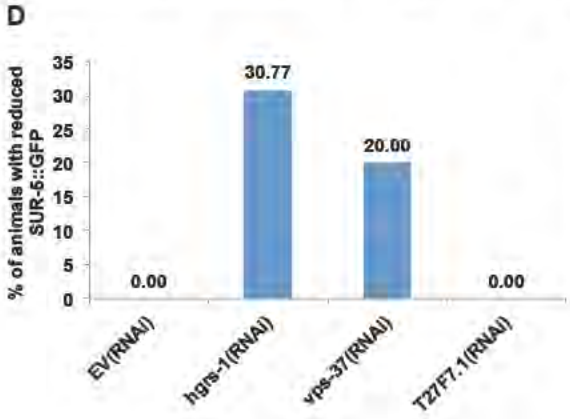

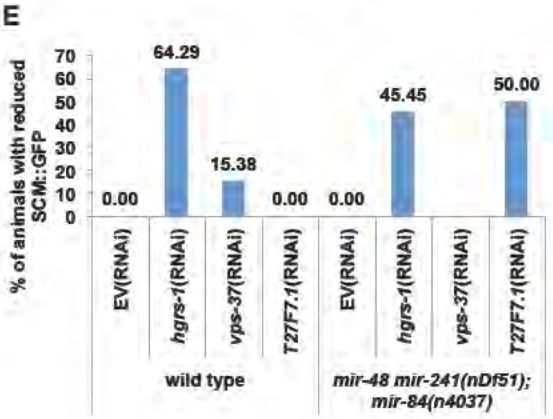

Figure 5.12 The effects of genes in the ESCRT complex on the phenotypes of miRNA mutants and miRNA target expression levels. (A) The *col-19::gfp* expression phenotype of wild type (VT1367) and *mir-48 mir-241(nDf51)* animals upon knocking down *hgrs-1*, *vps-37* and *T27F7.1*. (B) ASE neuron phenotype of wild type (VT2361) and *lsy-6(ot150)* animals upon knocking down *hgrs-1*, *vps-37* and *T27F7.1*. (C) Quantification of HBL-1::GFP::HBL-1 expression in wild type, *mir-48 mir-241(nDf51); mir-84(n4037)* and *alg-1(tm492)* animals upon EV, *hgrs-1*, *vps-37* and *T27F7.1* RNAi. (D) Quantification of the reduced expression of SUR-5::GFP in wild type animals upon EV, *hgrs-1*, *vps-37* and *T27F7.1* RNAi. (E) Quantification of the reduced expression of SCM::GFP in wild type and *mir-48 mir-241(nDf51); mir-84(n4037)* animals upon knocking down *hgrs-1*, *vps-37* and *T27F7.1*.

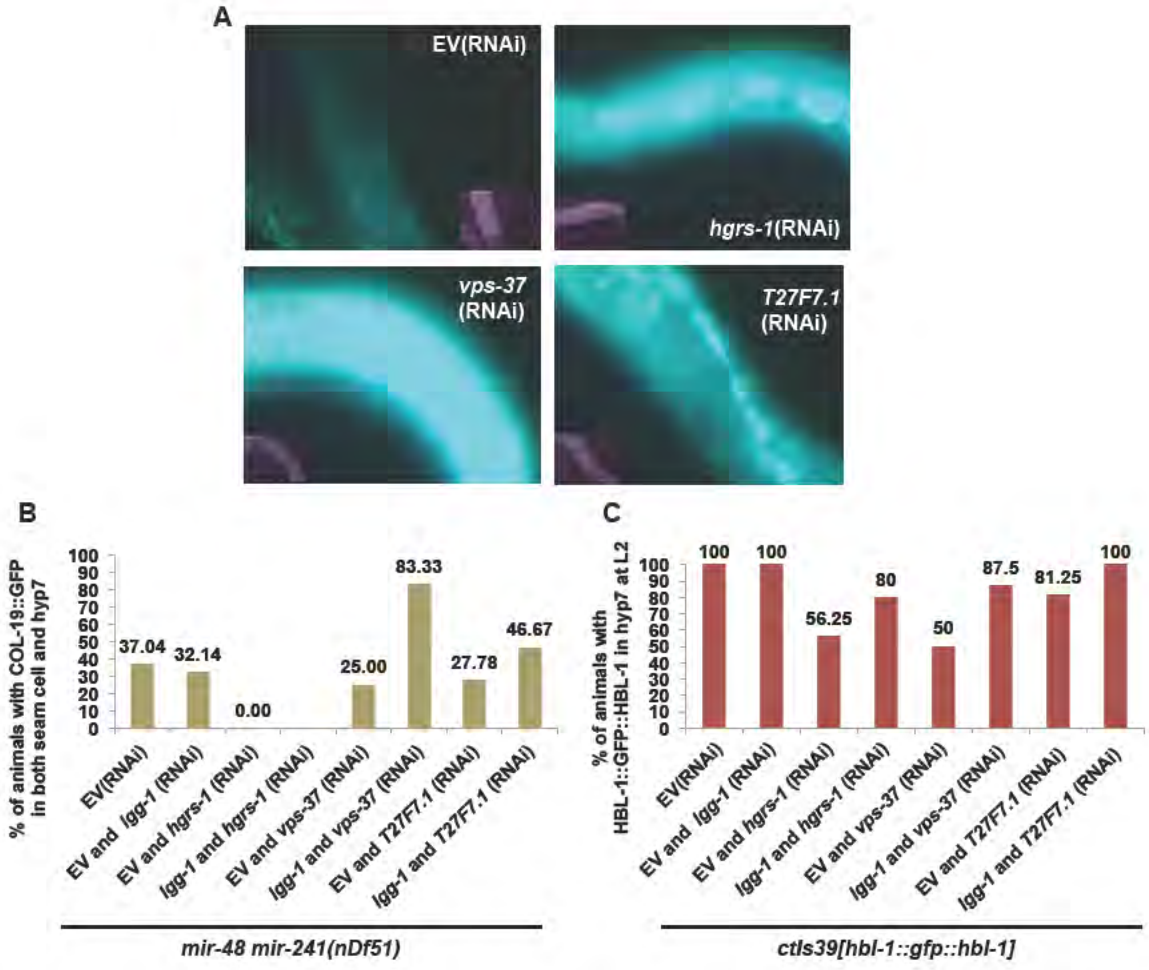

Figure 5.13 The reduced GFP expression caused by ESCRT gene knock down may be due to an enhanced autophagy activity. (A) Images showing LGG-1::GFP::LGG-1 expression of wild type animals upon knocking down *hgrs-1*, *vps-37* and *T27F7.1*. (B) The *col-19::gfp* expression phenotype of *mir-48 mir-241(nDf51)* animals upon knocking down *hgrs-1*, *vps-37* and *T27F7.1* in combination with *lgg-1* RNAi. (C) Quantification of HBL-1::GFP::HBL-1 in wild type animals upon knocking down *hgrs-1*, *vps-37* and *T27F7.1* in combination with *lgg-1* RNAi.

reduction of GFP expression caused by an elevated level of autophagy upon depleting *hgrs-1*, *vps-37* and *T27F7.1*.

Consistent with these findings, I also observed no co-localization between HGRS-1 and a miRISC factor NHL-2 (Figure 5.14), which indicates that the ESCRT complex does not directly interact with miRISC in *C. elegans*.

In conclusion, the ESCRT complex *hgrs-1*, *vps-37* and *T27F7.1* does not seems to directly modulate miRNA activity, and the elevated level of autophagy caused by *hgrs-1*, *vps-37* and *T27F7.1* RNAi seems to be the reason for the enhancement in *col-19::gfp* expression phenotype of *mir-48 mir-241(nDf51)* animals upon knocking down *hgrs-1*, *vps-37* and *T27F7.1*.

9. Prion-like proteins PQN-29 and PQN-67 suppress the *col-19::gfp* expression and adult alae phenotype of *mir-48 mir-241(nDf51)*.

Previous study has shown that human prion protein PrP^C binds to AGO protein and potentially provides the physical interaction between endosomal vesicles and miRISC (220). Therefore, I tested if the homologs of PrP^C in *C. elegans* (*pqn-29*, *pqn-67*) could have any modulation on the phenotypes of miRNA mutants. Interestingly, *pqn-29* and *pqn-67* seem to negatively modulate the *col-19::gfp* expression phenotype and adult alae phenotype of *mir-48 mir-241(nDf51)* animals (Figure 5.15A and C). However, knocking down *pqn-29* and *pqn-67* RNAi does not have any effect on the seam cell phenotype of *mir-48 mir-241(nDf51)* animals or the ASE neuron phenotype of *lsy-6(ot150)* animals (Figure 5.15B and D). Further studies are needed to figure out if the negative

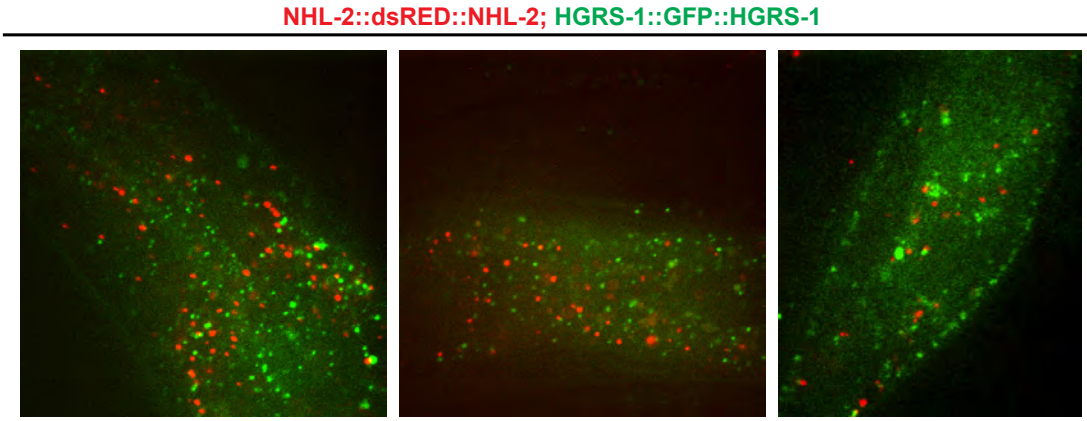

Figure 5.14 There seems to be no co-localization between miRISC and ESCRT complex. Confocal images showing NHL-2::dsRED::NHL-2 and HGRS-1::GFP::HGRS-1 expression in wild type animals.

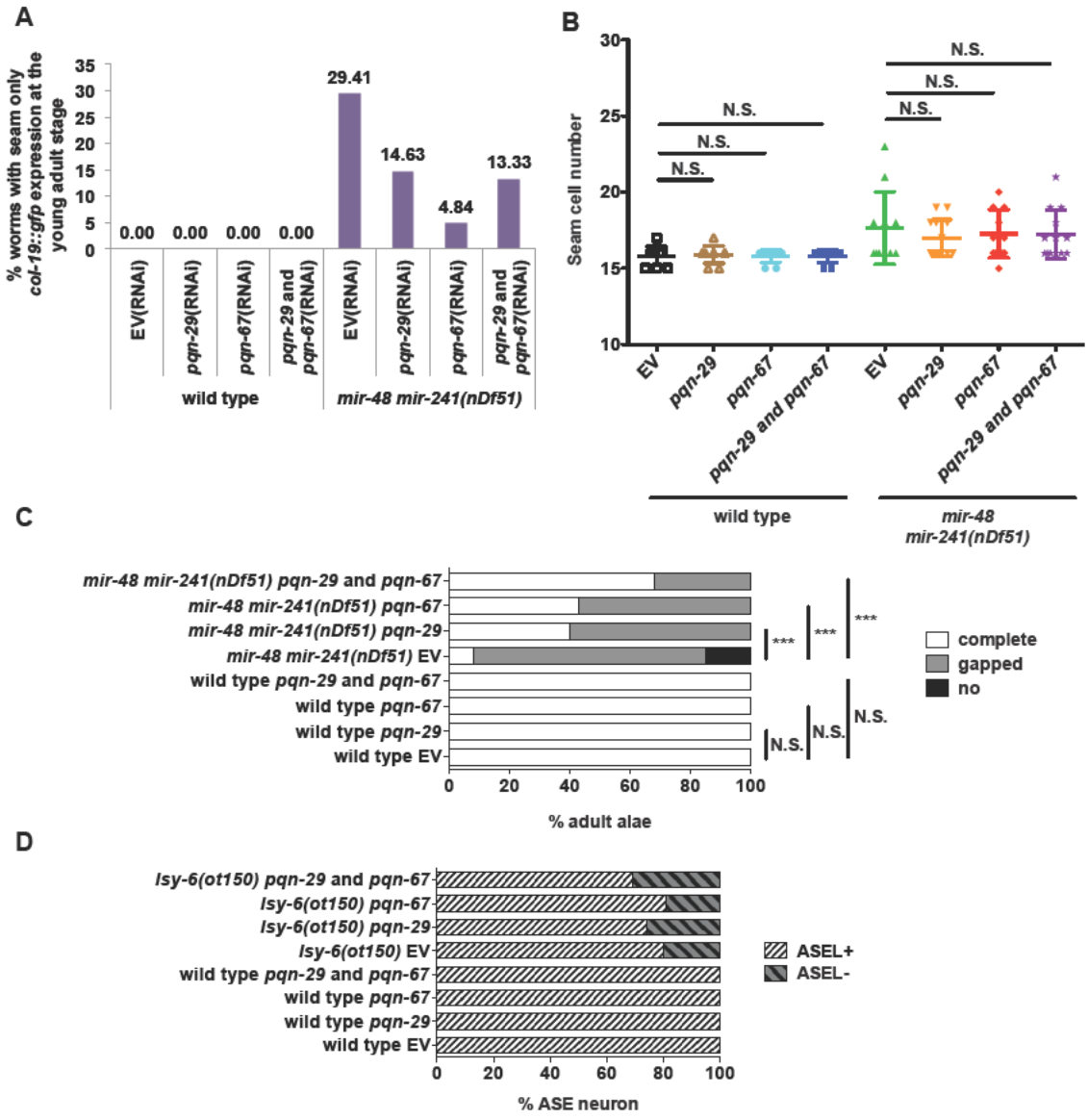

Figure 5.15 The effects of *pqn-29* and *pqn-67* on the phenotypes of miRNA mutants. (A) The *col-19::gfp* expression phenotype, (B) seam cell phenotype and (C) adult alae phenotype of wild type (VT1367) and *mir-48 mir-241(nDf51)* animals upon knocking down *pqn-29, pqn-67,* and *pqn-29 and pqn-67* together. (C) ASE neuron phenotype of wild type (VT2361) and *lsy-6(ot150)* animals upon knocking down *pqn-29, pqn-67,* and *pqn-29 and pqn-67* together. N.S. not significant, two-tailed *t*-test for seam cell phenotype.

modulation of the *col-19::gfp* expression phenotype and adult alae phenotype of *mir-48 mir-241(nDf51)* animals by *pqn-29* and *pqn-67* is through RAB-7.

10. RNAi for FMRP (*M88.5*) mildly suppresses the *let-7* family miRNA mutant's developmental timing phenotype.

The fragile X mental retardation protein (FMRP) has been shown before to regulate miRNA activity (221). Interestingly, I found that knocking down the *C. elegans* homolog of FMRP (*M88.5*) suppresses the seam cell phenotype of *mir-48 mir-241(nDf51)* animals (Figure 5.16). This suggests that *M88.5* might be a negative modulator of miRNA activity, however, the effects of *M88.5* on the phenotypes of other miRNA mutants are needed to test this hypothesis.

V.E. Discussion

Based on the results presented in this chapter, I have shown that the phenotypes of several miRNA mutants (sensitized genetic backgrounds) could be modulated by various cellular pathways, including endosomal trafficking, EGF signaling pathway. However, these modulators could function to affect miRNA activity directly or act downstream of miRNA pathway to exhibit their effects.

There are three major developmental timing phenotypes examined here: 1) the *col-19::gfp* expression phenotype; 2) the adult alae phenotype; 3) the seam cell phenotype. Based on our findings, it seems that these three heterochronic phenotypes are not always consistent with each other and they could be affected differently by the same modulator. The heterochronic defects in

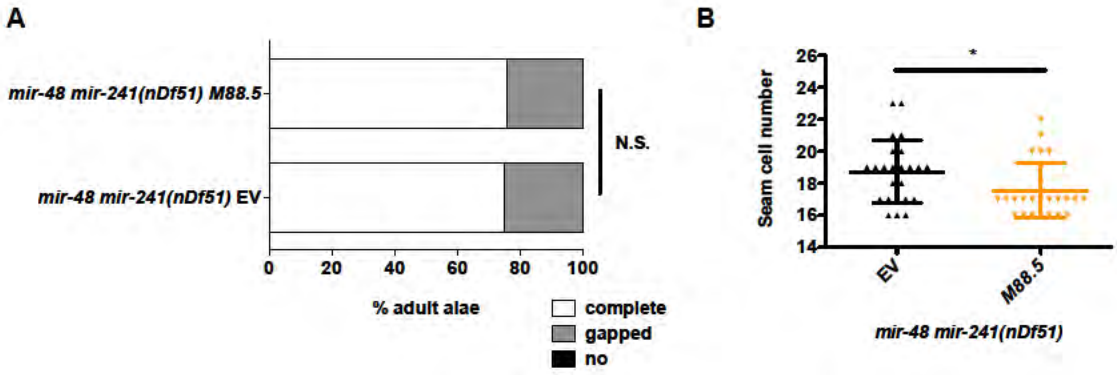

Figure 5.16 The effect of *M88.5*/FMRP on the heterochronic phenotypes of the *let-7* family miRNA mutant. (A) Adult alae and (B) seam cell phenotype of *mir-48 mir-241(nDf51)* animals upon knocking down *M88.5* at the young adult stage. * $p < 0.05$, N.S. not significant, chi-square test for adult alae phenotype, two-tailed *t*-test for seam cell phenotype.

C. elegans were originally defined as abnormal temporal patterns of cell lineage (77). Therefore, the seam cell phenotype should be the gold standard for heterochronic phenotypes, but other mechanisms (for instance, cell division) could also affect the seam cell lineage without changing the temporal patterns of seam cells (222), which might be independent from the *let-7* family miRNAs. Another phenotype of the heterochronic mutants is the adult alae phenotype and adult alae is an adult-specific cuticular structure produced only at the L4 molt. The adult alae phenotype is a great complement to the seam cell phenotype, but pathways other than the heterochronic pathway, for example, exocytosis of collagens, could also affect the production of adult alae. The adult specific collagen *col-19* is a downstream target of *let-7* and can be used as an indication of *let-7* family miRNA activity. There is a significant advantage in using the *col-19::gfp* phenotype because it can be used in large-scale screens whereas seam cell and adult alae phenotypes require much closer examination through high magnification fluorescent microscope. However, there are probably more pathways affecting this transcriptional reporter *col-19::gfp* expression in a *let-7* family miRNA independent manner. Therefore, all three developmental timing phenotypes should be examined to determine the effects of different modulators on *let-7* family miRNA activity.

The enhancement in the *col-19::gfp* expression of *mir-48 mir-241(nDf51)* animals by *rab-7* RNAi seems to be through the EGF pathway, and the EGF pathway suppresses the *col-19::gfp* expression of *mir-48 mir-241(nDf51)*

animals. However, regarding the adult alae phenotype, the EGF pathway mutants enhance, rather than suppress, the adult alae phenotype of *mir-48 mir-241(nDf51)* animals. This indicates that the EGF pathway might not be the downstream pathway required for the adult alae phenotype enhancement of *mir-48 mir-241(nDf51)* animals upon knocking down *rab-7*. I noticed that the cuticle looks generally weak under DIC microscopy upon *rab-7* RNAi, therefore, I propose that knocking down *rab-7* could affect the exocytosis of collagens, which could result in the enhancement of adult alae phenotype of *mir-48 mir-241(nDf51)* animals. Moreover, I have shown that knocking down *rab-7* delays the downregulation of *let-7* family miRNA targets HBL-1 and LIN-28, and I hypothesize that this regulation could be contributed by the inhibition of protein degradation caused by *rab-7* RNAi.

There is inconsistency between the effects of *rab-7* RNAi and *rab-7(ok511)* mutant on the phenotypes of miRNA mutants. *rab-7* RNAi enhances the phenotypes of *mir-48 mir-241(nDf51)* animals and *lsy-6(ot150)* animals. However, *rab-7(ok511)* homozygotes suppress the *col-19::gfp* expression phenotype but enhance the adult alae phenotype of *mir-48 mir-241(nDf51)* animals, whereas *rab-7(ok511)* heterozygotes enhance *col-19::gfp* expression phenotype but suppress the adult alae phenotype of *mir-48 mir-241(nDf51)* animals (Figure 5.5). Also, *rab-7(ok511)* homozygotes do not modulate the ASE neuron phenotype of *lsy-6(ot150)* animals. *rab-7(ok511)* is a putative null allele that removes about half of the *rab-7* coding region and potentially all the

promoter elements. The homozygotes of *rab-7(ok511)* produces dead embryos but they are able to develop normally possibly due to the maternal contribution of the RAB-7 protein. Although *rab-7(ok511)* animals probably have lower level of RAB-7 protein than wild type animals, the exact tissue distribution of the maternally loaded protein is unknown. Therefore, it is possible that *rab-7(ok511)* animals have more RAB-7 protein in the hypodermis and ASE neurons than wild type animals upon *rab-7* RNAi. Furthermore, different levels of RAB-7 might lead to accumulation of different endosomal vesicles, which could affect the miRNA phenotypes differently. So far, I do not yet know how exactly is the endosomal trafficking pathway affected by *rab-7(ok511)* and *rab-7* RNAi.

Interestingly, the EGF signaling pathway seems to function together with RAB-7 to exhibit the enhancement of the *col-19::gfp* expression phenotype of *mir-48 mir-241(nDf51)* animals. Loss-of-function mutants of EGF signaling pathway suppress the *col-19::gfp* expression phenotype of *mir-48 mir-241(nDf51)* animals but enhances the seam cell and adult alae phenotype *mir-48 mir-241(nDf51)* animals, which is another indication that the heterochronic phenotypes could be modulated differently. Our preliminary data suggest that the EGFR/Ras pathway might function to enhance the seam cell and adult alae phenotype, whereas the PI3K pathway may be responsible for the suppression of the *col-19::gfp* expression phenotype of *mir-48 mir-241(nDf51)* animals upon *let-23* RNAi.

Moreover, PI3K pathway and Ras pathway exhibit modulation on the seam cell phenotypes of *mir-48 mir-241(nDf51)* animals, which indicates that these two pathways might be involved in the regulation of developmental timing. However, both loss-of-function and gain-of-function mutants of *let-60* enhance the seam cell and adult alae phenotypes of *mir-48 mir-241(nDf51)* animals, which indicates that *let-60* might be able to affect heterochronic phenotypes through different mechanisms. Even though *let-23(sy1)* animals do not have any heterochronic defects, it is also possible that PI3K pathway and Ras pathway could inhibit and promote cell proliferation respectively to exhibit the seam cell and adult alae phenotypes. In order to dissect out the mechanisms, examination of the heterochronic phenotypes of these two pathways' mutants in the wild type background is needed in the future.

It should be noted that *mir-35* family mutants were only used in the RNAi screens for ESCRT and RAB genes. There are two reasons on why the embryonic lethality phenotype of *mir-35-41(lf)* animals is not ideal for the identification of miRNA modulators. First, to score the embryonic lethality phenotype is quite labor-intensive for large-scale screens. Second and more importantly, there are numerous pathways that can affect embryonic lethality independent of the *mir-35* family, which makes it difficult to identify bona fine miRNA modulators. In contrast, the *col-19::gfp* expression phenotype and ASE neuron phenotype are more specific to the activity of miRNAs and much easier to screen.

During these RNAi screens, I noticed that a significant number of *mir-48 mir-241(nDf51)* animals exhibit a “partial” *col-19::gfp* expression in the hyp7 and this “partial” *col-19::gfp* expression is almost completely at the posterior of the animal. It has been shown that Wnt ligands form a gradient along the worm’s anterior-posterior axis (223) and Wnt pathway is known regulate the developmental timing phenotypes (84, 222). Additionally, retromer complex functions in Wnt-producing cells to allow the formation of Wnt gradient (224) and retromer complex functionally interacts with RAB-7 as well (225). Therefore, I performed an RNAi screen on the effect of Wnt ligands and retromer complex on the *col-19::gfp* expression phenotype. However, I did not observe any significant modulation of the *col-19::gfp* expression phenotype of *mir-48 mir-241(nDf51)* animals upon knocking down Wnt ligands and retromer complex. It is possible that there is functional redundancy in the regulation of the *col-19::gfp* expression phenotype by these genes.

Additionally, I carried out an RNAi screen to test whether RNA helicases could affect miRNA activity. Many RNA helicases seem to be essential for worm’s survival, but there was one interesting finding that *ddx-23* positively modulates both the *col-19::gfp* expression phenotype of *mir-48 mir-241(nDf51)* animals and the ASE neuron phenotype of *lsy-6(ot150)* animals. Interestingly, a recent study has shown that *ddx-23* functions to regulate the processing of pri-miRNAs (226), which is consistent with our finding.

In conclusion, candidate-based RNAi screens allow us to study the modulation of different cellular pathways on the activity of miRNAs. Here I focused on the endosomal trafficking pathway and observed that several regulators of the endosomal trafficking pathway could modulate phenotypes associated with miRNA mutants. However, the modulation seems to be independent of miRNA pathway. Therefore, there could be indirect the interactions between miRNA pathway and other cellular pathways, which may be important in conferring the robustness in gene expression profiles under various conditions.

CHAPTER VI: Conclusions, discussion and future directions

VI.A. Summary of research

MiRNAs are important post-transcriptional regulators that control many developmental and physiological processes. In this thesis, I have shown that various environmental and cellular factors can modulate the activity of miRNAs, and that miRNAs function to confer developmental robustness under these perturbations.

1. Developmental timing pathway is integrated with innate immune pathway to regulate pathogen resistance and robust developmental cell fates.

The work in Chapter II and III demonstrated a reciprocal interaction between the developmental timing pathway and the p38 MAPK innate immune pathway centering on the *let-7* family miRNAs (Figure 6.1). A novel function of the p38 MAPK pathway was discovered in suppressing *let-7* family miRNAs upon *P. aeruginosa* infection, meanwhile, *let-7* family miRNAs negatively regulate pathogen resistance possibly through the p38 MAPK pathway and several heterochronic genes. In addition, the developmental timing regulator *lin-28* is upregulated upon *P. aeruginosa* infection and acts upstream of *let-7* family miRNAs to promote pathogen resistance. The feedforward loop involving *lin-28*, *let-7* family miRNAs and p38 could function to initiate the innate immune response upon a pathogen infection. And the full complement of *let-7* family miRNAs is required to maintain the invariant developmental timing process

during infection. Therefore, the interaction between heterochronic genes and innate immune pathway allows worms to monitor the physiological conditions while coordinate the robustness of developmental timing and pathogen response.

2. The miRNA pathway is modulated by various cellular components.

Besides environmental modulators, the activity of miRNAs can be affected by different cellular components and pathways as well. In Chapter IV, we found that the double-stranded RNA-binding protein Staufen (STAU-1) negatively modulates several miRNAs that control developmental timing and asymmetric neuronal cell fate specification in *C. elegans*. Also, our study reveals a novel finding that STAU-1 does not affect the levels of most small RNA populations including mature miRNAs, except a sub-population of endogenous siRNAs in the WAGO pathway. Interestingly, the 3'UTR of a miRNA target (*lin-14*) seems to be required for STAU-1-mediated modulation on miRNA activity. Therefore, Staufen negatively modulates the activity of the miRNA pathway downstream of miRNA biogenesis possibly through 3'UTR of miRNA targets, and this negative modulation of miRNA activity by Staufen is likely due to its role in promoting translation, rather than in mediating mRNA decay. Furthermore, other cellular pathways, for example, the endosomal trafficking pathway, can also affect the phenotypes associated with miRNA activity, but the modulation may not act directly through miRNAs.

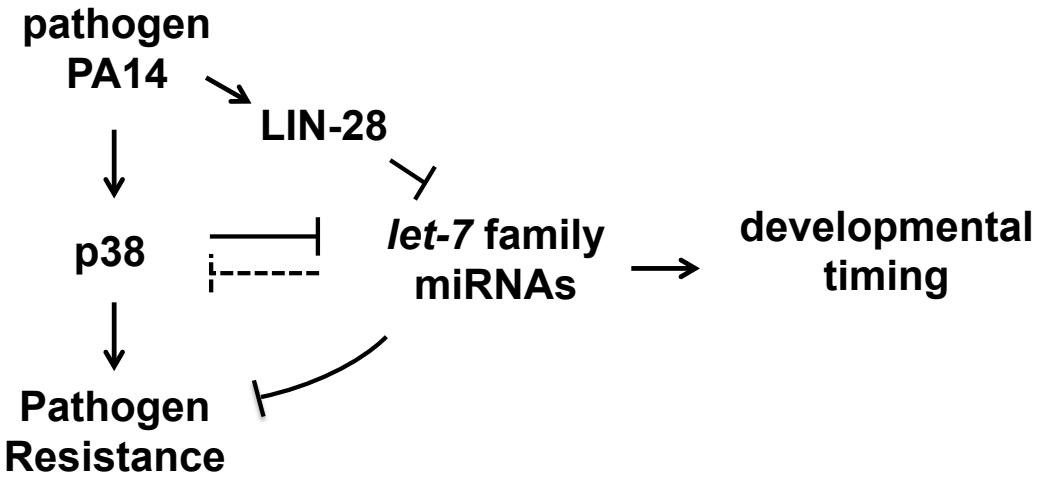

Figure 6.1 A diagram of the regulatory circuits involving heterochronic genes and the innate immune pathway in *C. elegans* upon *P. aeruginosa* infection. The dotted line indicates a proposed regulatory interaction not yet proven experimentally.

VI.B. MiRNAs and RNA-binding proteins: the evolutionary selection for biological robustness

1. Biological robustness.

Biological robustness refers to the maintenance of specific functionalities of the biological systems against perturbations (85). To cope with the unpredictable environments and the natural genetic mutations, organisms evolve various mechanisms to ensure their robust execution of fundamental processes. The findings here add to the increasing evidence suggest that miRNAs and RNA-binding proteins are important in the regulation of biological robustness.

2. Mechanisms of miRNAs and RNA-binding proteins in maintaining biological robustness.

Four mechanisms were proposed to ensure the robustness of a system: system control, alternative (or fail-safe) mechanisms, modularity and decoupling (85). Interestingly, our findings here indicate that miRNAs and RNA-binding proteins can be utilized in all these mechanisms.

System control includes feedback and feedforward regulatory circuits to confer a robust outcome. I have demonstrated that *let-7* family miRNAs and RNA-binding protein LIN-28 are involved in a feedforward loop with the p38 MAPK pathway to amplify the innate immune response (Figure 6.1), which could act like a “switch” to assist the host’s correct initiation of pathogen resistance programs upon infection.

The effects of *P. aeruginosa* and *stau-1* on the developmental timing phenotypes were only observed when a few members of the *let-7* family miRNAs are missing. Therefore, the genetic redundancy of the *let-7* family miRNAs is the fail-safe mechanism for the robust developmental cell fates against various internal and external perturbations, which is possibly the reason why this family of miRNAs evolve to consist many genomic copies in most organisms.

Modularity is a mechanism to restrain the perturbations locally thereby minimizing the effects on the whole system. To do that, multi-cellular organisms evolve specific functions for different cells or tissues. For example, the regulation of *let-7* family miRNAs by p38 was observed only in the intestine and hypodermis, while in the pharynx where *let-7* family miRNAs are highly expressed, there is no effect on the transcription of these miRNAs by p38. This indicates that different mechanisms are probably evolved in different tissues to ensure specific functionalities are carried out robustly.

Evolution requires organisms to maintain a degree of genetic diversity through random neutral mutations, which could be important for the adaptation of changing environments. Decoupling is an important mechanism that separates important phenotypes from these genetic variations to confer robustness. Since the double-stranded RNA-binding protein Staufen can regulate mRNA localization and translation, gaining of this gene during evolution is beneficial for organisms to carry out complex gene regulation. However, I have shown that Staufen has a negative effect on the miRNA pathway. Therefore, miRNAs must

utilize mechanisms like feedback loops and redundancy to decouple this effect of Staufen from important biological processes.

Collectively, the work presented in this thesis provides more evidence supporting the notion that numerous mechanisms employed by miRNAs and RNA-binding proteins are selected during evolution to control the robustness of biological processes. Studies on the functions of miRNAs and RNA-binding proteins under stresses other than *P. aeruginosa* infection are needed in the future to gain a more comprehensive understanding of the importance of miRNAs and RNA-binding proteins in regulating biological robustness.

VI.C. Sensitized genetic backgrounds to identify novel functions of miRNAs and miRNA modulators

One of the most important findings in this thesis is that a panel of miRNA and miRNA biogenesis factor mutants were established as sensitized genetic backgrounds and could be used to identify miRNA modulators and novel functions of miRNAs.

There are at least 110 miRNAs identified in *C. elegans* (227), but loss of most miRNAs and miRNA families do not exhibit any obvious developmental phenotypes (76, 228), which I think could be explained by several reasons. First, miRNA families could function redundantly with other miRNA families to regulate the same biological process. Second, the expression of miRNAs could be restricted to specific cell types (for example, neurons). As a result, the

phenotypes of these miRNA mutants could not be easily identified. Last, the functions of certain miRNAs could only be manifested under specific environmental and physiological conditions, which have not been examined yet.

A previous effort was made to identify the functions of individual miRNAs using sensitized genetic backgrounds (229). Specifically, the sensitized genetic background they employed was the null mutant of *alg-1*. Since there are two miRNA-specific AGO proteins in *C. elegans*, animals lacking *alg-1* do not exhibit any dramatic phenotype but their miRNA pathway is compromised. They generated mutants of individual miRNAs with *alg-1* null allele and examined the developmental timing phenotype, gonad migration phenotype, embryonic lethality and adult lethality phenotypes of these animals. Although several novel functions for miRNAs were identified in this study, not many phenotypes were tested to obtain a comprehensive understanding of the functions of individual miRNAs. However, *alg-1* null mutant could be added to our sensitized genetic backgrounds to identify modulators of the miRNA pathway as well.

Even though a lot of work has been done in this thesis to understand the functions of miRNAs and miRNA modulators, whole genome RNAi screens and more stresses should be applied to these sensitized genetic backgrounds in the future to gain more knowledge on the functions of miRNAs and the widespread modulation on the miRNA pathway.

VI.D. Connecting the dots among *let-7* family miRNAs, *P. aeruginosa* infection and Staufen

It has been shown in Chapter II that *let-7* family miRNA activity is significantly downregulated upon *P. aeruginosa* infection, albeit no dramatic change in the mature *let-7* family miRNA levels was observed. Furthermore, in Chapter IV, I demonstrated that Staufen negatively modulates miRNA activity without affecting mature miRNA levels. One hypothesis is that in addition to the transcriptional repression elicited by the p38 MAPK pathway, *P. aeruginosa* could suppress *let-7* family miRNA activity by boosting the level or activity of Staufen. To test this hypothesis, I examined the developmental timing phenotypes of the double mutant *stau-1(tm2266); mir-48 mir-241(nDf51)* on *P. aeruginosa*. Although no phenotypic enhancement was observed for this mutant on *P. aeruginosa* compared to the *E. coli* control (data not shown), it is possible that the phenotype of this mutant is not in the range of the sensitized genetic backgrounds. Therefore, I propose that other mutants of *stau-1* with *let-7* family miRNAs, which exhibit phenotypes in the range of sensitized genetic backgrounds, need to be examined to determine if Staufen is involved in the regulation of *let-7* family miRNAs on *P. aeruginosa*.

Another open question is that whether Staufen is involved in the regulation of pathogen resistance against *P. aeruginosa* infection, and if so, whether *let-7* family miRNAs is required for this regulation. Previous studies have shown that *Drosophila* and mammalian Staufen proteins are localized to P-body or stress

granules to potentially regulate stress response (181, 230). Also, a recent CLIP experiment identified that mammalian Staufen1 binds to the 3'UTR of *xbp1*, an important regulator of the ER stress pathway, and regulate its mRNA's cytosolic splicing and stability (178). The *C. elegans* homolog XBP-1 is known to be required for larval survival on *P. aeruginosa* (125). Therefore, it would be interesting to test whether *stau-1* mutants exhibit any survival phenotype on *P. aeruginosa* and if *xbp-1* and/or *let-7* family miRNAs are required for the phenotype.

VI.E. Concluding remarks

In this thesis, I have utilized sensitized genetic backgrounds to identify modulators of the miRNA pathway in *C. elegans*. First, I determined that *let-7* family miRNAs, *lin-28* and the p38 MAPK pathway function in a regulatory circuit to control pathogen resistance against *P. aeruginosa* infection, and *let-7* family miRNAs are important in conferring the robust developmental timing in *C. elegans* upon a pathogen infection. Second, the double-stranded RNA-binding protein Staufen was identified as a negative modulator of the miRNA pathway. This negative modulation of Staufen on miRNAs is carried out downstream of miRNA biogenesis, possible through the 3'UTR of miRNA targets. MiRNAs, *lin-28*, the p38 MAPK pathway and Staufen are all extremely conserved during evolution, and hence this study can enrich the knowledge of these pathways in other animal systems as well. Furthermore, the findings here also underscore the

emerging role of miRNAs in conferring robustness to developmental programs under various internal and external perturbations, which could provides us with a better understanding of the biological and pathological processes regulated by miRNAs and may potential aid the development of novel therapeutic interventions for diseases.

BIBLIOGRAPHY

1. Ambros V (2004) The functions of animal microRNAs. *Nature* 431:350–355.

2. Chang T-C, Mendell JT (2007) microRNAs in vertebrate physiology and human disease. *Annu Rev Genomics Hum Genet* 8:215–239.

3. Lee RC, Feinbaum RL, Ambros V (1993) The *C. elegans* heterochronic gene *lin-4* encodes small RNAs with antisense complementarity to *lin-14*. *Cell* 75:843–854.

4. Wightman B, Ha I, Ruvkun G (1993) Posttranscriptional regulation of the heterochronic gene *lin-14* by *lin-4* mediates temporal pattern formation in *C. elegans*. *Cell* 75:855–862.

5. Reinhart BJ et al. (2000) The 21-nucleotide *let-7* RNA regulates developmental timing in *Caenorhabditis elegans*. *Nature* 403:901–906.

6. Pasquinelli AE et al. (2000) Conservation of the sequence and temporal expression of *let-7* heterochronic regulatory RNA. *Nature* 408:86–89.

7. Bartel DP (2004) MicroRNAs: genomics, biogenesis, mechanism, and function. *Cell* 116:281–297.

8. He L, Hannon GJ (2004) MicroRNAs: small RNAs with a big role in gene regulation. *Nat Rev Genet* 5:522–531.

9. Lee Y et al. (2003) The nuclear RNase III Drosha initiates microRNA processing. *Nature* 425:415–419.

10. Nguyen TA et al. (2015) Functional Anatomy of the Human Microprocessor. *Cell* 161:1374–1387.

11. Yi R, Qin Y, Macara IG, Cullen BR (2003) Exportin-5 mediates the nuclear export of pre-microRNAs and short hairpin RNAs. *Genes Dev* 17:3011–3016.

12. Lund E, Güttinger S, Calado A, Dahlberg JE, Kutay U (2004) Nuclear export of microRNA precursors. *Science* 303:95–98.

13. Bernstein E, Caudy AA, Hammond SM, Hannon GJ (2001) Role for a bidentate ribonuclease in the initiation step of RNA interference. *Nature* 409:363–366.

14. Hutvágner G et al. (2001) A cellular function for the RNA-interference

enzyme Dicer in the maturation of the *let-7* small temporal RNA. *Science* 293:834–838.

15. Grishok A et al. (2001) Genes and mechanisms related to RNA interference regulate expression of the small temporal RNAs that control *C. elegans* developmental timing. *Cell* 106:23–34.

16. Mah SM, Buske C, Humphries RK, Kuchenbauer F (2010) miRNA*: a passenger stranded in RNA-induced silencing complex? *Crit Rev Eukaryot Gene Expr* 20:141–148.

17. Wu L, Belasco JG (2008) Let me count the ways: mechanisms of gene regulation by miRNAs and siRNAs. *Molecular Cell* 29:1–7.

18. Bartel DP (2009) MicroRNAs: target recognition and regulatory functions. *Cell* 136:215–233.

19. Ding L, Spencer A, Morita K, Han M (2005) The developmental timing regulator AIN-1 interacts with miRISCs and may target the argonaute protein ALG-1 to cytoplasmic P bodies in *C. elegans*. *Molecular Cell* 19:437–447.

20. Zhang L et al. (2007) Systematic identification of *C. elegans* miRISC proteins, miRNAs, and mRNA targets by their interactions with GW182 proteins AIN-1 and AIN-2. *Molecular Cell* 28:598–613.

21. Behm-Ansmant I et al. (2006) mRNA degradation by miRNAs and GW182 requires both CCR4:NOT deadenylase and DCP1:DCP2 decapping complexes. *Genes Dev* 20:1885–1898.

22. Eulalio A, Huntzinger E, Izaurralde E (2008) GW182 interaction with Argonaute is essential for miRNA-mediated translational repression and mRNA decay. *Nat Struct Mol Biol* 15:346–353.

23. Zekri L, Huntzinger E, Heimstädt S, Izaurralde E (2009) The silencing domain of GW182 interacts with PABPC1 to promote translational repression and degradation of microRNA targets and is required for target release. *Mol Cell Biol* 29:6220–6231.

24. Huntzinger E, Braun JE, Heimstädt S, Zekri L, Izaurralde E (2010) Two PABPC1-binding sites in GW182 proteins promote miRNA-mediated gene silencing. *EMBO J* 29:4146–4160.

25. Jinek M, Fabian MR, Coyle SM, Sonenberg N, Doudna JA (2010) Structural insights into the human GW182-PABC interaction in

microRNA-mediated deadenylation. *Nat Struct Mol Biol* 17:238–240.

26. Chekulaeva M et al. (2011) miRNA repression involves GW182-mediated recruitment of CCR4-NOT through conserved W-containing motifs. *Nat Struct Mol Biol* 18:1218–1226.

27. Fabian MR et al. (2011) miRNA-mediated deadenylation is orchestrated by GW182 through two conserved motifs that interact with CCR4-NOT. *Nat Struct Mol Biol* 18:1211–1217.

28. Braun JE, Huntzinger E, Fauser M, Izaurralde E (2011) GW182 proteins directly recruit cytoplasmic deadenylase complexes to miRNA targets. *Molecular Cell* 44:120–133.

29. Kuzuoglu-Öztürk D, Huntzinger E, Schmidt S, Izaurralde E (2012) The *Caenorhabditis elegans* GW182 protein AIN-1 interacts with PAB-1 and subunits of the PAN2-PAN3 and CCR4-NOT deadenylase complexes. *Nucleic Acids Research* 40:5651–5665.

30. Rosa A, Spagnoli FM, Brivanlou AH (2009) The miR-430/427/302 family controls mesendodermal fate specification via species-specific target selection. *Developmental Cell* 16:517–527.

31. Taganov KD, Boldin MP, Chang K-J, Baltimore D (2006) NF-kappaB-dependent induction of microRNA miR-146, an inhibitor targeted to signaling proteins of innate immune responses. *Proc Natl Acad Sci USA* 103:12481–12486.

32. Rayner KJ et al. (2010) MiR-33 contributes to the regulation of cholesterol homeostasis. *Science* 328:1570–1573.

33. Karres JS, Hilgers V, Carrera I, Treisman J, Cohen SM (2007) The conserved microRNA miR-8 tunes atrophin levels to prevent neurodegeneration in Drosophila. *Cell* 131:136–145.

34. He L et al. (2005) A microRNA polycistron as a potential human oncogene. *Nature* 435:828–833.

35. Johnson SM et al. (2005) *RAS* is regulated by the *let-7* microRNA family. *Cell* 120:635–647.

36. Johnson CD et al. (2007) The *let-7* microRNA represses cell proliferation pathways in human cells. *Cancer Research* 67:7713–7722.

37. Takamizawa J et al. (2004) Reduced expression of the *let-7* microRNAs

in human lung cancers in association with shortened postoperative survival. *Cancer Research* 64:3753–3756.

38. Yanaihara N et al. (2006) Unique microRNA molecular profiles in lung cancer diagnosis and prognosis. *Cancer Cell* 9:189–198.

39. Kim J et al. (2007) A MicroRNA feedback circuit in midbrain dopamine neurons. *Science* 317:1220–1224.

40. Chendrimada TP et al. (2005) TRBP recruits the Dicer complex to Ago2 for microRNA processing and gene silencing. *Nature* 436:740–744.

41. Melo SA et al. (2009) A *TARBP2* mutation in human cancer impairs microRNA processing and DICER1 function. *Nat Genet* 41:365–370.

42. Paroo Z, Ye X, Chen S, Liu Q (2009) Phosphorylation of the human microRNA-generating complex mediates MAPK/Erk signaling. *Cell* 139:112–122.

43. Kawahara Y, Zinshteyn B, Chendrimada TP, Shiekhattar R, Nishikura K (2007) RNA editing of the microRNA-151 precursor blocks cleavage by the Dicer-TRBP complex. *EMBO Rep* 8:763–769.

44. Kawahara Y et al. (2008) Frequency and fate of microRNA editing in human brain. *Nucleic Acids Research* 36:5270–5280.

45. Heale BSE et al. (2009) Editing independent effects of ADARs on the miRNA/siRNA pathways. *EMBO J* 28:3145–3156.

46. Alarcón CR, Lee H, Goodarzi H, Halberg N, Tavazoie SF (2015) N6-methyladenosine marks primary microRNAs for processing. *Nature* 519:482–485.

47. Viswanathan SR, Daley GQ (2010) Lin28: A microRNA regulator with a macro role. *Cell* 140:445–449.

48. Viswanathan SR, Daley GQ, Gregory RI (2008) Selective blockade of microRNA processing by Lin28. *Science* 320:97–100.

49. Van Wynsberghe PM et al. (2011) LIN-28 co-transcriptionally binds primary *let-7* to regulate miRNA maturation in *Caenorhabditis elegans*. *Nat Struct Mol Biol* 18:302–308.

50. Heo I et al. (2008) Lin28 mediates the terminal uridylation of let-7 precursor MicroRNA. *Molecular Cell* 32:276–284.

51. Hagan JP, Piskounova E, Gregory RI (2009) Lin28 recruits the TUTase Zcchc11 to inhibit let-7 maturation in mouse embryonic stem cells. *Nat Struct Mol Biol* 16:1021–1025.

52. Lehrbach NJ et al. (2009) LIN-28 and the poly(U) polymerase PUP-2 regulate *let-7* microRNA processing in *Caenorhabditis elegans*. *Nat Struct Mol Biol* 16:1016–1020.

53. Heo I et al. (2009) TUT4 in concert with Lin28 suppresses microRNA biogenesis through pre-microRNA uridylation. *Cell* 138:696–708.

54. Jones MR et al. (2009) Zcchc11-dependent uridylation of microRNA directs cytokine expression. *Nat Cell Biol* 11:1157–1163.

55. Nolde MJ, Saka N, Reinert KL, Slack FJ (2007) The *Caenorhabditis elegans* pumilio homolog, *puf-9*, is required for the 3'UTR-mediated repression of the *let-7* microRNA target gene, *hbl-1*. *Dev Biol* 305:551–563.

56. Kedde M et al. (2010) A Pumilio-induced RNA structure switch in p27-3' UTR controls miR-221 and miR-222 accessibility. *Nature Publishing Group* 12:1014–1020.

57. Kedde M et al. (2007) RNA-binding protein Dnd1 inhibits microRNA access to target mRNA. *Cell* 131:1273–1286.

58. Glorian V et al. (2011) HuR-dependent loading of miRNA RISC to the mRNA encoding the Ras-related small GTPase RhoB controls its translation during UV-induced apoptosis. *Cell Death Differ* 18:1692–1701.

59. Kim HH et al. (2009) HuR recruits let-7/RISC to repress c-Myc expression. *Genes Dev* 23:1743–1748.

60. Kundu P, Fabian MR, Sonenberg N, Bhattacharyya SN, Filipowicz W (2012) HuR protein attenuates miRNA-mediated repression by promoting miRISC dissociation from the target RNA. *Nucleic Acids Research* 40:5088–5100.

61. Tominaga K et al. (2011) Competitive regulation of nucleolin expression by HuR and miR-494. *Mol Cell Biol* 31:4219–4231.

62. Young LE, Moore AE, Sokol L, Meisner-Kober N, Dixon DA (2012) The mRNA stability factor HuR inhibits microRNA-16 targeting of COX-2. *Mol Cancer Res* 10:167–180.

63. Rybak A et al. (2009) The *let-7* target gene mouse *lin-41* is a stem cell specific E3 ubiquitin ligase for the miRNA pathway protein Ago2. *Nat Cell Biol* 11:1411–1420.

64. Zhang P, Zhang H (2013) Autophagy modulates miRNA-mediated gene silencing and selectively degrades AIN-1/GW182 in *C. elegans*. *EMBO Rep* 14:568–576.

65. Vasquez-Rifo A et al. (2013) A new role for the GARP complex in microRNA-mediated gene regulation. *PLoS Genet* 9:e1003961.

66. Hammell CM, Lubin I, Boag PR, Blackwell TK, Ambros V (2009) *nhl-2* Modulates microRNA activity in *Caenorhabditis elegans*. *Cell* 136:926–938.

67. Ramachandran V, Chen X (2008) Degradation of microRNAs by a family of exoribonucleases in *Arabidopsis*. *Science* 321:1490–1492.

68. Chatterjee S, Großhans H (2009) Active turnover modulates mature microRNA activity in *Caenorhabditis elegans*. *Nature* 461:546–549.

69. Baccarini A et al. (2011) Kinetic analysis reveals the fate of a microRNA following target regulation in mammalian cells. *Curr Biol* 21:369–376.

70. Marcinowski L et al. (2012) Degradation of cellular mir-27 by a novel, highly abundant viral transcript is important for efficient virus replication in vivo. *PLoS Pathog* 8:e1002510.

71. Chatterjee S, Fasler M, Büssing I, Großhans H (2011) Target-mediated protection of endogenous microRNAs in *C. elegans*. *Developmental Cell* 20:388–396.

72. Hammell CM, Karp X, Ambros V (2009) A feedback circuit involving let-7-family miRNAs and DAF-12 integrates environmental signals and developmental timing in *Caenorhabditis elegans*. *Proc Natl Acad Sci USA* 106:18668–18673.

73. Brenner S (1974) The genetics of *Caenorhabditis elegans*. *Genetics* 77:71–94.

74. Abbott AL et al. (2005) The *let-7* MicroRNA Family Members *mir-48*, *mir-84*, and *mir-241* Function Together to Regulate Developmental Timing in *Caenorhabditis elegans*. *Developmental Cell* 9:403–414.

75. Johnston RJ, Hobert O (2003) A microRNA controlling left/right neuronal

asymmetry in *Caenorhabditis elegans*. *Nature* 426:845–849.

76. Alvarez-Saavedra E, Horvitz HR (2010) Many Families of *C. elegans* MicroRNAs Are Not Essential for Development or Viability. *Current Biology* 20:367–373.

77. Ambros V, Horvitz HR (1984) Heterochronic mutants of the nematode *Caenorhabditis elegans*. *Science* 226:409–416.

78. Moss EG, Lee RC, Ambros V (1997) The Cold Shock Domain Protein LIN-28 Controls Developmental Timing in *C. elegans* and Is Regulated by the *lin-4* RNA. *Cell* 88:637–646.

79. Hristova M, Birse D, Hong Y, Ambros V (2005) The *Caenorhabditis elegans* heterochronic regulator LIN-14 is a novel transcription factor that controls the developmental timing of transcription from the insulin/insulin-like growth factor gene *ins-33* by direct DNA binding. *Mol Cell Biol* 25:11059–11072.

80. Vadla B, Kemper K, Alaimo J, Heine C, Moss EG (2012) *lin-28* controls the succession of cell fate choices via two distinct activities. *PLoS Genet* 8:e1002588.

81. Slack FJ et al. (2000) The *lin-41* RBCC gene acts in the *C. elegans* heterochronic pathway between the *let-7* regulatory RNA and the LIN-29 transcription factor. *Molecular Cell* 5:659–669. Available at: http://ac.els-cdn.com/S1097276500802452/1-s2.0-S1097276500802452-main.pdf?_tid=1a619fc6-3284-11e3-99ce-00000aacb35e&acdnat=1381503051_51436cf0973c221f04518028134ddc17.

82. Abrahante JE et al. (2003) The *Caenorhabditis elegans* hunchback-like Gene *lin-57*/*hbl-1* Controls Developmental Time and Is Regulated by MicroRNAs. *Developmental Cell* 4:625–637.

83. Rougvie AE, Ambros V (1995) The heterochronic gene *lin-29* encodes a zinc finger protein that controls a terminal differentiation event in *Caenorhabditis elegans*. *Development* 121:2491–2500.

84. Ren H, Zhang H (2010) Wnt signaling controls temporal identities of seam cells in *Caenorhabditis elegans*. *Dev Biol* 345:144–155.

85. Kitano H (2004) Biological robustness. *Nat Rev Genet* 5:826–837.

86. Cohen SM, Brennecke J, Stark A (2006) Denoising feedback loops by

thresholding--a new role for microRNAs. *Genes Dev* 20:2769–2772.

87. Martinez NJ et al. (2008) A *C. elegans* genome-scale microRNA network contains composite feedback motifs with high flux capacity. *Genes Dev* 22:2535–2549.

88. Tsang J, Zhu J, van Oudenaarden A (2007) MicroRNA-mediated feedback and feedforward loops are recurrent network motifs in mammals. *Molecular Cell* 26:753–767.

89. Hornstein E, Shomron N (2006) Canalization of development by microRNAs. *Nat Genet* 38 Suppl:S20–S24.

90. Ebert MS, Sharp PA (2012) Roles for MicroRNAs in Conferring Robustness to Biological Processes. *Cell* 149:515–524.

91. Gursky VV, Surkova SY, Samsonova MG (2012) Mechanisms of developmental robustness. *BioSystems* 109:329–335.

92. Posadas DM, Carthew RW (2014) MicroRNAs and their roles in developmental canalization. *Curr Opin Genet Dev* 27:1–6.

93. Li X, Cassidy JJ, Reinke CA, Fischboeck S, Carthew RW (2009) A microRNA imparts robustness against environmental fluctuation during development. *Cell* 137:273–282.

94. Burke SL, Hammell M, Ambros V (2015) Robust Distal Tip Cell Pathfinding in the Face of Temperature Stress Is Ensured by Two Conserved microRNAS in *Caenorhabditis elegans*. *Genetics* 200:1201–1218.

95. Iliopoulos D, Hirsch HA, Struhl K (2009) An Epigenetic Switch Involving NF-κB, Lin28, Let-7 MicroRNA, and IL6 Links Inflammation to Cell Transformation. *Cell* 139:693–706.

96. Fazi F et al. (2005) A minicircuitry comprised of microRNA-223 and transcription factors NFI-A and C/EBPalpha regulates human granulopoiesis. *Cell* 123:819–831.

97. Li Z, Lu Y, Xu X-L, Gao F-B (2013) The FTD/ALS-associated RNA-binding protein TDP-43 regulates the robustness of neuronal specification through microRNA-9a in *Drosophila*. *Hum Mol Genet* 22:218–225.

98. Zhang X, Zabinsky R, Teng Y, Cui M, Han M (2011) microRNAs play critical roles in the survival and recovery of *Caenorhabditis elegans* from

starvation-induced L1 diapause. *PNAS* 108:17997–18002.

99. Hochbaum D et al. (2011) DAF-12 regulates a connected network of genes to ensure robust developmental decisions. *PLoS Genet* 7:e1002179.

100. Goljanek-Whysall K et al. (2011) MicroRNA regulation of the paired-box transcription factor Pax3 confers robustness to developmental timing of myogenesis. *Proc Natl Acad Sci USA* 108:11936–11941.

101. Cassidy JJ et al. (2013) miR-9a minimizes the phenotypic impact of genomic diversity by buffering a transcription factor. *Cell* 155:1556–1567.

102. McJunkin K, Ambros V (2014) The embryonic *mir-35* family of microRNAs promotes multiple aspects of fecundity in *Caenorhabditis elegans*. *G3 (Bethesda)* 4:1747–1754.

103. Eulalio A, Huntzinger E, Izaurralde E (2008) Getting to the Root of miRNA-Mediated Gene Silencing. *Cell* 132:9–14.

104. Schulman BRM, Esquela-Kerscher A, Slack FJ (2005) Reciprocal expression of *lin-41* and the microRNAs *let-7* and *mir-125* during mouse embryogenesis. *Dev Dyn* 234:1046–1054.

105. Roush S, Slack FJ (2008) The *let-7* family of microRNAs. *Trends Cell Biol* 18:505–516.

106. Großhans H, Johnson T, Reinert KL, Gerstein M, Slack FJ (2005) The temporal patterning microRNA *let-7* regulates several transcription factors at the larval to adult transition in *C. elegans*. *Developmental Cell* 8:321–330.

107. Lin S-Y et al. (2003) The *C. elegans* hunchback Homolog, *hbl-1*, Controls Temporal Patterning and Is a Probable MicroRNA Target. *Developmental Cell* 4:639–650.

108. Aballay A, Ausubel FM (2002) *Caenorhabditis elegans* as a host for the study of host-pathogen interactions. *Curr Opin Microbiol* 5:97–101.

109. Schulte LN, Eulalio A, Mollenkopf H-J, Reinhardt R, Vogel J (2011) Analysis of the host microRNA response to Salmonella uncovers the control of major cytokines by the *let-7* family. *EMBO J* 30:1977–1989.

110. Chen X-M, Splinter PL, O'Hara SP, LaRusso NF (2007) A cellular micro-RNA, *let-7i*, regulates Toll-like receptor 4 expression and contributes to

cholangiocyte immune responses against *Cryptosporidium parvum* infection. *J Biol Chem* 282:28929–28938.

111. Hu G et al. (2009) MicroRNA-98 and *let-7* confer cholangiocyte expression of cytokine-inducible Src homology 2-containing protein in response to microbial challenge. *J Immunol* 183:1617–1624.

112. Liu F et al. (2013) Nuclear Hormone Receptor Regulation of MicroRNAs Controls Innate Immune Responses in *C. elegans*. *PLoS Pathog* 9:e1003545.

113. Stiernagle T (2006) Maintenance of *C. elegans*. *WormBook*:1–11.

114. Powell JR, Ausubel FM (2008) Models of *Caenorhabditis elegans* infection by bacterial and fungal pathogens. *Methods Mol Biol* 415:403–427.

115. Yang J-S et al. (2011) OASIS: online application for the survival analysis of lifespan assays performed in aging research. *PLoS ONE* 6:e23525.

116. Frøkjær-Jensen C et al. (2008) Single-copy insertion of transgenes in *Caenorhabditis elegans*. *Nat Genet* 40:1375–1383.

117. Irazoqui JE et al. (2010) Distinct pathogenesis and host responses during infection of *C. elegans* by *P. aeruginosa* and *S. aureus*. *PLoS Pathog* 6:e1000982.

118. Timmons L, Court DL, Fire A (2001) Ingestion of bacterially expressed dsRNAs can produce specific and potent genetic interference in *Caenorhabditis elegans*. *Gene* 263:103–112.

119. Fraser AG et al. (2000) Functional genomic analysis of *C. elegans* chromosome I by systematic RNA interference. *Nature* 408:325–330.

120. Shivers RP et al. (2010) Phosphorylation of the conserved transcription factor ATF-7 by PMK-1 p38 MAPK regulates innate immunity in *Caenorhabditis elegans*. *PLoS Genet* 6:e1000892.

121. MacNeil LT, Watson E, Arda HE, Zhu LJ, Walhout AJM (2013) Diet-induced developmental acceleration independent of TOR and insulin in *C. elegans*. *Cell* 153:240–252.

122. Reimmann C et al. (1997) The global activator GacA of *Pseudomonas aeruginosa* PAO positively controls the production of the autoinducer *N*-butyryl-homoserine lactone and the formation of the virulence factors

pyocyanin, cyanide, and lipase. *Mol Microbiol* 24:309–319.

123. Tan MW, Rahme LG, Sternberg JA, Tompkins RG, Ausubel FM (1999) *Pseudomonas aeruginosa* killing of *Caenorhabditis elegans* used to identify *P. aeruginosa* virulence factors. *Proc Natl Acad Sci USA* 96:2408–2413.

124. Kim DH et al. (2002) A conserved p38 MAP kinase pathway in *Caenorhabditis elegans* innate immunity. *Science* 297:623–626.

125. Richardson CE, Kooistra T, Kim DH (2010) An essential role for XBP-1 in host protection against immune activation in *C. elegans*. *Nature* 463:1092–1095.

126. Shivers RP, Kooistra T, Chu SW, Pagano DJ, Kim DH (2009) Tissue-specific activities of an immune signaling module regulate physiological responses to pathogenic and nutritional bacteria in *C. elegans*. *Cell Host and Microbe* 6:321–330.

127. Roush SF, Slack FJ (2009) Transcription of the *C. elegans let-7* microRNA is temporally regulated by one of its targets, *hbl-1*. *Dev Biol* 334:523–534.

128. Hammell M et al. (2008) mirWIP: microRNA target prediction based on microRNA-containing ribonucleoprotein–enriched transcripts. *Nat Meth* 5:813–819.

129. Troemel ER et al. (2006) p38 MAPK regulates expression of immune response genes and contributes to longevity in *C. elegans*. *PLoS Genet* 2:e183.

130. Garigan D et al. (2002) Genetic analysis of tissue aging in *Caenorhabditis elegans*: a role for heat-shock factor and bacterial proliferation. *Genetics* 161:1101–1112.

131. Hada K et al. (2010) The nuclear receptor gene *nhr-25* plays multiple roles in the *Caenorhabditis elegans* heterochronic gene network to control the larva-to-adult transition. *Dev Biol* 344:1100–1109.

132. Kim DH et al. (2004) Integration of *Caenorhabditis elegans* MAPK pathways mediating immunity and stress resistance by MEK-1 MAPK kinase and VHP-1 MAPK phosphatase. *Proc Natl Acad Sci USA* 101:10990–10994.

133. Mizuno T et al. (2004) The *Caenorhabditis elegans* MAPK phosphatase

VHP-1 mediates a novel JNK-like signaling pathway in stress response. *EMBO J* 23:2226–2234.

134. Pujol N et al. (2008) Distinct Innate Immune Responses to Infection and Wounding in the *C. elegans* Epidermis. *Current Biology* 18:481–489.

135. Ziegler K et al. (2009) Antifungal Innate Immunity in *C. elegans*: PKCδ Links G Protein Signaling and a Conserved p38 MAPK Cascade. *Cell Host and Microbe* 5:341–352.

136. Livingstone C, Patel G, Jones N (1995) ATF-2 contains a phosphorylation-dependent transcriptional activation domain. *EMBO J* 14:1785–1797.

137. De Graeve F, Bahr A, Chatton B, Kedinger C (2000) A murine ATFa-associated factor with transcriptional repressing activity. *Oncogene* 19:1807–1819.

138. Martinez NJ et al. (2008) Genome-scale spatiotemporal analysis of *Caenorhabditis elegans* microRNA promoter activity. *Genome Res* 18:2005–2015.

139. Richardson CE, Kinkel S, Kim DH (2011) Physiological IRE-1-XBP-1 and PEK-1 signaling in *Caenorhabditis elegans* larval development and immunity. *PLoS Genet* 7:e1002391.

140. Zou C-G, Ma Y-C, Dai L-L, Zhang K-Q (2014) Autophagy protects *C. elegans* against necrosis during *Pseudomonas aeruginosa* infection. *Proc Natl Acad Sci USA* 111:12480–12485.

141. Vadla B, Kemper K, Alaimo J, Heine C, Moss EG (2012) lin-28 controls the succession of cell fate choices via two distinct activities. *PLoS Genet* 8:e1002588. Available at: http://dx.plos.org/10.1371/journal.pgen.1002588.g005.

142. Voinnet O (2011) Micro-balancing innate immunity to *Salmonella*. *EMBO J* 30:1877–1879.

143. Tan MW, Ausubel FM (2000) *Caenorhabditis elegans*: a model genetic host to study *Pseudomonas aeruginosa* pathogenesis. *Curr Opin Microbiol* 3:29–34.

144. Pujol N et al. (2001) A reverse genetic analysis of components of the Toll signaling pathway in *Caenorhabditis elegans*. *Current Biology* 11:809–821.

145. Ren M, Feng H, Fu Y, Land M, Rubin CS (2009) Protein kinase D is an essential regulator of *C. elegans* innate immunity. *Immunity* 30:521–532.

146. Powell JR, Kim DH, Ausubel FM (2009) The G protein-coupled receptor FSHR-1 is required for the *Caenorhabditis elegans* innate immune response. *Proc Natl Acad Sci USA* 106:2782–2787.

147. Estes KA, Dunbar TL, Powell JR, Ausubel FM, Troemel ER (2010) bZIP transcription factor *zip-2* mediates an early response to *Pseudomonas aeruginosa* infection in *Caenorhabditis elegans*. *Proc Natl Acad Sci USA* 107:2153–2158.

148. Irazoqui JE, Ng A, Xavier RJ, Ausubel FM (2008) Role for beta-catenin and HOX transcription factors in *Caenorhabditis elegans* and mammalian host epithelial-pathogen interactions. *Proc Natl Acad Sci USA* 105:17469–17474.

149. Tenor JL, Aballay A (2008) A conserved Toll-like receptor is required for *Caenorhabditis elegans* innate immunity. *EMBO Rep* 9:103–109.

150. Seggerson K, Tang L, Moss EG (2002) Two genetic circuits repress the *Caenorhabditis elegans* heterochronic gene *lin-28* after translation initiation. *Dev Biol* 243:215–225.

151. McEwan DL, Kirienko NV, Ausubel FM (2012) Host translational inhibition by *Pseudomonas aeruginosa* Exotoxin A Triggers an immune response in *Caenorhabditis elegans*. *Cell Host and Microbe* 11:364–374.

152. Ren Z, Ambros VR (2015) *Caenorhabditis elegans* microRNAs of the *let-7* family act in innate immune response circuits and confer robust developmental timing against pathogen stress. *Proc Natl Acad Sci USA* 112:E2366–75.

153. Liu Z, Ambros V (1991) Alternative temporal control systems for hypodermal cell differentiation in *Caenorhabditis elegans*. *Nature* 350:162–165.

154. Van Hoof D et al. (2009) Phosphorylation dynamics during early differentiation of human embryonic stem cells. *Cell Stem Cell* 5:214–226.

155. Lukac M, Pier GB, Collier RJ (1988) Toxoid of *Pseudomonas aeruginosa* exotoxin A generated by deletion of an active-site residue. *Infect Immun* 56:3095–3098.

156. Yates SP, Jørgensen R, Andersen GR, Merrill AR (2006) Stealth and

mimicry by deadly bacterial toxins. *Trends in Biochemical Sciences* 31:123–133.

157. Fire A et al. (1998) Potent and specific genetic interference by double-stranded RNA in *Caenorhabditis elegans*. *Nature* 391:806–811.

158. Sagasti A et al. (2001) The CaMKII UNC-43 activates the MAPKKK NSY-1 to execute a lateral signaling decision required for asymmetric olfactory neuron fates. *Cell* 105:221–232.

159. Tanaka-Hino M et al. (2002) SEK-1 MAPKK mediates Ca2+ signaling to determine neuronal asymmetric development in *Caenorhabditis elegans*. *EMBO Rep* 3:56–62.

160. Chuang C-F, Bargmann CI (2005) A Toll-interleukin 1 repeat protein at the synapse specifies asymmetric odorant receptor expression via ASK1 MAPKKK signaling. *Genes Dev* 19:270–281.

161. Cohen P (2000) The regulation of protein function by multisite phosphorylation--a 25 year update. *Trends in Biochemical Sciences* 25:596–601.

162. Piskounova E et al. (2011) Lin28A and Lin28B inhibit let-7 microRNA biogenesis by distinct mechanisms. *Cell* 147:1066–1079.

163. Norris AD et al. (2014) A pair of RNA-binding proteins controls networks of splicing events contributing to specialization of neural cell types. *Molecular Cell* 54:946–959.

164. Kudlow BA, Zhang L, Han M (2012) Systematic Analysis of Tissue-Restricted miRISCs Reveals a Broad Role for MicroRNAs in Suppressing Basal Activity of the *C. elegans* Pathogen Response. *Molecular Cell* 46:530–541.

165. Pagano DJ, Kingston ER, Kim DH (2015) Tissue expression pattern of PMK-2 p38 MAPK is established by the miR-58 family in *C. elegans*. *PLoS Genet* 11:e1004997.

166. Krol J, Loedige I, Filipowicz W (2010) The widespread regulation of microRNA biogenesis, function and decay. *Nature Publishing Group* 11:597–610.

167. Fabian MR, Sonenberg N (2012) The mechanics of miRNA-mediated gene silencing: a look under the hood of miRISC. *Nat Struct Mol Biol* 19:586–593.

168. Bhattacharyya SN, Habermacher R, Martine U, Closs EI, Filipowicz W (2006) Relief of microRNA-mediated translational repression in human cells subjected to stress. *Cell* 125:1111–1124.

169. St Johnston D, Beuchle D, Nüsslein-Volhard C (1991) *Staufen*, a gene required to localize maternal RNAs in the Drosophila egg. *Cell* 66:51–63.

170. Li P, Yang X, Wasser M, Cai Y, Chia W (1997) Inscuteable and Staufen mediate asymmetric localization and segregation of *prospero* RNA during Drosophila neuroblast cell divisions. *Cell* 90:437–447.

171. Broadus J, Fuerstenberg S, Doe CQ (1998) Staufen-dependent localization of *prospero* mRNA contributes to neuroblast daughter-cell fate. *Nature* 391:792–795.

172. Ferrandon D, Elphick L, Nüsslein-Volhard C, St Johnston D (1994) Staufen protein associates with the 3'UTR of *bicoid* mRNA to form particles that move in a microtubule-dependent manner. *Cell* 79:1221–1232.

173. Ferrandon D, Koch I, Westhof E, Nüsslein-Volhard C (1997) RNA-RNA interaction is required for the formation of specific bicoid mRNA 3' UTR-STAUFEN ribonucleoprotein particles. *EMBO J* 16:1751–1758.

174. Shen CP, Jan LY, Jan YN (1997) Miranda is required for the asymmetric localization of Prospero during mitosis in Drosophila. *Cell* 90:449–458.

175. Köhrmann M et al. (1999) Microtubule-dependent recruitment of Staufen-green fluorescent protein into large RNA-containing granules and subsequent dendritic transport in living hippocampal neurons. *Mol Biol Cell* 10:2945–2953.

176. Kiebler MA et al. (1999) The mammalian staufen protein localizes to the somatodendritic domain of cultured hippocampal neurons: implications for its involvement in mRNA transport. *J Neurosci* 19:288–297.

177. Ricci EP et al. (2014) Staufen1 senses overall transcript secondary structure to regulate translation. *Nat Struct Mol Biol* 21:26–35.

178. Sugimoto Y et al. (2015) hiCLIP reveals the in vivo atlas of mRNA secondary structures recognized by Staufen 1. *Nature* 519:491–494.

179. Park E, Maquat LE (2013) Staufen-mediated mRNA decay. *Wiley Interdiscip Rev RNA* 4:423–435.

180. LeGendre JB et al. (2013) RNA targets and specificity of Staufen, a double-stranded RNA-binding protein in *Caenorhabditis elegans*. *J Biol Chem* 288:2532–2545.

181. Barbee SA et al. (2006) Staufen- and FMRP-containing neuronal RNPs are structurally and functionally related to somatic P bodies. *Neuron* 52:997–1009.

182. Peredo J, Villacé P, Ortín J, de Lucas S (2014) Human Staufen1 associates to miRNAs involved in neuronal cell differentiation and is required for correct dendritic formation. *PLoS ONE* 9:e113704.

183. Kim H et al. (2014) A co-CRISPR strategy for efficient genome editing in *Caenorhabditis elegans*. *Genetics* 197:1069–1080.

184. Arribere JA et al. (2014) Efficient marker-free recovery of custom genetic modifications with CRISPR/Cas9 in *Caenorhabditis elegans*. *Genetics* 198:837–846.

185. Zou Y et al. (2013) Developmental decline in neuronal regeneration by the progressive change of two intrinsic timers. *Science* 340:372–376.

186. Duchaine TF et al. (2006) Functional proteomics reveals the biochemical niche of *C. elegans* DCR-1 in multiple small-RNA-mediated pathways. *Cell* 124:343–354.

187. Sterling CH, Veksler-Lublinsky I, Ambros V (2015) An efficient and sensitive method for preparing cDNA libraries from scarce biological samples. *Nucleic Acids Research* 43:e1.

188. Martin M (2011) Cutadapt removes adapter sequences from high-throughput sequencing reads. *EMBnet journal*.

189. Langmead B, Trapnell C, Pop M, Salzberg SL (2009) Ultrafast and memory-efficient alignment of short DNA sequences to the human genome. *Genome Biol* 10:R25.

190. Griffiths-Jones S, Saini HK, van Dongen S, Enright AJ (2008) miRBase: tools for microRNA genomics. *Nucleic Acids Research* 36:D154–8.

191. Lee H-C et al. (2012) *C. elegans* piRNAs mediate the genome-wide surveillance of germline transcripts. *Cell* 150:78–87.

192. Robinson MD, McCarthy DJ, Smyth GK (2010) edgeR: a Bioconductor package for differential expression analysis of digital gene expression

data. *Bioinformatics* 26:139–140.

193. Zisoulis DG et al. (2010) Comprehensive discovery of endogenous Argonaute binding sites in *Caenorhabditis elegans*. *Nat Struct Mol Biol* 17:173–179.

194. Sarin S et al. (2007) Genetic screens for *Caenorhabditis elegans* mutants defective in left/right asymmetric neuronal fate specification. *Genetics* 176:2109–2130.

195. Gu W et al. (2009) Distinct argonaute-mediated 22G-RNA pathways direct genome surveillance in the *C. elegans* germline. *Molecular Cell* 36:231–244.

196. Shirayama M et al. (2012) piRNAs initiate an epigenetic memory of nonself RNA in the *C. elegans* germline. *Cell* 150:65–77.

197. Micklem DR, Adams J, Grünert S, St Johnston D (2000) Distinct roles of two conserved Staufen domains in *oskar* mRNA localization and translation. *EMBO J* 19:1366–1377.

198. Dugré-Brisson S et al. (2005) Interaction of Staufen1 with the 5' end of mRNA facilitates translation of these RNAs. *Nucleic Acids Research* 33:4797–4812.

199. Shi Z, Hayes G, Ruvkun G (2013) Dual regulation of the *lin-14* target mRNA by the *lin-4* miRNA. *PLoS ONE* 8:e75475.

200. Lewis BP, Burge CB, Bartel DP (2005) Conserved seed pairing, often flanked by adenosines, indicates that thousands of human genes are microRNA targets. *Cell* 120:15–20.

201. Jan CH, Friedman RC, Ruby JG, Bartel DP (2011) Formation, regulation and evolution of *Caenorhabditis elegans* 3'UTRs. *Nature* 469:97–101.

202. Gleghorn ML, Maquat LE (2014) 'Black sheep‘ that don’t leave the double-stranded RNA-binding domain fold. *Trends in Biochemical Sciences* 39:328–340.

203. Saito I, Matsuura T (1985) Chemical Aspects of UV-Induced Cross-Linking of Proteins to Nucleic Acids. Photoreactions with Lysine and Tryptophan. *American Chemical Society* 18:134–141.

204. Roegiers F, Jan YN (2000) Staufen: a common component of mRNA transport in oocytes and neurons? *Trends Cell Biol* 10:220–224.

205. Kennedy S, Wang D, Ruvkun G (2004) A conserved siRNA-degrading RNase negatively regulates RNA interference in *C. elegans*. *Nature* 427:645–649.

206. Lee RC, Hammell CM, Ambros V (2006) Interacting endogenous and exogenous RNAi pathways in *Caenorhabditis elegans*. *RNA* 12:589–597.

207. Pavelec DM, Lachowiec J, Duchaine TF, Smith HE, Kennedy S (2009) Requirement for the ERI/DICER complex in endogenous RNA interference and sperm development in *Caenorhabditis elegans*. *Genetics* 183:1283–1295.

208. Thomas MF et al. (2012) Eri1 regulates microRNA homeostasis and mouse lymphocyte development and antiviral function. *Blood* 120:130–142.

209. Lee YS et al. (2009) Silencing by small RNAs is linked to endosomal trafficking. *Nat Cell Biol* 11:1150–1156. Available at: http://www.nature.com/doifinder/10.1038/ncb1930.

210. Gibbings DJ, Ciaudo C, Erhardt M, Voinnet O (2009) Multivesicular bodies associate with components of miRNA effector complexes and modulate miRNA activity. *Nat Cell Biol* 11:1143–1149.

211. Wollert T et al. (2009) The ESCRT machinery at a glance. *J Cell Sci* 122:2163–2166.

212. Stenmark H (2009) Rab GTPases as coordinators of vesicle traffic. *Nat Rev Mol Cell Biol* 10:513–525.

213. Wang T, Ming Z, Xiaochun W, Hong W (2011) Rab7: role of its protein interaction cascades in endo-lysosomal traffic. *Cell Signal* 23:516–521.

214. Odorizzi G, Cowles CR, Emr SD (1998) The AP-3 complex: a coat of many colours. *Trends Cell Biol* 8:282–288.

215. Poteryaev D, Fares H, Bowerman B, Spang A (2007) *Caenorhabditis elegans* SAND-1 is essential for RAB-7 function in endosomal traffic. *EMBO J* 26:301–312.

216. Skorobogata O, Rocheleau CE (2012) RAB-7 antagonizes LET-23 EGFR signaling during vulva development in *Caenorhabditis elegans*. *PLoS ONE* 7:e36489.

217. Teis D, Huber LA (2003) The odd couple: signal transduction and

endocytosis. *Cellular and Molecular Life Sciences (CMLS)* 60:2020–2033.

218. Kaech SM, Whitfield CW, Kim SK (1998) The LIN-2/LIN-7/LIN-10 complex mediates basolateral membrane localization of the *C. elegans* EGF receptor LET-23 in vulval epithelial cells. *Cell* 94:761–771.

219. Djeddi A et al. (2012) Induction of autophagy in ESCRT mutants is an adaptive response for cell survival in *C. elegans*. *J Cell Sci* 125:685–694.

220. Gibbings D et al. (2012) Human prion protein binds Argonaute and promotes accumulation of microRNA effector complexes. *Nat Struct Mol Biol* 19:517–24– S1.

221. Jin P et al. (2004) Biochemical and genetic interaction between the fragile X mental retardation protein and the microRNA pathway. *Nat Neurosci* 7:113–117.

222. Harandi OF, Ambros VR (2015) Control of stem cell self-renewal and differentiation by the heterochronic genes and the cellular asymmetry machinery in Caenorhabditis elegans. *Proc Natl Acad Sci USA* 112:E287–96.

223. Coudreuse DYM, Roël G, Betist MC, Destrée O, Korswagen HC (2006) Wnt gradient formation requires retromer function in Wnt-producing cells. *Science* 312:921–924.

224. Port F et al. (2008) Wingless secretion promotes and requires retromer-dependent cycling of Wntless. *Nat Cell Biol* 10:178–185.

225. Balderhaar HJK et al. (2010) The Rab GTPase Ypt7 is linked to retromer-mediated receptor recycling and fusion at the yeast late endosome. *J Cell Sci* 123:4085–4094.

226. Chu Y-D, Chen H-K, Huang T, Chan S-P (2015) A novel function for the DEAD-box RNA helicase DDX-23 in primary microRNA processing in *Caenorhabditis elegans*. *Dev Biol*.

227. Ruby JG et al. (2006) Large-scale sequencing reveals 21U-RNAs and additional microRNAs and endogenous siRNAs in *C. elegans*. *Cell* 127:1193–1207.

228. Miska EA et al. (2007) Most *Caenorhabditis elegans* microRNAs are individually not essential for development or viability. *PLoS Genet* 3:e215.

229. Brenner JL, Jasiewicz KL, Fahley AF, Kemp BJ, Abbott AL (2010) Loss of individual microRNAs causes mutant phenotypes in sensitized genetic backgrounds in *C. elegans*. *Current Biology* 20:1321–1325. Available at: http://eutils.ncbi.nlm.nih.gov/entrez/eutils/elink.fcgi?dbfrom=pubmed&id=20579881&retmode=ref&cmd=prlinks.

230. Thomas MG, Martinez Tosar LJ, Desbats MA, Leishman CC, Boccaccio GL (2009) Mammalian Staufen 1 is recruited to stress granules and impairs their assembly. *J Cell Sci* 122:563–573.